HIV INFECTION IN THE POST-COMBINATION ANTIRETROVIRAL THERAPY ERA: A HUMAN MODEL OF IMMUNE AGING

by

Anthony Yu-Yang Hsieh

B.Sc., The University of British Columbia, 2013

A THESIS SUBMITTED IN PARTIAL FULFILLMENT OF

THE REQUIREMENTS FOR THE DEGREE OF

DOCTOR OF PHILOSOPHY

in

THE FACULTY OF GRADUATE AND POSTDOCTORAL STUDIES

(Pathology and Laboratory Medicine)

THE UNIVERSITY OF BRITISH COLUMBIA

(Vancouver)

August 2020

The following individuals certify that they have read, and recommend to the Faculty of Graduate and Postdoctoral Studies for acceptance, the dissertation entitled: **HIV infection in the post-combination antiretroviral therapy era: a human model of immune aging**

submitted by **Anthony Hsieh** in partial fulfillment of the requirements for

the degree of **Doctor of Philosophy**

in **Pathology and Laboratory Medicine**

Examining Committee:

Dr. Hélène C.F. Côté, Department of Pathology and Laboratory Medicine
Supervisor

Dr. Megan K. Levings, Department of Surgery
Supervisory Committee Member

Dr. Ivan Sadowski, Department of Biochemistry and Molecular Biology
University Examiner

Dr. Peter Lansdorp, Department of Medical Genetics
University Examiner

Additional Supervisory Committee Members:

Dr. Jacqueline Quandt, Department of Pathology and Laboratory Medicine
Supervisory Committee Member

Dr. Marc Horwitz, Department of Microbiology and Immunology
Supervisory Committee Member

Abstract

The deterioration of the immune system is a fundamental characteristic of aging and is accompanied by alterations in immune aging markers including shorter telomere length (TL), decreased mitochondrial DNA (mtDNA) content, and larger differentiated T cell populations. These same markers characterize an accelerated immune aging phenotype in people living with HIV (PLWH). Although HIV is successfully treated with combination antiretroviral therapy (cART), treatment is lifelong and does not fully eliminate the accelerated aging phenotype. Therefore, cART-controlled HIV infection can represent a human model of immune aging compared to the general population. The extent to which longitudinal changes in leukocyte TL (LTL) and blood mtDNA content inter-relate and are together influenced by HIV is unknown. Also unknown is whether slow progressors, a rare population who naturally control HIV without cART, are protected against HIV-mediated accelerated immune aging.

The goal of my research was to investigate aging markers in PLWH, considering HIV infection as a human model of immune aging.

First, I developed a monochrome multiplex quantitative PCR assay to measure mtDNA content quickly and accurately with low starting material. I measured blood mtDNA content, LTL, and their rates of change among 312 PLWH and 300 HIV-negative controls. I showed that faster rates of LTL attrition and blood mtDNA decline were associated with loss of HIV viral control. Faster LTL attrition was also associated with slower blood mtDNA content decline, regardless of HIV status. I then measured more granular markers of immune aging including lymphocyte

subset TL and T cell differentiation in 57 slow progressors with sex- and age-matched cART-controlled PLWH and HIV-negative controls. My analyses revealed that slow progressors had shorter immune subset TL and more differentiated CD8 T cells compared to both cART-controlled PLWH and HIV-negative controls, indicating that they experience even faster immune aging despite naturally controlling the disease.

My research confirms that uncontrolled chronic/latent viral infections such as HIV accelerate immune aging but demonstrates that naturally controlling HIV may also age immune cells. This suggests that preventing and controlling chronic/latent viral infections with therapy could extend lifespan and may represent an evolution to the paradigm of aging research.

Lay Summary

Our immune system weakens as we age, but it is difficult to study how and why because aging happens to everyone. My strategy was to study the cells of the immune system in people living with HIV, who age faster than the general population. To do so, I used blood samples and measured changes in DNA that normally occur with age and counted how many old and tired immune cells there were compared to young cells. I found that people with HIV who were not treated with medications to reduce the amount of virus aged faster than those who were. This even happened in an extraordinary group of people who do not get sick from HIV. My research shows that everybody living with HIV should receive treatment to slow immune aging and suggests that treating viruses that are even more common than HIV may slow aging for many more people.

Preface

This thesis represents my original work. The novel biological concepts, hypotheses, and research questions leading to the studies presented in this thesis are mine, developed with the help of my supervisor, Dr. Hélène Côté. They are based on topics of research proposed by a Canadian Institutes of Health Research Team Grant on Cellular Aging and HIV Comorbidities in Women and Children 2013-2018 (TCO-125269), on which Dr. Côté was the principal applicant. The research proposed in the grant, as well as my own research, largely involve participants and biospecimens from the Children and Women: AntiRetrovirals and Markers of Aging (CARMA) cohort. My research program benefited from the guidance of my supervisory committee, including Jacqueline Quandt, Marc Horwitz, Megan Levings, as well as Patrick Tang who was a past member. All studies were approved by the University of British Columbia Research Ethics Board (H08-02018). This thesis begins with an introductory chapter 1, followed by a methods publication as chapter 2, followed by 2 studies as chapters 3 and 4, and ends with a conclusion as chapter 5.

The purpose of chapter 1 is to present the overall theme of the thesis. It contains a literature review appropriate for a non-specialist scholar, which provides context for the impetus behind the research contained in subsequent chapters. Chapter 1 ends with research objectives and an overarching hypothesis. More granular and study-specific hypotheses are presented at the outset of the subsequent chapters. All figures in chapter 1 are original, based on data referred to, or concepts described in, the chapter itself.

A version of chapter 2 has been published as Hsieh AYY, Budd MA, Deng D, Gadawska I, and Côté HCF (2008), **"A Monochrome Multiplex qPCR Assay for the Measurement of mtDNA content"**, *Journal of Molecular Diagnostics*, 20(5):612-620. I am the first author of this manuscript, and contributed 80% of the experimental design, data collection, and writing, as well as all of the statistical analysis. Matthew Budd contributed to 10% of the writing. David Deng and Izabella Gadawska each performed several qPCR assays, which amounted to 20% of the data collection. Hélène Côté provided the scientific inspiration behind this manuscript, gave guidance relating to experimental design, and contributed to 10% of the writing. Unlike the publication, the supplementary material is now integrated into the main text, the acknowledgements section is removed, and any abbreviations that were defined in chapter 1 were not defined again in chapter 2.

A version of chapter 3 has been submitted as Hsieh AYY, Kimmel E, Pick N, Sauvé L, Brophy J, Kakkar F, Bitnun A, Murray MCM, Côté HCF, and the CIHR Team in Cellular Aging and HIV Comorbidities in Women and Children (CARMA), **"Inverse relationship between leukocyte telomere length attrition and blood mitochondrial DNA content loss over time",** to the journal *Aging (Albany NY)*. It is currently undergoing author minor revisions to address the peer reviewers' comments prior to resubmission. I am the first author of this manuscript, and contributed 90% of the experimental design and writing, 60% of the data collection, and all of the statistical analysis. Elana Kimmel, a summer student working under my mentorship, performed several qPCR assays, which amounted to 40% of the data collection. Neora Pick, Laura Sauvé, Jason Brophy, Fatima Kakkar, Ari Bitnun, and Melanie Murray contributed to the initial study design as well as manuscript editing. Hélène Côté provided the scientific inspiration

behind this manuscript, gave guidance relating to experimental design, and contributed to 10% of the writing. Similar to chapter 2, the supplementary material in the original submission is now integrated into the main text, the acknowledgements section is removed, and any abbreviations previously defined were not defined again. In addition, the section describing methods is moved from after the discussion to before the results, consistent with the other chapters of this thesis. The introduction section of the submission is also moved and integrated into chapter 1 to avoid repetition. Instead, chapter 3 begins with an abbreviated introduction, including specific hypotheses.

Chapter 4 is a manuscript in preparation, tentatively titled **"HIV Slow Progressors experience accelerated aging compared to HIV Non-Slow Progressors"**. I am the first author of this manuscript. While co-authorship has yet to be finalized, it will include Beheroze Sattha, Izabelle Gadawski, Mahtab Gill, Nicole Bernard, Cecile Tremblay, and Hélène Côté. For this manuscript, I contributed 70% of the data collection, 90% of the writing, and all the statistical analyses. Beheroze Sattha prepared blood biospecimens for storage prior to the experiments. Izabelle Gadawski and Mahtab Gill performed qPCR assays totaling 30% of the data collection. Nicole Bernard and Cecile Tremblay are investigators from the Canadian Cohort of HIV+ Slow Progressors. They helped facilitate the collaboration between their cohort and CARMA, as well as contributed to the initial study design. Hélène Côté provided the scientific inspiration behind this manuscript, gave guidance relating to experimental design, and contributed to 10% of the writing. As with chapter 3, the introductory material is integrated into chapter 1, and chapter 4 begins with an abbreviated introduction, including specific hypotheses. For readability, study group abbreviations were defined again even though they were previously defined in chapter 1.

Chapter 5 summarizes the scientific findings of the thesis and expands on their translational significance. This chapter also explores future studies based on the data and novel biological concepts presented in this thesis.

Table of Contents

List of Tables

List of Figures

List of Symbols and Abbreviations

β	Effect size
ρ_C	Lin's concordance correlation coefficient
ACB	African/Caribbean/Black
AIC	Akaike information criterion
ALB	Albumin
ANOVA	Analysis of variance
CARMA	Children and Women: AntiRetrovirals and Markers of Aging
cART	Combination antiretroviral therapy
CCR5	C-C motif chemokine receptor 5
CHO	Chinese hamster ovary
CMV	Cytomegalovirus
C_T	Cycle threshold
CV	Coefficient of variation
D-loop	Displacement loop
DMSO	Dimethyl sulfoxide
dPBS	Dulbecco's phosphate buffered saline
EBV	Epstein-Barr virus
EDTA	Ethylenediaminetetraacetic acid
FACS	Fluorescence-activated cell sorting
FBS	Fetal bovine serum
FISH	Fluorescence *in situ* hybridization

FMO	Fluorescence minus one
FVS700	Fixable Viability Stain 700
HBV	Hepatitis B virus
HCV	Hepatitis C virus
HEU	HIV-exposed uninfected
HLA	Human leukocyte antigen
HSV-1	Herpes simplex virus 1
HSV-2	Herpes simplex virus 2
IC	Internal control
INSTI	Integrase strand-transfer inhibitor
LTL	Leukocyte telomere length
MMqPCR	Monochrome multiplex qPCR
MT-CO1	Cytochrome c oxidase subunit 1
mtDNA	Mitochondrial DNA
nDNA	Nuclear DNA
NRTI	Nucleoside reverse transcriptase inhibitor
NSP	Non-slow progressor
PBMC	Peripheral blood mononuclear cell
PCA	Principal Component Analysis
PD-1	Programmed cell death protein-1
PI	Protease inhibitor
PLWH	People living with HIV
POLG2	Polymerase (DNA-directed), γ2, accessory subunit

pVL	Plasma viral load
QC	Quality control
qPCR	Quantitative PCR
ROS	Reactive oxygen species
SP	Slow progressor
T_{CM}	Central memory T cell
T_{EM}	Effector memory T cell
T_{EMRA}	Terminally-differentiated effector memory T cell
Tim-3	Immunoglobulin mucin-3
TL	Telomere length
T_N	Naïve T cell
T_{reg}	Regulatory T cell
TRF	Terminal restriction fragment
t-SNE	t-Distributed Stochastic Neighbor Embedding
UP	Uncontrolled progressor
VIF	Variance inflation factor
VZV	Varicella zoster virus
WB	Whole blood
WLWH	Women living with HIV
WHO	World Health Organization

Acknowledgements

I would like to thank the researchers, staff, and participants of the Children and Women: AntiRetrovirals and Markers of Aging (CARMA) cohort, without whom this work would not exist. I am grateful for all I have learned from the team and I am proud of the small contribution my research represents among the team's many scientific advances. I am also grateful to the University of British Columbia, the Department of Pathology and Laboratory Medicine, the Centre for Blood Research, the Canadian Institutes of Health Research, and the Canadian Association for HIV Research for funding my research and conference travel. My research was guided in part by my supervisory committee members Jacqueline Quandt, Marc Horwitz, Megan Levings, and Patrick Tang. They struck the perfect balance between critically assessing my work and helping me surmount obstacles. I would like to thank my committee chair Haydn Pritchard for his mentorship during my degree and providing perspective on what lies beyond.

The core of my PhD experience took place in the Côté lab. As one would expect from an accomplished scientist, my supervisor Hélène Côté is a font of knowledge, and her innate curiosity, ability to grasp complex ideas with ease, and relentless pursuit of excellence have been an inspiration to me. However, she is singular in her unwavering sense of morality and genuine care for her students. Over the years, I have witnessed how her leadership has led to a lab culture in which unabashed curiosity and scientific rigour coincide with earnest friendships. The depth of these friendships has been demonstrated by the sense of loss that followed each time a fellow student graduated. Previous students Sara Saberi, Marta Salvador Ordoño, Micah Piske, Matthew Budd, Abhinav Ajaykumar, and DeAnna Zanet are wonderful friends, and their input

into my research has had tremendous value. I would like to specifically acknowledge Abhinav, with whom I started my PhD. By a very wide margin, the strongest correlation that I present in this dissertation is the following: that in matters of both life and work, things turn out better when I run them by Abhinav first. He taught me how to ride a motorcycle. I will forever cherish our friendship. I have also forged meaningful friendships with my fellow graduate students Loïc Caloren, Nancy Yang, Adam Ziada, Rachel Dunn, and Marie-Soleil Smith. Their ability to continuously raise the bar of excellence makes me excited for the future of the lab. The outstanding undergraduate students whom I have had the privilege of mentoring, including Mahtab Gill, Nicolas Gauthier, Zhuo Chen, Aya Zakaria, Parmeet Shokar, Brian Shim, Prakruti Uday, Rutuja Pattanshetti, Mayanne Zhu, Elana Kimmel, Aïda Retta, Omair Arshad, and David Deng have each taught me at least as much as I have taught them. Finally, all of us trainees have benefitted from two lab technicians Izabelle Gadawski and Beheroze Sattha, who consistently and selflessly donated their time and energy to our work because they sincerely cared about us.

Lastly, I would like to thank my family and friends. My mom and dad, Joanne Tseng and Paul Hsieh, have always loved me with their time and their sacrifice. From immigrating to Canada 24 years ago to never missing a single moment of my childhood, they are eternal advocates for my well-being and success. As adults, my sister Angela Hsieh and I have always been separated by an ocean or a continent, yet that distance does not diminish the strength of her support. My lifelong friends, Ravi Nath, Jonathan Chan, and Wyatt Jang have stood by me and have grounded me with a perspective outside of academia. Finally, my girlfriend Shawna Stanwood, who has walked beside me on her own journey through a PhD program, understood the challenges that I faced better than anyone and gave her all in helping me overcome them.

For my mom and dad

Chapter 1: Introduction

1.1 Decline of immune function with age

The goal of aging research is to provide people with the opportunity to live long and healthy lives. The main challenges facing this endeavour are the increasing risks of illness and disability with age. One approach to overcome these challenges is to further our understanding of the processes that occur with aging.

The global impact of aging research continues to rise, along with the expansion of the global population itself. In 1990, approximately 1 in 17 people around the world were over 65 years old. This became 1 in 11 in 2019 and is projected to become 1 in 6 by 2050 [1]. Not only does understanding the drivers of human aging benefit an increasing number of people, but it may also lower healthcare costs currently expended on the elderly, thereby benefiting society at large.

The deterioration of the immune system is a fundamental characteristic of human aging. This is most directly observed as the weakening of immune function with older age and is supported by data linking impaired immune function with age-related morbidities and mortality. Among the elderly, there are ample data illustrating the clinical consequences of age-related immune decline, including increased vulnerability to infections [2], reactivation of chronic viral infections [3,4], reduced responsiveness to vaccines [5,6], and persistent inflammation [7], as well as the increased occurrence of age-associated diseases such as cardiovascular disease [8,9], liver disease [10], kidney disease [11,12], osteoporosis [13], and various cancers [14]. Together, these outcomes are likely related

to the holistic deterioration of the immune system, a phenomenon known as immunosenescence [15].

Immunosenescence can be evaluated using markers of immune aging that change as people age. Over the past several decades, much progress has been made in identifying these markers and determining which of them most strongly predict age-related comorbidities and/or mortality. Although immune aging markers and the degree to which they are affected by aging are well-characterized [16–18], comparatively fewer studies evaluate the potential for these markers to predict age-related diseases or mortality. Importantly, some of these are markers of cellular aging that can be measured in a single cell or any group of cells, while others describe the population sizes of specific immune cell subsets. This distinction may reflect discrete mechanisms of biological aging that may have implications with respect to their clinical relevance.

1.2 Cellular aging

1.2.1 Telomeres and mitochondrial DNA

For reasons of bioaccessibility and cost, markers of cellular aging are largely investigated as average measurements in circulating blood cells rather than in specific cell subsets or lymphoid tissues. Two of the most ubiquitous markers of cellular age are telomere length (TL) and mitochondrial DNA (mtDNA) copy number.

Telomeres are nucleoprotein complexes that cap chromosomes and, in most cells, shorten with each division. Leukocyte telomere length (LTL) is associated with age [16], and the rate of LTL attrition is more rapid during childhood (100-1,000 bp/year) [19,20] than adulthood (20-100 bp/year) [21–23]. Biological variability in LTL is attributed to genetics [24,25], sex [26,27], ethnicity [28,29], and other determinants of health including diet [30–32], exercise [33,34], and substance use such as tobacco smoking [35–40] and illicit drugs [41]. Shorter TL in leukocytes or peripheral blood mononuclear cells (PBMCs) is also associated with HIV [42–47], diabetes [48–50], Alzheimer's disease [51–53], and certain cancers [54,55]. Among older individuals, shorter TL is particularly predictive of cardiovascular disease [56–58] and mortality [59–61].

Mitochondria harbor multiple copies of mtDNA per cell, which replicate independently from nuclear DNA. Changes in mtDNA quality or quantity as well as decline in mitochondrial function are implicated in biological aging [62] and are primarily linked to metabolic and mitochondrial disorders [63–67]. Similarities also exist between whole blood (WB) mtDNA content per cell and LTL, whereby many diseases or conditions associated with shorter LTL are also associated with differences in mtDNA content. For example, decreased mtDNA content in various tissues are associated with HIV [68–74], diabetes [75], Alzheimer's disease [76], various cancers [77,78], and cardiovascular disease [79]. Tobacco smoking is also associated with altered mtDNA content in lung and buccal cells, though reports are inconsistent [80,81]. Compared to LTL, which is consistently reported to decline with age, WB mtDNA content is not as robust a marker of aging, with studies reporting negative [62], positive [82], non-linear [83,84], or no relationships [85] between mtDNA content and age.

Several proposals have arisen connecting these two markers of cellular aging mechanistically. Short telomeres trigger activation of p53, which arrests cell growth and induces apoptosis [86,87]. Activated p53 also binds to and inhibits *PGC-1α* and *PGC-1β*, the promoters of mitochondrial growth as well as mtDNA replication [88]. Thus, short telomeres and mitochondrial dysfunction may be mechanistically linked through p53 activation, potentially resulting in a relationship between TL and mtDNA content. The second mechanism involves the relationship between mtDNA and telomerase, the enzyme responsible for maintaining telomeres. Reactive oxygen species (ROS), which are produced as a byproduct of mitochondrial metabolism, can damage mtDNA. When intracellular concentrations of ROS reach a certain level resulting in a cellular state of oxidative stress, telomerase is exported from the nucleus and transported to the mitochondria where it protects mtDNA against oxidative damage [89,90]. When this occurs, telomerase neglects its primary function of maintaining TL. Similar to the mechanism involving p53, this protective function of telomerase could result in a relationship between TL and mitochondrial health. Despite the fact that TL and mitochondrial health appear to be governed by shared mechanisms, the relationship between LTL and WB mtDNA content is unclear based on cross-sectional studies [91–95] and has not yet been investigated longitudinally.

Literature on the two markers, LTL and WB mtDNA content, is prolific as both measures are commonly used across many fields of aging research, and improvements in measurement techniques continue to be needed. In the case of TL, several measurement techniques exist, including terminal restriction fragment (TRF) length analysis by Southern blot, flow-fluorescence *in situ* hybridization (FISH) of telomere repeats, and quantitative polymerase chain reaction (qPCR), each of which has advantages and disadvantages [96]. TRF analysis is based on

quantifying telomeric DNA on an agarose gel by excluding genomic DNA using restriction digest [97]. Due to the nature of agarose gel quantification, a large amount (several µg) of DNA is required, and the procedure is laborious. TL measurements using FISH rely on quantification of fluorescently labelled peptide nucleic acid probes hybridized to telomeric DNA [98]. This technique is often applied using flow cytometry to quantify these probes and is able to measure the average TL of individual cells. However, like TRF analysis, a large amount of starting material is required, and the procedures are time-intensive. The only technique that is practical for large studies of many hundreds or thousands of biospecimens is qPCR, which involves measurements of PCR-amplified telomeric DNA using specially designed PCR primers specific to telomeric repeats [99]. This technique requires low starting material (ng or pg of DNA) and the procedure is relatively quick. An even more time-efficient iteration of this method, known as monochrome multiplex qPCR (MMqPCR), is the most suitable technique for high-throughput applications [100]. Regardless of measurement technique, an assay with low variance is often required to draw biologically or clinically meaningful conclusions with statistical significance given achievable sample sizes because the age-associated loss of these markers occurs relatively slowly. For example, LTL decline with age occurs on the order of 5% per decade for adults [21–23]. Consequently, assays with a coefficient of variation (CV) of 10% will produce LTL measurements within a range equivalent to a decade of chronological aging only 38% of the time, assuming a normal distribution in measurement error. Assays with 5% and 2.5% CVs will achieve the same result 68% and 95% of the time, respectively. Given that the loss of LTL as a result of HIV infection approximates that seen for a single decade of aging [42], adequately powered studies investigating the impact of HIV on LTL typically require large sample sizes. Because of this, each study presented in this dissertation involves hundreds of biospecimens and

MMqPCR was chosen as the most suitable measurement technique. By decreasing the cost of these measurement techniques, high-throughput data and adequately powered statistical analyses will become more accessible and ubiquitous. Similarly, reducing the technical complexity of these assays by incorporating the use of a commercially available qPCR reaction mix would reduce the barrier to entry. These concepts are addressed in two publications describing MMqPCR-based techniques for measuring TL [101] and mtDNA content [102]. The latter is included as chapter 2 of this thesis.

While both LTL and WB mtDNA content are considered markers of aging, LTL is the more robust predictor of age. However, even though LTL reliably declines with older age, inter-individual variability introduced by both genetics and the external environment is such that many 60-year-old people have longer LTL than many 20-year-old people in a healthy population. Thus, to increase the precision and interpretability of aging studies, additional variables are required in addition to LTL and WB mtDNA content to appropriately characterize aging of the immune system rather than aging of individual cells.

1.3 Immune aging

1.3.1 T cell subsets

Of the many immune markers that are modulated by age, alterations in the distribution of T cell subsets are among the most prominent. CD4 and CD8 T lymphocytes represent the two principal T cell subpopulations. The ratio of CD4:CD8 T cells decreases with age and predicts morbidity and mortality [103,104]. Changes in cell subset distribution also occur within the two compartments,

albeit at different magnitudes. For example, the skewing of CD8 T cells away from the less differentiated naïve phenotype and towards the most differentiated memory phenotype is foremost among signs of immune aging [18,105]. In contrast, while a similar development in differentiation markers occurs in the CD4 compartment, their progression is much slower [106]. These changes are largely governed by two age-associated mechanisms: decline in thymic production and cumulative replication burden.

The most prominent phenotypic change with age is seen in the CD8 T cell population. Because thymic output disproportionately replenishes the CD4 compartment [107,108], the driving force behind CD8 T cell differentiation is more likely lifetime exposure to immune challenges that repeatedly compel T cell activation and proliferation. As the immune system experiences recurring immune challenges, the CD8 T cell compartment undergoes differentiation and repeated activation, increasing the proportion of highly differentiated cells [109]. The consequences of this process are highlighted among the elderly, whose extended accumulated history of immune stimuli leads to immunosenescence and eventually compromised immunity. This concept was elegantly demonstrated by an *in vitro* study demonstrating weakening T cell activation with repeated antigenic stimulation as measured by spikes of telomerase activity [110].

Repeated T cell activation and proliferation also prompt telomere shortening at the cellular level, and critically short telomeres lead to either cellular apoptosis or senescence [111]. The mechanism that determines whether a cell becomes apoptotic or senescent remains unclear [112,113], but it follows that as the highly differentiated T cell population accumulates with age, a subpopulation of senescent cells also accrues. Senescent T cells lack the CD28 costimulatory molecule [114],

secrete pro-inflammatory molecules [115], are resistant to apoptosis [116], and typically do not regain proliferative capacity [117]. Moreover, senescent cells have both cytotoxic [117] and suppressive [118] properties and may be predictive of morbidity and mortality in the elderly [17]. It is worth noting that the senescent T cell phenotype is distinct from the exhausted T cell phenotype. Unlike senescent cells, exhausted cells typically arise from chronic viral infection and express different markers such as programmed cell death protein-1 (PD-1) and immunoglobulin mucin-3 (Tim-3) [119]. In short, markers of senescent and exhausted T cells describe distinct phenotypes, and the accumulation of both cell types contributes to the general immunosenescence phenotype.

1.3.2 Regulatory T cells

The model for age-related decline in immune function continues to grow in complexity. For example, the decline of immune function with age is also partially attributed to immune suppression, specifically through the activity of a small subpopulation of CD4-expressing regulatory T cells (T_{regs}) with immunosuppressive properties [120]. T_{regs} primarily inhibit activation and proliferation of both CD4 and CD8 T cells [121], especially those with differentiated effector phenotypes [122]. The primary function of the T_{reg} population is to prevent immune hyperactivation. T_{regs} are implicated in autoimmune disorders [123–126] and appear to activate during infection, resulting in suppressed immune responses [127]. Importantly, ample data exist showing that the size of the T_{reg} population increases with age [122,128–130] with greater immunosuppressive activity per cell than their younger counterparts [129–131]. It is likely that these changes to the T_{reg} compartment contribute to age-related immune decline, however the exact mechanism is unclear.

1.3.3 B cells

B cell immunity also deteriorates with age, which translates notably into reduced response to influenza vaccines among the elderly [132,133]. Similar to aging in the T cell population, differentiation markers within the B cell population appear to be modulated by age [134–136]. However, these changes are less consistent compared to the age-related changes in the T cell compartment, making them less suitable as markers of immune aging. Instead, the changes to the B cell population can be more clearly assessed functionally. Older age is accompanied by a reduced capacity to respond to new antigenic challenge [137,138], reduced repertoire diversity [139,140], decreased antibody production via a reduction in capacity for class switch recombination [141], as well as an accumulation of a senescent and pro-inflammatory subpopulation [142]. These changes are thought to weaken B cell function, contributing to reduced vaccine response among the elderly, though this has not been directly linked mechanistically.

Because aging is ubiquitous, it is a unique challenge to study human aging using methods typically employed in studies of disease - that is, comparing a group of participants afflicted with the disease with a group of unaffected controls. However, a possible approach is to compare groups of individuals who are affected or not by a disease known to accelerate human aging. As such, this thesis uses HIV infection as a human model of immune aging.

1.4 HIV epidemiology and combination antiretroviral therapy (cART)

As of the end of 2018, an estimated 37.9 million people are living with HIV worldwide [143]. Of these, 95.5% are adults and 64.6% have access to antiretroviral therapy. During 2018, 1.7 million people were newly infected with HIV and over 700,000 died from AIDS-related disease.

Without treatment, HIV infection begins with an acute phase lasting a few weeks to several months [144], during which the quantity of viral copies in the blood, commonly termed plasma viral load (pVL), increases suddenly and considerably. During the acute phase, virus-related mechanisms cause the CD4 T cell count to drop, and immune responses cause the CD8 T cell population to expand. A chronic phase follows, leading to years of asymptomatic disease, during which pVL decreases and reaches a relatively stable set point. Similarly, CD4 T cell count recovers partially, then slowly declines over time, while CD8 T cell count decreases and remains relatively stable. After several years, CD4 T cell attrition reaches a threshold where immunity is lost, leading to opportunistic infections, AIDS, and eventually death [145]. The severity of the acute phase, as well as the rate of disease progression during the chronic phase, varies between individuals. At one end of this distribution exists a small population of people in whom HIV disease progression occurs so slowly that they are given a separate classification as slow progressors (SPs). The SP population will be investigated as a potential protective model against HIV-mediated accelerated immune aging and will be described later in this chapter.

HIV is a lifelong infection, and there is no cure. However, combination antiretroviral therapy (cART) successfully extends the lifespan of people living with HIV (PLWH) by inhibiting HIV replication and preventing AIDS. Current guidelines from the World Health Organization (WHO) recommend treating PLWH as soon as possible, regardless of disease progression [146]. However, previous recommendations for cART initiation depended on a combination of CD4 T cell count, comorbidities, coinfections, and/or other factors such as pregnancy [147]. These previous recommendations, along with reduced access to cART in certain regions, mean that not

all treated PLWH were on cART during the acute phase of infection. The course of HIV disease progression and the effect of cART are illustrated in **Figure 1.1**.

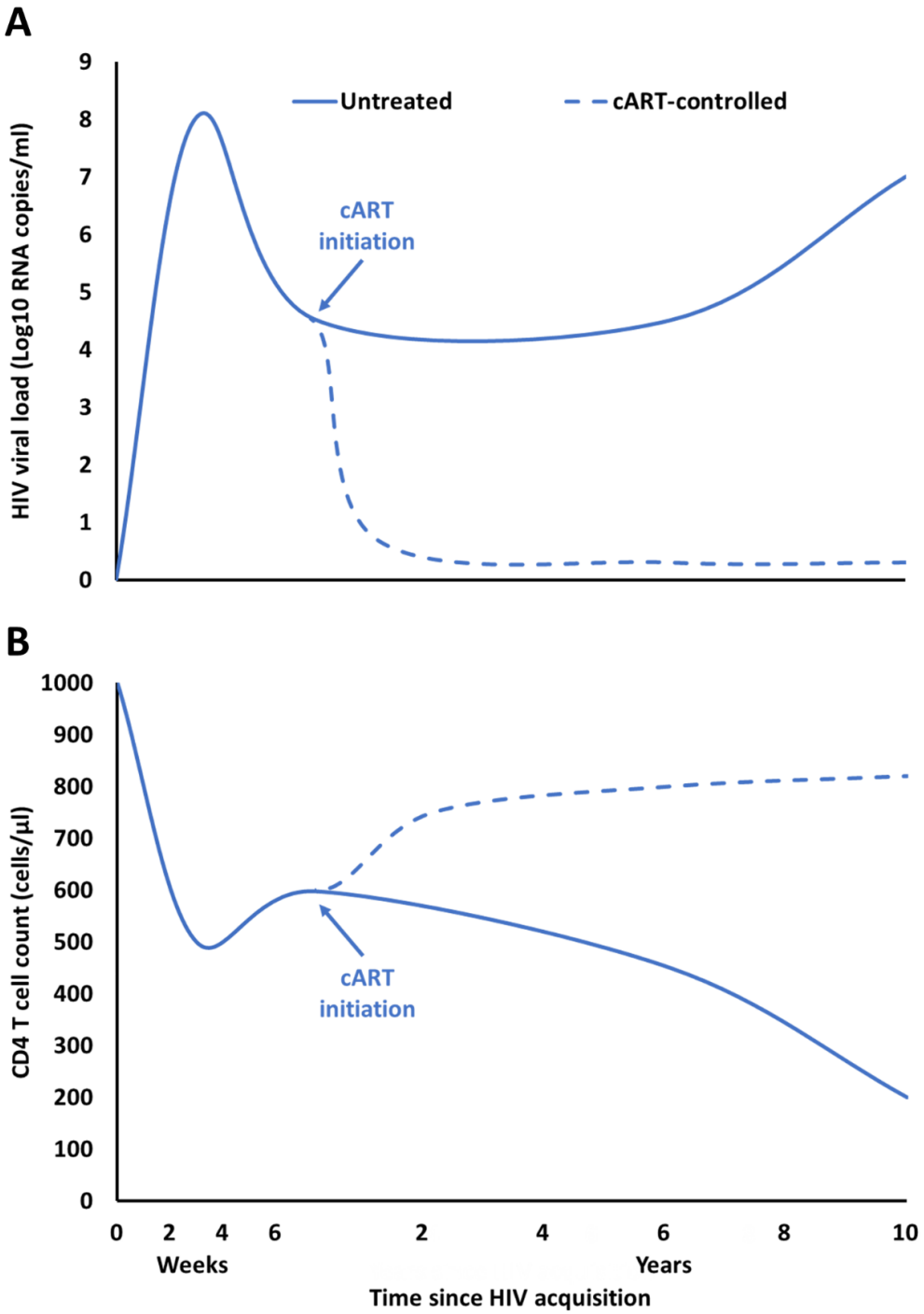

Figure 1.1 Schematic of disease progression in PLWH with and without cART.
HIV viral control and immunodeficiency as measured by viral load and CD4 count among PLWH with and without cART. In PLWH on cART, treatment initiation is assumed to occur between the acute and chronic phases.

Treatment with cART takes the form of a combination of 3 or 4 antiretroviral drugs belonging to at least 2 drug classes. Each drug class targets and inhibits a different portion of the HIV replication cycle. For example, nucleoside reverse transcriptase inhibitors (NRTIs) are nucleoside analogues that, once phosphorylated intracellularly, are incorporated into elongating DNA where they terminate reverse transcription of the viral RNA. Similarly, protease inhibitors (PIs) are substrate analogues that block HIV protease from cleaving HIV polyproteins into mature viral proteins. Some drug combinations, such as those that include the newer integrase strand-transfer inhibitors (INSTIs) that prevent HIV DNA integration into the human genome, are able to achieve viral suppression faster than older combinations [148,149].

In the context of immune aging, certain cART drugs are known to affect TL and mtDNA content. For example, NRTIs can lead to both shorter TL [150,151] and mtDNA content depletion [152,153] *in vitro*. However, it is an ongoing challenge to disentangle the effects of cART and HIV on markers of immune aging because long-term cART is not given to people who are uninfected and untreated HIV itself affects both markers. More granular analysis of immune studies with large sample sizes is needed to isolate the effect of specific drug combinations in order to further understand the relative impact of cART and HIV on immune aging.

The rising age of the global population has begun to intersect and compound the age-related burdens of PLWH. In every region of the world, the proportion of PLWH over 50 years old continues to increase and this proportion was estimated to approach 50% by 2020 in Europe and North America [154]. As such, studying the effect of HIV on accelerated aging may not only

deepen our understanding of biological aging in general, but may also provide much needed insight on the vulnerable population of elderly PLWH.

1.5 HIV and age-related comorbidities

Despite the effectiveness of cART over the past 25 years, it is evident that PLWH, even those successfully treated with cART, are at higher risk of morbidity and mortality compared to the general population and that the risk increases with time following seroconversion [155,156]. People living with cART-controlled HIV are also still at higher risk for early-onset age-related comorbidities including cardiovascular disease [157–159], liver disease [160], kidney disease [160,161], osteoporosis [162,163], and non-AIDS-defining cancers [164]. In search of a cause that is still not yet fully understood, many studies have demonstrated immune abnormalities in PLWH that are similar to those seen in older people, such as reduced response to vaccines [165], less effective specialized B cell responses [166,167], increased risk of autoimmune diseases [168,169], persistently elevated inflammation [170,171], shorter TL in peripheral blood cells [42–47], and altered WB mtDNA content [68–74]. It is believed that HIV-mediated chronic immunologic stresses such as persistently elevated inflammation and immune activation are connected to this apparent accelerated aging phenotype [172–175].

Although there is a growing body of literature linking aging and HIV to either shorter LTL or altered WB mtDNA content individually, there is a paucity of research considering the two markers together and describing the relationship between the two, especially longitudinally. A study addressing this gap in knowledge is described in chapter 3.

Lastly, the accelerated aging phenotype seen in PLWH, including in those whose viremia is controlled by cART, should not be mixed with observations from the pre-cART era that describe the related but far more destructive effects of untreated and progressing HIV disease on immune aging. As such, an effort is made in this thesis to delineate the effect of HIV in the pre- and post-cART eras, with a focus on the latter as a human model of immune aging.

1.6 HIV and immune aging

1.6.1 CD4:CD8 T cell ratio

HIV is associated with shorter LTL and altered WB mtDNA content, but relatively little data exist describing the impact of HIV on these markers in specific lymphocyte subsets. Several studies from the pre-cART era have reported shorter TL in CD8 T cells [176,177] as well as in the subpopulation of senescent CD8+CD28- T cells [178]. Since the widespread use of cART, virtually no studies have investigated the impact of cART-controlled HIV on lymphocyte subset TL. One group showed a decrease in CD4 naïve T cell TL in PLWH within 1-3 years of HIV infection [179]. However, no data exist describing immune subset-specific TL or mtDNA content in people who have lived with chronic cART-controlled HIV for many years compared to HIV-negative controls.

In lieu of data on cellular aging markers within PBMC subsets, previous research has primarily characterized HIV-mediated immune aging by measuring changes in the proportion of PBMC subsets that bear similarities with the changes that occur during biological aging. Most notably, the well-characterized decline of CD4:CD8 T cell ratio seen in HIV infection remains one of the

most reliable markers of HIV-mediated immunopathology and HIV disease progression [180]. Specifically, CD4:CD8 ratio does not fully recover even after successful cART, and people living with cART-controlled HIV with a low CD4:CD8 ratio are at increased risk for non-AIDS comorbidities [181,182]. This is attributed to several mechanisms involving either CD4 T cell depletion or CD8 T cell expansion.

1.6.2 CD4 T cell depletion and CD8 T cell proliferation

Depletion of CD4 T cells is a hallmark of HIV infection and prevents effective immune response against the virus and eventually other pathogens. This is accomplished through several mechanisms including HIV-induced suppression of thymic proliferation [183], sequestration of CD4 T cells to lymph nodes [184], and CD4 T cell death. During acute infection, HIV replicates within and directly kills activated CD4 T cells, leading to an immediate drop in CD4 T cell count [185]. However, the rate of CD4 T cell depletion following the acute phase of infection is not consistent with the relatively low proportion of HIV-infected CD4 T cells. The majority of CD4 T cell death in HIV infection occurs via apoptosis in bystander cells that are not productively infected by HIV [186]. More recent evidence shows that >95% of these bystander CD4 T cells undergo a pro-inflammatory variant of programmed cell death known as pyroptosis [187]. This model of HIV-mediated CD4 T cell depletion provides a new perspective on the role of HIV-associated chronic inflammation and HIV disease progression, whereby CD4 T cell death through pyroptosis releases pro-inflammatory molecules that lead to further CD4 T cell death, in a positive feedback loop that occurs primarily in lymphoid tissue rather than circulating blood. CD4 T cell count recovers after cART but is not completely normalized, even after many years

of virologic suppression, especially in circumstances in which pre-cART baseline CD4 T cell count is low [188,189].

HIV infection is also associated with increased numbers of CD8 T cells, both in progressing disease [190] and after effective cART [191]. The expansion of the CD8 T cell compartment occurs quickly following initial infection, as virus-specific CD8 T cells proliferate in an attempt to control the primary infection [192,193]. However, following successful long-term treatment with cART, CD8 T cell count remains elevated in PLWH [194,195], especially if cART initiation occurs after the acute phase of infection [196]. Although CD4 count is the primary clinical measure of HIV disease progression, and indirectly HIV control, elevated CD8 T cell count after long-term cART is associated with non-AIDS mortality [197].

1.6.3 T cell differentiation

There is growing evidence that both the CD4 and CD8 T cell compartments are proportionately more differentiated among PLWH. In the CD4 T cell compartment, naïve cell subsets are reduced and memory cell subsets are expanded relative to total CD4 T cells [179,198]. This is primarily demonstrated in people living with progressing HIV disease, but is also observed in people who have lived with cART-controlled HIV for many years [199]. The impact of HIV on CD4 T cell maturation is dwarfed in magnitude compared to its effect on CD8 T cell subsets. The reduction of the naïve CD8 T cell population in people with progressing HIV disease is considerably more aggressive than that of the CD4 T cell compartment [198]. Moreover, PLWH also have expanded and highly differentiated CD8 T cell populations that are senescent or exhausted, likely caused by persistent immune stimulation and replication due to HIV infection

[200]. The senescent CD8 T cell population lacks CD28 expression and are incapable of proliferation upon activation [201]. This population is of particular interest because of its shorter TL in HIV [178] and the fact that the accumulation of these cells itself weakens immune responses [118]. HIV infection is associated with expanded senescent T cell populations in both cART-naïve [202] and cART-controlled [203] participants. Similarly, exhausted CD8 T cell populations in PLWH have severely limited proliferative capacity and express inhibitory receptors, including PD-1 [204,205] or Tim-3 [206]. Consequently, while CD8 T cells in PLWH outnumber those in the general population, their function is compromised by the accumulation of senescent and exhausted cells. Long-term treatment with cART also seems to have only limited success in altering the proportions of CD8 T cells at varying stages of maturation [194,195,207] regardless of time of cART initiation [208]. Importantly, the comparatively more aggressive effect of HIV on the differentiation of CD8 T cells compared to CD4 T cells is reminiscent of biological aging, as described earlier.

1.6.4 Regulatory T cells

Accelerated T cell differentiation may be the most obvious sign of accelerated immune aging among PLWH. However, HIV infection also disrupts two smaller lymphocyte populations that may also contribute to the accelerated aging phenotype: T_{regs} and B cells. Understanding the relationship between HIV infection and the immunosuppressive T_{reg} population has been marred by inconsistent classification of the T_{reg} phenotype, even with the wealth of data that exists. Several conflicting studies show the T_{reg} population in HIV infection to be either increased [209–215] or decreased [216–221]. Other reports in PLWH describe increased T_{reg} populations in lymphoid tissues and decreased T_{reg} populations in peripheral blood [222,223], or the opposite [210]. Others also

demonstrate treatment with cART normalizing T_{reg} populations [209,215,221] or cART having no effect [213,214]. However, it is clear that HIV compromises T_{reg} activity by directly infecting them and reducing their immunosuppressive activity, thereby destabilizing the homeostasis between T_{regs} and other activated T cells [224,225]. The relationship between HIV and the T_{reg} population is nuanced and, despite the number of studies that have been conducted, remains poorly understood, especially in the post-cART era. More data on T_{reg} population size and function in cART-treated individuals may alleviate this, but studies integrating other measures of immune competence and aging may be critical in meaningfully evolving our understanding of this relationship.

1.6.5 B cells

HIV infection also affects both the size and function of the B cell compartment. B cell abnormalities are observed in PLWH including maturation of differentiation phenotypes [226], as well as the accumulation of a senescent population [227], reminiscent of what is seen with chronological aging. Moreover, B cells in PLWH appear to be hyperactivated [228], yet their immune responses less effective [166,167] compared to HIV-negative controls. These abnormalities are linked to compromised antibody production and reduced response to vaccines [229,230], which may contribute to the accelerated immune aging phenotype among PLWH. Furthermore, cART only seems to partially recover skewed B cell subpopulations [231–233] as well as vaccine response [234].

1.6.6 The effect of PBMC distributions on LTL

Lastly, the impact of HIV infection on modulating the sizes and maturation of various PBMC subsets, especially the larger T cell populations, is likely to contribute to its effect on LTL. There is evidence that WB cell subsets intrinsically have different TL [235]. As expected, more differentiated T cells have shorter TL [200,236], and it appears that lymphocytes have longer TL than neutrophils [237]. Because of this, changes in neutrophil-lymphocyte ratio, as well as redistribution of PBMC subsets due to HIV infection or otherwise, would alter LTL. Therefore, HIV-mediated changes in LTL can be the result of either cell subset redistribution or cellular aging as measured by shorter TL in specific immune cell subsets, or both. It is unclear what the relative contributions of these different mechanisms are to shorter LTL in PLWH. It has been proposed that while LTL may provide an indication of immunocompetence, TL within relevant PBMC subsets is a more accurate marker of immune aging [238].

1.7 HIV and CMV coinfection

In PLWH, expansion of CD8 T cell memory populations appears to be driven by activation and proliferation of both HIV-specific and non-HIV-specific cells [200]. For example, in PLWH who are coinfected with other chronic viruses such as cytomegalovirus (CMV), Epstein-Barr virus (EBV), and influenza, CD8 T cell populations specific to these viruses are expanded during HIV primary infection [239], even though the composition of differentiated cells varies in each virus-specific population [240]. In particular, CMV coinfection is an important variable when considering chronic HIV infection as a human model of biological aging. As of 2016, an estimated 83% of the global population lives with CMV [241], with an even higher prevalence among PLWH [242,243]. CMV infection alone has a considerable effect on accelerating immune

aging and is associated with an immune phenotype linked to greater risk of mortality among the elderly [103] as well as signs of immunosenescence among young adults [244]. CMV infection is also associated with frailty [245], cardiovascular disease, and all-cause mortality [246,247].

Despite the fact that immune consequences of both HIV and CMV infection bear similarities with biological aging, the two viruses exert different effects on CD8 T cell differentiation. While HIV-specific CD8 T cells proliferate in response to infection, this population rapidly deteriorates upon cART initiation [248,249]. In contrast, the population of CMV-specific CD8 T cells continues to expand, occupying a continuously increasing proportion of the total memory CD8 T cell population in a progression known as "memory inflation" [250,251]. Furthermore, CMV-specific CD8 T cells are more differentiated, have shorter TL, and are more similar with age-associated senescent populations than their HIV-specific counterparts [252–254], although both populations lack expression of CD28. It is also worth noting that even though CMV infection is associated with shorter TL among T cells [255], its effect on LTL is less clear, with a study showing decreased LTL with CMV infection [256] and another showing no effect [257].

Regardless of the differences in immune aging between HIV and CMV infection and their relative impact, it appears that the consequences of coinfections are cumulative. Compared to PLWH who are CMV-negative, people living with cART-controlled HIV who are coinfected with CMV have increased CD8 T cell counts, expanded senescent CD8 T cell populations, decreased CD4:CD8 ratios, increased inflammation, as well as a persistently larger population of CMV-specific cells [258–260]. The pronounced effect of CMV in PLWH is consistent with a small randomized controlled trial of PLWH coinfected with CMV, in which those treated with the

antiviral medication valganciclovir had significantly reduced T cell activation compared to the untreated group [261]. Moreover, in a mixed population of people living with cART-controlled or uncontrolled HIV, those coinfected with CMV are considerably more likely to experience more severe non-AIDS comorbidities, especially cardiovascular and cerebrovascular diseases, compared to PLWH who are CMV seronegative [262]. PLWH who have detectable CMV viremia are also at higher risk of mortality [263]. Among a more homogenous population of people living with cART-controlled HIV, a link between CMV antibody titers and subclinical cardiovascular disease remains [264]. CMV appears to have the largest effect on immune aging among coinfections that commonly occur in PLWH, and it may be representative of a cumulative exacerbation of immune burden of coinfections with other chronic viruses such as hepatitis C virus (HCV) and hepatitis B virus (HBV), or other herpes viruses including EBV, Herpes simplex viruses 1 and 2 (HSV-1 and HSV-2), as well as Varicella zoster virus (VZV). More research is needed to determine whether the accumulation of chronic/latent viral infections is associated with a corresponding progressive deterioration of the immune system.

1.8 HIV slow progressors

1.8.1 Prevalence and subgroups

In consideration of HIV infection as a human model of immune aging, it would be useful to study PLWH who appear to have a natural defense against the virus, or at least a resistance against the typical rate of disease progression. These SPs can control HIV and impede disease progression in the absence of cART with varying degrees of success. Among PLWH, estimates of SP prevalence range from 0.3% to 25% [265–269]. More recent estimates are on the lower end of

that spectrum [270–273] likely because the threshold for cART initiation has become more stringent with time, leading to earlier cART initiation and a greater chance that a person would have begun treatment prior to being identified as an SP. The wide variance in prevalence estimates is at least in part the result of a lack of consensus in defining the SP population, which itself reflects the heterogeneity of this population in terms of the effectiveness of their natural defense against HIV infection.

This heterogeneity has also led to the subcategorization of the SP population, although the number of subgroups, their subgroup names, and their defining characteristics also fluctuate. All SP definitions share the common attribute of resistance to HIV disease progression in the absence of cART. Beyond this, subcategorization is based on the level of viral control as measured by HIV pVL, immune integrity as measured by CD4 count, and/or duration of HIV infection without progression to AIDS while cART-naïve. Those with the highest level of natural HIV control are known as elite controllers. Elite controllers are the rarest subgroup of SPs, comprising of <0.5% of PLWH [270,274] who can maintain undetectable HIV pVL. However, this is a moving target, as detection limits of assays measuring viremia improve over time. In fact, modern assays with a limit of detection approximately 100-fold lower than previous methods reveal that the majority of elite controllers have very low level viremia [275], which appears to be higher than that of cART-controlled PLWH [276]. Virologic controllers are another subgroup who can maintain a detectable but low HIV pVL, typically <2,000 or <3,000 copies/ml. Most published studies required elite and/or virologic controller classifications to also include a minimum duration of infection of typically 7 to 10 years [266–268,270,272–274], while others used a less stringent minimum duration of 2 years or less [271,276,277]. Lastly, non-virologic

controllers have higher HIV pVL than virologic controllers, the former describing PLWH who have the least control over viremia, yet do not progress to AIDS. This subgroup is typically distinguished from progressors by a minimum duration of infection of typically 7 to 10 years, a threshold guided by the average time of progression to AIDS and resembling the criteria used in many elite and virologic controller definitions. For all SP subgroups, many studies require the maintenance of immune competence as measured by a minimum CD4 count [265–267,270,272,273], which can range from 200-500 cells/mm^3, but this requirement is not consistently implemented [274,276,277]. In summary, while there are common trends among SP subgroup definitions, there is no consensus on the quantitative characteristics that define each subgroup, and many previous studies exploring the immune differences between SP subgroups do not describe exactly the same populations. **Figure 1.2** describes the prevalence of SPs and elite controllers relative to the entire populations of PLWH and PLWH on cART, and **Figure 1.3** describes HIV disease progression in the same four populations.

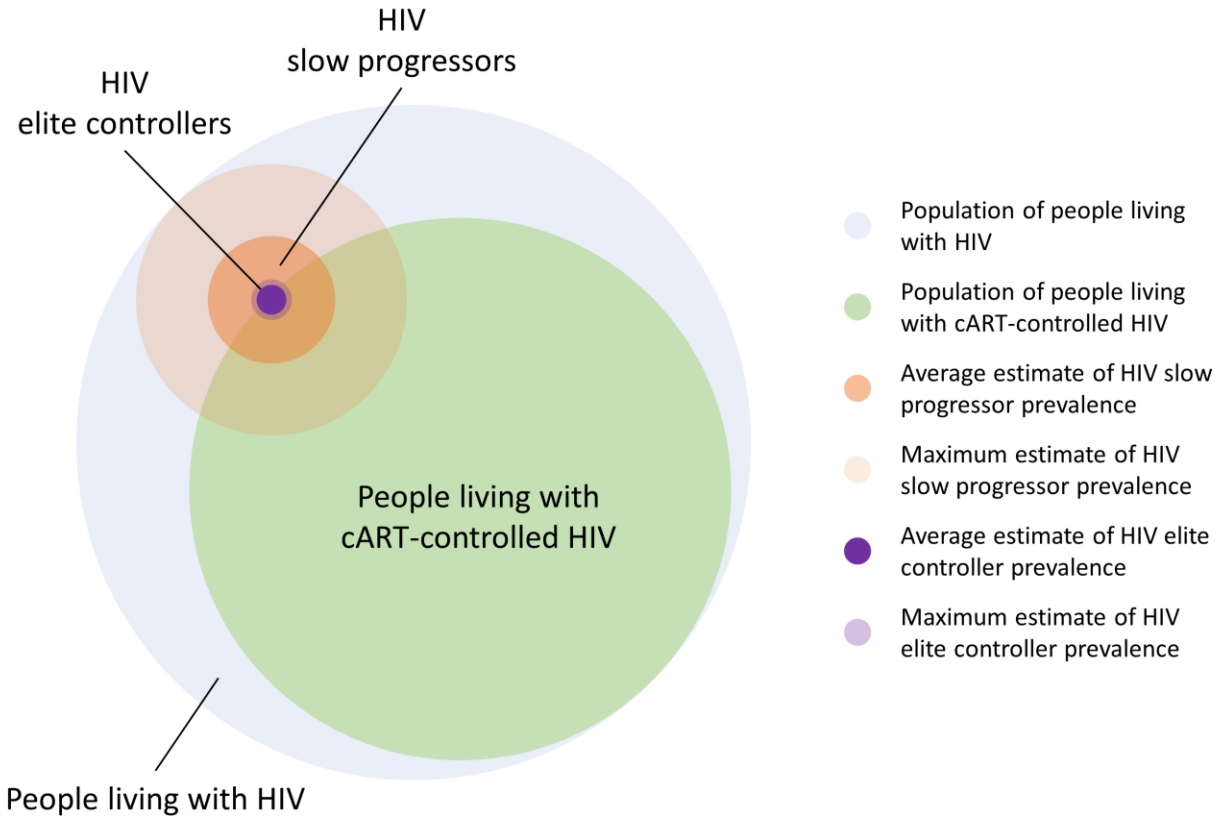

Figure 1.2 Prevalence of SPs and elite controllers.
Prevalence of SPs and elite controllers are shown relative to the population of PLWH using the sizes of the circles. The populations of PLWH with and without cART are shown in the green and blue circles, respectively. The prevalence of SPs and elite controllers among PLWH are shown as the orange and purple circles. Average and maximum prevalence estimates are shown for SP and elite controller populations as darker and lighter orange and purple circles. The overlap between people living with cART-controlled HIV and SPs/elite controllers demonstrate that a proportion of SPs/elite controllers may not be identified as such if they are on cART.

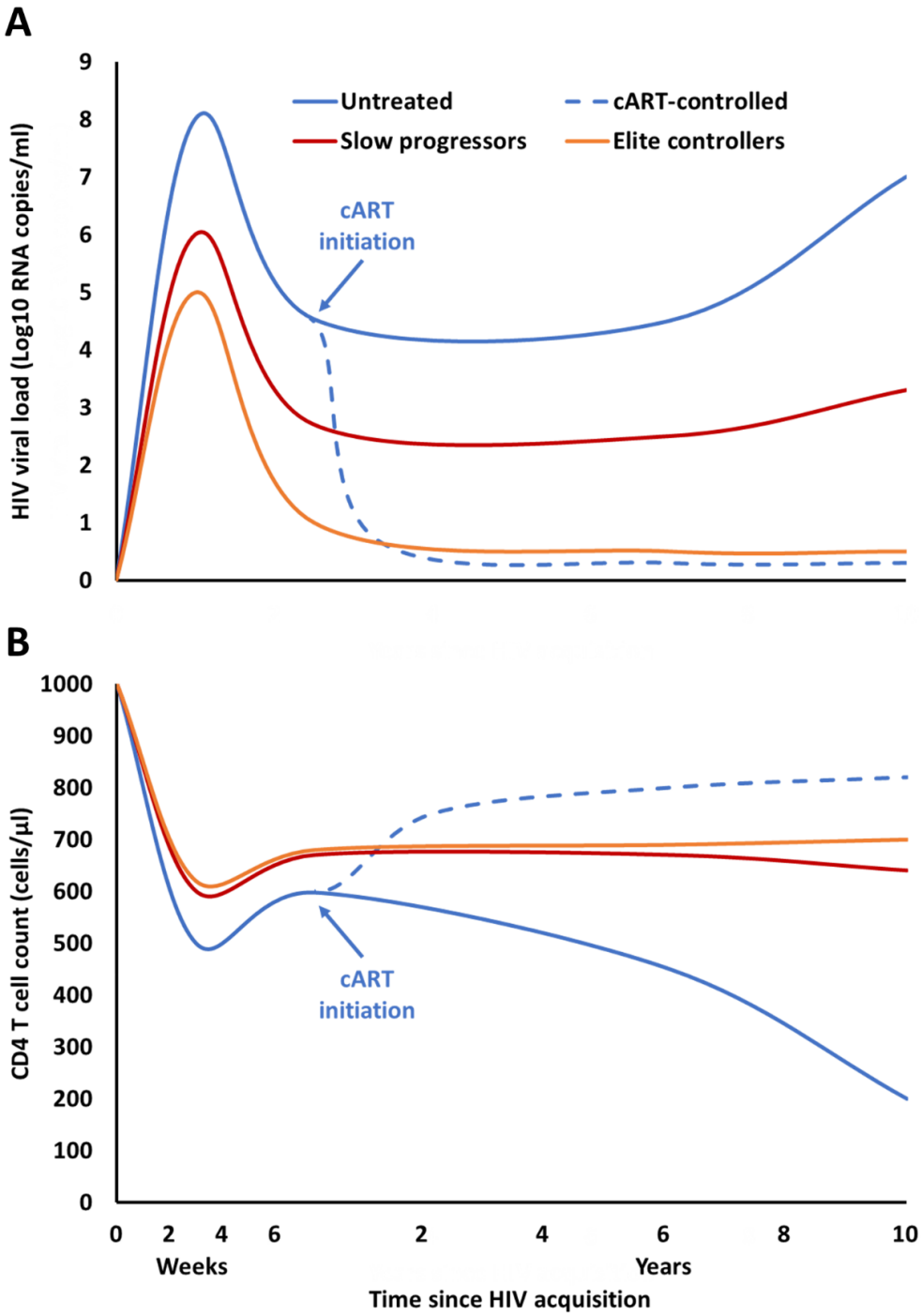

Figure 1.3 Schematic of disease progression in PLWH with and without cART, including SPs and elite controllers.
HIV viral control and immunodeficiency as measured by viral load and CD4 count among PLWH with and without cART, including SPs and elite controllers. In PLWH on cART, treatment initiation is assumed to occur between the acute and chronic phases.

1.8.2 Putative mechanisms

The source of the natural protection against HIV among SPs remains a mystery, with no unifying characteristics among this heterogeneous population. Of note, two genetic traits are overrepresented among SPs: a 32 base pair deletion in the C-C motif chemokine receptor 5 gene known as *CCR5Δ32* and the human leukocyte antigen (HLA) class I allele *HLA-B57*. *CCR5* encodes a coreceptor that certain variants of HIV require for entry into CD4 T cells, and *CCR5Δ32* encodes a truncated receptor that prevents HIV entry and infection [278]. As such, people with homozygous *CCR5Δ32* alleles are highly resistant to infection of these variants [279,280], and heterozygous *CCR5Δ32* is associated with slow disease progression [281–283]. The prevalence of individuals with *CCR5Δ32* alleles is more than twice as high in SPs compared to progressors [281,284]. HLAs are a class of molecules that, in the context of HIV, present viral antigens to CD8 T cells, allowing those cells to identify and kill infected cells. The *HLA-B57* allele is associated with slow progression with prevalence estimates up to ten times higher among SPs than progressors [274,277,285,286]. The mechanism by which *HLA-B57* confers protection against HIV is unclear, but there is some evidence suggesting that CD8 T cells specific to HIV antigens presented by *HLA-B57* have greater proliferative capacity [287] and resistance to T_{reg} suppression [288] compared to other CD8 T cells. Although *CCR5Δ32* and *HLA-B57* represent two genetic markers that confer the most protection against HIV, many SPs do not possess either allele. Furthermore, many other alleles, including other HLA alleles, have higher representation among the SP population [289].

Slow progression can also be partially attributed to infection with strains of HIV that are less virulent. For example, certain deletions in the HIV *nef* gene have been associated with slow

progression [290,291], and viruses isolated from SPs occasionally have reduced replicative capacity [292–294]. However, replication-competent HIV has also been isolated from elite controllers [295], suggesting that even PLWH with the highest level of natural viral control can do so independent of strain-specific characteristics.

In 2015, the WHO recommended cART in all PLWH regardless of CD4 count when it became evident that early treatment initiation results in better clinical outcomes [146]. Prior to this, cART was initiated based on disease progression as indicated by CD4 count, which led to SPs often being left untreated for many years. Therefore, the window of opportunity to study SPs in the context of HIV-mediated accelerated immune aging is closing. It is unknown whether the SP ability to control HIV also confers protection against HIV-mediated immune aging, and one of the primary goals of this thesis is to ascertain whether this natural defense is associated with a more favourable immune aging profile compared to people living with uncontrolled and/or cART-controlled HIV.

1.8.3 Immune aging

Little is known about immune aging in SPs, though poorer non-AIDS health outcomes have been seen among SPs compared to cART-controlled PLWH. According to one study that collected data from multiple sites across the United States, rate of hospitalizations among elite controllers appeared to be higher than among people living with cART-controlled HIV, especially hospitalizations related to cardiovascular disease [296].

Among SPs, PBMC TL appears to be shorter than that of HIV-negative controls and comparable to that of progressors [297]. However, TL measurements in the CD8 T cell compartment are comparable between SPs and HIV-negative controls, which are themselves longer than those of progressors [298]. Furthermore, among HIV-specific CD8 T cells, SPs have longer TL as well as higher telomerase activity compared to uncontrolled progressors (UPs) [299]. Consistent with the above TL studies, a previous study showed that SPs have younger CD8 T cell distributions, with more naïve CD8 T cells and fewer senescent CD8 T cells compared to progressors [300]. The opposite is true when comparing SPs with HIV-negative controls, who have an even less differentiated CD8 T cell population. Taken together, these studies suggest that the CD8 T cell compartments of SPs are protected against immune aging, although this protection does not extend to the entire PBMC compartment. The lack of comparison to cART-controlled PLWH in these studies limits the interpretability of this result and its impact in the post-cART era. Importantly, it remains unknown whether SP status is superior to cART in the context of protection against HIV-mediated immune aging. **Figure 1.4** illustrates CD8 T cell differentiation with age in untreated and treated PLWH as well as the HIV-negative general population, while describing the putative protective effect of SP and elite controller status.

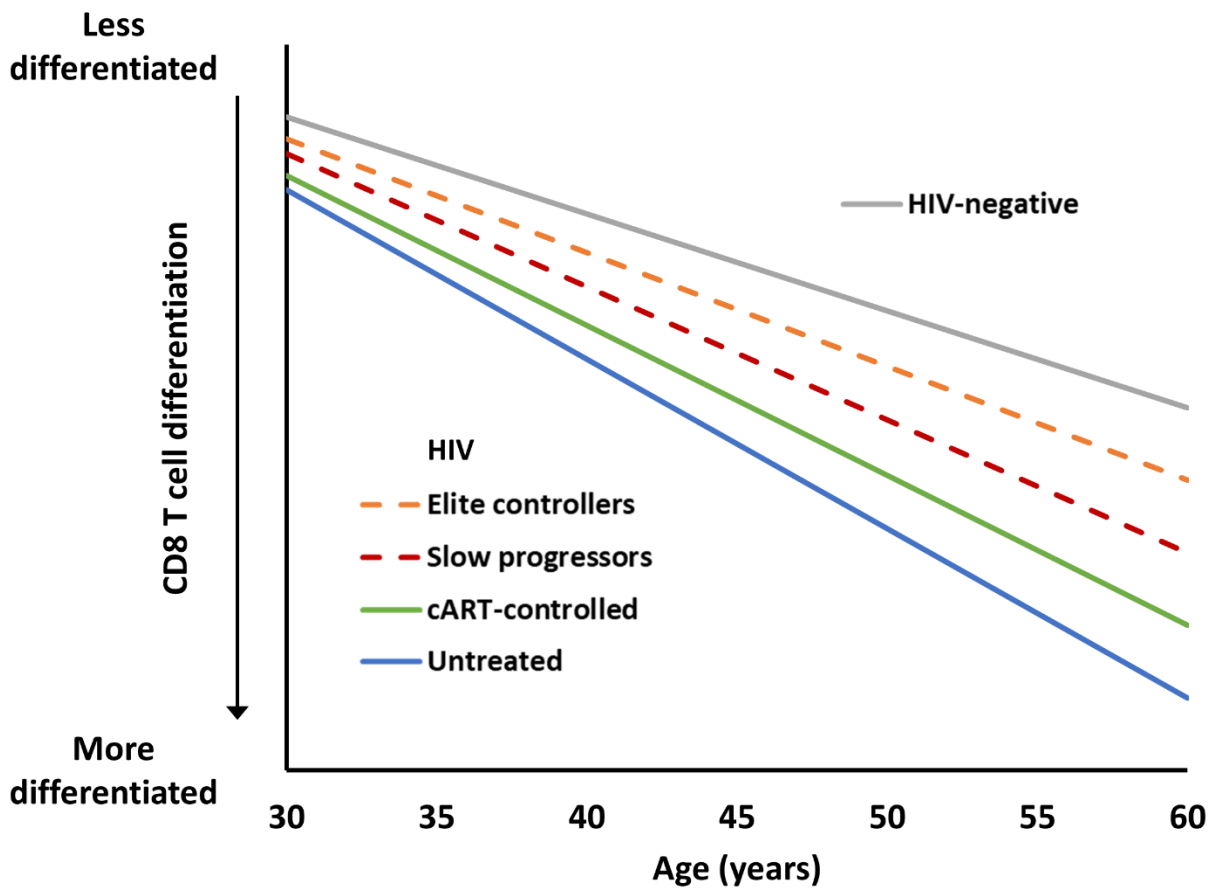

Figure 1.4 Schematic of CD8 T cell differentiation with age.
CD8 T cell differentiation declines with age in the HIV-negative general population. This effect is exacerbated in PLWH and is only partially mitigated by cART. The putative effect of SP and elite controller status is also indicated by dashed lines. In this schematic, SP and elite controller status is assumed to mitigate CD8 T cell differentiation with age, and HIV acquisition is assumed to occur prior to 30 years of age.

Differences in immune aging markers between SPs and cART-controlled PLWH are not well-characterized. One study showed that HIV elite controllers have higher levels of T cell activation compared to both cART-controlled PLWH and HIV-negative controls [301]. Aging markers were not assessed, though it is possible that the HIV elite controllers maintained abnormal T cell activation as a consequence of naturally controlling HIV replication. Furthermore, in the same study, higher T cell activation was associated with lower CD4 T cell count, even among elite controllers, leading the authors to suggest that T cell activation is a better indicator of disease progression than HIV replication.

Despite the growing body of literature supporting HIV-mediated accelerated immune aging, even among people successfully treated with cART, several key questions remain. It is unclear to what extent T cell subset aging is affected by cART-controlled HIV infection relative to progressors. In addition, it remains unclear to what extent HIV SPs are protected against HIV-mediated immune aging overall. If SPs show signs of alleviated immune aging compared to UPs or even cART-controlled PLWH, then investigating immunity in this unique population may benefit aging research in the general population. Whereas cART-controlled PLWH may be a human model of immune aging, SPs may be a protective model against it. Conversely, if HIV SPs show signs of accelerated immune aging compared to cART-controlled PLWH, then this population may be an example of antagonistic pleiotropy [302], in which mechanisms that serve a protective role in the present may become detrimental in the future. To date, no sufficiently powered study has compared immune aging in SPs to cART-controlled PLWH, especially with more granular assessments of immune aging such as measuring TL within relevant immune subsets. To address this, an in-depth investigation into immune aging markers in SPs, cART-

controlled PLWH, UPs, and HIV-negative controls was conducted in order to directly address the potential benefit of treating SPs and/or elite controllers with cART and is described in chapter 4.

1.9 Objectives and main hypothesis

The principal goal of my PhD research was to investigate markers of aging in PLWH using HIV infection as a human model of aging.

My objectives were to:

1. Develop an MMqPCR assay to measure mtDNA content for use in PBMC subsets that, relative to previously established qPCR assays, has (Chapter 2)
    a. high concordance,
    b. a low limit of detection, and
    c. a low assay variance.

2. In a large (N~300 per group) sample of PLWH and HIV-negative controls, investigate the (Chapter 3)
    a. effect of HIV infection and HIV-related clinical parameters on LTL and WB mtDNA content and
    b. relationship between LTL and WB mtDNA content
    both cross-sectionally and longitudinally.

3. In a smaller (N~55 per group) sample of SPs, cART-controlled PLWH, UPs, and HIV-negative controls, characterize (Chapter 4)
    a. the in-depth impact of HIV on cellular and immune markers of aging and
    b. immune aging in SPs as a potential protective model of HIV-mediated accelerated aging.

The overarching hypothesis of my research was that parameters representing HIV replication and effective viral control, including pVL and SP status, would be associated with indicators of immune aging such as the telomere-mitochondria axis of cellular aging, T cell differentiation,

and the accumulation of senescent CD8 T cells. More granular descriptions of my research hypotheses are included in chapters 3 and 4.

Chapter 2: A monochrome multiplex real-time quantitative PCR assay for the measurement of mitochondrial DNA content

2.1 Introduction

Mitochondria contain multiple copies of circular mtDNA that code for some of the proteins necessary for oxidative phosphorylation, as well as 22 tRNAs and two rRNAs [303]. MtDNA replicates independently of both cellular division and mitochondrial proliferation, although the number of mtDNA copies per cell is typically maintained within a homeostatic range [304,305]. The copy number of mtDNA per cell can be modulated on the basis of the cell's energetic needs as well as the presence of the nuclear-encoded mitochondrial transcription factor A, which acts on the promoter regions of mtDNA to regulate replication and transcription [306–308].

Altered levels of mtDNA copies per cell (mtDNA content) in various tissues have been associated with aging [62,309] and may be a physiological response to oxidative stress [80,310]. MtDNA content has been examined in the context of numerous diseases and conditions. For example, measurable changes in mtDNA content have been reported in various forms of cancer [77,78,311], diabetes [75,312,313], and in HIV-infected individuals either untreated or treated with certain antiretroviral therapy regimens [68,70,73]. Some studies demonstrate the depletion of mtDNA content by HIV infection longitudinally [68,71]. MtDNA quantification is also of particular interest as a potential marker for mitochondrial dysfunction in critical care [314] as well as metabolic comorbidities such as hyperlactatemia [315], myopathy and cardiomyopathy [63,64,316], peripheral and optic neuropathies [65,317], and lipodystrophy [318]. Furthermore, reduced mtDNA content is a

hallmark of mitochondrial DNA depletion syndrome, a heterogeneous set of genetic disorders that may clinically present as hepatic failure, encephalopathy, and myopathy [66,67]. To date, the usefulness of mtDNA content as a diagnostic and/or molecular screening tool remains a matter of debate because of the current paucity of mechanistic evidence in various disease states, unknown sensitivity and specificity, and a scarcity of prospective cohort studies demonstrating causality [319–321]. Nevertheless, it is likely that the use of mtDNA content measurements in both clinical and research settings will become more prevalent as data are generated and their biological relevance is more clearly established. Real-time qPCR is the preferred method of measuring mtDNA content because of its applicability in both fresh and archived tissues, its high-throughput nature, and extensive use history for more than a decade.

In 2009, Cawthon [100] described an MMqPCR technique for the measurement of telomere length, exploiting copy number differences and melting temperatures of single-copy and telomeric DNA amplicons. Our group has previously described optimization conditions for this technique on the LightCycler 480 platform (Roche Molecular Systems, Pleasanton, CA) with SYBR green intercalating fluorescent dye [101]. Herein, we implement the MMqPCR method for the measurement of mtDNA content on the basis of the same principles. We present quality control considerations and quantify assay variance, and we juxtapose the performance of this assay relative to the gold standard monoplex qPCR.

2.2 Materials and methods

2.2.1 Ethics statement

This study was approved by the University of British Columbia Research Ethics Board. All study participants and volunteer blood donors provided written informed consent.

2.2.2 Study specimens

Human tissues (n = 130) and cultured human cell specimens (n = 30) were used in this study. Our sample of convenience consisted of human DNA from the following tissues: WB (n = 46), mouth swab (n = 30), as well as biopsy samples of skeletal muscle (n = 35), subcutaneous fat (n = 4), heart (n = 4), liver (n = 4), lung (n = 4), and kidney (n = 3). These were randomly selected from a DNA biobank of specimens from previously published studies [322–324]. In addition, cultured human cells were used: JEG-3 (ATCC-HTB-36) and BeWo (ATCC-CCL-98) placental cells, CCRF-CEM (ATCC-CRM-CCL-119) T-lymphoblast cells, and HEK-293 (ATCC-CRL-1573) embryonic kidney cells. As part of other studies, cultured cells had been exposed to HIV antiretrovirals, some of which affect mtDNA content [73].

2.2.3 DNA extraction and storage

Total genomic DNA from WB (0.1 ml) and cultured cells (approximately 1×10^6 cells) was extracted using the QIAamp DNA Mini Kit (Qiagen, Hilden, Germany) on the QIAcube, according to the manufacturer's blood and body fluid protocol, with modifications as previously described [325]. Total DNA from muscle, fat, heart, liver, lung, and kidney tissues was collected and extracted as described in previous studies [322–324].

2.2.4 MMqPCR

MtDNA content was defined as the ratio of the copy number of mitochondrial genomes normalized to the copy number of a single-copy nuclear gene. Fragments of the mitochondrial displacement loop (D-loop) and albumin (*ALB*) were used as mtDNA and nuclear DNA (nDNA) sequences, respectively. Both sequences were amplified in a single 10-μL reaction containing 1× LightCycler SYBR Green I Master (Product number 04707516001; Roche Molecular Systems), 0.9 μmol/L of each of the following four primers (AlbuF, AlbdR, D-loop_MPLX_F, and D-loop_MPLX_R), 1.2 mmol/L ethylenediaminetetraacetic acid (EDTA), and 2 μL of genomic DNA template (approximately 0.3 to 35 ng/μL). Primers were high-performance liquid chromatography purified (Integrated DNA Technologies, Coralville, IA), and their sequences are presented in **Table 2.1**. Noncomplementary tags were added to the 5′ end of the primer sequences to modify amplicon melting temperatures. Degenerate bases in D-loop primers were incorporated to accommodate common mtDNA sequence variants, as reported in Mitomap (http://www.mitomap.org, last accessed October 4, 2017), an integrated database of human mtDNA sequence variants [326]. The thermal cycling program started with a 95°C enzyme activation (hot-start) incubation for 15 min and was followed by 40 cycles of 94°C for 15 s, 62°C for 10 s (2.2°C/s), 74°C for 15 s, 84°C for 10 s, and 88°C for 15 s, with two signal acquisitions at the end of the 74°C and 88°C stages. Temperature ramping rates were all 4.4°C/s unless specified.

Table 2.1 Primer sequences.

Assay Type	Target	Accession no.*	Amplicon size, bp	Forward Primer	Forward Primer Nucleotide Sequence	Reverse Primer	Reverse Primer Nucleotide Sequence
Monoplex qPCR	*MT-CO1*	NC_012920.1	197	CCOI1F	5'-TTCGCCGACCGTTGACTATT -3'	CCOI2R	5'-AAGATTATTACAAATGCATGGGC -3'
Monoplex qPCR	*POLG2*	NM_007215.3	186	ASPG3F	5'-GAGCTGTTGACGGAAAGGAG -3'	ASPG4R	5'-CAGAAGAGAATCCCGGCTAAG -3'
Monoplex qPCR	D-loop	NC_012920.1	150	MT325F	5'-CACAGCACTTAAACACATCTCTGC -3'	MT474R	5'-AGTATGGGAGTGRGAGGGRAAAA -3'
Monoplex qPCR	*ALB*	NM_000477.5	44	AlbuFM	5'-AAATGCTGCACAGAATCCTTG -3'	AlbdRM	5'-GAAAAGCATGGTCGCCTGTT -3'
MMqPCR	*ALB*	NM_000477.5	98	AlbuF	5'-**CGGCGGCGGGCGGCGCGGGCTGGGCGG**AAATGCTGCACAGAATCCTTG -3'	AlbdR	5'-**GCCCGGCCCGCCGCGCCCGTCCCGCCG**GAAAAGCATGGTCGCCTGTT -3'
MMqPCR	D-loop	NC_012920.1	173	D-loop_MPLX_F	5'-<u>ACGCTCGACA</u>CACAGCACTTAAACACATCTCTGC -3'	D-loop_MPLX_R	5'-<u>GCTCAGGTCATAC</u>AGTATGGGAGTGRGAGGGRAAAA -3'

Boldfaced nucleotides represent noncomplementary GC clamps, and underlined nucleotides represent noncomplementary bases added to increase the melting temperature of the amplicon. Degenerate (50% A, 50% G) bases are represented by R. *https://www.ncbi.nlm.nih.gov

A standard curve was included on each plate ($r > 0.999$), consisting of a mixture of two pCR2.1-TOPO plasmids, each containing one of the amplicons. The two plasmids were mixed at a 50:1 ratio of D-loop/*Alb*, serially diluted 1:5 to obtain a range of 3250 to 1.27×10^9 copies of D-loop and 65 to 2.5×10^7 copies of *ALB*. A total of 40 DNA specimens were assayed in duplicate in each run.

Data were acquired on the LightCycler 480 software version 1.5.1.62 SP2. The signal acquired at 88°C is reflective of only *ALB* amplicon copy number, given that the D-loop amplicon dissociates at a lower temperature. Although the 74°C signal technically represents the sum of both D-loop and *ALB* amplicons, the quantity of *ALB* is negligible at cycle threshold (C_T) given the usually much higher amount of D-loop. Therefore, the 74°C C_T can be used to calculate D-loop copy number, and the 88°C C_T can be used to calculate *ALB* copy number.

Data from an MMqPCR run were exported from the LightCycler 480 software as one text file and imported into Microsoft Excel (Microsoft Corp., Redmond, WA) to delineate the D-loop (74°C) and *ALB* (88°C) signals with the program and segment markers specified by the LightCycler 480 software. Using the thermal cycling program described herein, D-loop data are recorded in Program 2, Segment 3, and *ALB* data are recorded in Program 2, Segment 5. Once separated, data for each amplicon were individually exported as text files and converted into grid format using LC480 Conversion version 2.0. Baseline corrections and C_T determination were done on the LinRegPCR software version 2012.1, as previously described [327]. Both programs are freely available from the Heart Failure Research Center (Amsterdam, the Netherlands; http://www.hartfaalcentrum.nl/index.php?main=files&sub=0, last accessed September 25, 2017).

More details regarding data analysis workflow can be found in a previous publication by our group [101].

2.2.5 Monoplex qPCR

Monoplex qPCR was based on a previously described fluorescein probe method [73] adapted to the SYBR intercalating dye. DNA samples were assayed twice by monoplex qPCR, amplifying two different sets of mtDNA and nDNA amplicons each time, each gene in a separate qPCR. In the first set, primers complementary to the cytochrome c oxidase subunit 1 (*MT-CO1:* CCOI1F and CCOI2R) and polymerase (DNA-directed), γ2, accessory subunit (*POLG2:* ASPG3F and ASPG4R) were used as the mitochondrial and single-copy nuclear genes, respectively. In the second set, the same D-loop (MT325F and MT474R) and *ALB* (AlbuFM and AlbdRM) sequences as above were amplified, although the D-loop and *ALB* monoplex primers did not contain any noncomplementary tags (**Table 2.1**). Quantification of both genes within a set took place in different wells but on the same plate.

Each 10-μL reaction consisted of 1× LightCycler SYBR Green I Master, 1 μmol/L each of forward and reverse primers, and 2 μL of genomic DNA template (approximately 0.3 to 35 ng/μL). The thermal cycling program started with 95°C enzyme activation (hot-start) incubation for 10 min. This was followed by 45 cycles of 95°C for 5 s, 60°C for 10 s (2.2°C/s), and 74°C for 5 s, with signal acquisition at the end of the 60°C stage and temperature ramping at 4.4°C/s unless indicated. Data were acquired on the LightCycler 480 software version 1.5.1.62 SP2.

A standard curve for each gene was included on each plate. The standard curves for the *MT-CO1*/*POLG2* set consisted of 1:10 serial dilutions of a cloned plasmid (pCR2.1-TOPO; Invitrogen, Carlsbad, CA) containing a single copy of both *MT-COI* and *POLG2* amplicons, with a linear range of 4.3×10^0 to 4.3×10^6 copies ($r > 0.999$). For the D-loop/*Alb* set, the same standard curve as for MMqPCR was used for convenience. A total of 17 DNA specimens were assayed in duplicate per run.

Data from each gene were independently exported from the LightCycler 480 software as text files and processed with LC480 Conversion and LinRegPCR, as described in the MMqPCR assay above. The data do not need to be sorted by acquisition because each amplicon was measured in separate PCRs.

2.2.6 qPCR quality control

In-house quality control (QC) practices have been established for this assay. These involve a run-specific QC followed by a specimen-specific QC. To ensure the quality of any given run, two internal controls (ICs) and a negative control were included on each plate. One IC was composed of pooled WB DNA extracts from 12 volunteers, and the other was DNA extracted from SK-BR-3 (ATCC-HTB-30) mammary gland epithelial cells. The negative control consisted of DNA elution buffer (Buffer AE; Qiagen) in place of template DNA. For an MMqPCR run to pass QC, it must not violate more than one of the following criteria: i) IC measurements in each run must fall within 2 SDs of IC measurements from previous runs performed under the same conditions; ii) PCR efficiencies of each gene (as determined by the standard curve) must each lie between 90% and 100% (1.80- to 2.00-fold amplification per

cycle); iii) differences in PCR efficiencies between the two genes must be <2.5%; iv) the mean of the difference between duplicate mtDNA content measurements must be <10%; and v) signal in the negative control must be absent or negligible (>3C_t below the last standard).

Specimen-specific QC was based on variation between specimen duplicates. For MMqPCR, data for individual extracts are accepted if mtDNA content measurements (D-loop/*Alb* ratio) between duplicates varies by <15%. In monoplex qPCR, data for individual extracts are accepted if both individual genes and their ratio (mtDNA content) measurements between duplicates vary by <20%. For both methods, DNA extracts that do not meet QC criteria are repeated in duplicate. If the repeated measurement still does not meet QC criteria, the CV of all four replicates is determined, and the average of the four replicates is accepted if their CV is <10%. Otherwise, data for that DNA extract are excluded from the analysis. In this study, approximately 5% of initial measurements needed to be repeated, and all repeated data were accepted.

More detail on MMqPCR QC can be found in our previous publication [101].

2.2.7 Statistical analysis

All qPCR data were log transformed for statistical analyses. Correlations between monoplex qPCR and MMqPCR were tested using Pearson's correlations on XLSTAT 2013 version 1.01 (Addinsoft, Paris, France). Concordances between assays were determined with Lin's concordance correlations (ρ_C) using online software provided by the National Institute of Water and Atmospheric Research in New Zealand (https://www.niwa.co.nz/node/104318/concordance,

last accessed September 25, 2017). Reproducibility was evaluated by comparing measurements made across several runs with those of the same DNA samples on a single repeat run. Intra-assay variability was determined from the CV of 12 to 20 replicate measurements of an IC on a single run. Interassay variability was derived from the CV of an IC included in 6 to 22 runs. Reproducibility and variability data were collected by several operators within our group. All available data from all operators are presented herein.

2.3 Results

The principle of this novel mtDNA content MMqPCR technique was influenced by a telomere MMqPCR technique [100] that our group previously optimized for the LightCycler platform [101]. The MMqPCR design offers improvements in time effectiveness and cost-effectiveness while diminishing the impact of pipetting error.

This assay relies on the addition of extra nucleotides to the PCR primers to alter the dissociation temperatures of the two amplicons. This was done such that the signal of only one amplicon can be acquired at a higher temperature than the signal from both. Herein, longer GC-rich tags were added to *ALB* MMqPCR primers (as with the original telomere publication [100]) and shorter tags were added to D-loop MMqPCR primers. Consequently, the combined D-loop/*ALB* signal can be acquired at 74°C, whereas only the *ALB* signal is acquired at 88°C. Both acquisitions occur within each cycle, facilitating duplex signal acquisition similar to that of duplex probe-based qPCR assays. Because mtDNA genomes typically greatly outnumber nuclear genomes, the 74°C acquisition can be used to directly estimate D-loop copy number. A schematic of the cycling

program as well as amplification profiles of the mitochondrial and nuclear amplicons can be found in **Figure 2.1**.

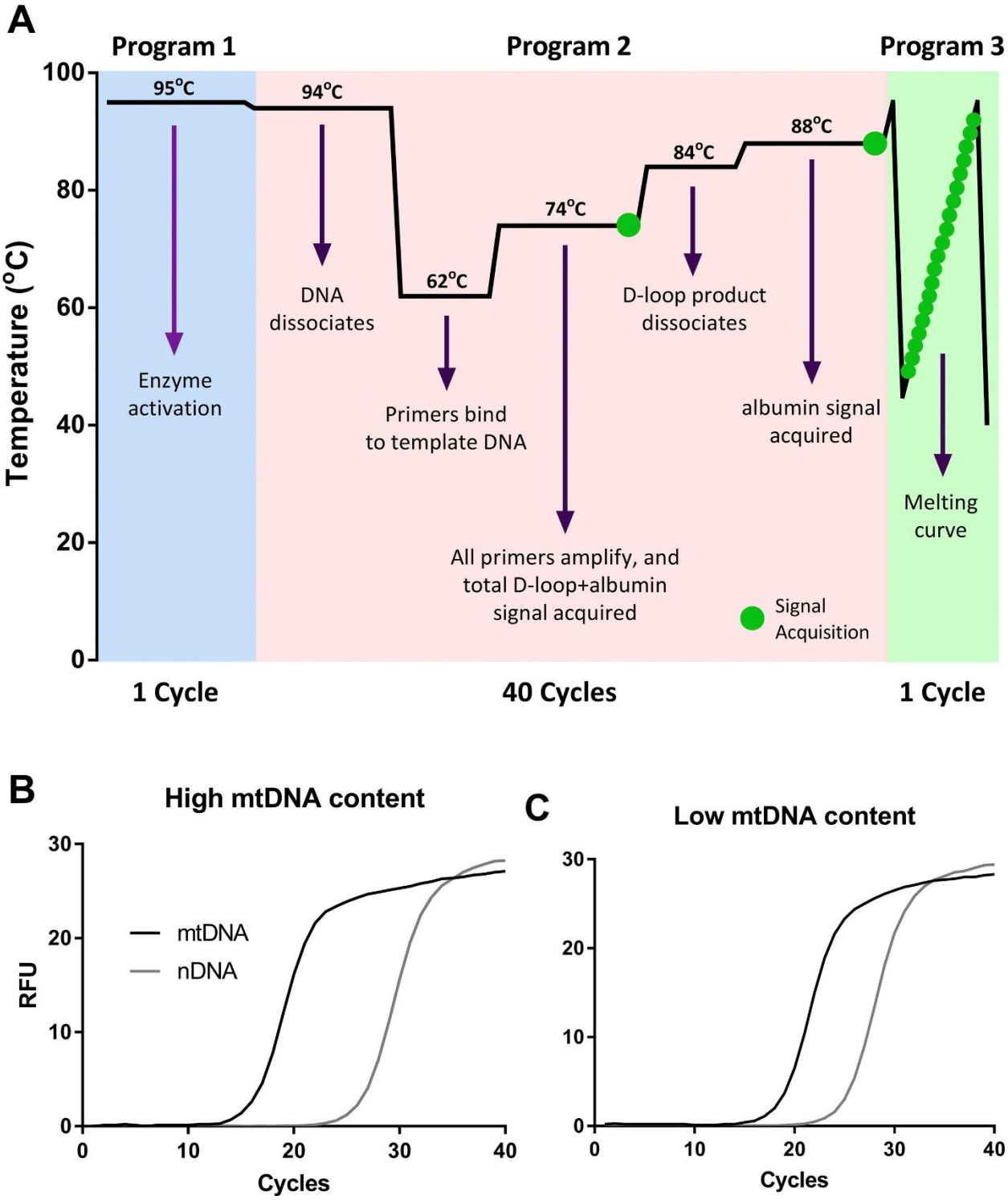

Figure 2.1 qPCR cycling program and amplification profiles.
(A) Schematic describing qPCR cycling program. Amplification profiles of mtDNA and nuclear DNA showing **(B)** high and **(C)** low mtDNA content DNA specimens. RFU, relative fluorescence units.

2.3.1 Agreement between monoplex qPCR and MMqPCR

In this study, DNA specimens from diverse human tissues (**Table 2.2**) were assayed with MMqPCR (D-loop/*ALB*) and two versions of the monoplex qPCR (*MT-CO1*/*POLG2* and D-loop/*ALB*) to perform comparisons between the two techniques. The MMqPCR targets the same D-loop and *ALB* sequences as one of the monoplex qPCR assays.

Table 2.2 mtDNA content of human tissues or specimens.

Tissue or specimen (N)	**mtDNA content median** [interquartile range] (range)
Muscle (35)	2012 [1684-3031] (511-7524)
Fat (4)	501 [343-667] (138-893)
Heart (4)	3169 [2891-3543] (2772-3951)
Kidney (3)	571 [407-929] (243-1286)
Liver (4)	994 [600-1272] (179-1347)
Lung (4)	420 [113-910] (73-1494)
Mouth Swab (30)	236 [175-298] (103-437)
Whole Blood (46)	99 [66-117] (39-196)
Cultured immortalized cells (30)*	264 [183-509] (40-1946)

MtDNA content is the ratio of the copy number of mitochondrial genomes normalized to the copy number of a single-copy nuclear gene. *Cultured cells were exposed to mtDNA content-altering antiretroviral drugs.

There was a strong correlation (Pearson's $r > 0.98$) and agreement (Lin's $\rho_C > 0.95$) between MMqPCR data and both forms of monoplex qPCR (**Figure 2.2**, **A** and **B**). Lin's concordance correlation coefficient [328] as reported herein, is a reproducibility index that evaluates goodness of fit to a line with a slope of 1 that passes through the origin. This metric is sensitive to systematic variance between assays that changes the slope or y-intercept in a line of best fit, but would not be reflected in the Pearson's correlation. Although the robust Pearson's correlation indicated that both measures were proportional, the strong Lin's concordance also confirms that one assay approximated the exact values of the other assay. MtDNA content measurements extended linearly from 39 to 7524 copies of D-loop per copy of *ALB*, across a nearly 200-fold range. In subanalyses involving only blood or muscle tissue that covered narrower ranges (approximately fivefold range for blood and approximately 15-fold range for skeletal muscle), correlations ranged from $0.80 < r < 0.90$ (**Figure 2.3**). Correlations of individual gene measurements between MMqPCR and monoplex qPCR among all DNA samples were also robust, spanning $0.96 < r < 0.98$ (**Figure 2.4**).

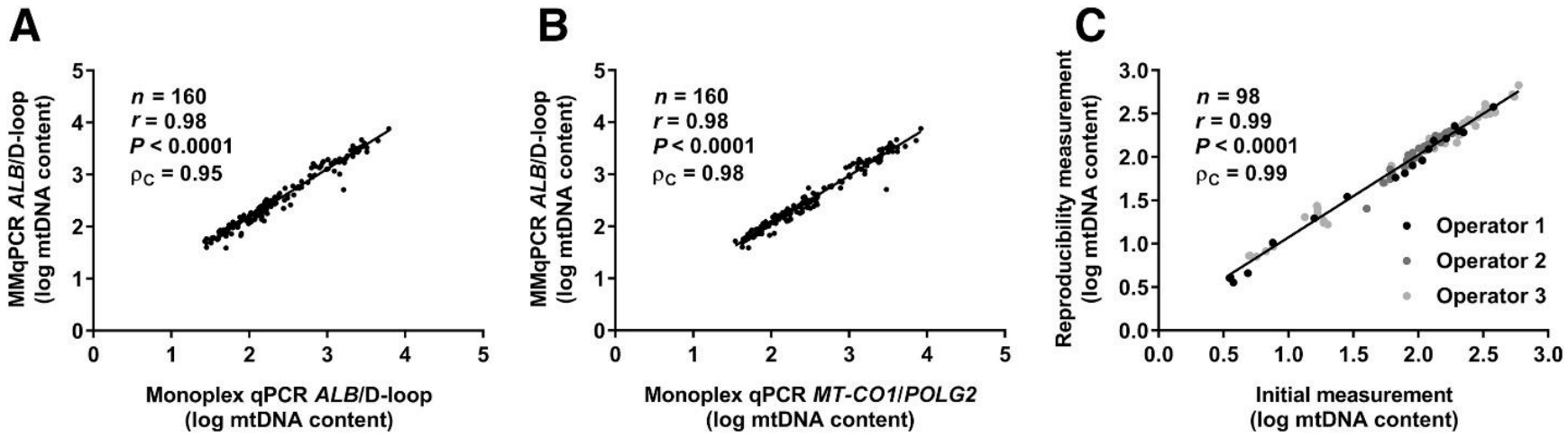

Figure 2.2 Concordance between mtDNA content of MMqPCR vs. monoplex qPCR (n=160) and assay reproducibility (n=98).
Pearson's correlations between **(A)** MMqPCR (*ALB*/D-loop) *vs.* monoplex qPCR (*ALB*/D-loop), and **(B)** MMqPCR (*ALB*/D-loop) *vs.* monoplex qPCR (*MT-CO1*/*POLG2*) are shown. **(C)** Pearson's correlation of MMqpCR assay reproducibility from three operators (n=18, n=28, and n=52) are shown in aggregate.

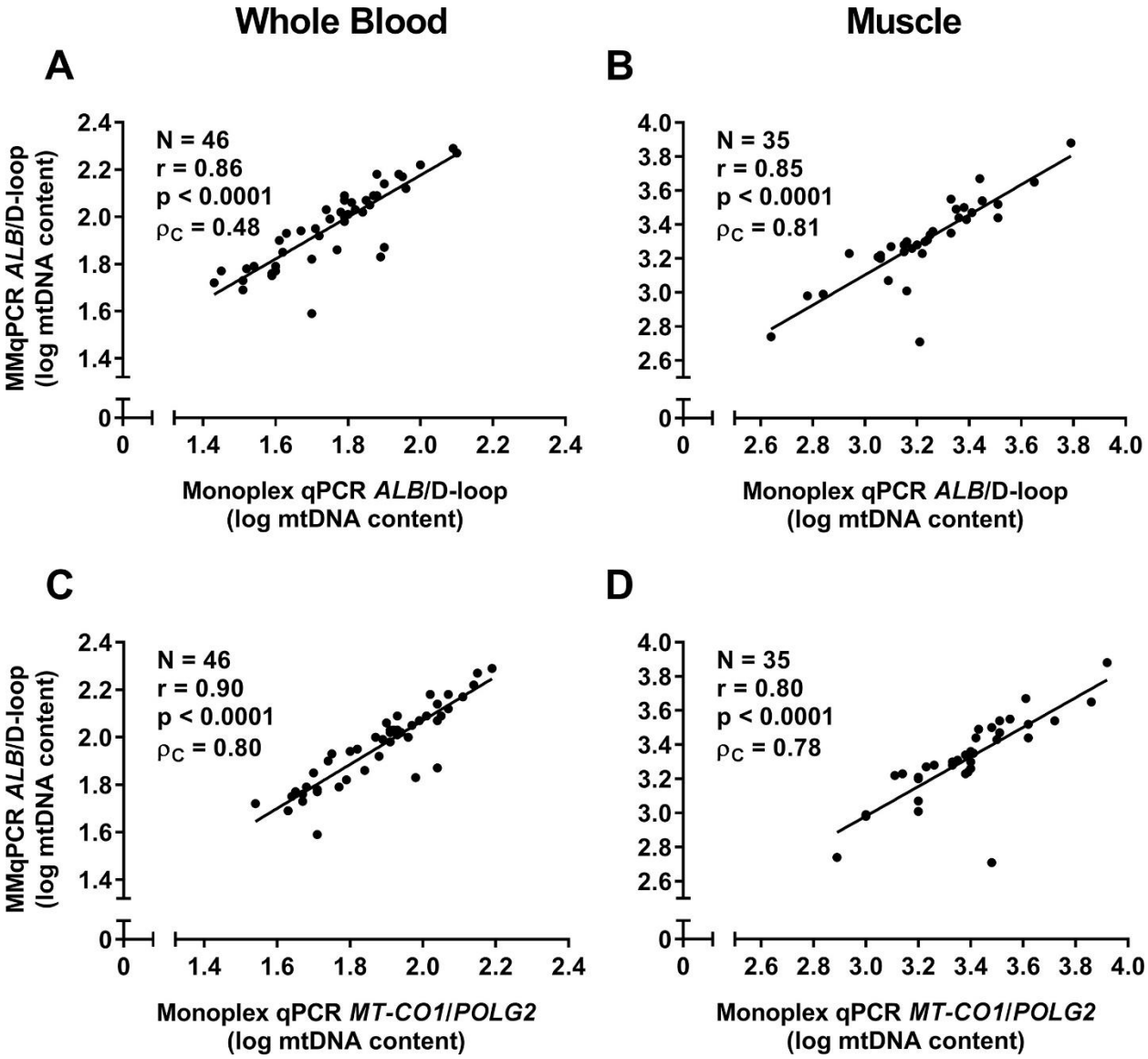

Figure 2.3 Subanalysis of concordances between MMqPCR and monoplex qPCR of whole blood and muscle samples.
Pearson's correlations between **(A)** MMqPCR (ALB/D-loop) and monoplex qPCR (ALB/D-loop) of whole blood, **(B)** MMqPCR (ALB/D-loop) and monoplex qPCR (ALB/D-loop) of muscle, **(C)** MMqPCR (ALB/D-loop) and monoplex qPCR (MT-CO1/POLG2) of whole blood, and **(D)** MMqPCR (ALB/D-loop) and monoplex qPCR (MT-CO1/POLG2) of muscle are shown. mtDNA, mitochondrial DNA.

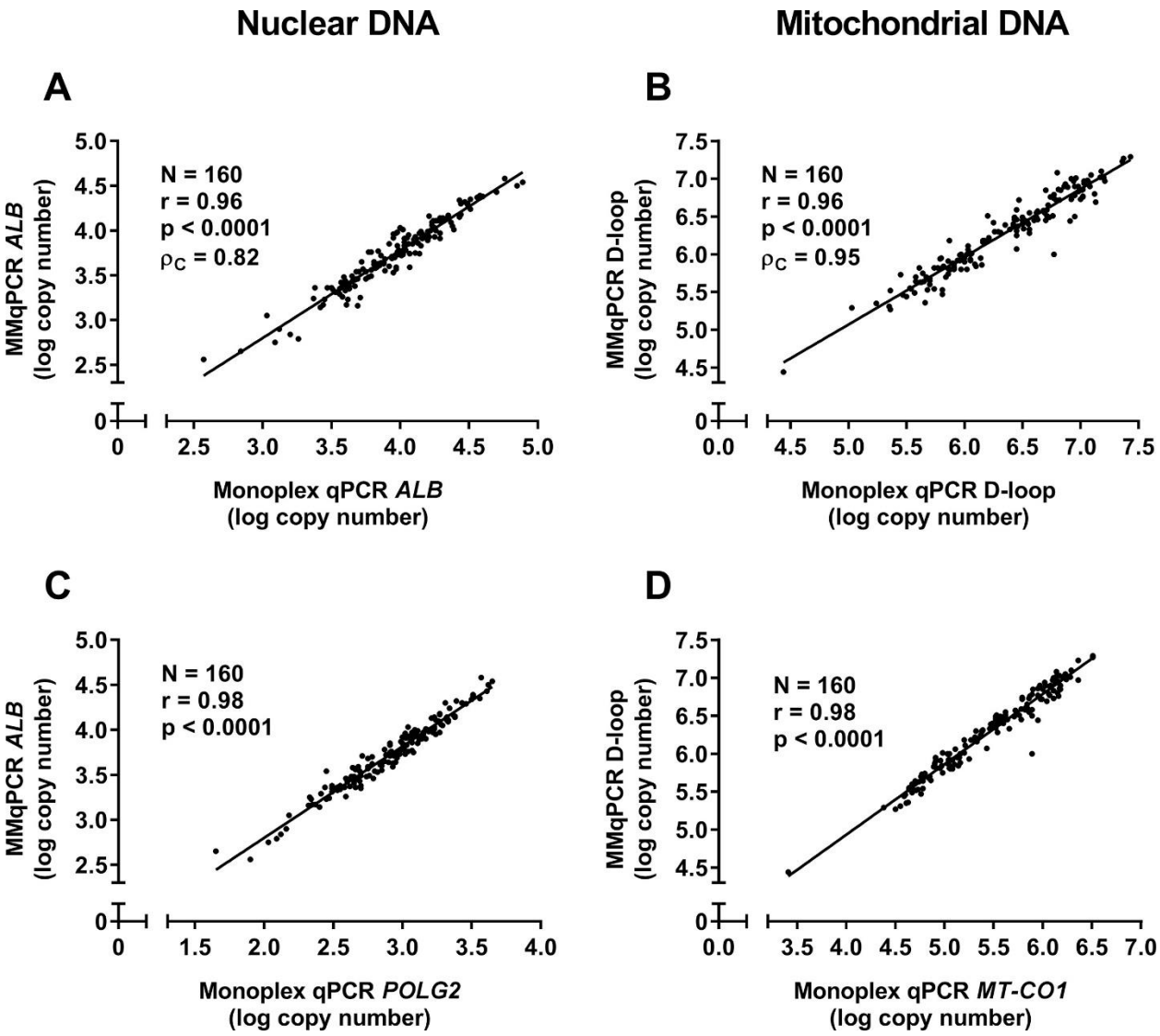

Figure 2.4 Subanalysis of concordances between nuclear and mitochondrial DNA copy numbers of MMqPCR versus monoplex qPCR.
Pearson's correlations between **(A)** MMqPCR (ALB) and monoplex qPCR (ALB), **(B)** MMqPCR (D-loop) and monoplex qPCR (D-loop), **(C)** MMqPCR (ALB) and monoplex qPCR (POLG2), and **(D)** MMqPCR (D-loop) and monoplex qPCR (MT-CO1) are shown. Lin's concordance (ρ_C) is shown only for ALB and D-loop data, because POLG2 and MT-CO1 data are not calibrated for absolute quantification.

2.3.2 MMqPCR reproducibility and variability

Data collected by multiple operators over a period of 2 years were used to assess the real-life reproducibility and variability of this assay. Each of three operators repeated a random subset (n = 18 to 52) of their DNA sample from previous studies (E. Kimmel, M. Budd, and M. Zhu, unpublished data). The correlations between initial and repeated measurements on a different day were $0.96 < r < 0.99$ for all operators. Taken together (**Figure 2.2C**), the overall correlation (r) and agreement (ρ_C) were 0.99 and 0.99, respectively.

Interassay variability measured across 6 to 22 runs was determined for five different operators, and these ranged from 2.9% to 6.2% for the low IC and from 4.8% to 9.2% for the high IC. Intra-assay variability (n = 12 to 20) ranged between 4.3% and 7.9%, measured by four independent operators.

2.3.3 Amplicon specificity

Both D-loop and *ALB* MMqPCR products were visualized on agarose gel electrophoresis (**Figure 2.5A**). In separate reactions containing only one set of primer pairs, only the corresponding product is seen. This was demonstrated using both ICs, because their DNA are derived from different sources.

The C_T values of both 74°C and 88°C acquisitions were used to monitor amplification in the presence of the *ALB* primer pair, the D-loop primer pair, or both. With both sets of primers present, the C_T of the 74°C acquisition was considerably lower than that of the 88°C acquisition (**Figure 2.5B**), as would be expected given the greater abundance of the D-loop amplicon. The

actual ΔCT between the two temperatures is related to the measured mtDNA content. When only *ALB* primers were present, the C_T values of both acquisitions were identical, indicating that the *ALB* signal measured at 74°C may also be measured at 88°C. When only D-loop primers were present, there was no signal in the 88°C acquisition, indicating that the D-loop amplicon measured in the 74°C acquisition is fully dissociated at 88°C. These results demonstrate the specificity of the 74°C and 88°C acquisitions by showing that D-loop, but not *ALB*, is dissociated at 88°C.

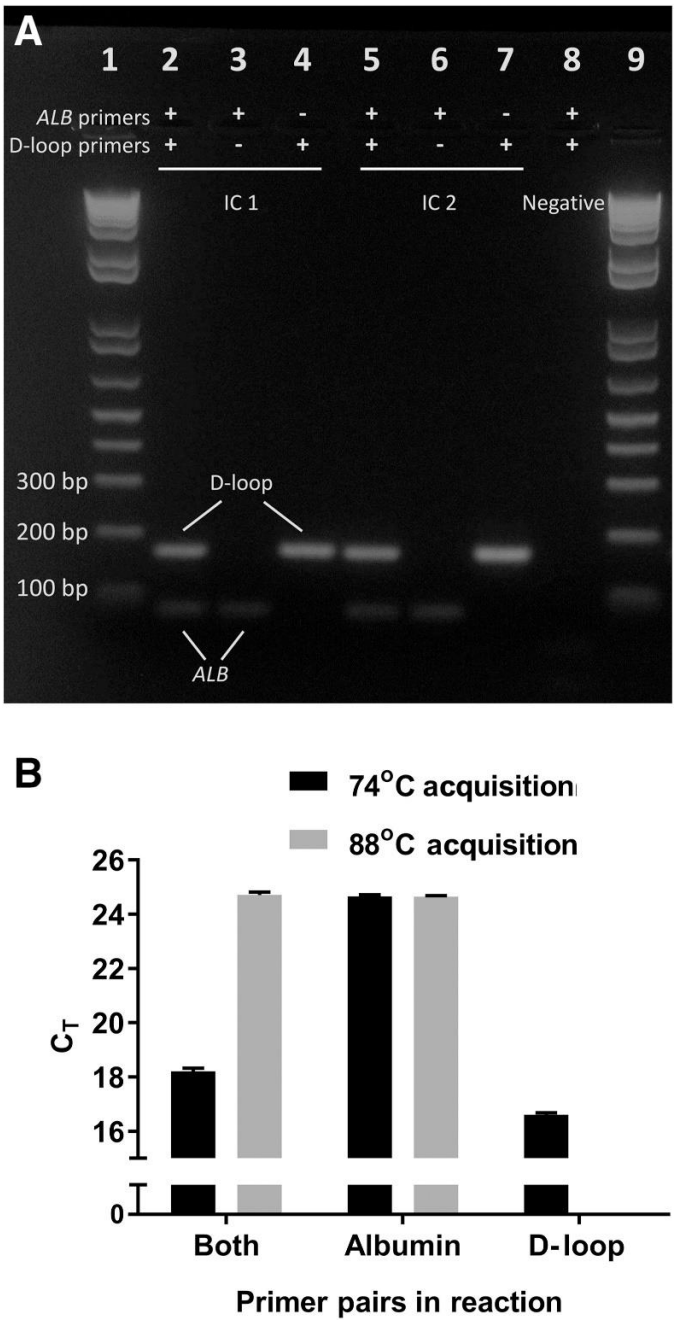

Figure 2.5 MMqPCR primer and signal acquisition specificity.
(A) Visualization of MMqPCR amplicons on 2.5% agarose gel. Lanes 1 and 9 were loaded with 1kb Plus DNA ladder. Lanes 2 through 4 show PCR products from reactions with both primer sets, the *ALB* primer pair, and the D-loop primer pair, respectively, amplified from an IC. Lanes 5 through 7 show the same arrangement of reactions amplified from the second IC. Lane 8 is a negative control (DNA elution buffer) with all primers. All PCR products were diluted 1:10 prior to loading onto the gel. **(B)** C_T values of both 74ºC and 88ºC acquisitions are shown in reactions containing all primers, the *ALB* primer pair, and the D-loop primer pair. C_T values are derived from 8 technical replicates, and error bars are standard deviation. The small difference in 74ºC C_T values between reactions with and without the albumin primer is related to the influence of the albumin primer on the background fluorescence.

2.3.4 Assay limitations

In most biological tissues, the copy number of mtDNA greatly exceeds that of nDNA. Under these typical circumstances, the amount of *ALB* amplicon in the 74°C acquisition is negligible, so the 74°C signal can be directly used to calculate D-loop copy numbers. However, in scenarios where mtDNA copies do not vastly outnumber nDNA copies, *ALB* amplicons detected by the 74°C acquisition will artificially inflate calculated D-loop values and the MMqPCR assay will overestimate mtDNA content. To determine the critical D-loop/*ALB* ratio below which this error inflates the inherent intra-assay variability, both ICs were quantified with a series of standard curves constructed using different ratios of D-loop and *ALB* plasmids. Standard curves below the critical ratio would be affected by the same error, and calibration based on such standard curves would, therefore, underestimate the true D-loop/*ALB* ratio of the ICs. Given this, the critical standard curve ratio below which measured IC ratios are underestimated reflects the minimum mtDNA/nDNA ratio in the template DNA that can be accurately quantified using this method.

According to the data, standard curves with a D-loop/*ALB* ratio of at least 20 were needed to accurately quantify mtDNA content of either IC (**Figure 2.6A**). Standard curves with a D-loop/*ALB* ratio of 50 were used in this study. By doing so, the assay avoids the error mentioned above and maximizes the quantifiable range of template DNA copy number when measuring mtDNA content in various tissues. As expected, there was no such minimum ratio when tested using monoplex qPCR (**Figure 2.6A**).

The limit of quantification of the MMqPCR assay was determined by replicate measurements of serially diluted pooled WB DNA samples. The attempts to quantify <82 pg of template DNA per reaction were constrained by rapidly increasing variance attributable to sampling error (**Figure 2.6B**). As such, 82 pg/reaction is reported as the lower limit of reliable quantification.

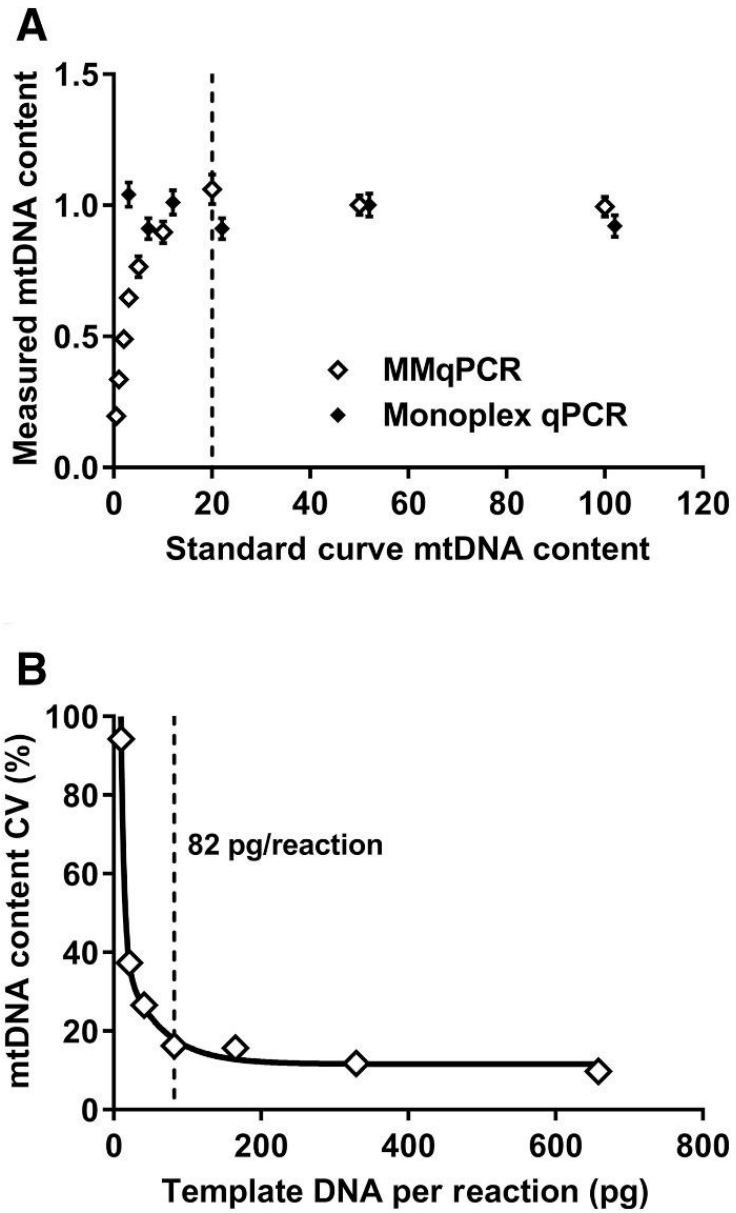

Figure 2.6 MMqPCR minimum quantifiable mtDNA content and limit of quantification.
(A) MtDNA content of an IC were calculated from both MMqPCR and monoplex qPCR using standard curves prepared with different ratios of *ALB* and D-loop plasmids. The vertical dotted line marks the minimum quantifiable mtDNA content (20) using MMqPCR. IC mtDNA content values represent 6 technical replicates. Error bars represent standard deviation. **(B)** The CV of MtDNA content measurements of serially diluted quantities of human WB DNA are shown. Each data point is derived from 20 technical replicates, and the vertical dotted line indicates the limit of quantification: ~82 pg/reaction.

2.4 Discussion

MtDNA content is an increasingly prevalent biomarker across both clinical and basic research, particularly in studies of bioenergetics, mitochondrial disease, drug toxicity, and aging. Thus far, the most widespread and cost-effective method of mtDNA content measurement involves quantification of mitochondrial and nuclear genomes using either two qPCRs or two multiplexed hybridization probes in a single reaction. Deriving mtDNA content from two reactions introduces pipetting and interreaction variability, whereas hybridization probes are generally more expensive than DNA intercalating dyes and more sensitive to batch-to-batch or lot variability. Herein, we apply the MMqPCR technique to the measurement of mtDNA, developing a one-tube monochromatic multiplex assay using the DNA-intercalating dye SYBR Green.

To properly assess the agreement between the MMqPCR assay and classic monoplex qPCR, a diverse set of study applications were simulated by testing diverse human tissues with a broad range of mtDNA content, a commonly assayed specimen at the low end of the biological range of mtDNA content; mitochondria-rich tissues, such as skeletal muscle and heart, were used to represent the higher range. To demonstrate the effectiveness of this assay with *in vitro* experiments that may require measurement of mtDNA content values outside the typical biological range, cultured human cells exposed to HIV antiretrovirals were assayed. This study is strengthened by the comparison of MMqPCR measurements with two monoplex qPCR data sets, including one that exploits the same complementary regions of D-loop and *ALB* as the MMqPCR assay. The latter revealed the variability (3%) that may be attributed solely to the difference between monoplex and multiplex. The comparison between D-loop/*ALB* MMqPCR and *MT*-

CO1/*POLG2* monoplex qPCR also captured the variability introduced by changing the PCR targets, and no meaningful decrease was detected because the correlation with the MMqPCR was similarly high. more stringent quality control may be applied to the MMqPCR assay compared with the monoplex qPCR (<15% difference between duplicates compared with <20%) without increasing the number of repeated measurements.

Given the increasing number of studies reporting mtDNA content measurements in translational and clinical settings, it is paramount to both quantify and reduce the assay's variability. Herein, we report reproducibility and variability metrics from three to five operators over a 2-year period. the realistic influence of interoperator variance was captured, in addition to other factors, such as different reagent lots and instrument maintenance. As such, these data represent a valid prediction of assay performance in the hands of future operators from other groups.

As with all qPCR assays, the amount of template DNA must exceed the limit of quantification to attain an accurate measurement. Herein, the limit of quantification (82 pg/reaction) was determined to be on the order of 10 nuclear genomes [329,330] and well below biospecimens with a scarcity of genetic material, such as dried blood spots [331]. In addition, the mtDNA/nDNA ratio in the DNA assayed was demonstrated to exceed 20 for accurate quantification. This is intrinsic to the MMqPCR design, where the 74°C signal is directly used to quantify one of the amplicons (in this case the D-loop amplicon). As such, the amplicon detected by the 88°C acquisition (in this case the *ALB* amplicon) must have a negligible influence on the 74°C acquisition. Typically, the mtDNA content of a physiologically relevant DNA sample will be substantially >20. In the sample, WB mtDNA content ranged from 39 to 196, with a median value of 99 (**Table 2.2**). WB

mtDNA content levels reported in the literature, measured using absolute quantification methods, were similar (on the order of approximately 100 copies of mtDNA/nDNA), and even pathologies associated with decreased WB mtDNA content still yielded mtDNA/nDNA ratios >20 [332–334]. However, in cases in which cells or tissues may harbor low mtDNA content, this assay may overestimate mtDNA content. A correction would need to be made to account for this error, possibly by spiking the DNA specimens with a known quantity of plasmid DNA containing the mtDNA amplicon to decrease the influence of the *ALB* amplicon on the 74°C signal. In the analysis, the known copy number of the spiked plasmid would be subtracted to derive the original quantity of mtDNA. An alternative may be to simply repeat low mtDNA content specimens using monoplex qPCR.

The MMqPCR assay is a considerable logistical improvement on existing methods for the quantification of mtDNA content. With the described protocol, the cost per sample may be reduced by roughly 2.3× compared with a monoplex qPCR protocol, in which two genes are assayed on a single plate.

This work also serves as a proof of concept for MMqPCR applications beyond the original telomere assay, as first suggested by Cawthon [100]. These data suggest that existing two-reaction qPCR assays may possibly be adapted to the MMqPCR technique, which may greatly benefit other high-throughput applications. It is fortunate that, like telomeric DNA, mtDNA greatly outnumber nDNA. Future development of MMqPCR assays to simultaneously measure near-equal quantities of DNA would be hindered by the minimum quantifiable ratio discussed above and would require the artificial increase of one of the amplicons.

As with telomere length measurements, MMqPCR would be expected to become the method of choice in studies aiming to quantify mtDNA content. As more data on mtDNA content are being generated to bolster our understanding of this biomarker, the demand for low -cost high-throughput assays will grow. The advances in time efficiency and cost-effectiveness and the reduction of variability inherent to MMqPCR will be essential to this process.

Chapter 3: Inverse relationship between leukocyte telomere length attrition and blood mitochondrial DNA content loss over time

3.1 Abbreviated introduction to chapter

There is growing evidence relating both aging and HIV to either shorter LTL or altered WB mtDNA content individually, but no studies to date have described the inter-relationship between these two markers longitudinally, in the context of HIV or in the general population. The objectives of this study were to investigate the effect of HIV and HIV-related clinical parameters on two aging markers, LTL and WB mtDNA content, as well as the relationship between them. These relationships were examined both cross-sectionally and longitudinally in a sample of 312 women living with HIV (WLWH) and 300 HIV-negative participants. We hypothesized that HIV infection would be associated with shorter LTL and/or faster LTL attrition, as well as decreased WB mtDNA content and/or faster WB mtDNA content loss. Furthermore, we hypothesized that LTL and WB mtDNA content would be positively associated cross-sectionally and/or longitudinally.

3.2 Methods

3.2.1 Study sample

Study participants included all non-pregnant women and girls ≥12 years old living with or without HIV enrolled in the Children and Women: AntiRetrovirals and Markers of Aging (CARMA) cohort between December 2008 and August 2017. WLWH were enrolled in the

CARMA cohort during routine clinical visits at four locations across Canada: British Columbia Women's Hospital in Vancouver, British Columbia; the Centre Hospitalier Universitaire Sainte-Justine in Montreal, Quebec; the Hospital for Sick Children in Toronto, Ontario; and the Children's Hospital of Eastern Ontario in Ottawa, Ontario. CARMA study participant visits occurred annually between 2008-2013, and every 2-3 years thereafter. The majority (293/300) of the HIV-uninfected participants were invited to participate through word of mouth and advertisements placed in regions of Vancouver that have higher representation of at-risk individuals. The remaining 7 were born from mothers living with HIV previously enrolled in CARMA and are HIV-exposed uninfected (HEU) participants. Written informed consent was provided by adult participants, and assent from pediatric participants was obtained with parent/legal guardian consent. This study was approved by the University of British Columbia Research Ethics Board at the Children's and Women's Hospital (H08-02018). Further details on CARMA enrolment have been previously described [42].

Study participants total 328 WLWH and 318 HIV-negative women and girls. Of these, one participant was excluded because no blood was collected and 33 were excluded because of missing demographic or clinical data that was deemed essential *a priori* (**Figure 3.1**). These variables included age, ethnicity, tobacco smoking, cannabis use, alcohol use, opioid use, HCV infection ever, and HIV status for all participants, as well as current HIV pVL, and CD4 count at visit for WLWH. Other data considered included BMI, household income, highest education level completed, HCV viremia, highest HIV pVL ever recorded (peak pVL), lowest CD4 count recorded, and platelet count (**Table 3.1**). For participants with ≥2 study visits at least one year

apart, the last visit was used for cross-sectional analyses, and the earliest (or baseline) and latest visits were used for longitudinal analyses.

In total, cross-sectional analyses included 312 WLWH and 300 HIV-negative participants. Longitudinal analyses included 228 WLWH and 68 HIV-negative participants.

Table 3.1 Essential and non-essential variables

Essential Variables	Non-Essential Variables
Age	BMI
Ethnicity	Household Income
Tobacco Smoking	Highest Education
Alcohol Use	HIV Peak Viral Load
Cannabis Use	ART-naïve at visit
Opioid Use	Lowest CD4 Count Recorded
HIV Status	HBV Infection Ever
HIV Viral Load	HCV Active Infection
CD4 Count	Platelet Count
HCV Infection Ever	

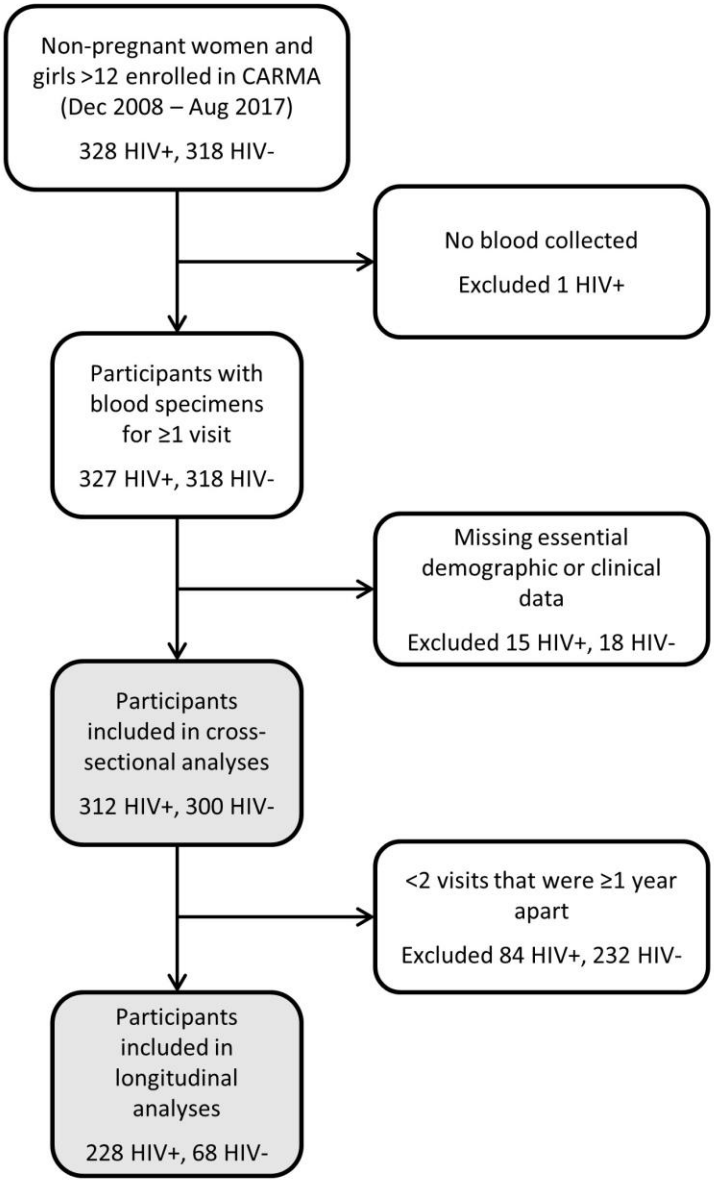

Figure 3.1 Study selection schematic.
Inclusion and exclusion criteria for present study are described. Required demographic or clinical data include age, ethnicity, opioid use, cigarette smoking, cannabis use, alcohol use, HIV status, HIV viral load, CD4 count, and HCV infection ever. Shaded boxes indicate samples for analysis.

Demographic data were self-reported at study entry for all participants, and substance use data were self-reported during study visits for participants ≥14 years old. HIV clinical information were collected from medical records when available. ART-naïve status, on/off cART, and the third drug of the cART regimen at visit were collected from medical records. HCV and HBV infection history were self-reported and confirmed by medical records when available. Missing data from essential variables were imputed from the nearest visit with available data, except for detectable/undetectable HIV pVL, which was imputed from on/off ART at visit, and vice versa. Of the 8 variables that required imputation, an average of 1.5% of the data were imputed ranging from 0.3% to 2.4%.

3.2.2 Biospecimen collection and qPCR

WB was collected and stored at -80°C until genomic DNA was extracted from 100 µl of WB using the QIAamp DNA Mini Kit on the QIAcube (Qiagen, Hilden, Germany) according to the manufacturer's blood and body fluid protocol. DNA was eluted in 100 µl of Buffer AE which contains 0.5 mM EDTA and 10 mM Tris-Cl, pH 9.0, and stored at -80°C until assayed.

Relative LTL and mtDNA content were measured in duplicate by MMqPCR as previously described [101,102]. TL was defined as the ratio between telomeric DNA quantity and the copy number of a single-copy nuclear gene, *ALB*. MtDNA content measured the ratio of mitochondrial genome copy number, measured using a segment of the mitochondrial displacement loop, to *ALB* copy number. The TL assay was calibrated using fluorescent *in situ* hybridization such that each unit of relative TL approximates 1 kb of telomeric DNA, whereas the mtDNA content assay provides the mtDNA to nuclear DNA ratio.

For both assays, quality control was applied as previously described [101,102]. Briefly, individual assays were accepted or rejected based on the measurements of two internal controls, the amplification efficiency of both amplicons as calculated using a standard curve, the average variability between all technical duplicates in the plate, and a negative control. Measurements of individual specimens were accepted if they fell within the linear range of the assay and if the difference between technical duplicates was <15%. Measurements that were not accepted were repeated at most once more and subjected to the same QC criteria. All qPCR data assayed for this study passed QC.

3.2.3 Statistical analyses

To evaluate the relationship between potential explanatory variables and our measures of interest, namely LTL and mtDNA content and the change in these over time, possible associations were first explored with univariate analyses using Pearson's or Spearman's correlation, one-way analysis of variance (ANOVA), Kruskal-Wallis, Student's t-, or Mann-Whitney U tests. Variables that were important in univariate analysis ($P<0.15$) were candidates for inclusion in multivariable models. The final models for each measure of interest included all essential variables as described above and were constructed in a stepwise manner, by minimizing the Akaike information criterion (AIC). While possible interactions were explored, none offered substantial model improvement. Chi-Square contingency tables, Kruskal-Wallis tests, and Spearman's correlation were used to detect collinearity among variables, and variance inflation factors (VIF) were calculated to characterize the influence of collinearity in the models. To further test the robustness of final models, subgroup analyses (such as among a specific ethnicity

or HIV group), and sensitivity analyses were done to investigate the effect of HIV clinical variables and non-essential variables, but with reduced power.

In cross-sectional models involving all participants, potential explanatory variables first included age, ethnicity, tobacco smoking, cannabis use, alcohol use, opioid use, HIV status, and HCV infection history. In models restricted to WLWH only, the above variables were considered in addition to CD4 count and detectable HIV pVL. LTL was also considered in all WB mtDNA content models and vice versa. After the final model was developed, the following non-essential variables were considered in sensitivity analyses with reduced power: household income, highest education level completed, HCV detectable pVL, HIV peak pVL, CD4 nadir, ART-naïve status, and third drug in the cART regimen. HBV infection history was considered only in HIV subanalyses, as only 2 HIV-uninfected participants were ever infected with HBV. Longitudinal models included LTL and WB mtDNA content at first visit as well as changes in HIV detectable pVL and on/off ART as additional potential explanatory variables. The subgroup model of ΔLTL/year among HIV-uninfected participants considered only continuous variables (age, baseline LTL, and ΔWB mtDNA content/year) because of reduced sample size.

Statistical analyses were performed using XLSTAT version 2019.1.1.

3.3 Results

3.3.1 Study sample

Characteristics of the study participants are shown in **Table 3.2**. Cross-sectional analyses included 312 WLWH and 300 HIV-negative participants. WLWH were slightly younger, with a median (range) age of 41 (14-69) *vs.* 44 (15-78) years (p=0.042). WLWH were also more likely to be African/Caribbean/Black (ACB), current tobacco smokers, current prescribed opioid users, have past or present HBV or HCV infections, and less likely to be White, Asian, current drinkers, have a household income >15000 CAD/year, and have any college education compared to HIV-negative controls. Body mass index and cannabis use did not differ between groups. Among WLWH, 70% of participants had an undetectable HIV pVL (<50 HIV RNA copies/ml) and 82% were on cART at visit.

Table 3.2 Study sample characteristics

	Cross-Sectional Sample (N=612)			**Longitudinal Sample** (N=296)		
	HIV+ (N=312)	**HIV-** (N=300)	**P-value**	**HIV+** (N=228)	**HIV-** (N=68)	**P-value**
Age, years	41 [31,50] (14,69)	44 [31,55] (15,78)	**0.042**	38 [29,46] (12,67)	36 [27,48] (12,73)	0.859
Time between visits, years				4 [2,6] (1,8)	3 [2,5] (1,7)	**< 0.001**
BMI, kg/m^2 (N=603)	24.9 [21.4,30.0] (15.0,48.6)	24.6 [21.4,29.7] (14.0,52.9)	0.608	24.0 [21.3,28.8] (16.0,46.6)	23.5 [20.5,28.7] (15.3,42.3)	0.526
Ethnicity						
White	131 (42)	153 (51)	**< 0.001**	94 (41)	37 (54)	**0.003**
African/Black/Caribbean	72 (23)	19 (6)		51 (22)	3 (4)	
Indigenous	78 (25)	79 (26)		58 (25)	16 (24)	
Asian	8 (3)	28 (9)		8 (4)	7 (10)	
Other[a]	23 (7)	21 (7)		17 (7)	5 (7)	
Household income >$15000 CAD/year (N=553)	127 (48)	170 (59)	**0.009**	95 (48)	40 (67)	**0.011**
Highest level of education (N=552)						
Any College	114 (43)	200 (69)	**< 0.001**	93 (47)	44 (73)	**0.005**
High School Graduate	54 (21)	30 (10)		38 (19)	6 (10)	
Some High School	80 (30)	53 (18)		56 (28)	9 (15)	
Grade School	15 (6)	6 (2)		11 (6)	1 (2)	
Cigarette smoking[b]						
Current	122 (39)	85 (28)	**0.010**	85 (37)	13 (19)	**0.002**
Past	69 (22)	67 (22)		54 (24)	12 (18)	
Never	121 (39)	148 (49)		89 (39)	43 (63)	

	Cross-Sectional Sample (N=612)			**Longitudinal Sample** (N=296)		
Cannabis[b]						
Current	77 (25)	72 (24)	0.853	59 (26)	15 (22)	0.664
Past	67 (21)	60 (20)		49 (21)	13 (19)	
Never	168 (54)	168 (56)		120 (53)	40 (59)	
Alcohol[b]						
Current	150 (48)	199 (66)	**< 0.001**	113 (50)	44 (65)	**0.039**
Past	87 (28)	61 (20)		63 (28)	17 (25)	
Never	75 (24)	40 (13)		52 (23)	7 (10)	
Current any opioid use[b]	69 (22)	32 (11)	**< 0.001**	51 (22)	3 (4)	**< 0.001**
Prescribed opioid use	62 (20)	25 (8)	**< 0.001**	47 (21)	1 (1)	**< 0.001**
Heroin use	17 (5)	13 (4)	0.523	15 (7)	0 (0)	**0.030**
HIV Detectable pVL at visit, >50 copies/ml[b,c]	95 (30)			63 (28)		
HIV Peak pVL >100000 copies/ml (N=248)	111 (45)			87 (48)		
CD4 count at visit, cells/µL[b]	540 [348,733] (10,2380)			500 [348,683] (14,1370)		
CD4 nadir, cells/µL (N=260)	221 [130,350] (1,1110)			216 [118,330] (1,900)		
ART-naïve (N=278)	10 (4)			11 (5)		
On cART at visit[b]	255 (82)			195 (86)		

	Cross-Sectional Sample (N=612)			**Longitudinal Sample** (N=296)		
HBV ever infected (N=395)	29 (13)	2 (1)	**< 0.001**	9 (26)	0 (0)	**0.011**
HCV ever infected	109 (35)	45 (15)	**< 0.001**	79 (35)	9 (13)	**< 0.001**
Platelet Count, 10^9/L (N=429)	227 [178,274] (40,663)	235 [213,281] (82,464)	**0.005**	233 [184,274] (45,489)	272 [217,277] (172,316)	0.240
Relative LTL	7.1 [6.4,7.8] (4.8,11.5)	7.4 [6.7,8.1] (4.8,11.3)	**0.004**	7.0 [6.3,7.8] (4.7,10.5)	7.5 [6.9,8.4] (5.1,10.5)	**< 0.001**
ΔLTL/year				0.01 [-0.10,0.11] (-0.94,1.8)	-0.05 [-0.26,0.09] (-1.18,0.74)	**0.020**
WB mtDNA content	101 [78,131] (4,265)	112 [85,146] (4,379)	**0.004**	143 [109,171] (4,277)	129 [96,154] (4,231)	**0.025**
WB ΔmtDNA content/year				-10 [-15,-1] (-76,77)	-7 [-16,8] (-32,37)	**0.013**

Data are number (%) of individuals or median [interquartile range] (range). Number of participants with available data indicated beside variables with incomplete data. P-values indicate Mann-Whitney U or Chi-Squared Tests depending on type of variable.
Abbreviations: ART, antiretroviral therapy; BMI, body mass index; cART, combination antiretroviral therapy; CAD, Canadian dollars; HBV, hepatitis B virus; HCV, hepatitis C virus; LTL, leukocyte telomere length; mtDNA, mitochondrial DNA; pVL, plasma viral load; WB, whole blood.

[a] a combination of South Asian, Hispanic, or other

[b] at last visit for longitudinal sample

[c] 22 lost HIV viral control and 41 participants gained HIV viral control between longitudinal visits

3.3.2 Cross-sectional LTL and WB mtDNA content decline with age but are not inter-related

WLWH had shorter LTL (median 7.1 *vs.*7.4) and lower WB mtDNA content (median 101 *vs.* 112) than HIV-negative controls before (**Table 3.2**, $p \leq 0.004$) and after adjusting for age ($P \leq 0.002$). Among all participants, relative LTL declined with age (**Figure 3.2A**), with an average loss of approximately 33 bp of telomeric DNA per year ($R^2=0.17$, $P<0.0001$). LTL was modulated by HIV status whereby the decline in LTL with age was faster among WLWH with detectable pVL compared to HIV-negative controls. WB mtDNA also declined with age (**Figure 3.2B**), although with a weaker relationship ($R^2=0.03$, $P<0.001$), that was not modulated by HIV. Despite the fact that both markers declined with age, they were not associated with one another (**Figure 3.2C**) ($R^2=0.004$, $P=0.14$).

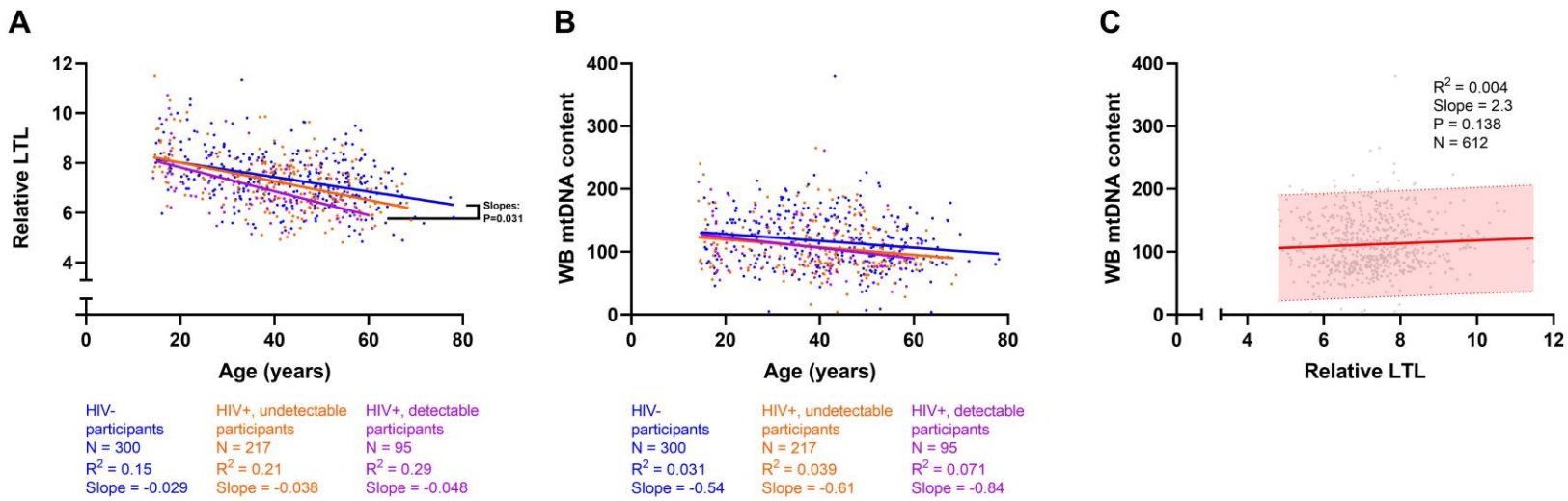

Figure 3.2 Cross-sectional univariate associations between LTL, WB mtDNA content, and age.
Among 612 participants, **(a)** LTL declines with age (R^2=0.17, Slope=-0.03, Pearson's P<0.0001); as does **(b)** WB mtDNA content (R^2=0.03, Slope=-0.57, P<0.0001). Both measures also decline within each HIV sub-group (all p<0.01). Linear regressions of HIV-, HIV+ undetectable pVL, and HIV+ with detectable pVL participants are shown in blue, orange, and magenta, respectively. Differences between slopes were tested and showed that **(a)** LTL declines faster among HIV+ detectable pVL participants than in HIV- controls. **(c)** No detectable relationship exists between LTL and WB mtDNA content (P=0.138). The shaded area indicates the 95% prediction interval. Coefficients of determination (R^2) are shown.

3.3.3 Cross-sectional predictors of LTL

Among all participants, the final multivariable model for LTL (N=612, R^2=0.28) indicated that HIV infection (either with detectable or undetectable pVL), current tobacco smoking, and older age were independently associated with shorter LTL. In contrast, alcohol use, and ACB or Asian ethnicities were associated with longer LTL (**Figure 3.3A**). Cannabis use showed no effect on LTL. In an HIV+ subgroup model (**Figure 3.3B**), in addition to the above factors, detectable HIV pVL was also independently associated with shorter LTL compared to undetectable HIV pVL, (N=312, R^2=0.31). Among HIV-negative participants, current smoking remained associated (N=300, R^2=0.28) with shorter LTL, but current alcohol did not (**Figure 3.3C**). Models showing non-standardized effect sizes are shown in **Figure 3.4**. Although substance use was considered when building our model, to ensure the validity of our findings in the general population, we performed sub-group analyses among participants who never used tobacco, cannabis, or opioids (**Figure 3.5A-C**). Similarly, informed by past studies that showed effects on LTL by chronic co-infections [42], we analyzed participants with no history of either HCV or HBV infection (**Figure 3.5D**). All models showed essentially the same effects as the main model although in the smaller never smoker and never HBV/HCV-coinfected groups, the effect size of undetectable HIV infection was similar but the confidence interval became broader and significance was lost. The effect of detectable HIV infection remained in all sub-group models. Taken together, these secondary models confirmed the robustness of the effects observed in our main model.

3.3.4 Cross-sectional predictors of WB mtDNA content

The final multivariable model for WB mtDNA content (N=612, R^2=0.10) indicated that HIV infection and older age were independently associated with decreased WB mtDNA content, while ACB and Indigenous ethnicities, as well as current alcohol use showed an association with increased WB mtDNA content (**Figure 3.3D**). Contrary to the LTL models, no difference was detected between participants with detectable or undetectable HIV pVL (**Figure 3.3E**). Once again, we carried out sub-group analyses as above and found that older age remained in all models while the effect of HIV was detected sporadically, likely due to lower power and wider confidence intervals (**Figure 3.6**).

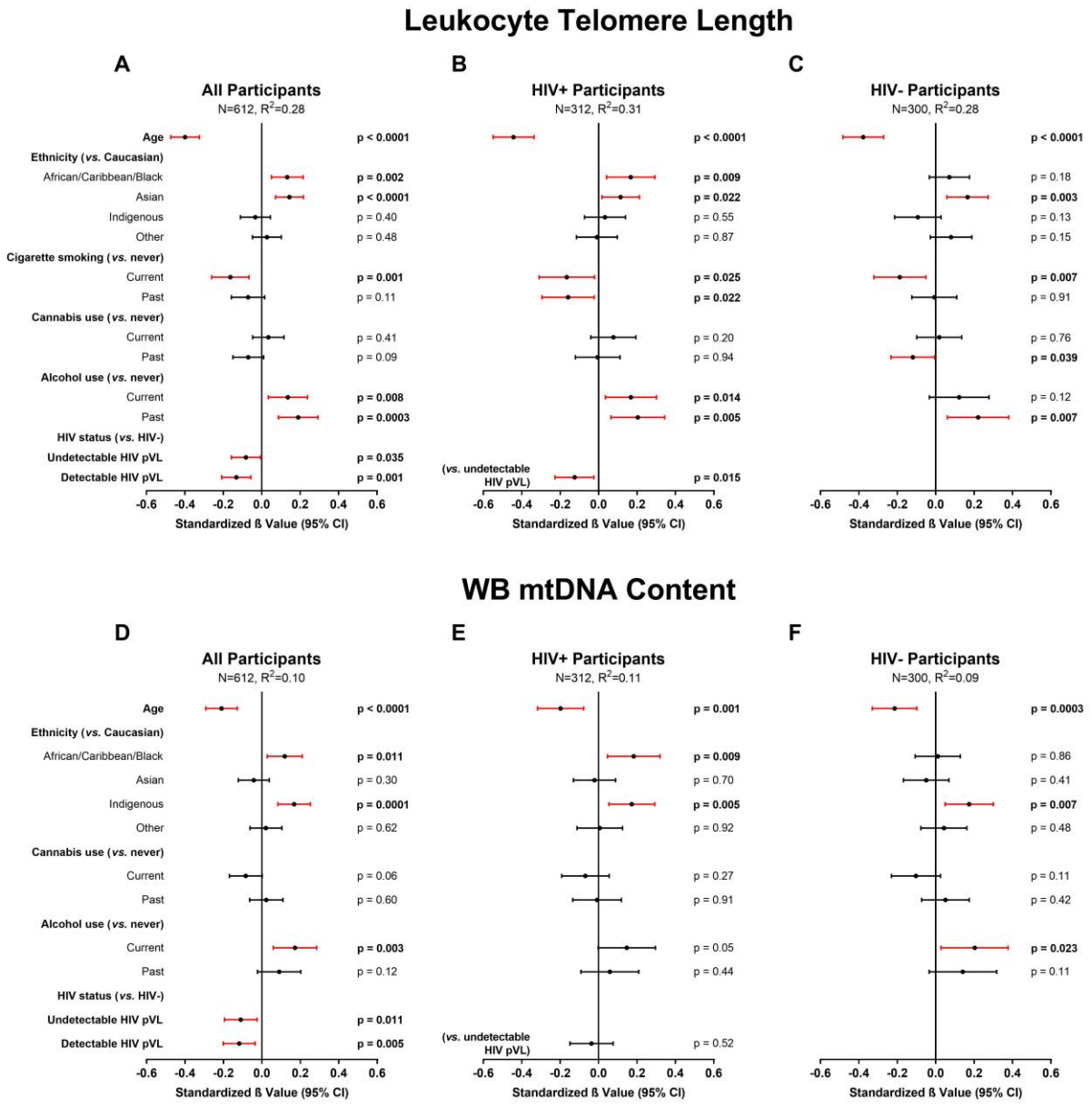

Figure 3.3 Multivariable modelling of cross-sectional LTL and WB mtDNA content.
Final selected multivariable linear regression models of cross-sectional LTL (VIF≤2.1) in **(a)** all, **(b)** HIV+, and **(c)** HIV- participants, and WB mtDNA content (VIF≤1.3) in **(d)** all, **(e)** HIV+, and **(f)** HIV- participants. Final models among all participants were selected automatically by minimizing AIC. Statistical significance depicted by red confidence intervals; negative standardized β values indicate associations with either shorter LTL or lower WB mtDNA content and vice versa. Coefficients of determination (R^2) are shown for each model. The models show that after adjusting for age, ethnicity and substance use, HIV infection is independently associated with shorter LTL and lower WB mtDNA content. Detectable HIV viremia was associated with shorter LTL but not WB mtDNA content.

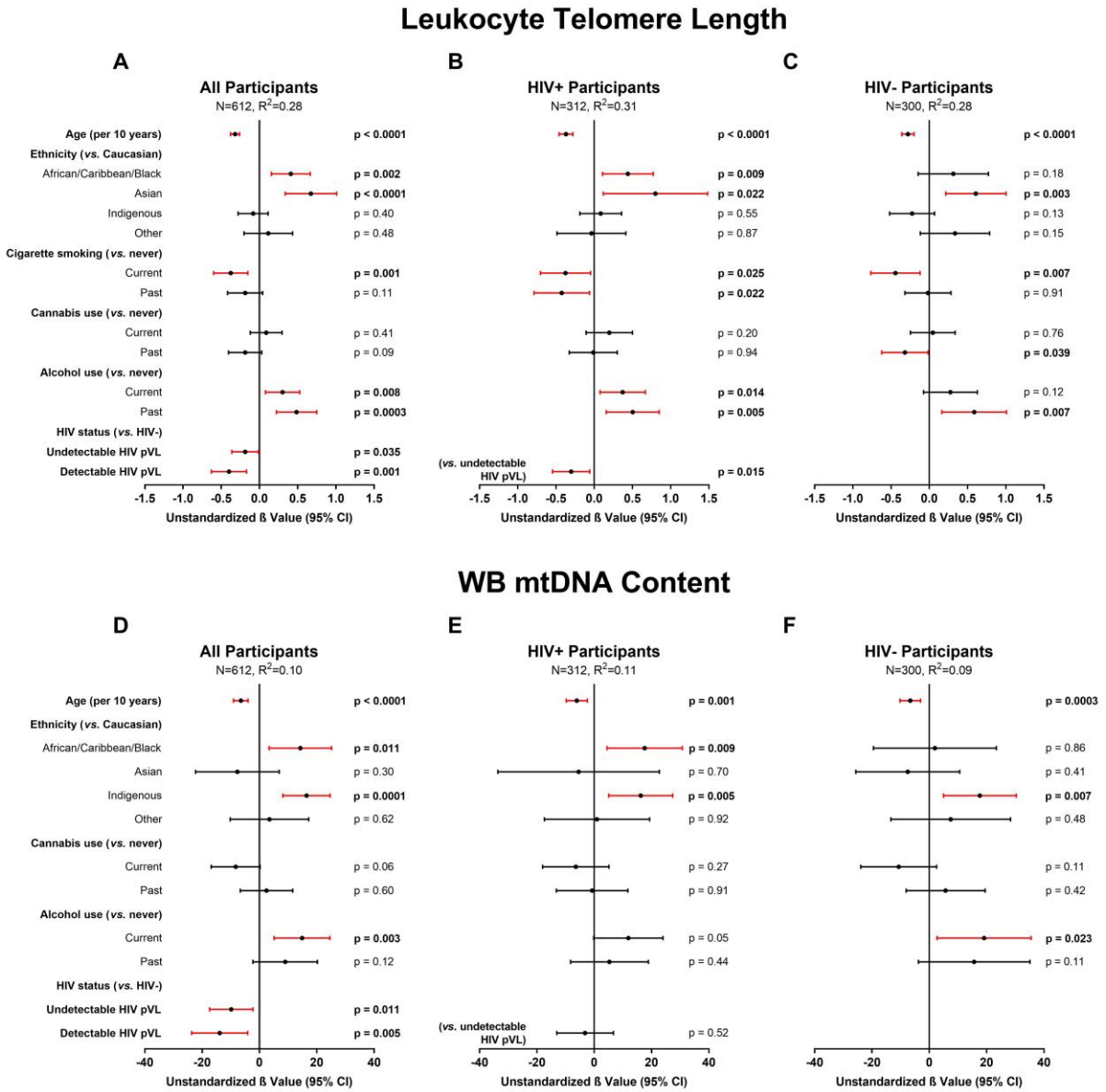

Figure 3.4 Multivariable modelling of cross-sectional LTL and WB mtDNA content with unstandardized effect sizes (β).

Final selected multivariable linear regression models of cross-sectional LTL (VIF≤2.1) in **(a)** all, **(b)** HIV+, and **(c)** HIV- participants, and WB mtDNA content (VIF≤1.3) in **(d)** all, **(e)** HIV+, and **(f)** HIV- participants. Final models among all participants were selected automatically by minimizing Akaike's Information Criterion. Statistical significance depicted by red confidence intervals; negative unstandardized β values indicate associations with either shorter LTL or lower WB mtDNA content and vice versa. Coefficients of determination (R^2) are shown for each model.

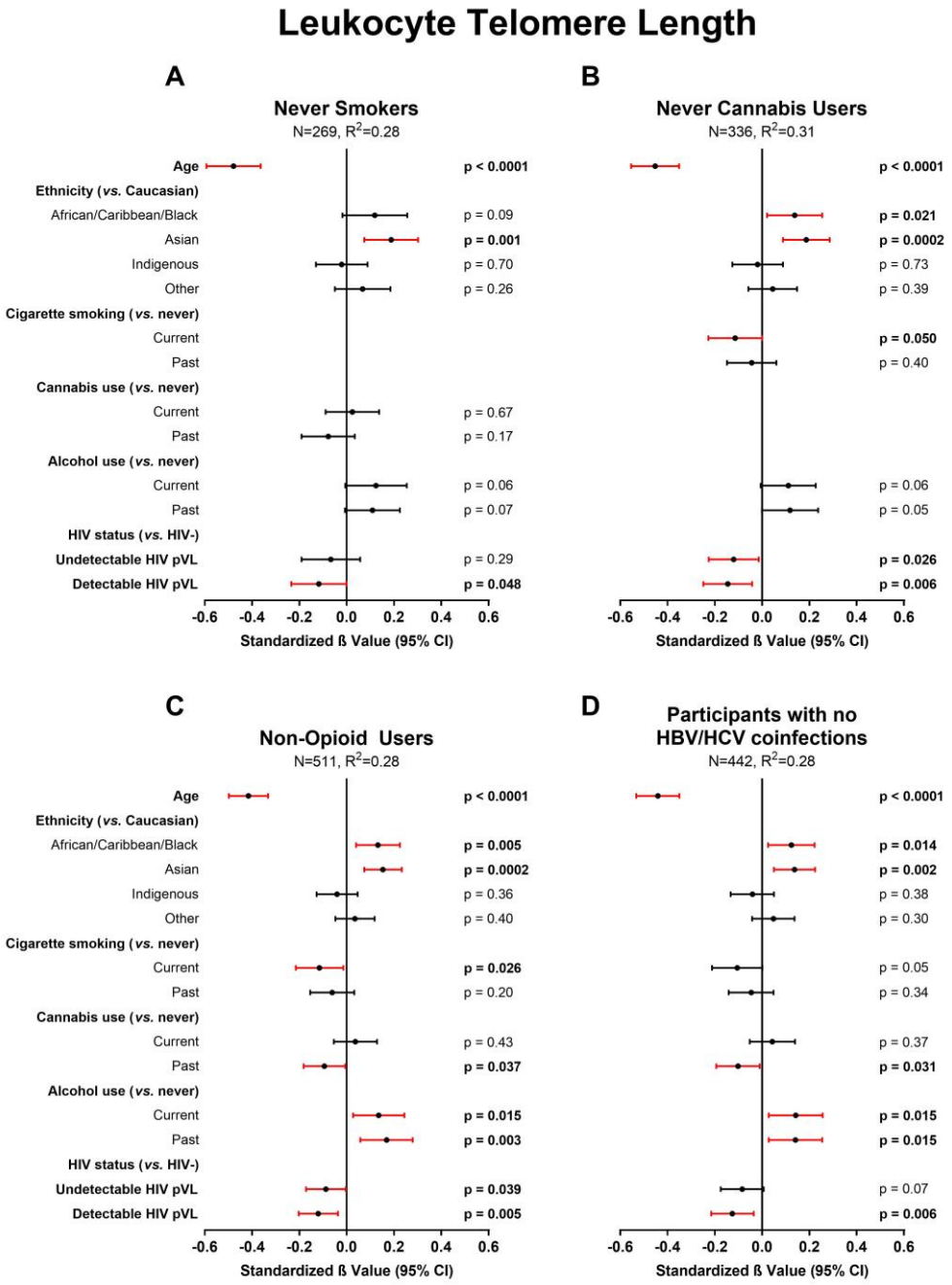

Figure 3.5 Subgroup analyses of cross-sectional LTL.
Multivariable subgroup analyses of LTL (VIF≤1.7) among **(a)** never smokers, **(b)** never cannabis users, **(c)** non-opioid users, and **(d)** participants with no history of HBV or HCV coinfection. Statistical significance depicted by red confidence intervals; negative standardized β values indicate associations with shorter LTL and vice versa. Coefficients of determination (R^2) are shown for each model.

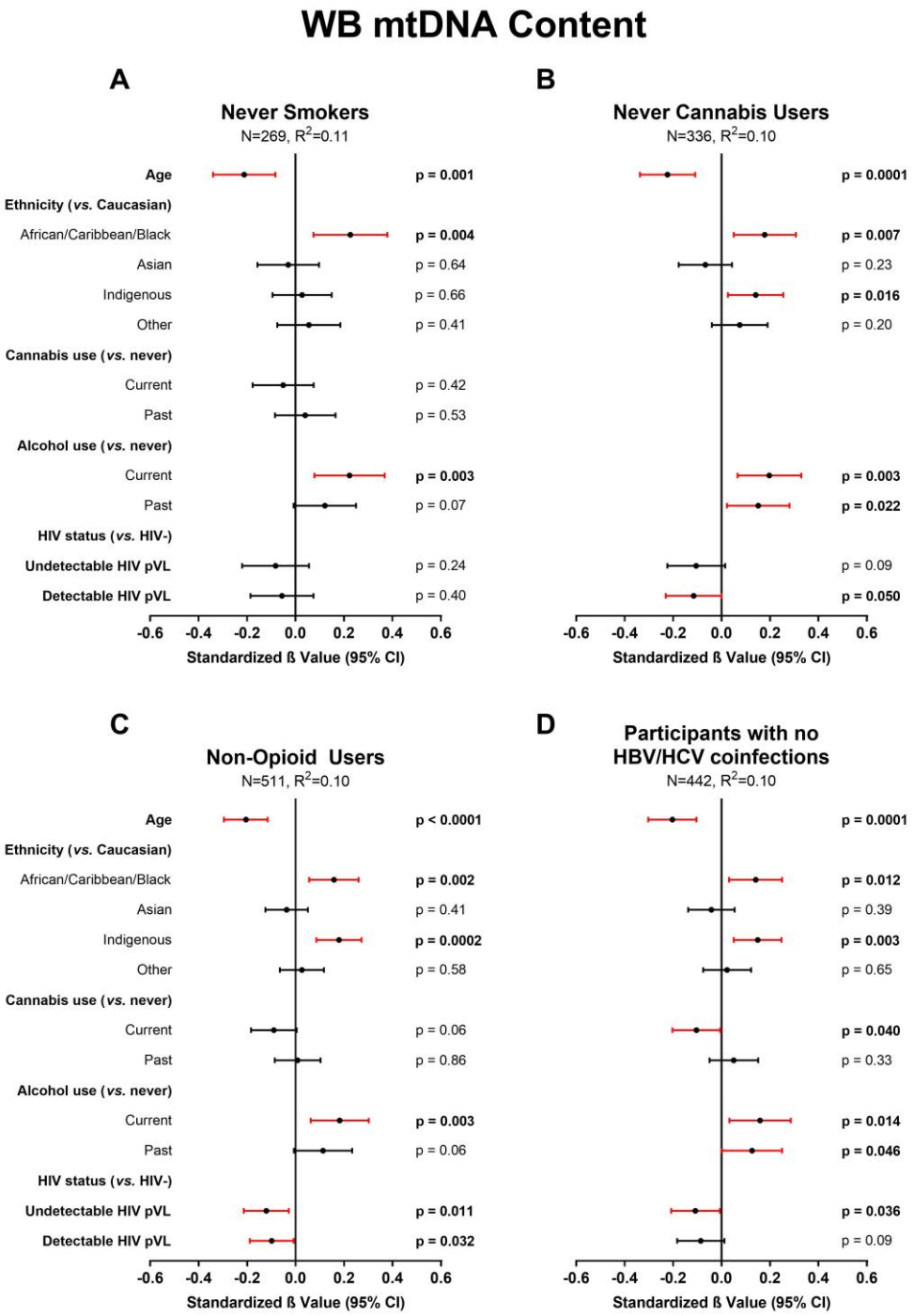

Figure 3.6 Subgroup analyses of cross-sectional WB mtDNA content.
Multivariable subgroup analyses of WB mtDNA content (VIF≤1.4) among **(a)** never smokers, **(b)** never cannabis users, **(c)** non-opioid users, and **(d)** participants with no history of HBV or HCV coinfection. Statistical significance depicted by red confidence intervals; negative standardized β values indicate associations with lower WB mtDNA content and vice versa. Coefficients of determination (R^2) are shown for each model.

Sensitivity models were constructed including platelet count data that were available for a subset of study participants. Here, higher platelet count showed an association with higher WB mtDNA content (**Figure 3.7A-C**) and the relationship between older age and decreased WB mtDNA content remained, but the effect of HIV was lost. However, in these models the sample size of the HIV- group was considerably reduced (N=121 *vs.* N=300).

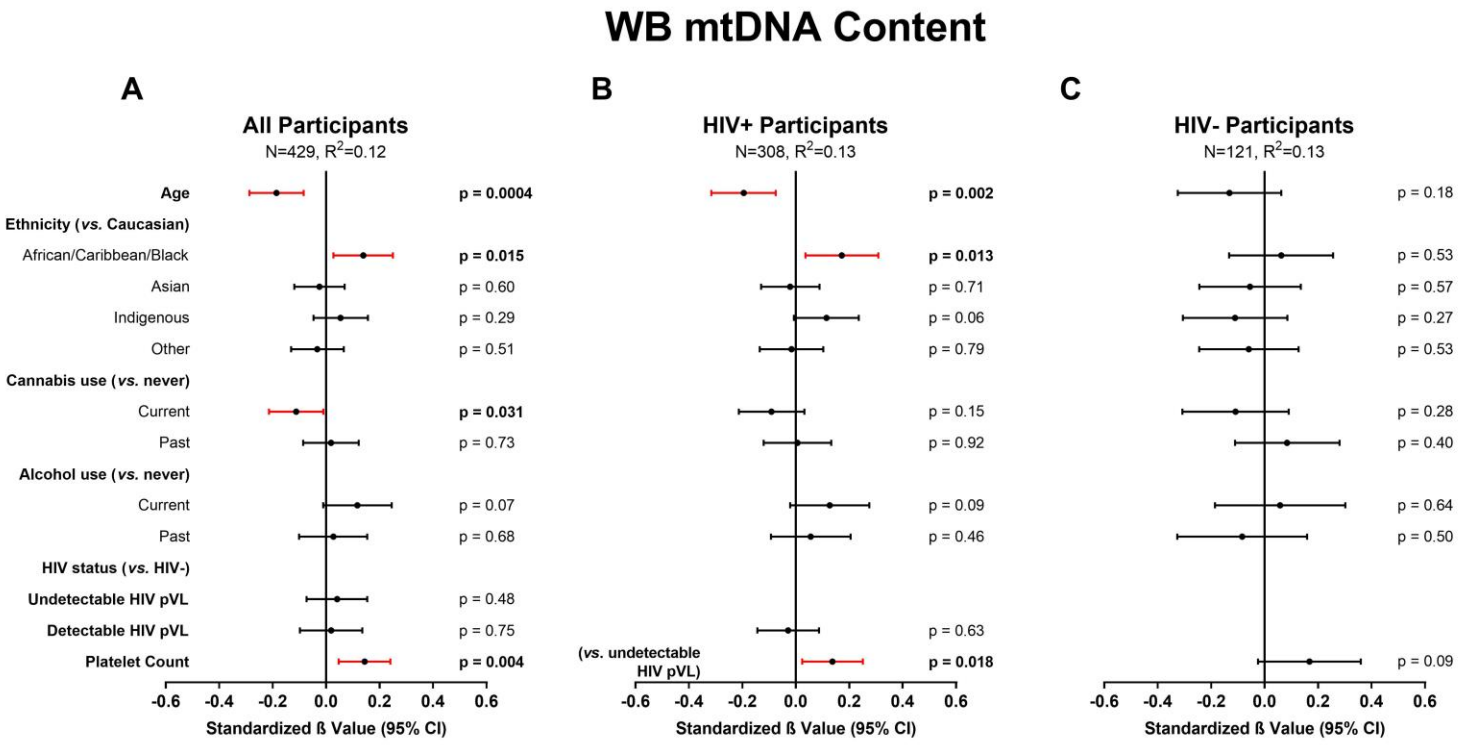

Figure 3.7 Sensitivity analyses of cross-sectional WB mtDNA content with platelet count.
Multivariable sensitivity analyses of WB mtDNA content with platelet count (VIF≤1.3) among in **(a)** all (P<0.0001), **(b)** HIV+ (P<0.0001), and **(c)** HIV- (P<0.11) participants. Statistical significance depicted by red confidence intervals; negative standardized β values indicate associations with lower WB mtDNA content and vice versa. Coefficients of determination (R^2) are shown for each model.

3.3.5 Longitudinal changes in LTL and mtDNA are inversely related

Having determined that both age and HIV affect our two markers cross-sectionally, we then examined the dynamics of the two markers over time, as well as their longitudinal relationship. Of the 612 participants studied cross-sectionally, 228 WLWH and 68 HIV-negative participants had at least one visit ≥1 year earlier, and were included in the longitudinal analyses. Characteristics of the longitudinal subset were similar to whole group (**Table 3.2**) with the exception that age was similar between groups, and baseline mtDNA content was higher in WLWH than HIV-negative controls. A median [IQR] of 4 [2,6], and 3 [2,5] years elapsed between longitudinal visits in WLWH and HIV-negative controls, respectively.

A significant negative relationship was observed between ΔLTL/year and WB ΔmtDNA content/year (R^2=0.13, P<0.001) (**Figure 3.8A**). Overall, participants who lost LTL the fastest were also most likely to have gained mtDNA over the same period (**Figure 3.8B**) and vice-versa whereby those who lost mtDNA the fastest were more likely to have gained LTL (**Figure 3.8C**).

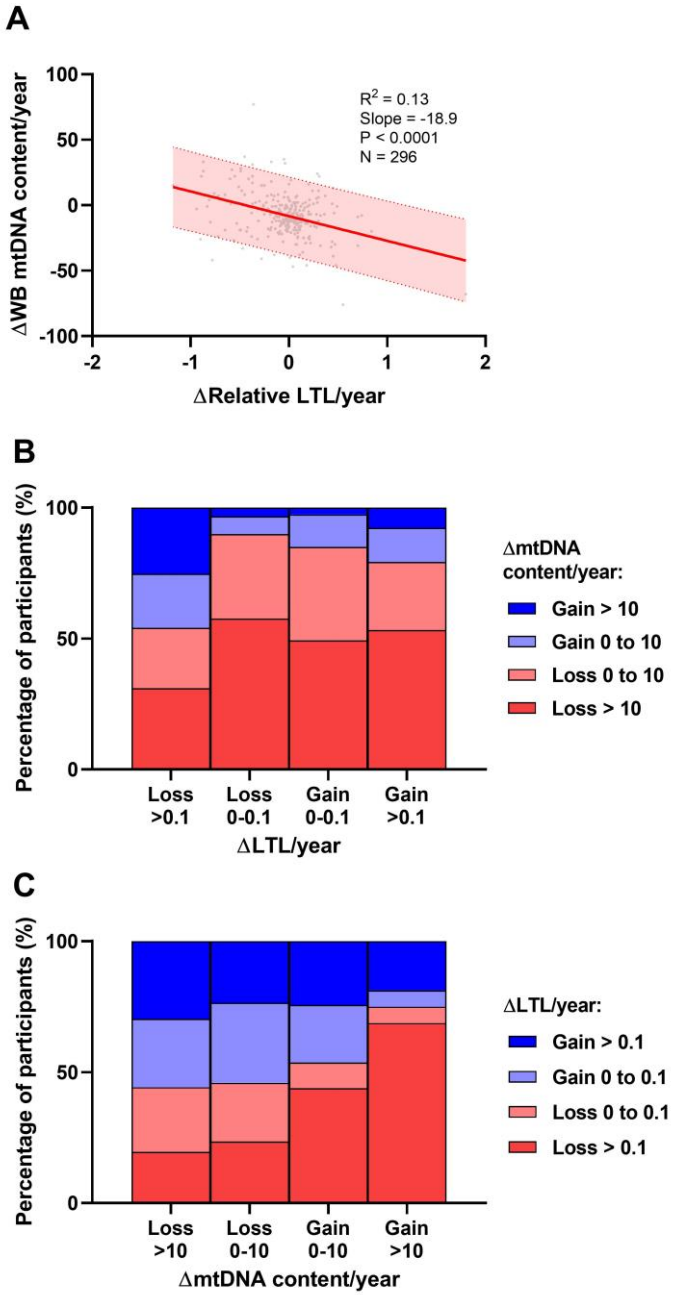

Figure 3.8 Univariate associations between longitudinal rates of change in LTL and WB mtDNA content. **(a)** Data show an inverse relationship between ΔLTL/year and WB ΔmtDNA content/year. Shaded area represents the 95% prediction interval. Coefficient of determination (R^2) and Pearson's P-value shown. **(b)** Participants were categorized based on a small (<0.1) or large (>0.1) loss or gain of ΔLTL/year and further stratified according to a small (<10) or large (>10) loss or gain of WB ΔmtDNA content/year. These data show that participants who lost LTL fastest were more likely to preserve or gain WB mtDNA content. **(c)** Similarly, participants were categorized based on WB ΔmtDNA content/year and stratified according to ΔLTL/year. The data show that participants who lost WB mtDNA fastest were more likely to preserve LTL and vice versa.

3.3.6 Predictors of longitudinal change in LTL

In the univariate analysis, overall relative LTL shortened by 0.036 units per year among all participants. This represents a loss of approximately 36 bp per year, in close agreement with the population attrition rate estimate (33 bp per year) seen in the cross-sectional analysis (**Figure 3.2A**). These univariate investigations were validated by multivariable modelling (N=296, R^2=0.33), where we observed that a slower decrease in WB mtDNA content/year was a strong predictor of faster LTL loss (**Figure 3.9A**), as was having longer LTL at baseline. Older age at baseline was also associated with faster LTL loss while past alcohol use, current opioid use, as well as ACB and Asian ethnicities were associated with slower loss of LTL (**Figure 3.9A**), reminiscent of the cross-sectional analysis. In contrast to the cross-sectional finding, tobacco smoking and undetectable HIV did not show an effect on LTL attrition rate. However, among WLWH, LTL was lost faster in those with a detectable HIV pVL at last visit (**Figure 3.9B**). Among HIV-negative participants (**Figure 3.9C**) only age, baseline LTL and WB ΔmtDNA content were included due to the reduced sample, and they all showed similar effects as those seen in the all participants model. Models showing non-standardized effect sizes are shown in **Figure 3.10**. In all subgroup analyses that excluded substance users or co-infections (**Figure 3.11**), slower loss of WB mtDNA content/year and longer baseline LTL remained independently associated with faster LTL attrition. Similar to the cross-sectional sub-group models, the effect of HIV lost significance in some models, likely due to reduced power.

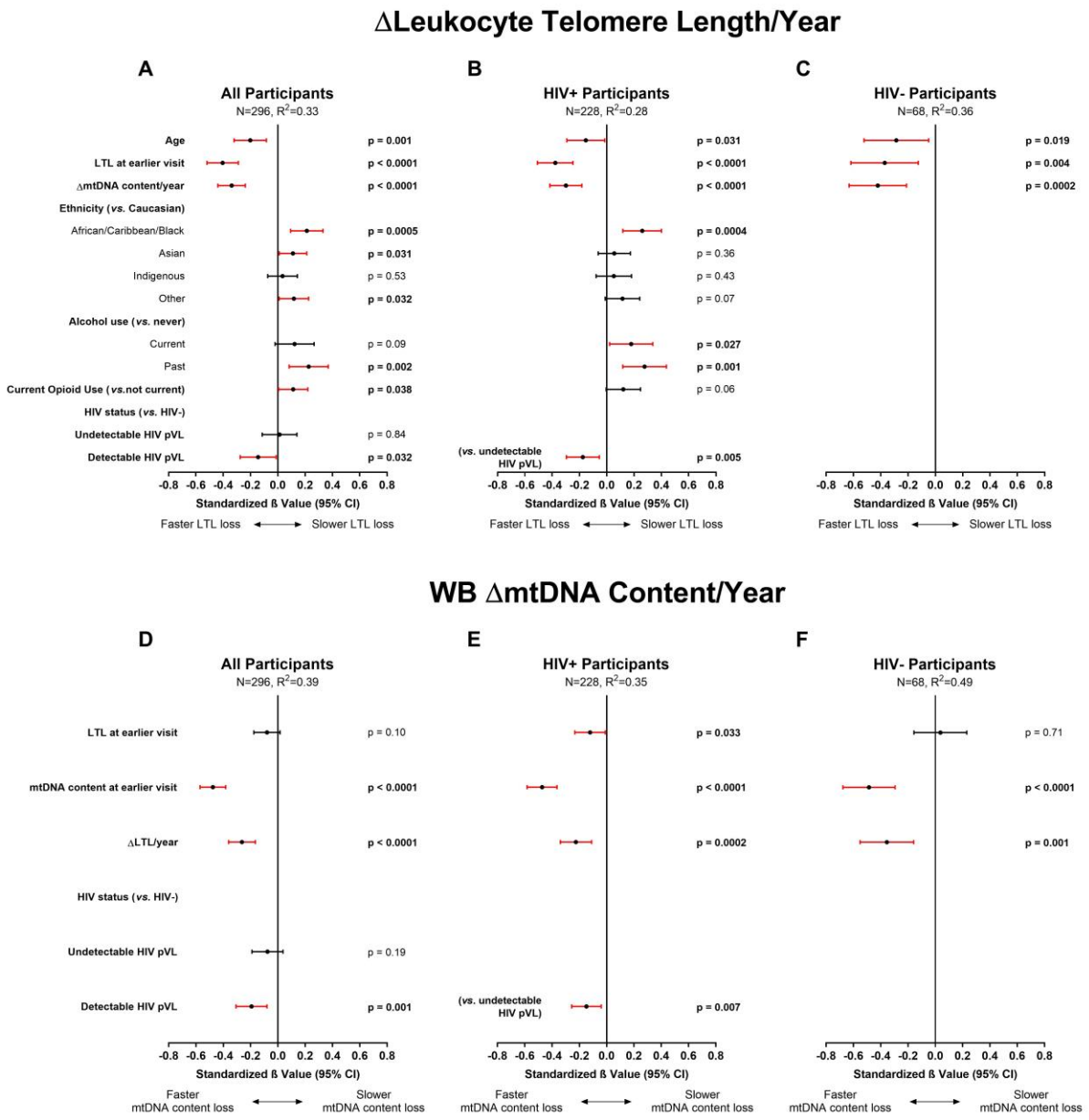

Figure 3.9 Multivariable modelling of longitudinal rates of change in LTL and WB mtDNA content.
Final selected multivariable linear regression models of longitudinal ΔLTL/year (VIF≤1.5) in **(a)** all, **(b)** HIV+, and **(c)** HIV- participants, and WB ΔmtDNA content/year (VIF≤1.2) in **(d)** all, **(e)** HIV+, and **(f)** HIV- participants. Final models among all participants were selected automatically by minimizing AIC. Statistical significance depicted by red confidence intervals; negative standardized β values indicate associations with either faster LTL loss or faster WB mtDNA content loss and vice versa. Coefficients of determination (R^2) are shown for each model. The ΔLTL/year models show that after adjusting for age and LTL at baseline, ethnicity, and substance use, a slower loss of WB mtDNA/year is significantly independently associated with faster LTL attrition. Similarly, the models for WB ΔmtDNA content/year show that after adjusting for LTL and WB mtDNA at baseline, a slower rate of LTL attrition is independently associated with faster loss of WB mtDNA content. Detectable HIV viremia was associated with faster decline in both markers.

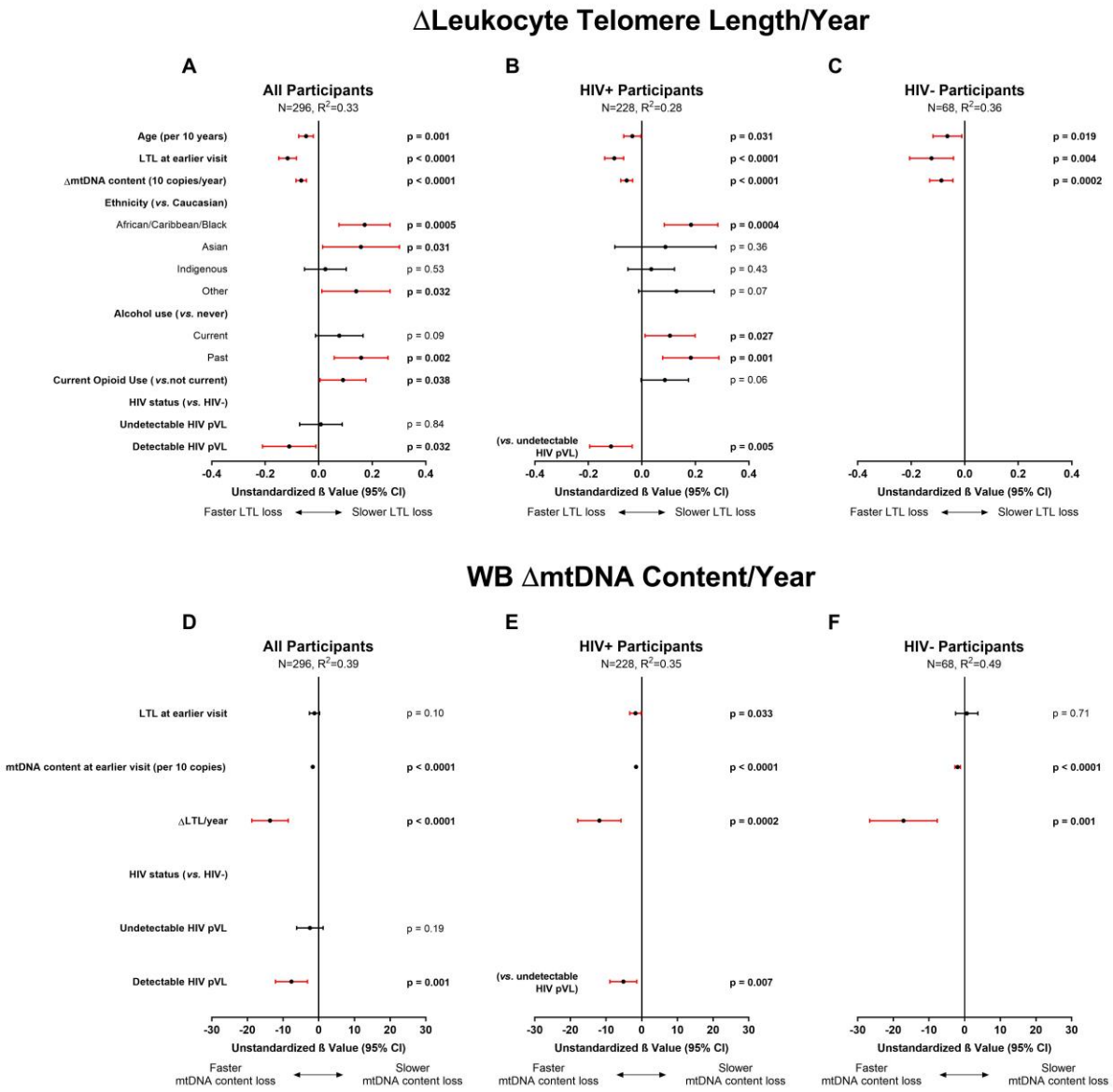

Figure 3.10 Multivariable modelling of longitudinal change in LTL and WB mtDNA content with unstandardized effect sizes (β).

Final selected multivariable linear regression models of longitudinal LTL (VIF≤1.5) in **(a)** all, **(b)** HIV+, and **(c)** HIV- participants, and WB mtDNA content (VIF≤1.2) in **(d)** all, **(e)** HIV+, and **(f)** HIV- participants. Final models among all participants were selected automatically by minimizing AIC. Statistical significance depicted by red confidence intervals; negative standardized β values indicate associations with either faster LTL loss or faster WB mtDNA content loss and vice versa. Coefficients of determination (R^2) are shown for each model.

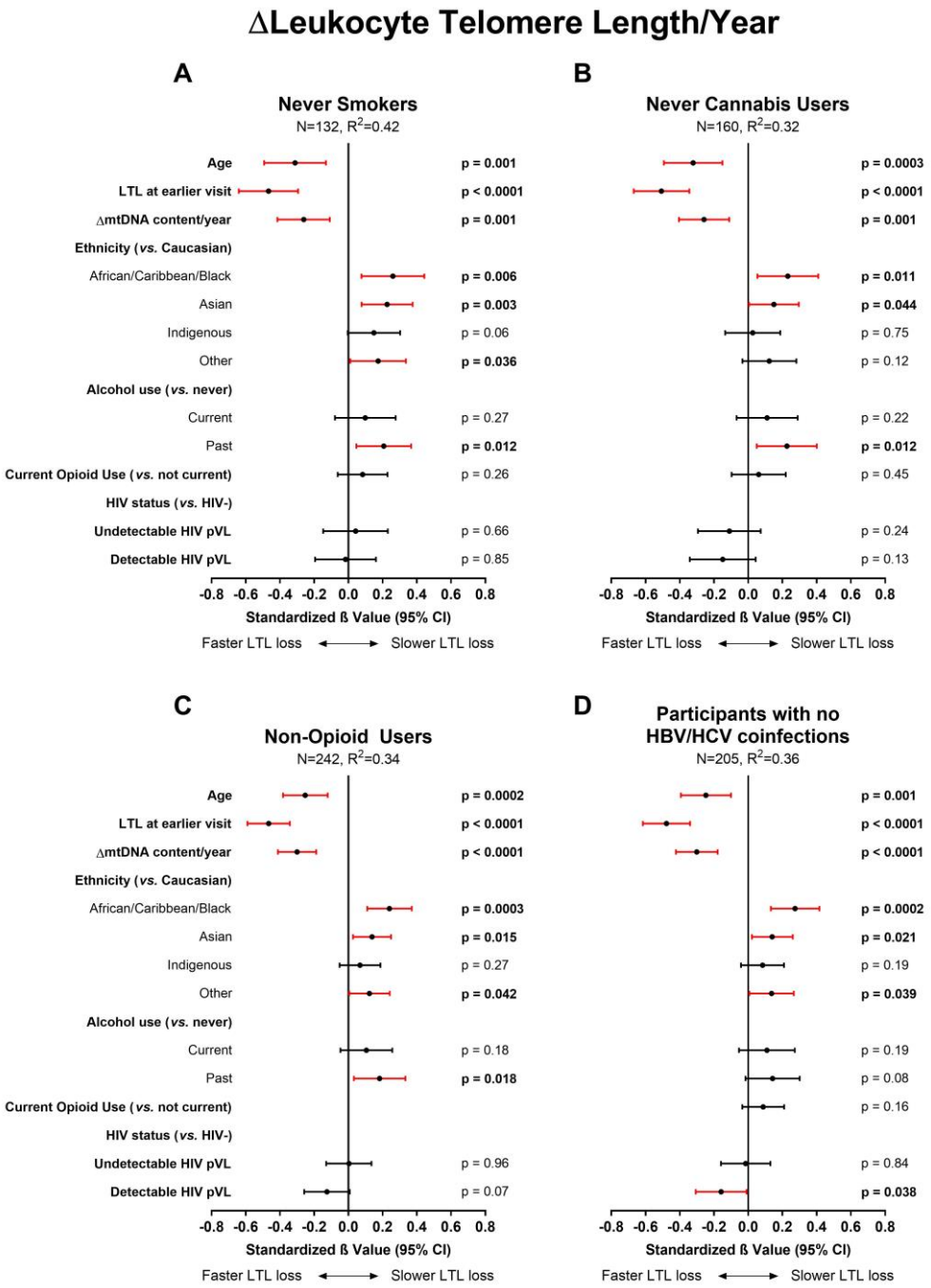

Figure 3.11 Subgroup analyses of longitudinal change in LTL.
Multivariable subgroup analyses of longitudinal ΔLTL/year (VIF≤1.7) among **(a)** never smokers, **(b)** never cannabis users, **(c)** non-opioid users, and **(d)** participants with no history of HBV or HCV coinfection. Statistical significance depicted by red confidence intervals; negative standardized β values indicate associations with faster LTL loss and vice versa. Coefficients of determination (R^2) are shown for each model.

Taken together, our data show that the main predictors of faster LTL attrition were having longer LTL at baseline and a slower WB mtDNA content decline over time. Our data also point toward faster LTL attrition among those who have a detectable HIV pVL while those who maintain viral control showed rates of LTL loss essentially identical to HIV-negative individuals.

3.3.7 Predictors of longitudinal change in WB mtDNA content

In WLWH and controls, WB mtDNA content decreased by a median of 10 and 7 copies of mtDNA per copy of nDNA per year, respectively (**Table 3.2**). Similar to what was observed for ΔLTL, in the final model of WB ΔmtDNA content (N=296, R^2=0.39), detectable HIV infection, higher WB mtDNA content at baseline, and slower LTL attrition rate were each independently associated with a faster decline in WB mtDNA content (**Figure 3.9D**). Among WLWH (**Figure 3.9E**) and HIV-negative controls (**Figure 3.9F**), the same associations were seen. Furthermore, compared to WLWH with undetectable HIV pVL, having a detectable HIV pVL at last visit was associated with faster WB mtDNA content decline (**Figure 3.9E**). Sub-group analyses were highly similar to the all-participant model (**Figure 3.12**) and the effect of viremia persisted in all models. Adding platelet counts to the WB ΔmtDNA content models had no effect, and platelet count itself showed no association with WB ΔmtDNA content (**Figure 3.13**).

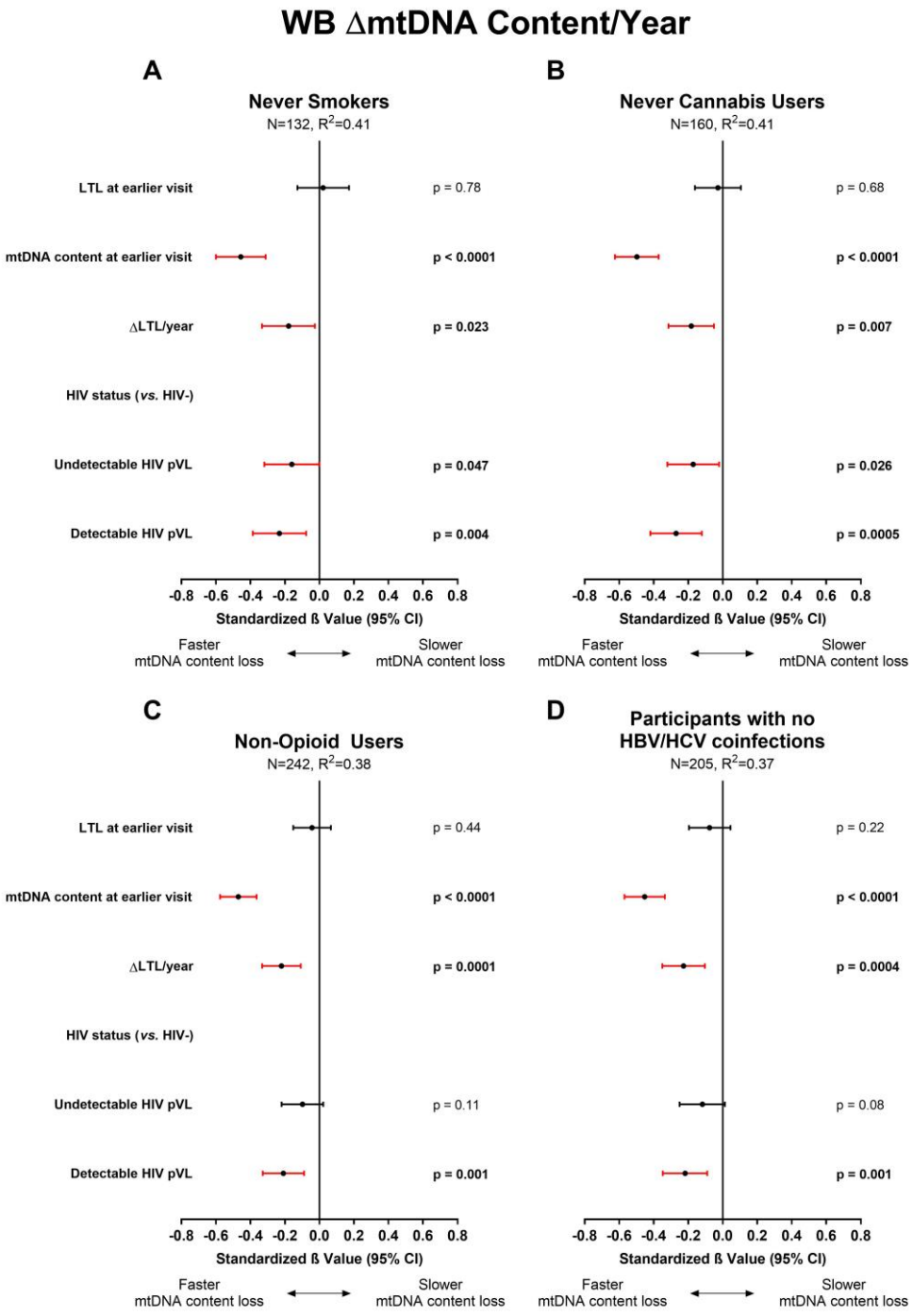

Figure 3.12 Subgroup analyses of longitudinal change in WB mtDNA content.
Multivariable subgroup analyses of longitudinal WB ΔmtDNA content/year (VIF≤1.3) among **(a)** never smokers, **(b)** never cannabis users, **(c)** non-opioid users, and **(d)** participants with no history of HBV or HCV coinfection. Statistical significance depicted by red confidence intervals; negative standardized β values indicate associations with faster WB mtDNA content loss and vice versa. Coefficients of determination (R^2) are shown for each model.

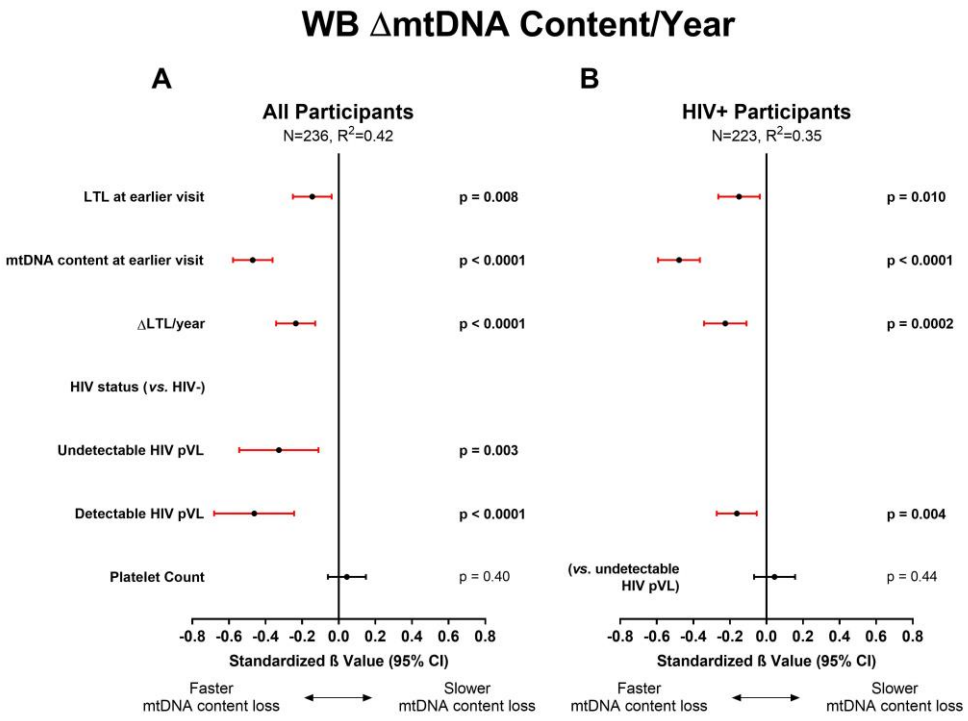

Figure 3.13 Sensitivity analyses of change in longitudinal WB mtDNA content with platelet count. Multivariable sensitivity analyses of WB ΔmtDNA content/year with platelet count (VIF≤1.2) among in **(a)** all and **(b)** HIV+ participants. Statistical significance depicted by red confidence intervals; negative standardized β values indicate associations with faster WB mtDNA content loss and vice versa. Coefficients of determination (R^2) are shown for each model.

Overall, as seen for the change in LTL, the strongest predictors of faster decrease in WB mtDNA content were higher WB mtDNA content at baseline and slower LTL loss. In addition, having a detectable HIV pVL accelerated mtDNA loss.

3.4 Discussion

This is the first human cohort study to incorporate both LTL and WB mtDNA content measures and their rates of change over time, adjusting for relevant covariates. Our primary finding is that the rates of change in the two measures are inversely associated, meaning that while both decline with age, a faster decline in one marker is observed if the decline in the other is slower, and vice-versa. We further show the negative impact of uncontrolled HIV viremia on both LTL and WB mtDNA content loss longitudinally. Given that both markers were measured using the same technique (MMqPCR) on the same cohort specimens, this study was uniquely suited to characterize the relative effect of predictors, as well as the influence of one marker on the other. These data highlight the importance of investigating both LTL and WB mtDNA content as complementary and non-independent markers of aging.

The inverse relationship between LTL and mtDNA content attrition rates, seen in both the ΔLTL/year and the ΔmtDNA content/year models, is a novel finding and sheds light on previously proposed mechanisms that implicate a relationship between telomere and mitochondrial biology. This effect is consistent with the dual functions of telomerase. While the classical function of telomerase is to maintain telomeres, *in vitro* research has demonstrated that under oxidative stress conditions, the enzymatic subunit of telomerase translocates to the mitochondria where it exerts a protective function against oxidative damage but appears to

neglect telomere maintenance [89,90]. A similar phenomenon may be occurring *in vivo* when mitochondria require protection, potentially resulting in mitigated mtDNA loss at the cost of higher LTL attrition rate, as seen here. If so, this would suggest that upon oxidative stress challenge, telomerase confers a necessary and immediate protection to the mitochondria at the expense of the long-term benefit of telomere maintenance. Future longitudinal studies with a longer interval between measures are needed to determine if this apparent "yin and yang" effect persists over longer periods of time. It should also be confirmed in an independent cohort.

The rate of LTL attrition observed agrees with previous research [21] and is consistent between our cross-sectional and longitudinal data. Although WB mtDNA content also declined with age, both univariable and multivariable analyses explained a smaller percentage of the total variance compared to that of LTL models. Given that the variability of the two assays is comparable [101,102], this suggests that either WB mtDNA content is intrinsically more stochastic, or that the mtDNA analyses presented here missed key explanatory variables. Such yet unidentified variables may partially explain the inconsistency in previous attempts by researchers to establish WB mtDNA content as a robust marker of aging. A potential confounder that we addressed in WB mtDNA content models was platelets, which may lead to overestimation of WB mtDNA content. Two studies have shown that a very large increase in platelet mtDNA contribution would be necessary to meaningfully affect WB mtDNA content measurement [335,336], and others found no relationship between platelet count and WB mtDNA content [73,337]. Based on this and our own unpublished data in a non-HIV sample, we did not initially intend to include platelet count in our analyses. However, a recent study highlighted the importance of platelet count in studies investigating the effect of HIV on WB mtDNA content [74]. Therefore, to increase the

rigor of our analysis, we analyzed a subset of our participants for whom platelet count data were available to investigate the role of platelets in WB mtDNA content and its change over time. We found that platelet count had no effect on our longitudinal models. Despite a modest reduction in power, the effects of HIV on faster WB mtDNA attrition as well as the inverse relationship between the rates of change in LTL and WB mtDNA content over time persisted. However, while platelet count affected WB mtDNA content cross-sectionally, its inclusion resulted in a substantial reduction in sample size and the effect of HIV lost statistical significance. It remains unclear whether the well-established relationship between HIV and decreased WB mtDNA content is partially driven by thrombocytopenia in people living with HIV.

We could not detect any significant cross-sectional relationship between LTL and WB mtDNA content, whether univariately or multivariately, in contrast to some studies in healthy adults that reported a modest correlations (R^2=0.15, and R^2=0.03) [91,95]. The reason for this is unclear and may be related to differences in the assays used and the range they yield. There could also be a bias toward not reporting negative findings (i.e. no correlation) by other studies. Furthermore, past studies did not examine this relationship while adjusting for covariates and confounders.

HIV infection and uncontrolled viremia have been previously associated with both shorter LTL [42] and lower mtDNA content [73,74]. Based on non-standardized effect sizes, our study demonstrates that the independent effects on LTL by HIV infection, uncontrolled HIV viremia, and current tobacco smoking are each similar to approximately one decade of chronological aging. Furthermore, we show that the decline of both LTL and mtDNA content with age is accelerated in participants with uncontrolled HIV viremia, emphasizing the importance of

maintaining HIV viral control. This is supported by model estimates showing that having uncontrolled viremia increases the LTL loss per year of aging from approximately 30 bp to more than 100 bp.

Previous research has shown early and rapid LTL decline following HIV acquisition [43,338], which may result from an initial HIV-induced immune activation leading to rearrangement of leukocyte subsets. It is possible that a similar phenomenon is occurring here, where immune cell proliferation triggered by actively replicating HIV results in faster apparent attrition of both LTL and WB mtDNA content. A recent study demonstrated faster mtDNA content attrition among WLWH who were approximately 50 years old compared to controls [74]. However, more research with longitudinal samples spanning longer periods of time is necessary to determine whether this effect is transient or carries long-term consequences. Indeed, these findings are in keeping with the model of HIV-mediated accelerated aging and may explain the link between HIV and aging comorbidities. While HIV represents a valuable model of accelerated human aging, other chronic and proinflammatory diseases such as diabetes, rheumatoid arthritis, and other chronic/latent viral infections associated with aging comorbidities may similarly modulate LTL and mtDNA content.

In support of previous research, we show that tobacco smoking is robustly independently associated with shorter LTL. In most subgroup analyses, this effect exists only among current smokers, suggesting that smoking cessation confers a LTL benefit, as reported by others [36]. However, it is unclear why the benefit of smoking cessation was not detected among WLWH. It is possible that time since smoking cessation differed between groups. Alternatively, the

mechanism by which LTL recovers after smoking cessation may be adversely affected by the presence of HIV. Smoking was also not associated with LTL attrition rate, likely because the time elapsed between longitudinal visits was insufficient for the effect of smoking to reach a detectable size.

In contrast, alcohol use was associated with longer LTL, slower LTL attrition, and increased WB mtDNA content. While this may seem to contradict some research reporting shorter LTL in people who abuse alcohol [339], other studies are less clear as to the relationship between LTL and moderate alcohol consumption [57,340]. Our definition for this variable was any alcohol use regardless of quantity, which does not imply abuse and would also include low to moderate users. Moreover, unlike tobacco smoking or opioid use, alcohol use is lower among our WLWH. The apparent association between alcohol use and both longer LTL and increased WB mtDNA content may therefore be the result of nested effects with unknown factors more prevalent among the HIV-negative group, and not fully addressed by the covariates considered herein. It is also possible that we detected a spurious finding, as the association with alcohol disappeared in some subgroup analyses. Nevertheless, the associations between alcohol and the markers studied here is of interest and should be reproduced in an independent cohort, along with a more granular analysis of alcohol consumption, with respect to frequency and quantity.

While differences in LTL dynamics between men and women exist, this study includes only female participants. As such, we are not able to comment on whether the same predictors of LTL and WB mtDNA content would be seen in men. Furthermore, this analysis also does not

consider the intensity and frequency of substance use. The role of sex and substance use should therefore be further examined.

In summary, we describe a novel relationship between longitudinal LTL and WB mtDNA dynamics, whereby better preservation of LTL appears to occur at the cost of mtDNA loss and vice versa. We also validate the cross-sectional predictors of LTL and WB mtDNA content that have been previously shown. In addition, we demonstrate that for women living with HIV, loss of viral control exacerbates both LTL and WB mtDNA content attrition and may contribute to biological aging. Taken together, our findings provide further evidence supporting the importance of consistently maintaining HIV viral control. Given that the effects of HIV viremia are believed to be largely related to chronic inflammation, it is possible that other proinflammatory conditions would similarly exacerbate cellular aging through related mechanisms. Our findings further imply that future longitudinal studies of either LTL or WB mtDNA content as a biomarker should also consider the other given their strong relationship.

Chapter 4: HIV slow progressors experience accelerated aging compared to HIV non-slow progressors

4.1 Abbreviated introduction to chapter

Despite the growing body of literature supporting HIV-mediated accelerated immune aging in the HIV population, even among people successfully treated with cART, several key questions remain. It is unknown to what extent T cell subset TL is affected by cART-controlled HIV infection. In addition, it remains unknown to what extent HIV slow progressors (SPs) are protected against HIV-mediated immune aging. To date, no sufficiently powered study has compared immune aging in SPs to non-slow progressors (NSPs). A primary goal of this study was to investigate markers of immune aging in HIV with more granularity, such as TL within relevant immune cell subsets, and investigate any differences in SPs. We hypothesized that HIV infection would be associated with shorter TL in senescent CD8 T cells, decreased mtDNA content in senescent CD8 T cells, increased senescent:proliferative CD8 T cell ratio, larger populations of differentiated CD8 T cells, and/or smaller populations of naïve CD8 T cells. We further hypothesized that SP status would confer protection against aging in one or more of the markers described above.

4.2 Materials and methods

4.2.1 Study sample

Study participants were PLWH and HIV-negative controls enrolled in the CARMA cohort [42] and the Canadian Cohort of HIV+ Slow Progressors [341] between November 2006 and May 2017. HIV study groups were defined as in **Table 4.1**, with SP subgroups as previously described [341]. Briefly, participants were considered SPs if they could be classified into the following groups at study entry: elite controllers with undetectable (<50 HIV-RNA copies/ml) pVL, virologic controllers with 50-3000 HIV-RNA copies/ml, or non-virologic controllers with >3000 HIV-RNA copies/ml who had been living with HIV for >7 years without cART. All SPs were cART-naïve and had a CD4 count >500/mm^3 at study entry. Although sustaining viral control or remaining cART-naïve at visit was not a requirement among SP groups, both were fairly well maintained. At visit, all elite controllers were cART-naïve and 7 of 28 had detectable pVL. Of these, 4 elite controllers had 50 or 51 HIV-RNA copies/ml and the remaining 3 had <500 HIV-RNA copies/ml. Among the remaining 29 SPs, 2 were on cART at visit with undetectable pVL. One virologic controller had 3648 HIV-RNA copies/ml at visit, while the remaining virologic controllers maintained <3000 HIV-RNA copies/ml at visit. Participants were categorized as NSPs if they were not cART-naïve at baseline and had undetectable pVL at visit. Among participants with detectable pVL at visit, those who were not SPs were categorized as uncontrolled progressors (UPs). All participants provided written informed consent.

Table 4.1 Description of HIV study groups

Study Group	CD4 T cell count at baseline (cells/µl)	Viral load at baseline (HIV-RNA copies/ml)	Time Since HIV Diagnosis (years)	ART Naïve at baseline	Viral load at visit (HIV-RNA copies/ml)
Slow progressor (SP)					
Elite controller	>500	<50	-	Yes	-
Virologic controller	>500	50-3000	-	Yes	-
Non-virologic controller	>500	>3000	>7	Yes	-
Non-slow progressor (NSP)	-	-	-	No	<50
Uncontrolled progressor (UP)*	-	-	-	-	≥50

*Only participants who were not categorized as SPs were considered for inclusion as UPs

Sample selection is described in **Figure 4.1**. SPs were age- and sex-matched 1:1:1:1 to NSPs, UPs, and HIV-negative controls. SPs and UPs were participants enrolled in either the Canadian Cohort of HIV+ Slow Progressors or CARMA, whereas NSPs and HIV-negative controls were all participants enrolled in CARMA. CARMA participants were predominantly women, so only a random subset of men from the Canadian Cohort of HIV+ Slow Progressors with available biospecimens were considered for sample selection in order to balance sex between cohorts. Matching was done systematically by applying an algorithm that matched SPs with NSPs, UPs, and HIV-negative individuals of the same sex by minimizing age difference. For rare situations in which two SPs were matched to the same individual, a substitute was matched to one of the SPs such that the average absolute age difference across all matches was minimized. If one of the specimens was rejected for failing QC at the cell sorting stage, it was replaced by the next available unique specimen closest in age. Lastly, although there were enough UP participants to match to each SP, comparing SPs to UPs was not a focus in this study, and as such, only 14 participants from each cohort were randomly selected for matching to SPs.

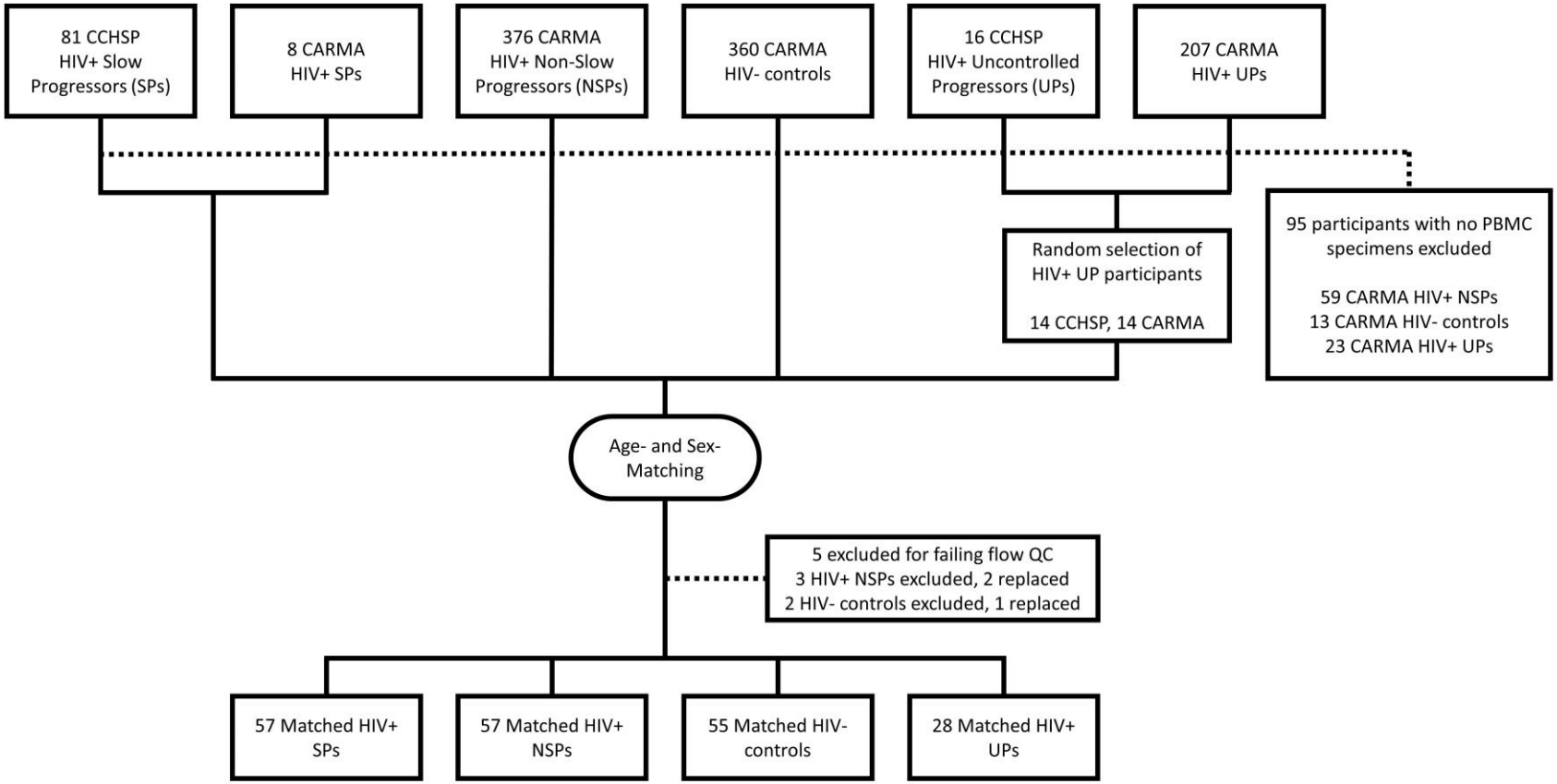

Figure 4.1 Schematic of the study sample selection.
In summary, 57 SP participants were age- and sex-matched with 57 NSP participants (57:57). Of these, 55 were matched to HIV-negative controls (55:55:55) and 28 were matched to UP participants (28:28:28:28). All SP women and a subset of randomly selected SP men were initially included from all Canadian Cohort of HIV+ Slow Progressors (CCHSP) participants with available biospecimens.

4.2.2 Demographic and clinical data collection

Age, sex, ethnicity, date of HIV diagnosis, peak HIV pVL, and CD4 nadir were collected at study entry. Tobacco smoking status, BMI, CD4 count, and HIV viral load were collected at each study visit. Complete cART history was documented, from which cART status at visit was derived. During data collection, ethnicity was categorized as African/Caribbean/Black, Asian/South Asian, Hispanic, Indigenous, White, or other. However, there were few Asian/South Asian and Hispanic participants, and as such, they were grouped together with the "other" category for statistical analyses. Smoking status was trichotomized into current, past, or never smoker. History of HBV and HCV was collected by self-report, and CMV status was determined by serology at visit.

4.2.3 Blood collection and processing

WB was collected at study entry and each study visit. For CARMA participants, PBMCs were isolated within 48 h of blood collection using Ficoll-Paque™ Plus (Cat# 17-1440-02, Sigma-Aldrich, St. Louis, MO, US) density gradient centrifugation according to manufacturer's recommendations. PBMCs were frozen at -80°C in Chinese hamster ovary (CHO) media (Cat# 10743-011, Thermo Fisher Scientific, Waltham, MA, US) with 10% dimethyl sulfoxide (DMSO, Cat# D2650-100ML, Sigma-Aldrich) for 24 h and then stored in liquid nitrogen until needed. PBMCs were available for all participants, but WB was available for CARMA participants only. PBMCs from the Canadian Cohort of HIV+ Slow Progressors were provided to us from their specimen bank committee.

4.2.4 Fluorescence-activated cell sorting (FACS)

Immunophenotyping and live cell sorting of four lymphocyte subsets (B cells, CD4+ T cells, proliferative CD8+CD28+ T cells, and senescent CD8+CD28- T cells) were done simultaneously using an 11-colour flow cytometry panel. Cryopreserved PBMCs initially prepared from 1.5-6.0 ml of whole blood were rapidly thawed in 10 ml pre-warmed RPMI-1640 (Cat# A10491-01, Thermo Fisher Scientific) supplemented with 10% fetal bovine serum (FBS, Cat# 12483-020, Thermo Fisher Scientific), then washed twice in Dulbecco's phosphate buffered saline (dPBS, pH 7.0-7.3, Cat# 14190-136, Thermo Fisher Scientific) with 2% FBS. Cells were stained in 100 µl for viability using Fixable Viability Stain 700 (FVS700) and surface markers using the following fluorescently-conjugated monoclonal antibodies that were individually titrated: CD45-BV510, CD3-PerCP-Cy5.5, CD4-BV786, CD8-PE-Cy7, CD28-BV421, CD27-APC, CD45RA-PE, CD25-BB515, CD127-PE-CF594, and CD19-APC-eFluor780. Cells were washed again in dPBS+2% FBS, filtered through a 40 µm cell strainer (Cat# 10199-654, VWR International, Radnor, PA, US) and immediately sorted on a Moflo Astrios EQ cell sorter (Beckman Coulter, Indianapolis, IN, USA). Gating strategy, reagent list, and instrument emission filters are shown in **Figure 4.2** and **Table 4.2**. Briefly, lymphocytes were gated on morphology using light scatter and live leukocytes as $CD45^{+}FVS700^{dim}$ cells. Within live lymphocytes, $CD3^{-}CD19^{+}$ cells were sorted as B cells, $CD3^{+}CD19^{-}CD4^{+}CD8^{-}$ cells as CD4+ T cells, $CD3^{+}CD19^{-}CD4^{-}CD8^{+}CD28^{+}$ cells as proliferative CD8+ T cells, and $CD3^{+}CD19^{-}CD4^{-}CD8^{+}CD28^{-}$ cells as senescent CD8+ T cells. Lysis buffer (200 µl, buffer AL, Qiagen) was added to the sorted cell pellets before they were stored at -80°C until DNA extraction. For quantification of CD4+ and CD8+ T cell subsets, naïve (T_N), central memory (T_{CM}), effector memory (T_{EM}), and terminally-differentiated effector memory (T_{EMRA}) cells were defined using $CD45RA^{+}CD27^{+}$, $CD45RA^{+}CD27^{-}$,

$CD45RA^{-}CD27^{-}$, and $CD45RA^{+}CD27^{-}$, respectively. T_{regs} were defined as $CD127^{-}CD25^{+}$ cells within the CD4+ T cell population. For two populations that showed lower resolution (B cells and T_{reg}), fluorescence minus one (FMO) controls were used to define gates. In this study, cell subset population sizes are expressed as the proportion of cells relative to the larger cell compartment, such as $\%T_{regs}$ within the CD4 compartment, rather than an absolute cell count per volume of blood.

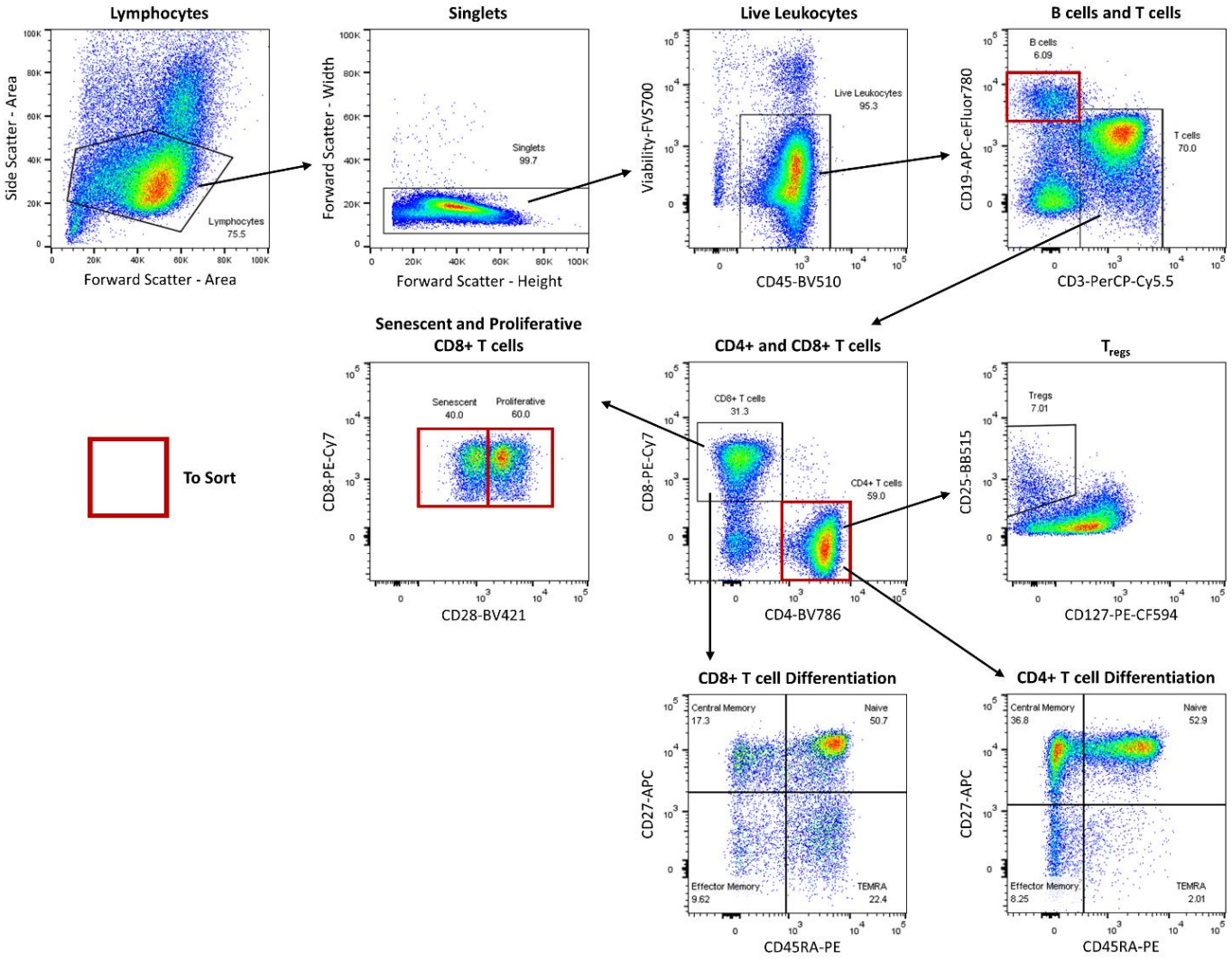

Figure 4.2 PBMC flow cytometry immunophenotyping gating strategy.
Numbers indicate population size as a percentage of parent gate. Sorted populations are marked by red boxes.

Table 4.2 Antibodies used for cell sorting

Antibody/Stain	Clone	Fluorochrome	Vendor	Cat. Number	Laser Line (nm)	Emission filters (nm)
Mouse Anti-Human CD28	CD28.2	BD Horizon™ BV421	BD Biosciences	562613	405	448/59
Mouse Anti-Human CD45	HI30	BD Horizon™ BV510	BD Biosciences	563204	405	513/26
Mouse Anti-Human CD4	SK3	BD Horizon™ BV786	BD Biosciences	563877	405	795/70
Mouse Anti-Human CD25	M-A251	BD Horizon™ BB515	BD Biosciences	565096	488	510/20
Mouse Anti-Human CD3	UCHT1	PerCP-Cy™5.5	BD Biosciences	560835	488	710/45
Mouse Anti-Human CD45RA	HI100	PE	BD Biosciences	561883	561	579/16
Mouse Anti-Human CD127	HIL-7R-M21	BD Horizon™ PE-CF594	BD Biosciences	562397	561	664/22
Mouse Anti-Human CD8	RPA-T8	PE-Cy™7	BD Biosciences	560917	561	795/70
Mouse Anti-Human CD27	M-T271	APC	BD Biosciences	561786	640	671/30
Fixable Viability Stain		BD Horizon™ FVS700	BD Biosciences	564997	640	722/44
Mouse Anti-Human CD19	HIB19	APC-eFluor® 780	Thermo Fisher Scientific	47-0199-42	640	795/70

The cryopreserved PBMCs used in this study were collected by two cohort studies over a period spanning ten years and in multiple centres across Canada. All specimens were thawed and stained by the same individual a few hours prior to cell sorting, which was done by a single experienced technician in 25 experiments over 13 months. All fluorescence-activated cell sorting (FACS) experiments were done using the same compensation matrix on the same instrument, which underwent daily QC. PBMC specimens that showed <25% viable cells during flow cytometry or had <5000 viable leukocytes (CD45+) in total were excluded. In total, 5 PBMC specimens (3%) were rejected and replaced with specimens that then passed QC. **Figure 4.3** describes a sensitivity analysis that was done among all specimens (N=32) with 25-75% viable cells, which showed a high concordance (R^2=0.97, ρ_c=0.98) between subset frequencies measured in viable cells compared to all cells. Lin's ρ_c is primarily used to quantify the agreement between two measures of the same variable and is used here to demonstrate the measurements using viable cells are representative of measurements of all cells.

Antibodies were titrated using a specimen with high cell density to ensure that study specimens were stained at a saturating concentration. Centralized manual gating for all specimens was done by a single individual with FlowJo (Version 10.4.2, FlowJo, Ashland, OR, US).

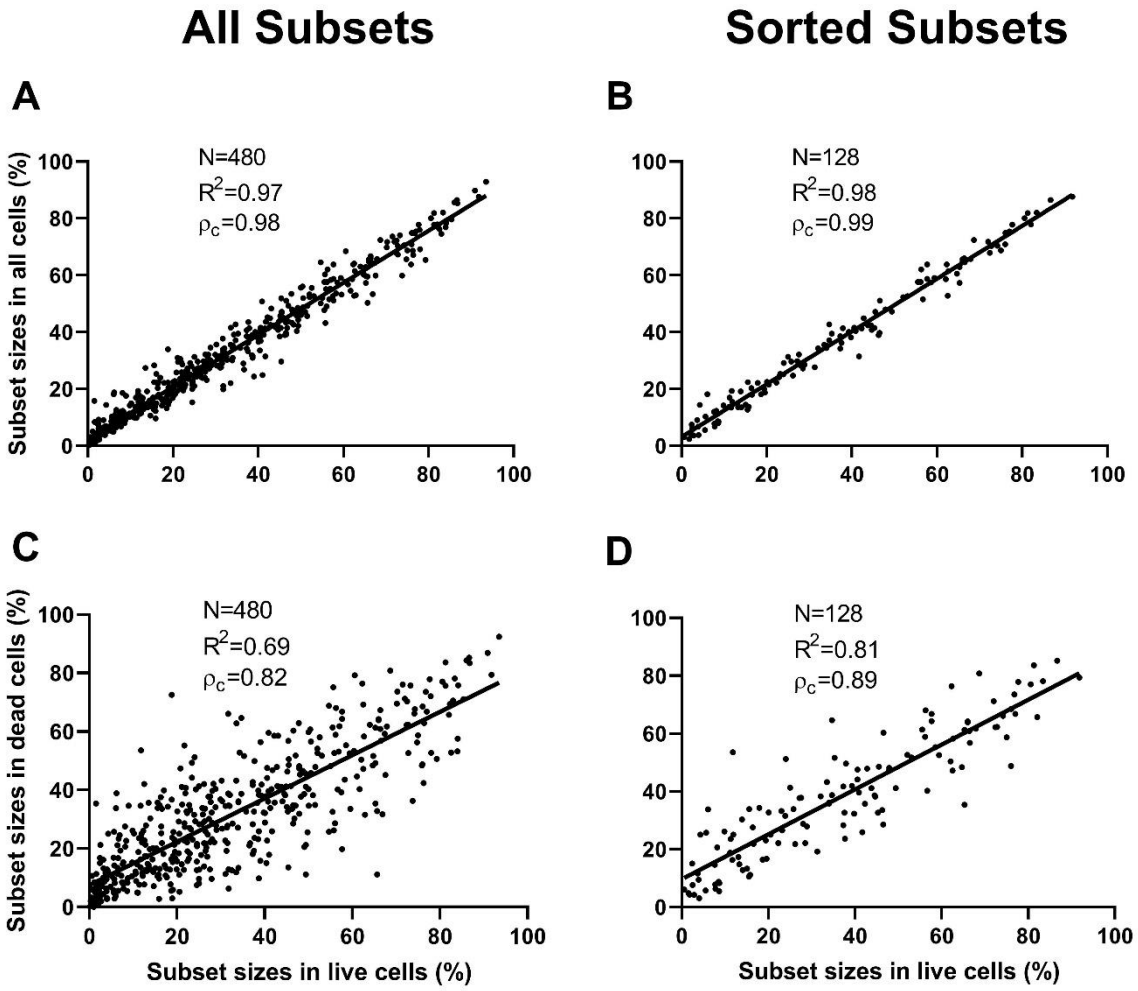

Figure 4.3 Concordance between live and all or dead cells in flow cytometry.
Concordance of subset frequencies between live and all cells among the 15 counted (A) and 4 sorted (B) subsets, and concordance of subset frequencies between live and dead cells among the 15 counted (C) and 4 sorted (D) subsets. Data shown from all 32 participants with leukocyte viability between 25-75%. Number of data points and Pearson's R^2 and Lin's ρ_c are shown.

A FACS IC was included in every cell sorting experiment to determine the inter-experiment variability present during immunophenotyping and cell sorting. The IC was cryopreserved aliquots from a large quantity of PBMCs pooled from four healthy donors that were isolated and frozen at the same time. Measurements of immune cell distributions and ratios showed a median CV of 9.0% (**Table 4.3**) across 25 experiments. Average variability (14% CV) was heavily influenced by very small subsets such as CD4+ T_{EMRA} (57% CV), which constituted <2% of all CD4+ T cells. The relationship between subset sizes and variability is demonstrated by **Figure 4.4**. The average inter-experiment CV of subset TL and mtDNA content were 14 and 40%, respectively. Sort purity was ~98%, randomly checked three times during data collection.

Table 4.3 Inter-experiment variability

Measured variables across 25 experiments	Mean Subset Size (%)	CV (%)
Lymphocytes	74	9
Live Leukocytes	93	9
B cells	6	15
T cells	71	5
CD4 T cells	58	4
CD4 T_N cells	48	7
CD4 T_{CM} cells	39	5
CD4 T_{EM} cells	11	28
CD4 T_{EMRA} cells	2	57
CD4 T_{reg} cells	5	30
CD8 T cells	34	6
CD8 T_N cells	47	10
CD8 T_{CM} cells	17	13
CD8 T_{EM} cells	12	23
CD8 T_{EMRA} cells	24	12
Proliferative CD8 T cells	61	5
Senescent CD8 T cells	39	8
	Average T cell Ratio	
CD4/CD8 T cell Ratio	1.70	9
Proliferative/Senescent CD8 T cell Ratio	1.57	13
	Average Subset TL	
CD4 T cell TL	8.14	10
Proliferative CD8 T cell TL	9.80	15
Senescent CD8 T cell TL	7.29	15
B cell TL	12.37	16
	Average Subset mtDNA content	
CD4 T cell mtDNA content	113	25
Proliferative CD8 T cell mtDNA content	142	38
Senescent CD8 T cell mtDNA content	79	51
B cell mtDNA content	180	47

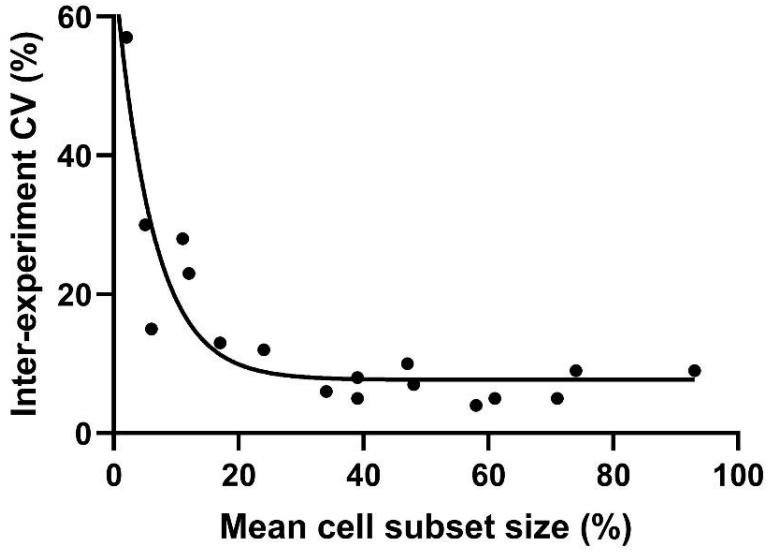

Figure 4.4 Relationship between mean cell subset size and inter-experiment CV.
Inter-experiment variability is affected by cell subset size. Cell subsets with a CV>20% all had mean cell subset sizes ≤12%. B cell subset size had uncharacteristically low variability relative to subset size, with 15% CV and a mean subset size of 6%.

4.2.5 DNA extraction and qPCR

Sorted cells and WB specimens were extracted using the QIAcube and QIAamp DNA Mini Kit (Qiagen, Hilden, Germany) according to the manufacturer's blood and body fluid protocol as previously described [325]. Extracted DNA samples were stored in buffer AE (Qiagen) at -80°C until qPCR was performed. MtDNA content and relative TL either within sorted cell subsets or in whole blood were assayed using monochrome multiplex qPCR as previously described [101,102]. MtDNA content was an absolute measure of the ratio between mitochondrial genome copies and single-copy nuclear gene copies. Here, fragments of the mitochondrial D-loop and *ALB* were used as mtDNA and nuclear DNA sequences, respectively [102]. TL was a relative measure defined as the ratio between relative quantities of telomeric DNA and *ALB*, expressed as a T/S (telomere/single-copy gene) ratio [101].

Quality control for both qPCR assays were applied as previously described [101,102]. Briefly, qPCR runs were accepted or rejected based on two qPCR ICs, a negative control, the amplification efficiency of the standard curve, and the average variability between technical duplicates. Individual measurements were accepted if the quantity of DNA fell within the linear range of the assay and the difference between technical duplicates was <20%. Most of the specimens excluded from analysis for not passing qPCR QC were the consequence of insufficient cell numbers within the sorted populations, resulting in DNA copy numbers below the linear range of the assay. Therefore, while immunophenotypic data exists for all participants, some analyses involving qPCR data exclude a portion of the participants.

4.2.6 Statistical analysis

To accommodate the large amount of data and number of variables of interest in this study, statistical analysis was organized into four stages. First, we investigated the intrinsic relationships of the cellular markers between blood cell fractions, irrespective of HIV status. We compared TL and mtDNA content levels between lymphocyte subsets and examined correlations between subsets. Paired Wilcoxon signed rank tests and Spearman's correlations were used because some subsets had non-parametric distributions. Here, our goal was to characterize differences and relationships between lymphocyte subsets, and a Bonferroni correction was applied to mitigate type I errors. The adjusted significance value was 0.00125.

Second, to determine which of the variables of interest should be further investigated through multivariable linear modelling, we carried out univariable comparisons using Mann-Whitney U tests between the 4 matched groups defined in **Figure 4.1** and chose those showing a statistically significant difference ($p<0.05$). For these analyses, if a data point from one participant was rejected due to qPCR QC, data from the three matched participants were also excluded. Univariable comparisons of LTL and WB mtDNA content between HIV groups included only HIV-negative and HIV NSP participants because WB was not available for HIV SP and UP participants from the Canadian Cohort of HIV+ Slow Progressors. Cell subset TL and mtDNA content were compared between all four HIV groups. First, pairwise comparisons between the larger SP, NSP, and HIV-negative groups were done, followed by pairwise comparisons between the smaller UP group and the other 3 groups separately. By doing so, all univariable comparisons could be made between matched participants without the smaller UP group (N=28) restricting the power of comparisons between the other 3 groups (N=55-57). The same approach

was used to compare CD4:CD8 T cell and proliferative:senescent CD8 T cell ratios, as well as B cell, T cell, CD4 T_{reg}, T_N, T_{CM}, T_{EM}, and T_{EMRA} compartment sizes. As our goal here was not to infer differences between groups, but rather to visualize the raw data and inform downstream analyses, corrections for multiple comparisons were not applied.

Third, multivariable linear regressions were used to model markers of aging among the matched study groups that were deemed important based on the above univariable analyses. Here, missing data for any given participant did not preclude inclusion of data from the matched participants since the models were adjusted for age and sex. Potential predictors and confounders were selected *a priori* based on prior literature and included age, sex, ethnicity, BMI, smoking status, and previous history of HCV and CMV infection. Model refinement was done by minimizing AIC which evaluates goodness of fit relative to model simplicity. In models restricted to PLWH, additional potential explanatory variables included HIV peak pVL and CD4 count at visit, except for the model describing CD4:CD8 ratio, in which CD4 count was excluded *a priori*. For all multivariable linear regressions, data were tested for non-normality using the Shapiro-Wilk test and transformed when necessary as indicated in the figure legends.

Lastly, two dimensionality reduction techniques were used to holistically visualize the differences between the matched study groups in relation to the immune aging markers studied here: Principal Component Analysis (PCA) and t-Distributed Stochastic Neighbor Embedding (t-SNE). Rather than modelling each variable of interest separately, these techniques allow us to take all the variables for which differences between HIV groups were detected ($p<0.05$) in multivariable linear regressions and combine them in a single model. Sensitivity analyses were

also done using either CD4 or senescent CD8 T cell TL in lieu of using all four subsets to demonstrate that missing data in the smaller B cell and proliferative CD8 T cell subsets did not introduce bias. Given that TL in all four subsets were collinear ($P<0.0001$), modelling one subset is likely to represent all four. All t-SNE models were generated using a perplexity of 15 with 5000 iterations. These hyperparameters were chosen as they yielded the greatest separation between HIV groups in the CD4 TL models. For both PCA and t-SNE, data were transformed to Z-scores prior to analysis.

Statistical analyses were performed using XLSTAT version 2018.7 and JMP Pro 14.3.0 using the "Rtsne" R package.

4.3 Results

4.3.1 Study sample

Study participant characteristics are shown in **Table 4.4**. This study was designed primarily to compare the three groups: SPs, NSPs, and HIV-negative controls. Analyses including UP participants constituted a secondary objective which has lower power. As such, balance of demographic and clinical characteristics in the three primary groups was considered separately from comparisons among all four groups. Half of the SP group were elite controllers, with 41% and 9% of the group categorized as virologic and non-virologic controllers, respectively. As per the study design, age and sex were well-balanced across all groups. The median [range] of all participants was 43[17-75] years old, and 57% of all participants were female. The HIV-negative group had lower BMI than the other HIV groups. Ethnicity was balanced between the

SP and NSP groups, but the HIV-negative control group had fewer ACB and more Indigenous participants, whereas the UP group had more ACB participants. SP participants were more likely never smokers and less likely past smokers compared to the other three groups. Viremia was detected in 58% of SP participants at visit. Peak pVL >100000 HIV-RNA copies/ml was more common among HIV NSP (54%) and UP (43%) participants compared to SP (2%) participants. Although CD4 count was similar between SP and NSP groups, UP participants had significantly lower CD4 count compared to the other HIV groups. Almost all SP participants were cART-naïve (95%) and off cART at visit (96%), whereas all but one NSP participants were on cART at visit. Among UP participants, 95% were cART-experienced and 11% of were on cART at visit. Years since HIV diagnosis and % of life since HIV diagnosis were balanced between the SP, NSP, and HIV-negative groups, whereas UP participants tended to have a higher % of life since HIV diagnosis. Both number and type of viral coinfections differed between groups. History of HBV infection was more prevalent among SO (33%) and UP (25%) participants compared to NSP (9%) and HIV-negative (0%) participants. In contrast, HCV infection history was balanced across all four groups, with a prevalence between 18 and 40%. CMV infection history was less prevalent among HIV-negative controls (49%) compared to any other group (75-82%).

Table 4.4 Study participant characteristics

	Slow Progressors (SPs) (N=57)	Non-Slow Progressors (NSPs) (N=57)	HIV-negative (N=55)	P-value[a]	Uncontrolled Progressors (UPs) (N=28)	P-value[b]
Age, years	43 [36,50] (17,73)	43 [36,50] (17,75)	43 [35,49] (17,60)	0.96	42 [35,50] (25,60)	0.98
Female sex	31 (54)	31 (54)	31 (56)	0.97	20 (71)	0.44
Ethnicity				**0.012**	(N=27)	**0.003**
White	35 (61)	29 (51)	34 (62)		9 (33)	
ACB	13 (23)	13 (23)	4 (7)		11 (41)	
Indigenous	5 (9)	7 (12)	15 (27)		6 (22)	
Other	4 (7)	8 (14)	2 (4)		1 (4)	
BMI, kg/m^2	27 [24,32] (18,51) (N=56)	26 [23,30] (20,46) (N=53)	24 [22,28] (19,40) (N=54)	**0.028**	25 [23,31] (18,42) (N=26)	0.07
Tobacco smoking		(N=56)		**0.010**		**0.030**
Current	21 (37)	20 (36)	26 (47)		13 (46)	
Past	5 (9)	18 (32)	9 (16)		5 (18)	
Never	31 (54)	18 (32)	20 (36)		10 (36)	
Currently detectable HIV pVL	33 (58)	0 (0)		**< 0.001**	28 (100)	**< 0.001**
HIV peak pVL >100000 copies/ml	1 (2)	27 (54) (N=50)		**< 0.001**	12 (43)	**< 0.001**
Current CD4 count/µl blood	606 [480,780] (290,1200)	560 [415,760] (90,1290) (N=56)		0.17	448 [268,643] (20,981)	**0.002**
Currently on cART	2 (4)	56 (98)		**< 0.001**	3 (11) (N=27)	**< 0.001**
Currently cART-naïve	54 (95)	0 (0) (N=56)		**< 0.001**	1 (4) (N=27)	**< 0.001**
Years since HIV diagnosis	6 [3,10] (1,27) (N=48)	7 [5,11] (1,20) (N=27)		0.34	9 [6,15] (3,24) (N=22)	0.12
Ever infected with HBV	19 (33)	5 (9)	0 (0)	**< 0.001**	7 (25)	**< 0.001**
Ever infected with HCV	10 (21) (N=48)	10 (18)	10 (18)	0.90	10 (40) (N=25)	0.11
Ever infected with CMV	33 (79) (N=42)	46 (82) (N=56)	26 (49) (N=53)	**0.0003**	15 (75) (N=20)	**0.001**
Slow progressor category	(N=56)					
Elite	28 (50)					
Virologic	23 (41)					
Non-virologic	5 (9)					

Data are presented as number (%) of individuals or median [interquartile range] (range). Number of participants with available data are indicated in smaller font when applicable. Comparisons were done using Kruskal-Wallis, Chi-Squared, or Mann-Whitney U Tests depending on data and number of groups.
Abbreviations: BMI, body mass index; cART, combination antiretrovrial therapy; HBV, Hepatitis B Virus; HCV, Hepatitis C virus; LTL, leukocyte telomere length; mtDNA, mitochondrial DNA; NSPs, non-slow progressors; pVL, plasma viral load; SPs, slow progressors; UPs, uncontrolled progressors
[a]Group comparisons among all slow progressors, non-slow progressors, and HIV-negative controls
[b]Group comparisons among all slow progressors, non-slow progressors, HIV-negative controls, and uncontrolled progressors

4.3.2 Comparisons between TL and mtDNA content in lymphocyte subsets and WB

Participants for whom complete qPCR data were available for all four sorted subsets were included in univariable analyses. Two-by-two paired comparisons between lymphocyte subsets revealed intrinsic differences with respect to the two cellular aging markers (**Figure 4.5**). Notably, proliferative CD8+ T cells had higher TL and mtDNA content than senescent CD8+ T cells, and B cells had the highest levels of both markers in the lymphocyte subsets investigated here. Furthermore, it appears that the subsets with higher TL also have higher mtDNA. When measured in WB, these markers were also significantly different than their subset measurements except for senescent CD8+ and proliferative CD8+ T cells for TL and mtDNA content, respectively.

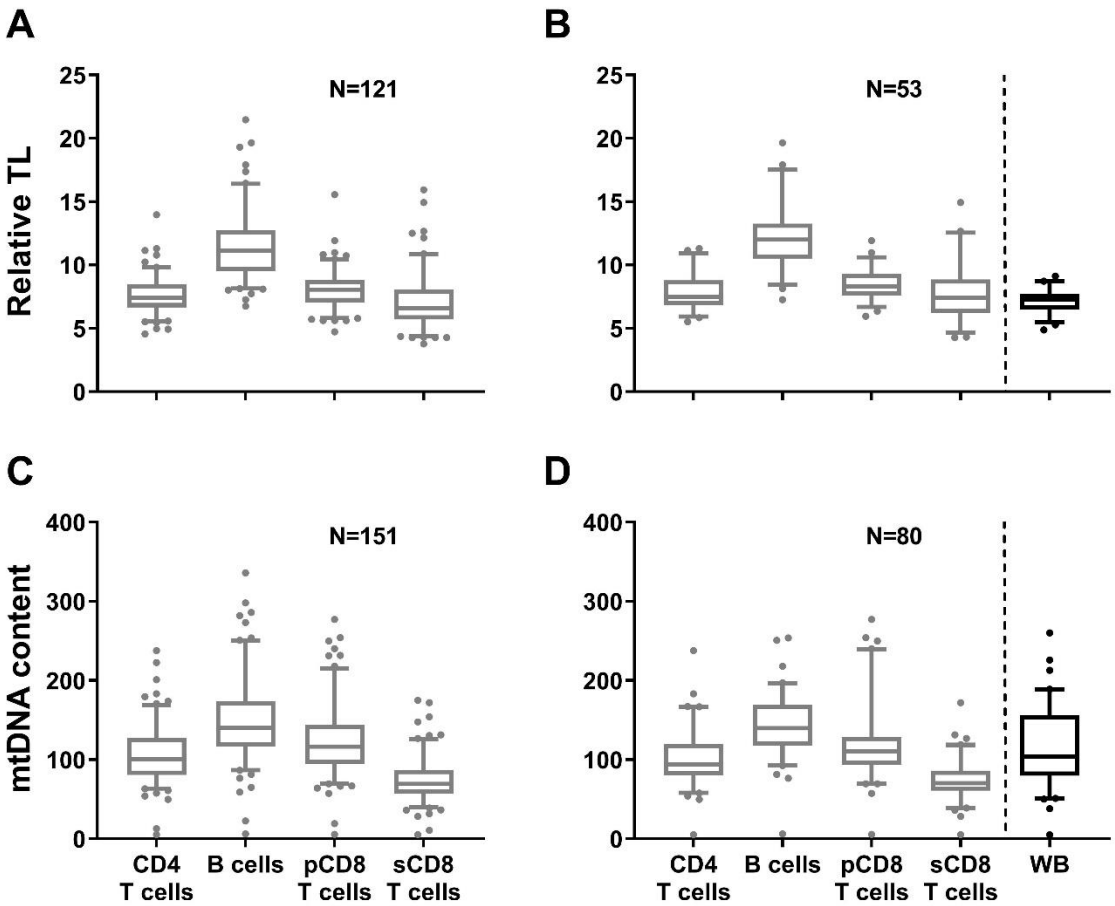

E

Cell subsets	CD4 T cells	sCD8 T cells	pCD8 T cells	B cells	LTL
CD4 T cells	x	**0.001***	**< 0.0001***	**< 0.0001***	0.016§
Senescent CD8 T cells	**< 0.0001†**	x	**< 0.0001***	**< 0.0001***	0.110§
Proliferative CD8 T cells	**< 0.0001†**	**< 0.0001†**	x	**< 0.0001***	**< 0.0001§**
B cells	**< 0.0001†**	**< 0.0001†**	**< 0.0001†**	x	**< 0.0001§**
WB mtDNA content	0.054‡	**< 0.0001‡**	0.628‡	**< 0.0001‡**	x

Shaded and non-shaded cells indicate analyses of TL and mtDNA content respectively.
Bonferroni's corrected significance value=0.00125. *N=121. §N=53. †N=151. ‡N=80.

Figure 4.5 Comparisons of TL and mtDNA content between lymphocyte subsets and leukocytes among all participants.
TL (A,B) and mtDNA content (C,D) among participants with data in all four sorted subsets only (left), as well as among participants with data in all four sorted subsets and WB (right). Boxplots show the median, interquartile and 5-95% percentile bars. Shaded and non-shaded cells in the table are paired Wilcoxon signed rank test P-values for TL and mtDNA content, respectively. Abbreviations: pCD8, proliferative CD8; sCD8, senescent CD8.

4.3.3 Associations of TL and mtDNA content between lymphocyte subsets

Within individuals, TL measurements were correlated between all lymphocyte subsets but not related to LTL, except for CD4 TL, which appeared to have a weak negative association with LTL (**Table 4.5**). Similarly, mtDNA content between all lymphocyte subsets were concordant and were all positively associated with WB mtDNA content (**Table 4.5**).

Table 4.5 Correlations between TL (shaded) and mtDNA (non-shaded) measurements in lymphocyte subsets and WB

		Telomere length				
mtDNA content	**Cell subsets**	CD4 T cells	Senescent CD8 T cells	Proliferative CD8 T cells	B cells	WB
	CD4 T cells	x	**0.428** **P < 0.0001**	**0.651** **P < 0.0001**	**0.399** **P < 0.0001**	-0.211 P = 0.039
	Senescent CD8 T cells	**0.602** **P < 0.0001**	x	**0.627** **P < 0.0001**	**0.484** **P < 0.0001**	-0.105 P = 0.319
	Proliferative CD8 T cells	**0.783** **P < 0.0001**	**0.661** **P < 0.0001**	x	**0.562** **P < 0.0001**	0.115 P = 0.299
	B cells	**0.542** **P < 0.0001**	**0.606** **P < 0.0001**	**0.702** **P < 0.0001**	x	0.012 P = 0.922
	WB	0.284 P = 0.002	0.266 P = 0.004	0.254 P = 0.007	**0.367** **P = 0.0001**	x

Shaded and non-shaded cells represent Spearman's rho and P-value, respectively. Bold rho values indicate significance.
All comparisons made with sample sizes between N=69-142 (TL) and N=104-172 (mtDNA). Bonferroni's corrected significance value=0.00125.

These data show that while TL and mtDNA content appear to be different between lymphocyte subsets, they remain highly correlated between the various subsets. The exception to this is LTL, which shows noticeably less or no correlation with TL in various cell subsets.

4.3.4 Univariable comparisons of aging markers between HIV groups

The CD4:CD8 T cell ratio was higher in the HIV-negative group than any HIV group, although the only detectable difference between HIV groups was that of UP participants having a lower ratio than SP participants (**Figure 4.6A-B**). Similarly, HIV-negative participants had higher proliferative:senescent CD8 T cell ratios than any HIV group. Here, UP participants had a lower ratio than NSP participants (**Figure 4.6C-D**). Both ratios were comparable between HIV SP and NSP groups. **Figure 4.7** shows an alternative visualization of the same comparisons using log-transformed data, which more clearly highlight the differences between groups.

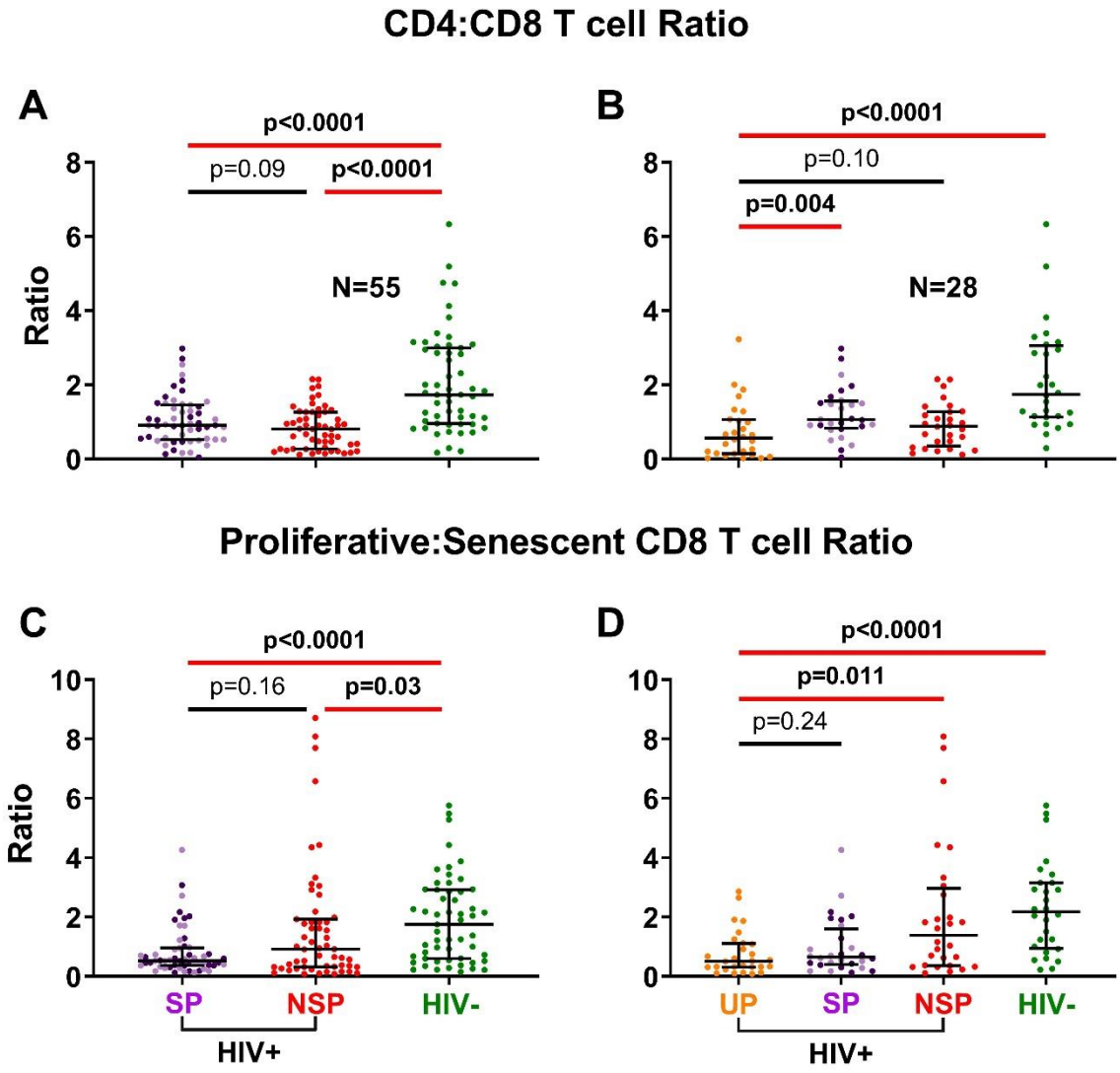

Figure 4.6 Comparisons of CD4:CD8 T cell and proliferative:senescent CD8 T cell ratios between matched HIV groups.
CD4:CD8 T cell ratio among matched (A) SP, NSP, and HIV-negative participants, as well as a sensitivity analysis (B) adding the matched UP group. Proliferative:senescent CD8 T cell ratio among (C) SP, NSP, and HIV-negative participants, as well as a sensitivity analysis (D) adding UP participants. Dark purple data points in the SP group indicate elite controllers. Median, interquartile range, and Mann-Whitney U P-values shown.

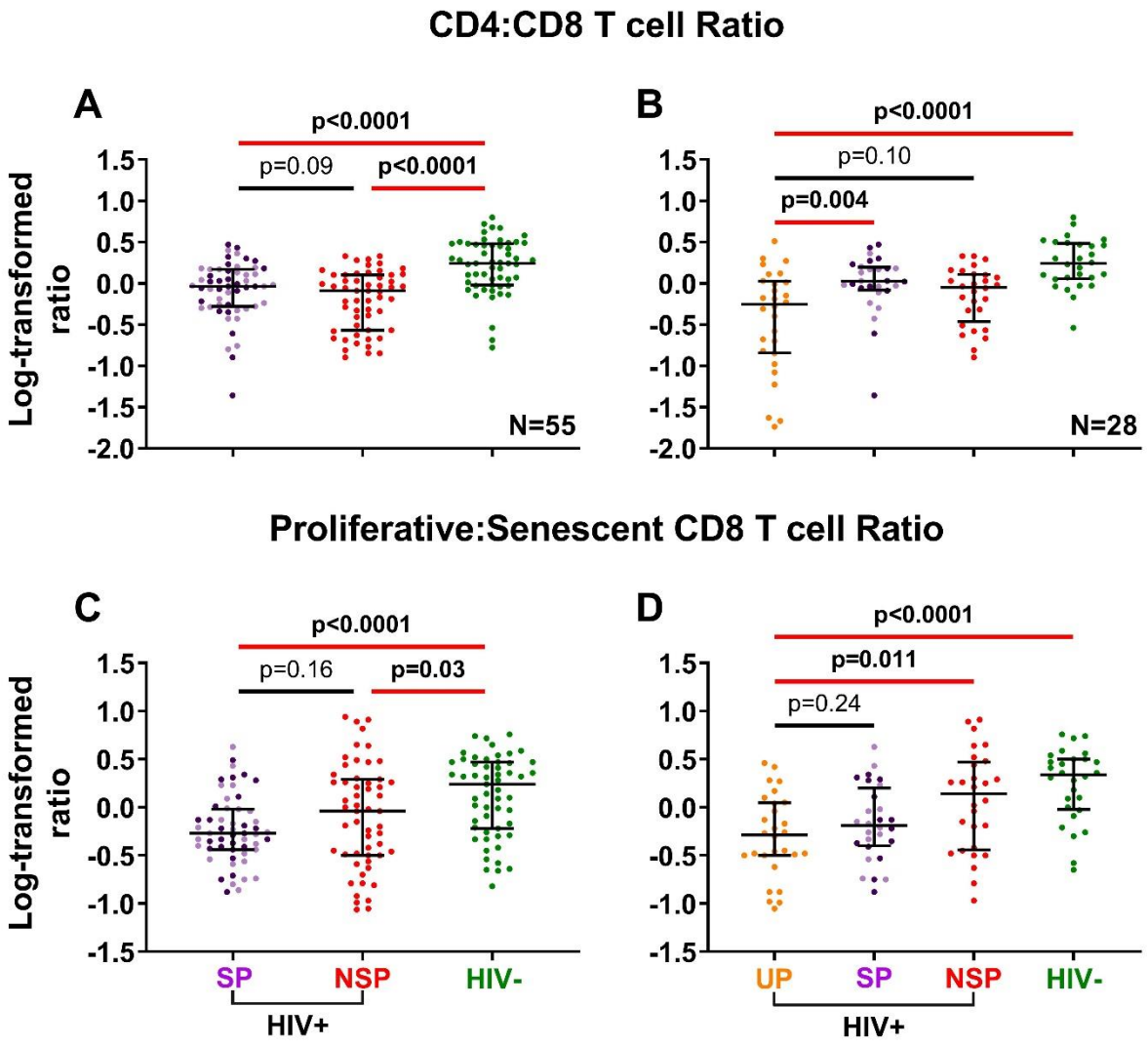

Figure 4.7 Comparisons of log-transformed CD4:CD8 T cell and proliferative:senescent CD8 T cell ratios between matched HIV groups.
Log-transformed CD4:CD8 T cell ratio among matched (A) SP, NSP, and HIV-negative participants, as well as a sensitivity analysis (B) adding the matched UP group. Log-transformed proliferative:senescent CD8 T cell ratio among (C) SP, NSP, and HIV-negative participants, as well as a sensitivity analysis (D) adding UP participants. Dark purple data points in the SP group indicate elite controllers. Median, interquartile range, and Mann-Whitney U P-values shown.

Within the CD4 T cell subset, SP participants had shorter TL compared to NSP participants (**Figure 4.8A**), and no other differences in CD4 TL were detected between groups (**Figure 4.8A-B**). HIV-negative participants had longer B cell TL than all HIV groups (**Figure 4.8C-D**) but there were no differences detected between of them. In proliferative CD8+ T cells, HIV-negative participants had longer TL compared to both SP and UP participants (**Figure 4.8E-F**). Finally, SP and UP participants had shorter senescent CD8+ T cell TL compared to both NSP and HIV-negative participants (**Figure 4.8G-H**), whereas no difference between SP and UP groups were detected. Elite controller status did not appear to be driving the effects detected here.

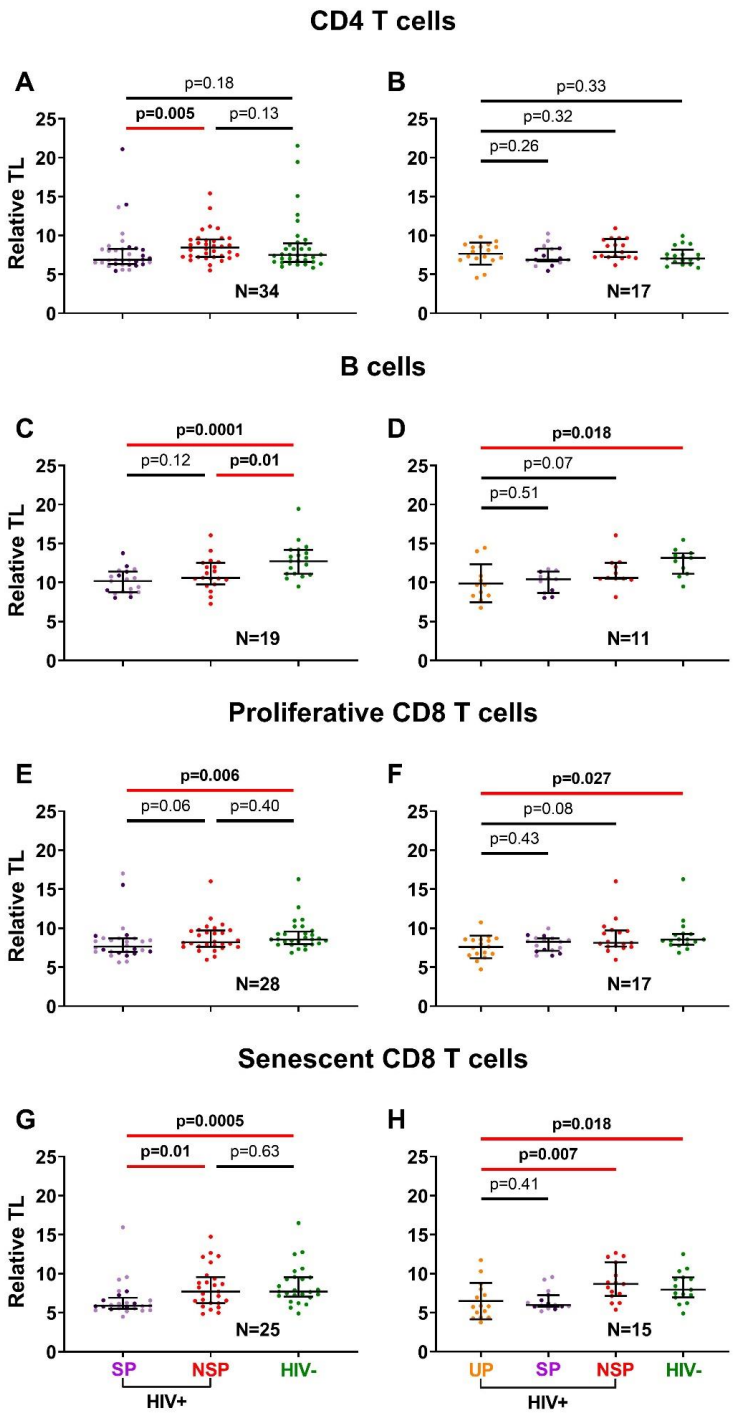

Figure 4.8 Comparisons of lymphocyte subset TL between matched HIV groups.
TL among SP, NSP, and HIV-negative participants (left), as well as sensitivity analyses adding UP participants (right), for CD4 T cells (A, B), B cells (C, D), proliferative CD8 T cells (E, F), and senescent CD8 T cells (G, H). Dark purple data points in the SP group indicate elite controllers. Median, interquartile range, and Mann-Whitney U P-values shown.

Differences in subset mtDNA content between groups were far less apparent (**Figure 4.9**). The only detectable difference between groups was NSP participants having increased proliferative CD8+ T cell mtDNA content compared to HIV-negative controls (**Figure 4.9E**). UP participants also trended towards having increased proliferative CD8+ T cell mtDNA content compared to HIV-negative controls, although the difference did not reach significance (P=0.062, **Figure 4.9F**).

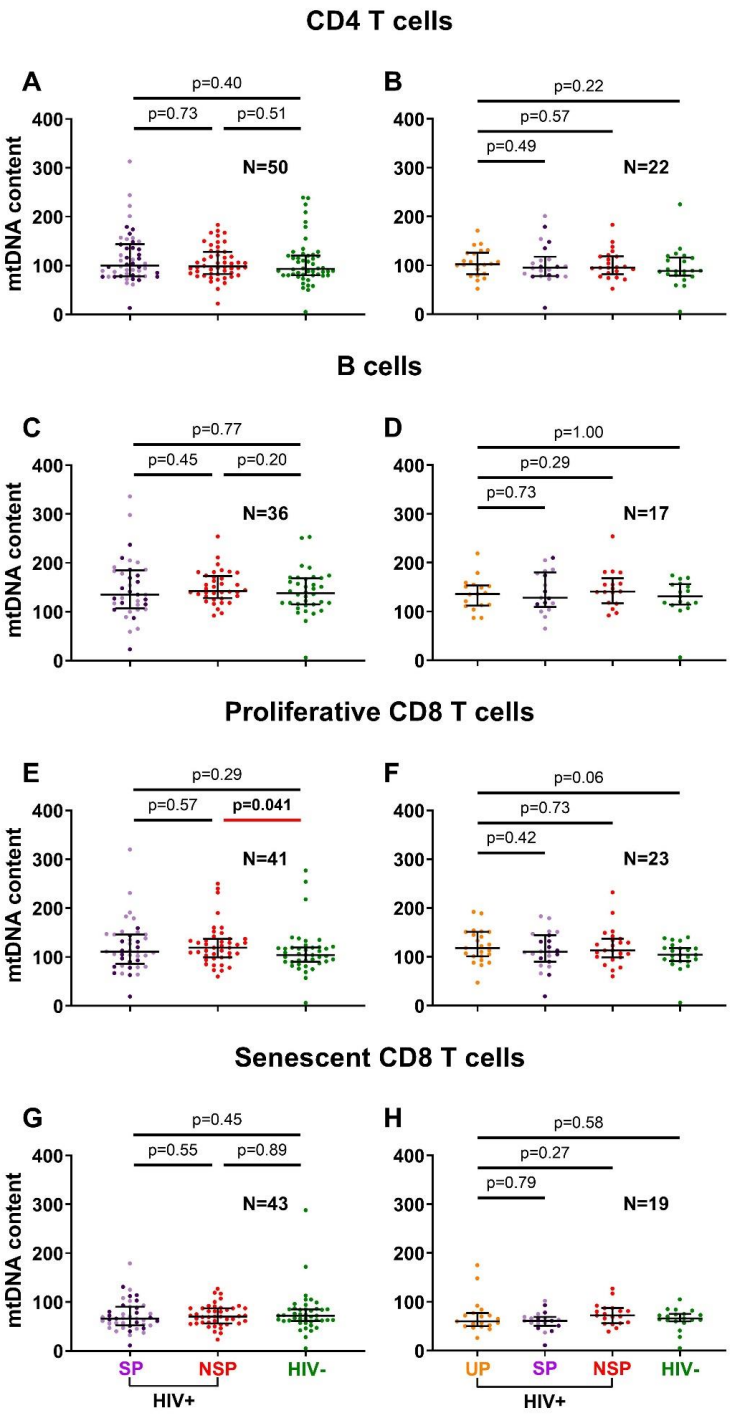

Figure 4.9 Comparisons of lymphocyte subset mtDNA content between matched HIV groups.
MtDNA content among SP, NSP, and HIV-negative participants (left), as well as sensitivity analyses adding UP participants (right), for CD4 T cells (A, B), B cells (C, D), proliferative CD8 T cells (E, F), and senescent CD8 T cells (G, H). Dark purple data points in the SP group indicate elite controllers. Median, interquartile range, and Mann-Whitney U P-values shown.

In LTL and WB mtDNA content, markers commonly measured in readily available biospecimens, no differences were detected between NSP and HIV-negative groups (**Figure 4.10**).

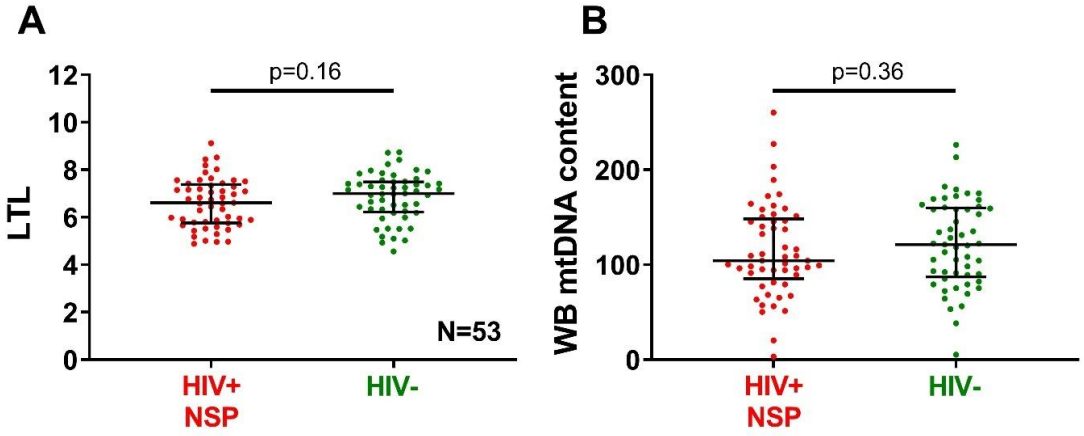

Figure 4.10 Comparison of LTL and WB mtDNA content between matched HIV groups.
LTL (A) and WB mtDNA content (B) among NSP and HIV-negative participants. HIV SP and UP participants were excluded because of unavailable WB biospecimens. Median, interquartile range, and Mann-Whitney U P-values shown.

Cell subset sizes related to T cell differentiation were also investigated. **Figure 4.11** provides a visual representation of T cell subsets at different states of differentiation, while **Figures 4.12** and **4.13** show the comparisons of the subset sizes between groups. In the CD4 T cell compartment, UP participants had a smaller T_N population than NSP, and SP participants had a larger T_{EM} population than HIV-negative controls (**Figures 4.11-4.12**). In the CD8 T cell compartment, SP participants had smaller T_N and larger T_{EM} populations than both NSP and HIV-negative groups (**Figures 4.11, 4.13**). Similarly, UP participants had a smaller T_N population than NSP and HIV-negative groups, but a larger T_{EM} population compared to only the HIV-negative controls. No differences in any cell subsets were detected between the SP and UP groups. Lastly, although NSP participants had a smaller T_{EM} population size than SPs, they had a larger T_{EM} population than HIV-negative controls. As before, the differences detected between SP participants and other groups do not seem to be driven by elite controller status.

Taken together, differences in CD4 lineage subsets between HIV groups were barely detectable and unrelated, potentially indicating spurious findings. In contrast, differences in CD8 lineage subsets were more robust, and the decreased T_N populations seen in SP and UP participants may be related to their increased T_{EM} populations.

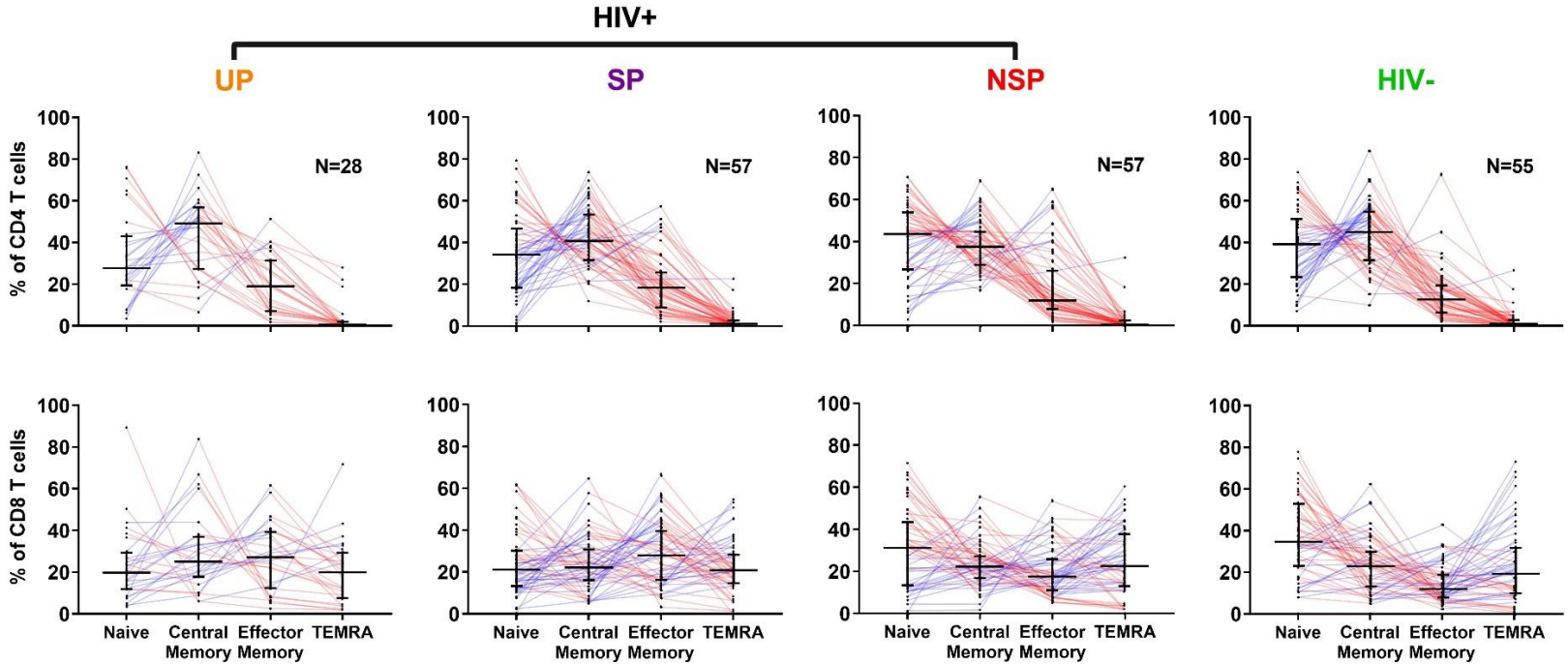

Figure 4.11 Visualization of T cell lineage subset population sizes.
CD4 and CD8 T_N, T_{CM}, T_{EM}, T_{EMRA} subset population sizes of SP, NSP, UP, and HIV-negative participants shown. Blue and red lines indicate increasing and decreasing populations sizes within an individual, respectively. Median and interquartile range shown.

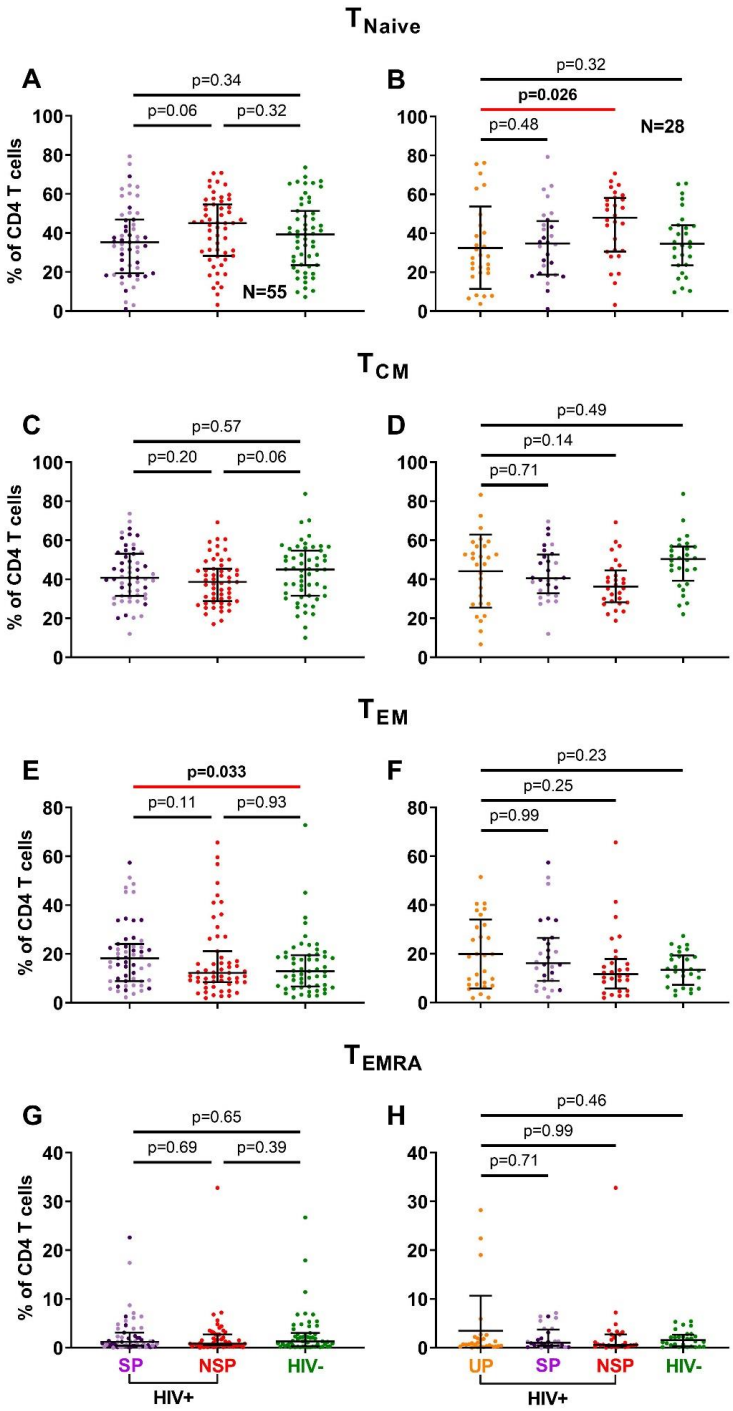

Figure 4.12 Comparisons of CD4 T cell lineage subset sizes between matched HIV groups.
Subset sizes among SP, NSP, and HIV-negative participants (left), as well as sensitivity analyses adding UP participants (right), for CD4 T_N (A, B), T_{CM} (C, D), T_{EM} (E, F), and T_{EMRA} (G, H). Dark purple data points in the SP group indicate elite controllers. Median, interquartile range, and Mann-Whitney U P-values shown.

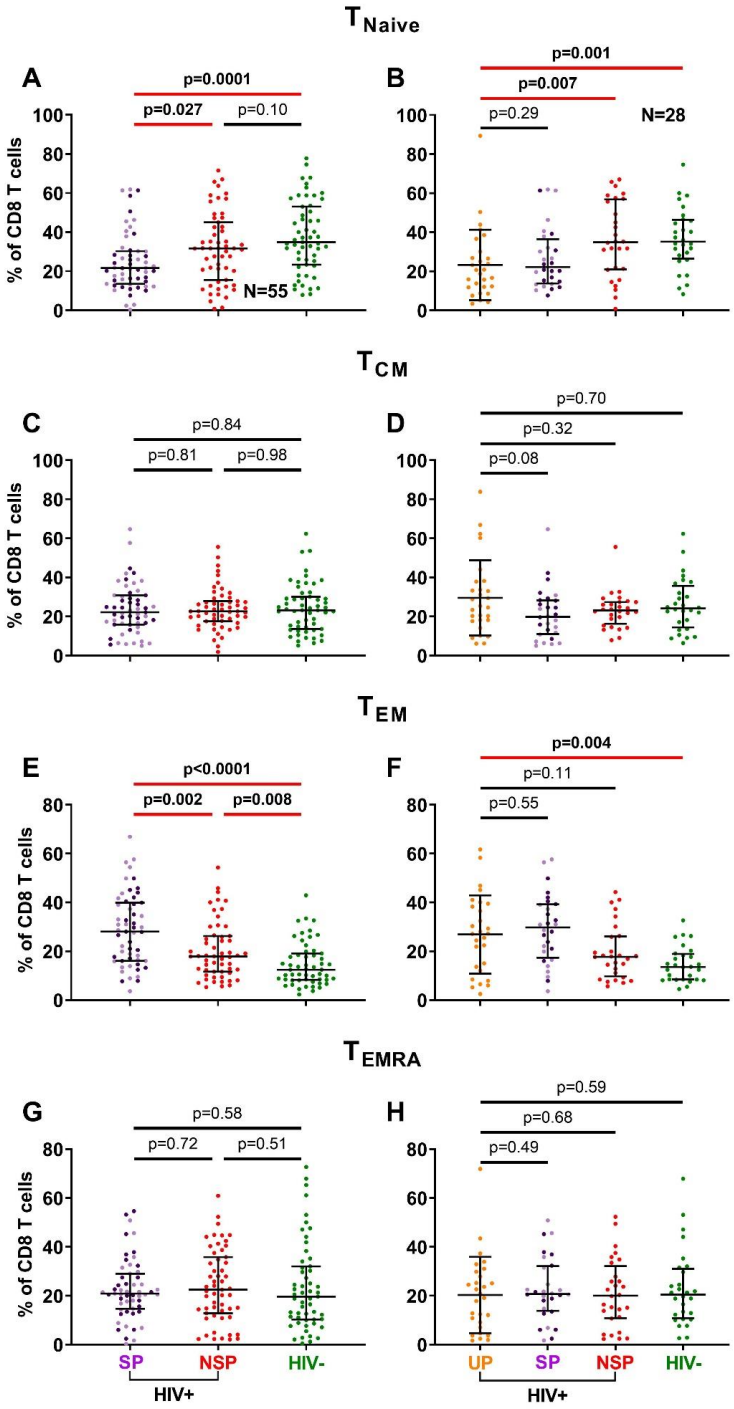

Figure 4.13 Comparisons of CD8 T cell lineage subset sizes between matched HIV groups.
Subset sizes among SP, NSP, and HIV-negative participants (left), as well as sensitivity analyses adding UP participants (right), for CD8 T_N (A, B), T_{CM} (C, D), T_{EM} (E, F), and T_{EMRA} (G, H). Dark purple data points in the SP group indicate elite controllers. Median, interquartile range, and Mann-Whitney U P-values shown.

No differences in B cell population sizes were detected between HIV groups (**Figure 4.14A-B**), whereas SPs had a larger T cell population than the HIV-negative controls, and the UPs had a larger T cell population than both SPs and HIV-negative controls (**Figure 4.14C-D**). Lastly, SP participants had a smaller T_{reg} population compared to NSP participants, with a non-significant trend in the same direction compared to HIV-negative controls (**Figure 4.14E-F**).

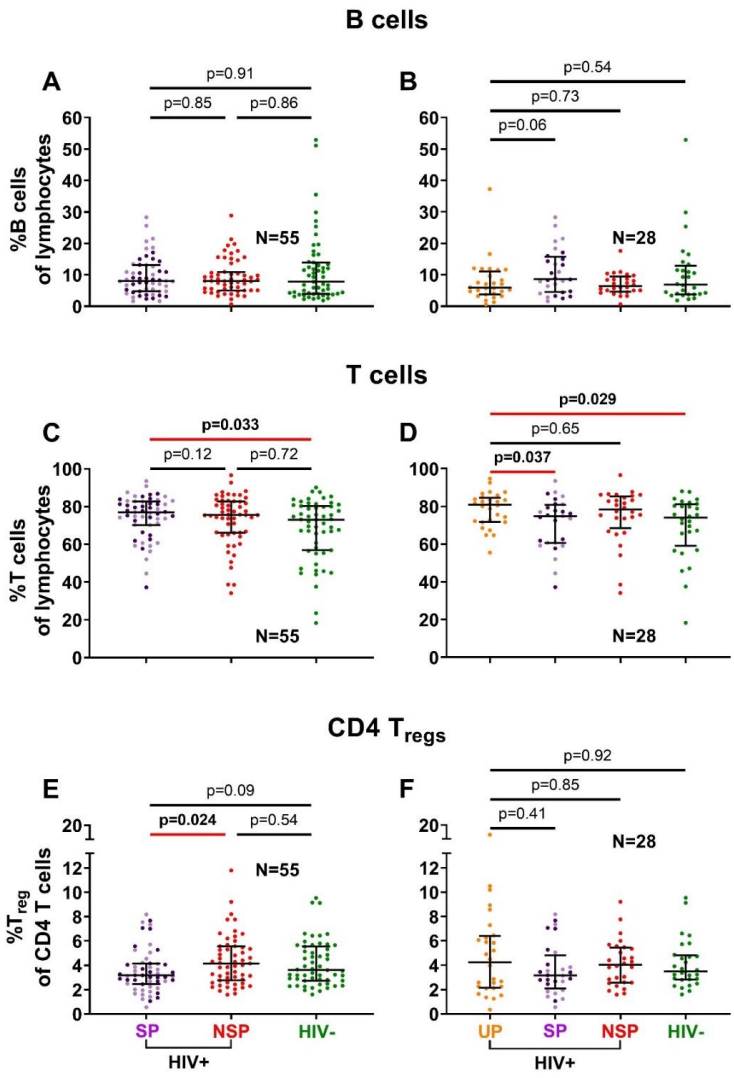

Figure 4.14 Comparisons of B cell, T cell, and CD4 T_{reg} compartment sizes between matched HIV groups. Compartment sizes among SP, NSP, and HIV-negative participants (left), as well as sensitivity analyses adding UP participants (right), for B cells (A, B), T cells (C, D), and CD4 T_{regs} (E, F). Dark purple data points in the SP group indicate elite controllers. Median, interquartile range, and Mann-Whitney U P-values shown.

4.3.5 Multivariable predictors of aging markers

Variables that were different (P<0.05) between HIV groups in univariable analyses were modelled using multivariable linear regressions.

SPs had higher CD4:CD8 ratio compared to NSP and UP participants and lower CD4:CD8 ratio compared to HIV-negative controls after adjusting for age, sex, and ethnicity, as well as HCV and CMV infection (N=156, R^2=0.49, **Figure 4.15A**). In the same model, female sex was independently associated with higher CD4:CD8 ratio, whereas ACB ethnicity and HCV infection ever were independently associated with lower CD4:CD8 ratio. Here, a trend was observed between CMV infection and lower CD4:CD8 ratio (P=0.08). In a similar model among PLWH only, having a peak HIV pVL >100000 HIV-RNA copies/ml was independently associated with lower CD4:CD8 ratio (**Figure 4.15B**). In this subgroup analysis with reduced power (N=103 PLWH of the N=156 total participants), the effects of sex and ACB ethnicity remained, while those of HIV group and HCV infection were lost.

The SP group had lower proliferative:senescent CD8 ratio compared to HIV-negative controls, but was not discernibly different from either NSP and UP groups (N=156, R^2=0.32, **Figure 4.15C**). Similar to the model describing CD4:CD8 ratio, female sex was independently associated with higher proliferative:senescent CD8 ratio and a trend was observed between CMV infection and lower proliferative:senescent CD8 ratio. In the subgroup analysis among PLWH, higher CD4 count was associated with higher proliferative:senescent CD8 ratio, while the effect of female sex remained (**Figure 4.15D**).

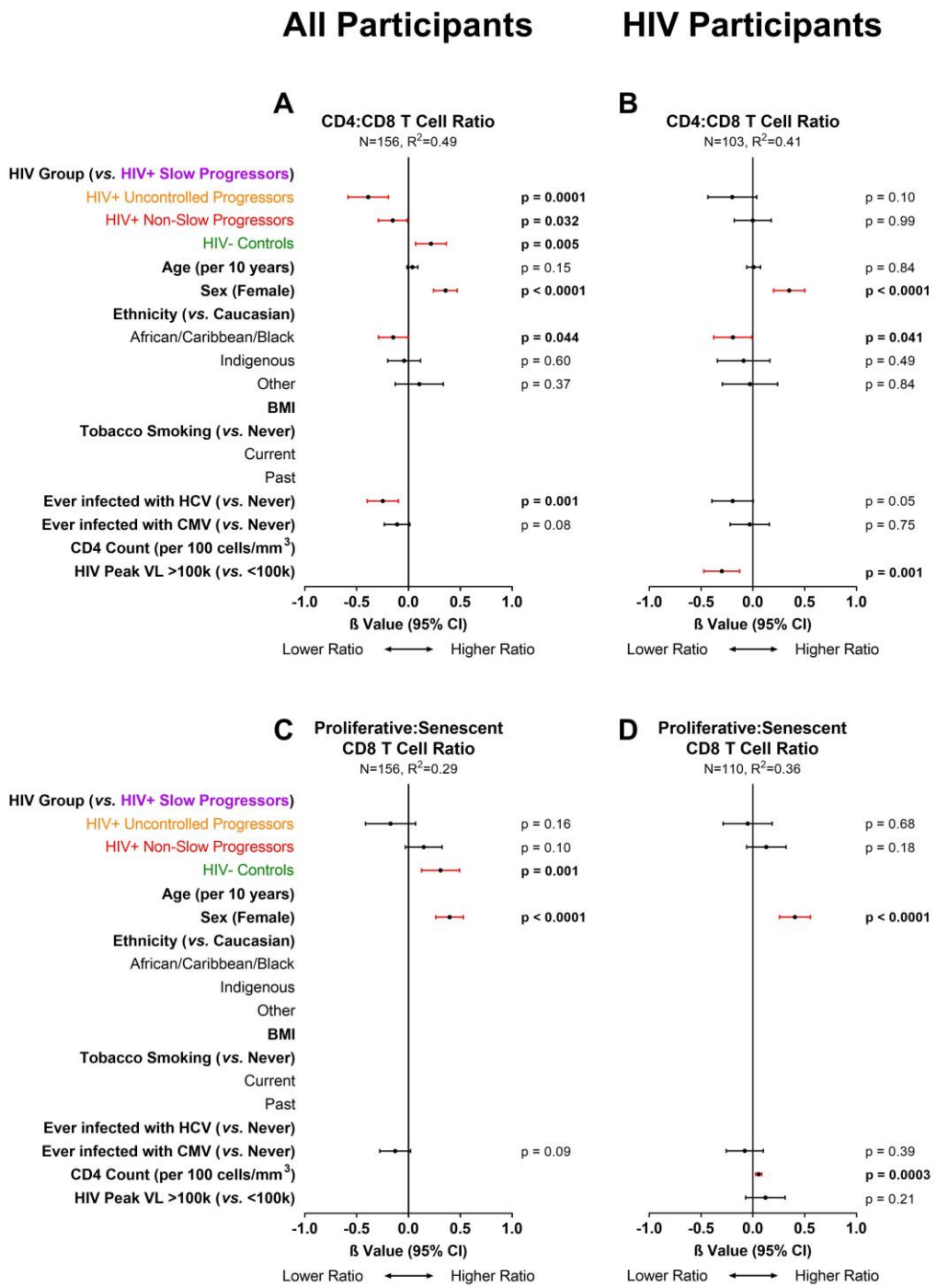

Figure 4.15 Multivariable modelling of CD4:CD8 and proliferative:senescent CD8 T cell ratios. Multivariable linear models of all participants (left) and subgroup analyses among PLWH (right) are shown, including models of CD4:CD8 (A-B) and proliferative:senescent CD8 T cell ratios (C-D). Both T cell ratios are log-transformed. Red confidence intervals indicate statistical significance. Coefficients of determination and unstandardized β values shown.

In all multivariable models describing TL within CD4, B cell, proliferative CD8, and senescent CD8 T cell subsets, SPs had shorter TL compared to NSPs and HIV-negative controls, whereas no differences were detected between SP and UP groups (N=100-127, model R^2=0.20-0.34, **Figures 4.16, 4.17**). In all T cell subsets, CMV infection was independently and significantly associated with shorter TL ($P \leq 0.022$, **Figure 4.16A,C** and **Figure 4.17A,C**), but no effect was detected in B cells (**Figure 4.16C**). Older age was associated with shorter TL only in CD4 T cells ($P<0.0001$, **Figure 4.16A**), and female sex was associated with shorter TL in CD4 T cells ($P<0.0001$, **Figure 4.16A**) and proliferative CD8 T cells (P=0.049, **Figure 4.17A**). ACB and indigenous ethnicities were associated with longer TL in B cells (P=0.017, **Figure 4.16C**) and senescent CD8 T cells (P=0.045, **Figure 4.17C**), respectively. In subgroup analyses among PLWH, higher CD4 count was associated with shorter CD4 T cell TL (P=0.042, **Figure 4.16B**), but not associated with TL in any other subset (**Figure 4.16D** and **Figure 4.17B,D**). HIV peak pVL also showed no association with TL in any subsets.

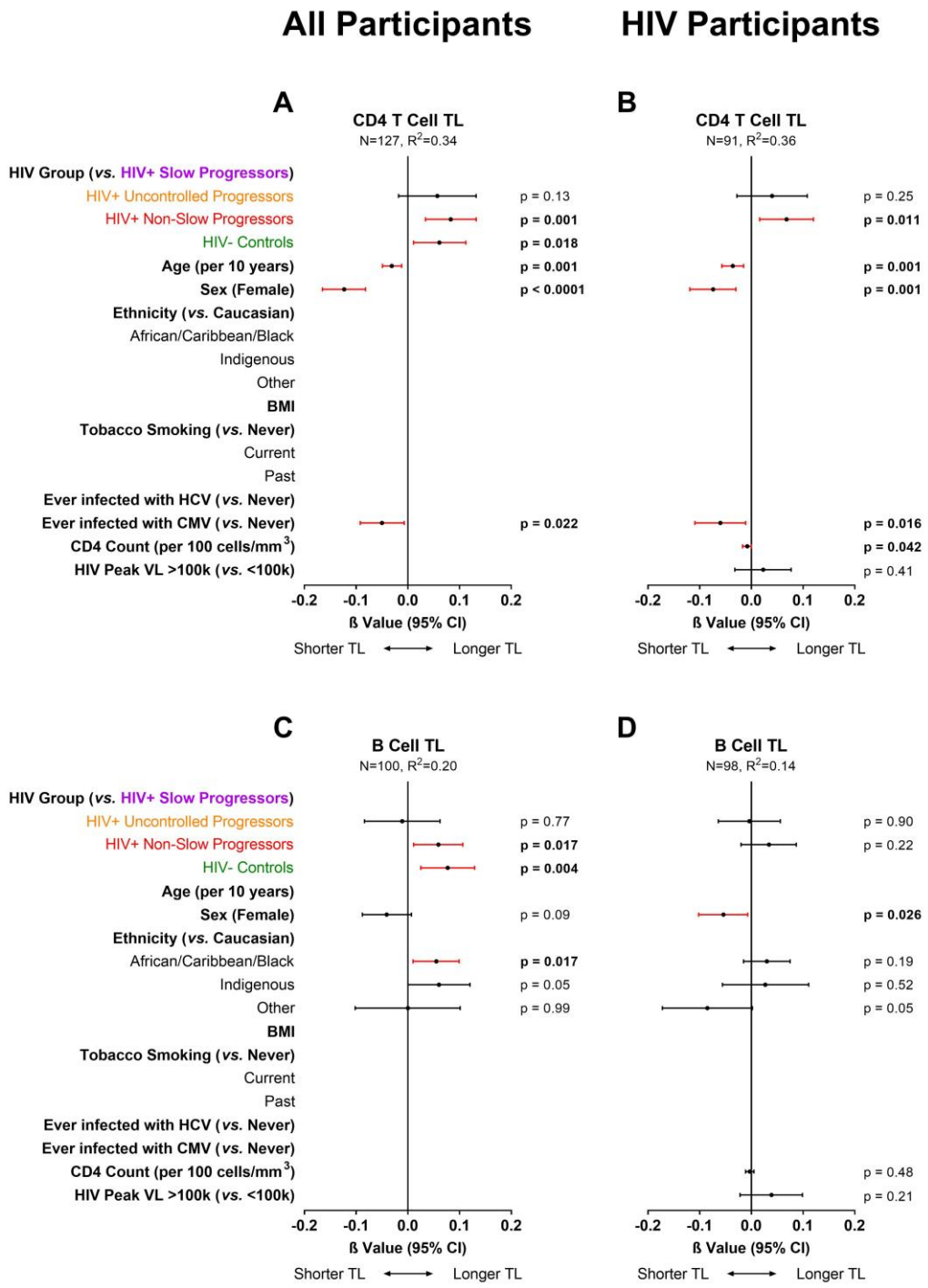

Figure 4.16 Multivariable modelling of CD4 T cell and B cell TL.
Multivariable linear models of all participants (left) and subgroup analyses among PLWH (right) are shown, including models of CD4 T cell (A-B) and B cell TL (C-D). Both subset TL variables are log-transformed. Red confidence intervals indicate statistical significance. Coefficients of determination and unstandardized β values shown.

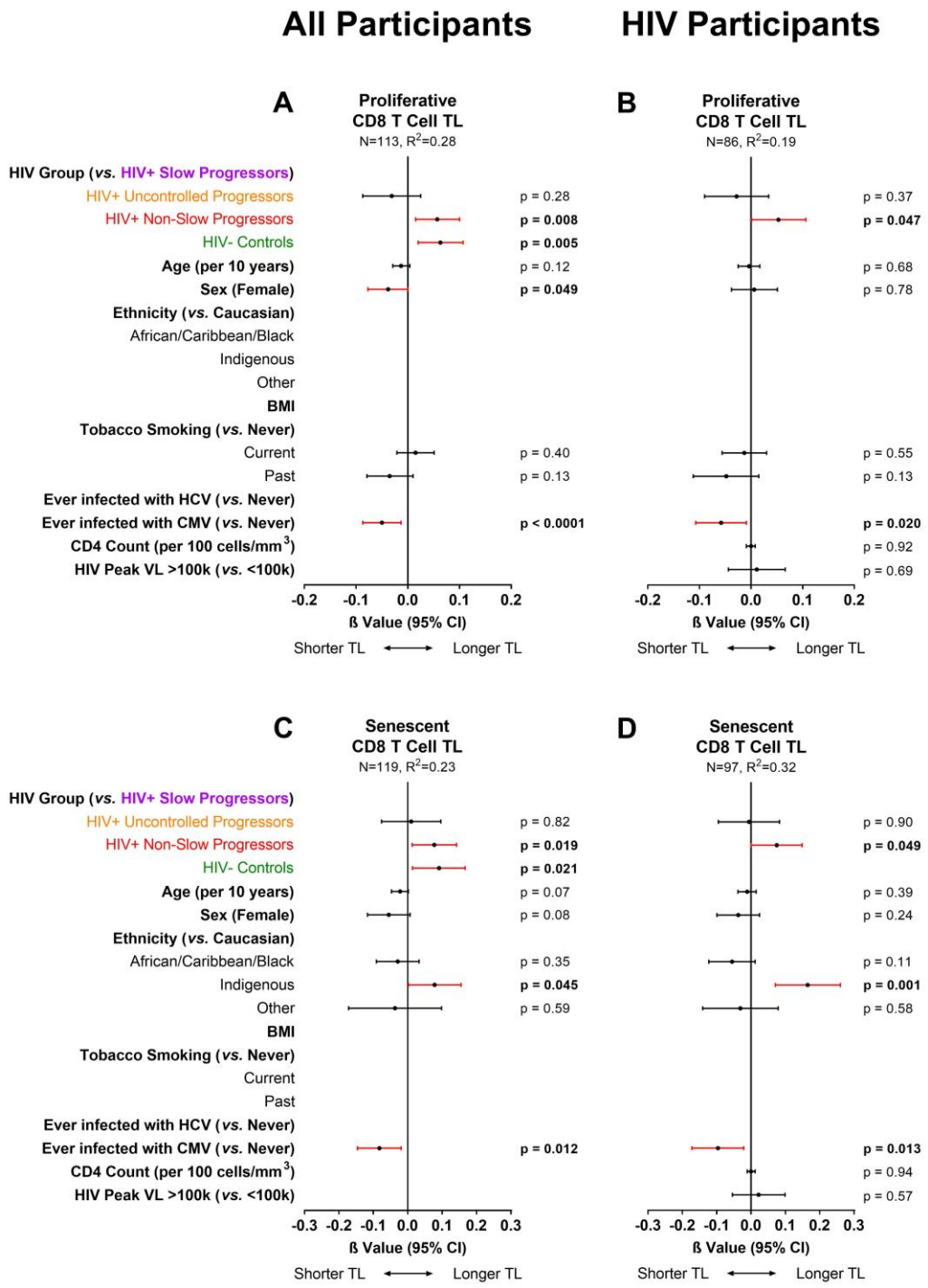

Figure 4.17 Multivariable modelling of proliferative and senescent CD8 T cell TL.
Multivariable linear models of all participants (left) and subgroup analyses among PLWH (right) are shown, including models of proliferative (A-B) and senescent CD8 T cell TL (C-D). Both subset TL variables are log-transformed. Red confidence intervals indicate statistical significance. Coefficients of determination and unstandardized β values shown.

NSPs had shorter LTL compared to HIV-negative controls (N=102, R^2=0.58, **Figure 4.18A**). Female sex (P<0.0001) and the other ethnicity category (P=0.010), which include Asian, South Asian, and Hispanic participants were also independently associated with longer LTL. A trend was observed between older age and shorter LTL (P=0.07), whereas tobacco smoking, BMI, HCV, and CMV infection were not associated with LTL.

No difference in WB mtDNA content was detected between NSPs and HIV-negative controls (N=102, $R^2$0.27, **Figure 4.18B**). Here, female sex (P<0.0001) and CMV infection (P=0.049) were independently associated with lower WB mtDNA content, and HCV infection (P=0.025) with higher WB mtDNA content. No relationship was detected between WB mtDNA content and age, ethnicity, tobacco smoking, or BMI.

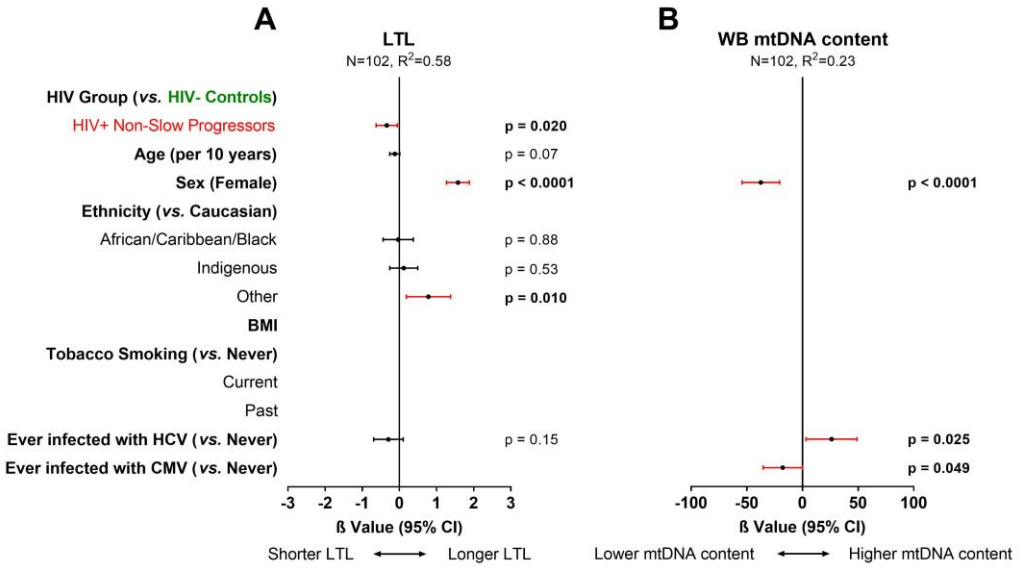

Figure 4.18 Multivariable modelling of LTL and WB mtDNA content.
Multivariable linear models of LTL (A) and WB mtDNA content (B). Red confidence intervals indicate statistical significance. Coefficients of determination and unstandardized β values shown.

A larger CD4 T_N compartment was independently associated with younger age and female sex, with no detectable association with HIV group (N=156, R^2=0.22, **Figure 4.19A**). BMI, HCV infection, and CMV infection had no effect. In a subgroup analysis among PLWH, SP status, higher BMI, and HIV peak pVL >100000 HIV-RNA copies/ml were independently associated with a smaller CD4 T_N population size (**Figure 4.19B**). The age and sex effects in the original model remained. A larger CD4 T_{EM} compartment size was independently associated with male sex and CMV infection (N=156, R^2=0.18, **Figure 4.19C**), and these effects remained in a subgroup analysis among PLWH (**Figure 4.19D**). No difference was detected in CD4 T_{EM} population size between HIV groups.

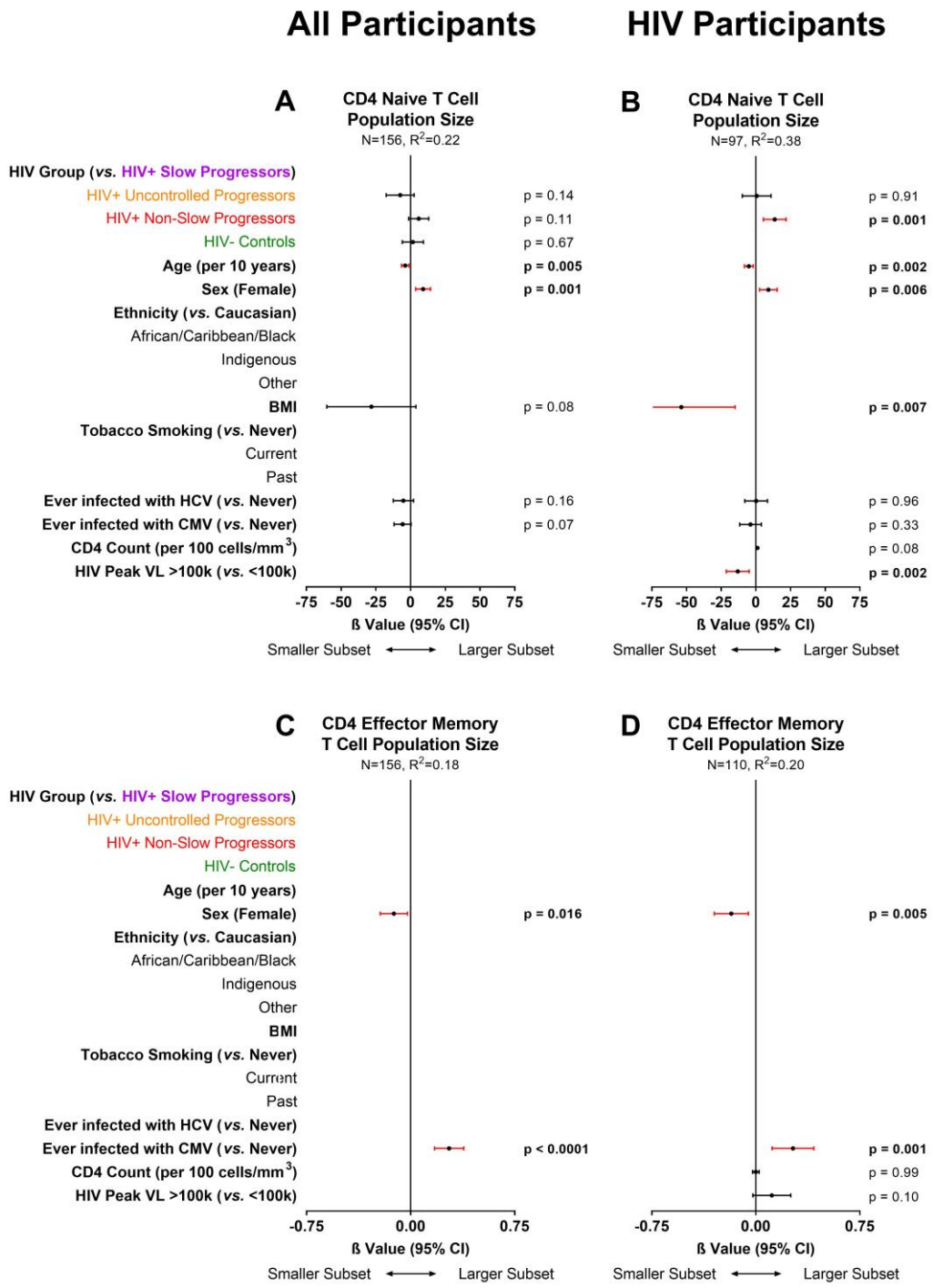

Figure 4.19 Multivariable modelling of CD4 T_N and T_{EM} subset sizes.
Multivariable linear models of all participants (left) and subgroup analyses among PLWH (right) are shown, including models of CD4 T_N (A-B) and T_{EM} (C-D) subset sizes. CD4 effector memory T cell population size is log-transformed. Red confidence intervals indicate statistical significance. Coefficients of determination and unstandardized β values shown.

In contrast with the CD4 compartment, CD8 differentiation subsets were different between HIV groups. SPs had a smaller CD8 T_N subset compared to NSPs and HIV-negative controls, but not UP participants (N=156, R^2=0.34, **Figure 4.20A**). Older age and CMV infection were independently associated with a smaller CD8 T_N subset, whereas female sex was independently associated with a larger subset. Among PLWH, higher CD4 count was independently associated with a larger CD8 T_N subset (**Figure 4.20B**). In this subgroup analysis, the effect of HIV group, sex, and CMV infection remained, but the effect of age was lost. The multivariable models describing CD8 T_{EM} population size revealed several associations in the opposite direction compared to those of CD8 T_N. SPs had a larger CD8 T_{EM} subset compared to NSPs and HIV-negative controls, but not UP participants (N=156, R^2=0.27, **Figure 4.20C**). CMV infection was independently associated with a larger CD8 T_{EM} subset, whereas age had no effect. In the HIV subgroup analysis, neither CD4 count nor HIV peak pVL was associated with CD8 T_{EM} population size (**Figure 4.20D**).

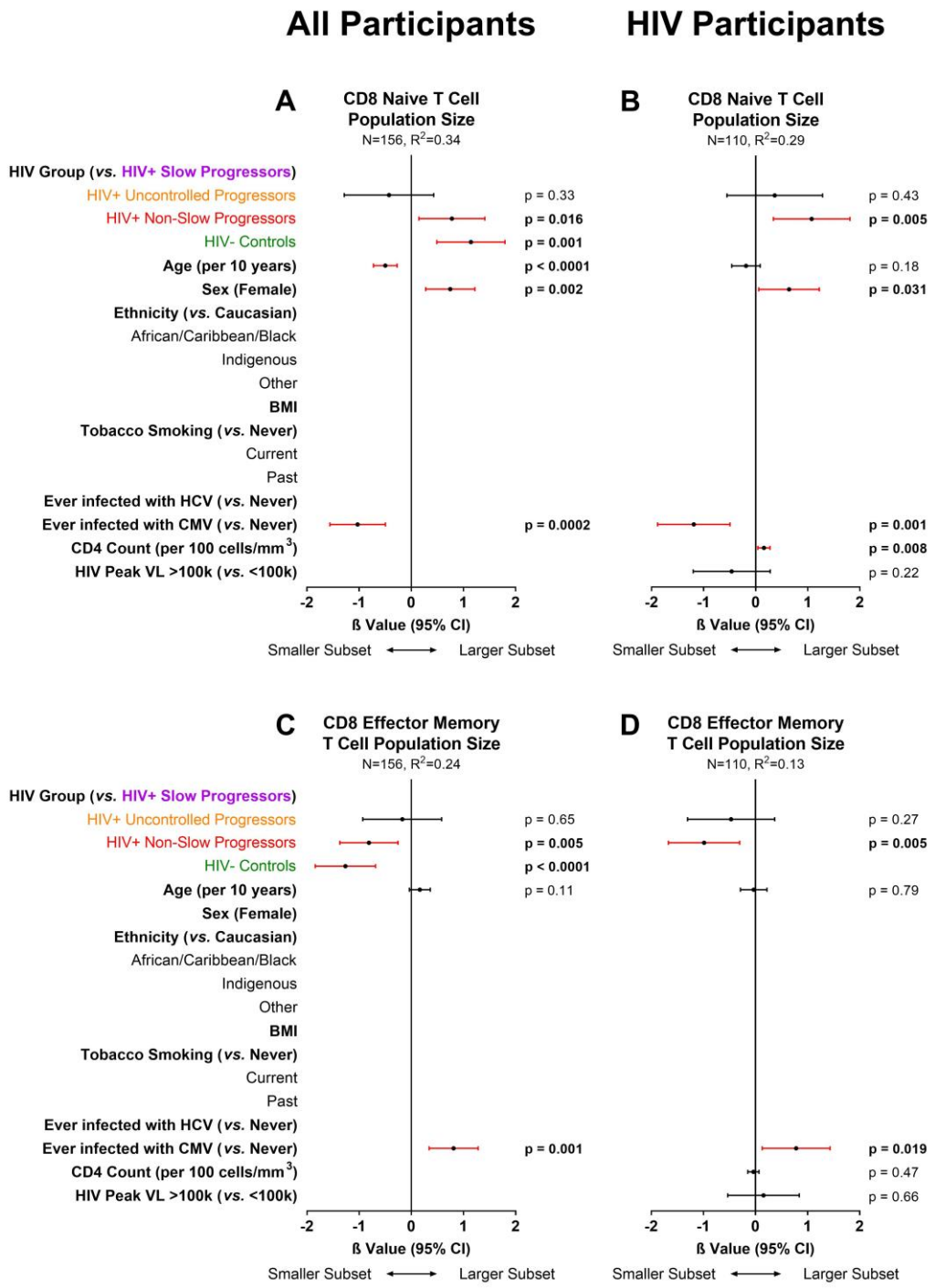

Figure 4.20 Multivariable modelling of CD8 T_N and T_{EM} subset sizes.
Multivariable linear models of all participants (left) and subgroup analyses among PLWH (right) are shown, including models of CD8 T_N (A-B) and T_{EM} (C-D) subset sizes. Both CD8 T cell subset population sizes are square root-transformed. Red confidence intervals indicate statistical significance. Coefficients of determination and unstandardized β values shown.

Female sex was independently associated with larger T cell population size, but the latter was not associated with any other explanatory variable studied here (N=156, R^2=0.29, **Figure 4.21A-B**). A larger T_{reg} population size was independently associated with male sex, lower BMI, and HCV infection, but not HIV group (N=156, R^2=0.19, **Figure 4.21C**). In the HIV subgroup analysis, a larger T_{reg} population size was independently associated with lower CD4 count but was not associated with HIV peak pVL. The effect of BMI in the above model remained, but the effects of sex and HCV infection were lost.

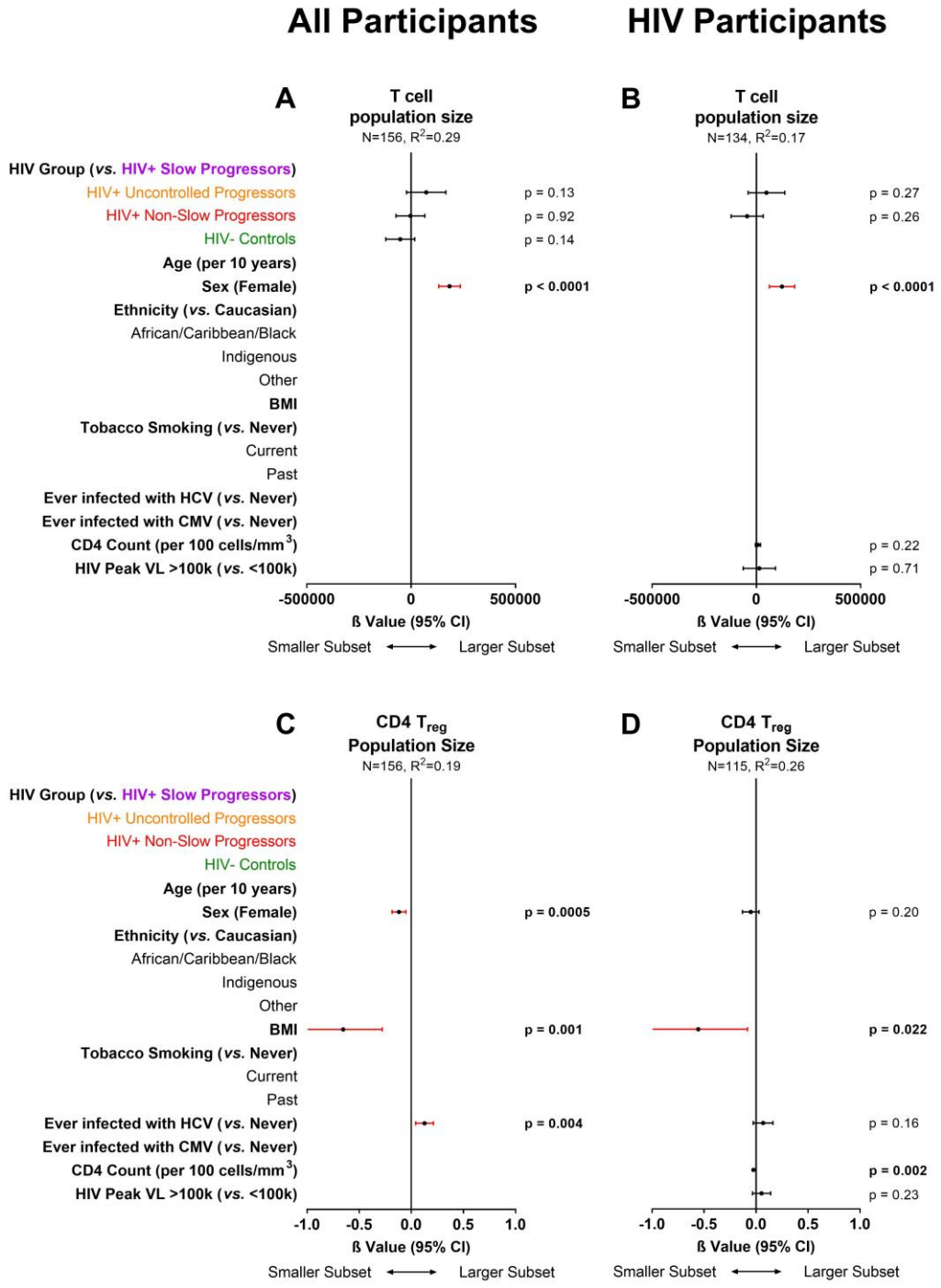

Figure 4.21 Multivariable modelling of T cell and CD4 T_{reg} subset sizes.
Multivariable linear models of all participants (left) and subgroup analyses among PLWH (right) are shown, including models of T cell (A-B) and CD4 T_{reg} (C-D) subset sizes. T cell and CD4 T_{reg} population sizes are cubed and log-transformed, respectively. Red confidence intervals indicate statistical significance. Coefficients of determination and unstandardized β values shown.

4.3.6 Dimensionality reduction visualization of aging markers

The multivariable linear regressions described above enable us to draw statistically stringent conclusions from the data, but they are limited by their capacity to model one variable of interest at a time. This makes complex datasets involving multiple variables of interest difficult to conceptualize. By using dimensionality reduction visualization techniques such as PCA and t-sne, we can visualize the relationships between any number of variables collapsed down to a two-dimensional plot. Using this plot, we can also visualize how HIV groups are associated with these variables. In the context of PCAs, these two dimensions are called principal components.

Here, we take all the variables of interest that multivariable linear regressions revealed to be different between HIV groups ($P<0.05$) and model them using PCA. The first two principal components (PC1 and PC2) are shown in **Figure 4.22A-B** (N=121, variance explained by PC1+PC2 = 66%). This model demonstrated collinearity in TL between CD4 T cells, B cells, and proliferative CD8 T cells, as suggested in earlier univariable analysis. The senescent CD8 T cell TL appeared to have the weakest association with the other subset TL measurements. Furthermore, CD4:CD8 T cell ratio, proliferative:senescent CD8 T cell ratio, and CD8 T_N subset size were also collinear. As expected, CD8 T_N and T_{EM} population sizes were inversely related. When PC1 and PC2 data points were categorized by HIV group, there was substantial overlap between participants in different groups (**Figure 4.22B**). Despite this, the position of the centroids of each group suggests that the greatest difference between groups exists between SPs and HIV-negative controls, with UPs more similar to SPs and NSPs more similar to HIV-negative controls. Moreover, the position of the centroids relative to vectors representing the original variables suggests that SPs tend to have larger CD8 T_{EM} populations, and that HIV-

negative controls tend to have larger CD8 T_N populations and higher CD4:CD8 ratio compared to the other groups. Overall, this PCA supports the findings of earlier linear regression models showing opposing relationships between CD8 T_N and T_{EM} population sizes with explanatory variables including HIV group, age, sex, and CMV infection (**Figure 4.20**).

A sensitivity PCA was done with CD4 TL instead of using TL from all four subsets (**Figure 4.22C-D**). This was done to increase power and mitigate the chance that missing TL data could introduce a bias in these models. In this sensitivity analysis, the explained variance increased but the separation between HIV groups appeared to be weaker (N=160, variance = 75%). Despite this, the greatest separation between groups remains between HIV SPs and HIV-negative controls, although the separation between NSPs and HIV-negative controls is greater relative to the earlier PCA. The opposing relationship between CD8 T_N and T_{EM} population sizes remained, as did the collinearity between CD4:CD8 and proliferative:senescent CD8 T cell ratios. As above, another sensitivity analysis was done using senescent CD8 TL instead of CD4 TL (N=153, **Figure 4.22E-F**). This was done to evaluate the robustness of the model when another cell subset is used to represent PBMC TL. Compared to the CD4 T cell TL model, the relationships between the other markers was virtually identical, reinforcing the robustness of the models. However, the HIV NSP group appeared to shift closer to the HIV UP population and away from the HIV-negative controls, although the centroids still indicate that SPs were most different from HIV-negative controls, and most similar with UP participants. These sensitivity models suggest that TL differences contribute substantially to the holistic differences between HIV groups, even when the other variables remain the same.

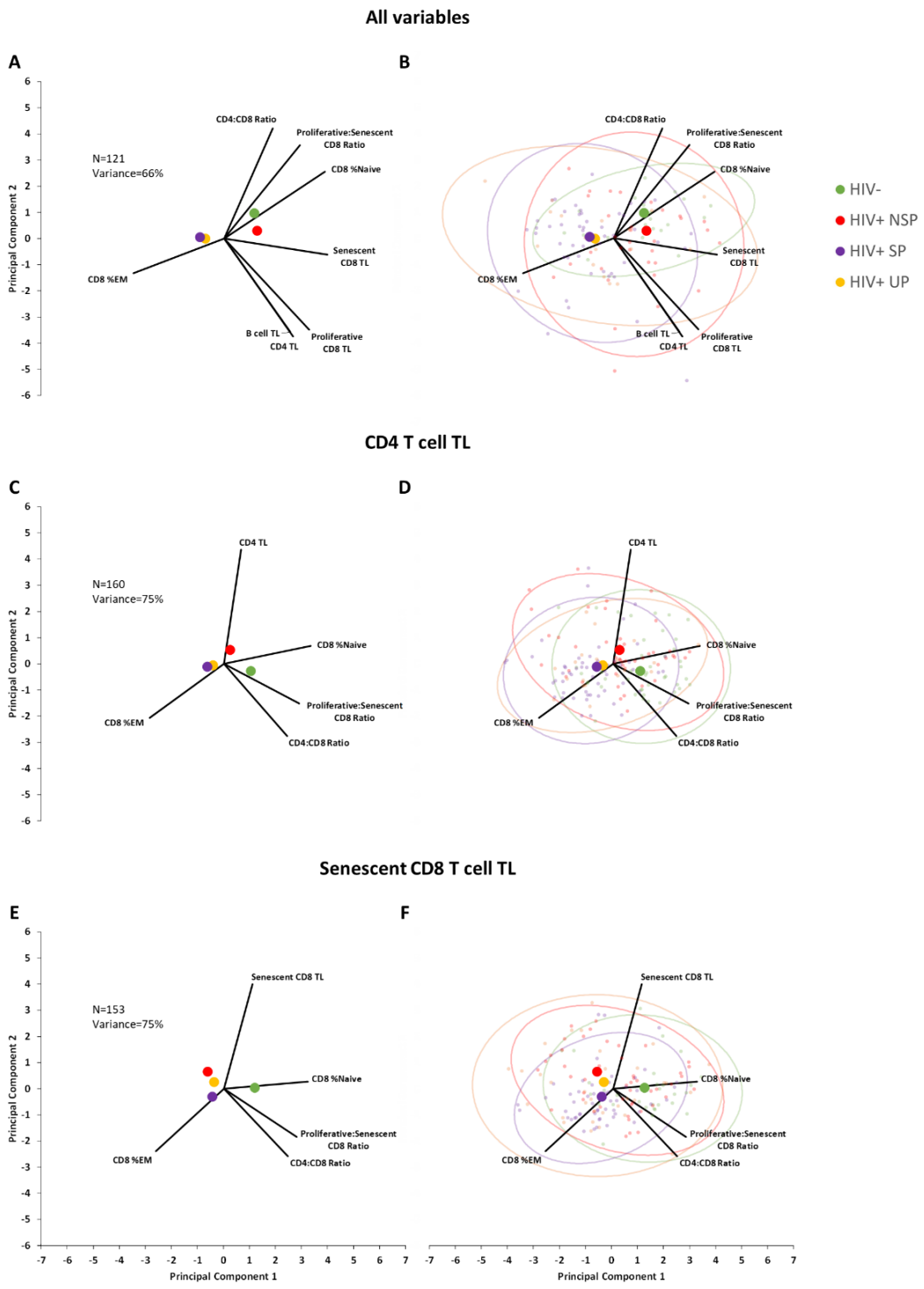

Figure 4.22 Dimensionality reduction visualization using PCA.
PCA biplots of the first two principal components are shown. Left and right panels show the same data, with data points and 95% confidence intervals of HIV groups shown on the right. Three models are depicted using TL data from all subsets (A-B), CD4 T cells (C-D), and senescent CD8 T cells (E-F). Loadings of explanatory variables are shown, and centroids of the four HIV groups are shown as large colour-coded dots on all panels.

In summary, PCA modelling revealed robust relationships between immune aging markers that persisted in sensitivity models where TL data from either the CD4 or senescent CD8 T cell compartment substituted those from all subsets. However, none of the PCA models showed truly distinct clustering of data by HIV groups, although the first two principal components explained 66-75% of the total variance. While it is possible that increasing sample size or number of relevant variables would more clearly resolve HIV groups, it is more likely that for the immune markers investigated here, the intrinsic variability within groups is greater than the variability between groups. Despite this, a recurring pattern was observed whereby SP participants were the most similar to UP participants and the most dissimilar with NSP participants and HIV-negative controls. The latter two groups were most closely associated in two of the three models. In relation to the original variables, SP participants tended to have larger CD8 T_{EM} and smaller CD8 T_N populations on average, while the opposite was true for the HIV-negative controls. Similarly, SPs and HIV-negative controls tended to have shorter and longer PBMC subset TL respectively, although this relationship was less clear than that seen with the CD8 T cell population sizes.

Dimensionality reduction visualization was then done using t-sne as an alternative to PCA. Unlike PCA, which models variables of interest linearly, t-sne is a non-deterministic technique sensitive to non-parametric relationships between variables. In many datasets, this is the superior technique for resolving clusters between groups.

A t-sne model using the same variables as the PCA was done, which demonstrated an apparent polarity between HIV groups, where a higher density of SP data points was plotted away from those of HIV-negative controls (**Figure 4.23A**). Although these data were still insufficient to

form distinct clusters, the difference between SP and HIV-negative groups was more evidently resolved compared to PCA generated from the same data. Clustering of the HIV NSP and UP groups was less apparent.

As with the PCA models, sensitivity t-sne models were created in which all PBMC subset TL were substituted by either CD4 of senescent CD8 T cell TL (**Figure 4.23B-C**). In the CD4 T cell TL model, the NSP data points appeared to be more strongly associated with those of the HIV-controls and less with the SP group. This may be the benefit of a larger sample size when only using TL data from one subset (N=160 and N=121). The UP group remains similarly unresolved, perhaps because of the comparatively lower sample size within that group. In both sensitivity models, the differences between the SP and HIV-negative groups remain. Together, these t-sne models indicate that including all PBMC subset TL data was not superior to only including TL data from one subset. This is in contrast with the PCAs, in which the overall separation between HIV groups was less easily discerned.

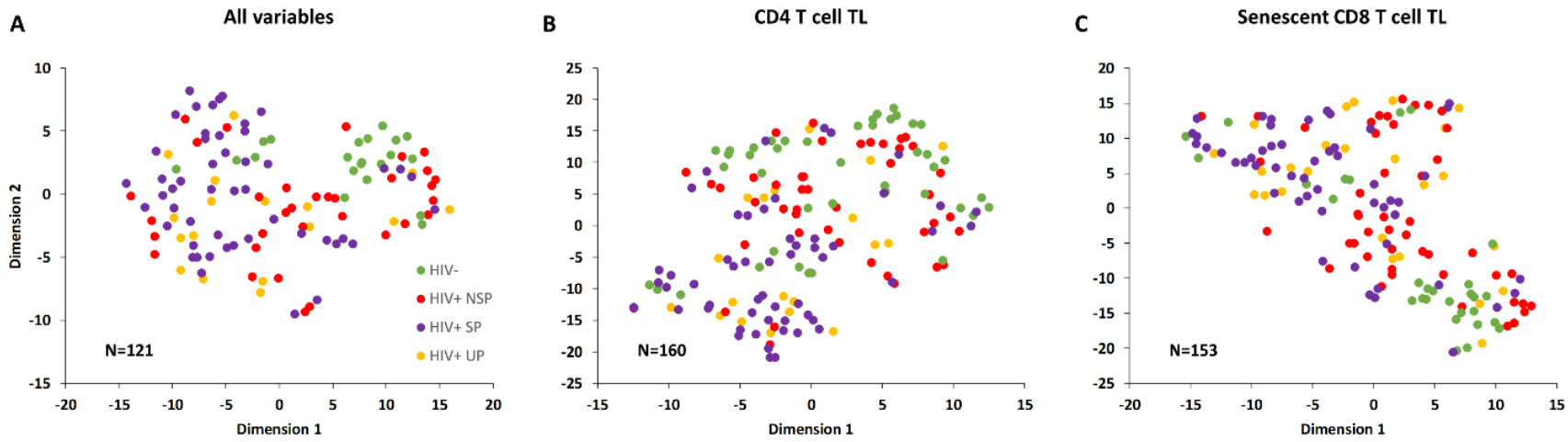

Figure 4.23 Dimensionality reduction visualization using t-sne.
Two-dimensional t-sne plots are shown, with TL data from all subsets (A), CD4 T cells (B), and senescent CD8 T cells (C). All t-sne analyses included immunophenotypic markers selected from multivariable linear regressions and were done with a perplexity of 15 and 5000 iterations.

4.4 Discussion

The purpose of this study was to characterize the differences in immune aging between people with naturally-controlled HIV, cART-controlled HIV, uncontrolled HIV, and no HIV. We sought to determine whether a person's natural ability to control HIV would translate to a natural defense against HIV-mediated accelerated immune aging. In contrast to our hypotheses, our analyses robustly demonstrated that SPs have an older immune aging profile than age- and sex-matched NSPs and HIV-negative controls, with a similar immune aging profile to UPs. Furthermore, we showed that HIV-mediated immune aging can be observed in specific cell types as well as in the T cell population holistically. This is demonstrated most explicitly in the SP participants, who have shorter TL in T cell subsets and expanded populations of more differentiated CD8 T cells compared to HIV-negative controls. These results support treatment of SPs, even elite controllers who can maintain undetectable HIV pVL, and provide insight on the role of chronic viral infections in aging in general.

We first characterized the degree to which cellular aging markers in PBMC subsets were mutually related. Specifically, we sought to ascertain whether HIV-induced changes in WB markers such as LTL and WB mtDNA content were driven by cellular aging or redistribution of cellular subsets. We found that although cellular markers were correlated between all four subsets among our entire sample, these markers were also different between specific subsets within individuals. For example, proliferative CD8 T cells intrinsically had higher TL than senescent CD8 T cells, and B cells intrinsically had higher TL and mtDNA content compared to T cell subsets. This suggests that while the variability between subsets was larger than the variability within subsets, individuals with evidence of greater cellular aging for a given marker

in one subset tended to show the same in all subsets. Furthermore, the correlations within lymphocyte subsets were much higher than the correlations between lymphocyte subsets and WB, although WB mtDNA was a better proxy of lymphocyte subsets than LTL. These results imply that neutrophils exert immense influence on LTL, suggesting that studies aiming to characterize lymphocyte TL should measure PBMC TL rather than LTL or incorporate both LTL and neutrophil-lymphocyte ratio into a multivariable analysis.

We also found that HIV status was associated with both more differentiated T cell distributions as well as shorter cell subset TL. Furthermore, the effect of HIV group on TL in all four PBMC subsets were similar. This, in conjunction with the collinearity in TL between PBMC subsets, suggests that HIV has a negative and uniform effect on TL in PBMCs. Together, these analyses indicate that HIV-mediated immune aging, and perhaps immune aging in general, affects both markers of cellular aging as well as T cell subset distributions. It remains unclear whether these effects represent a single phenomenon, or whether immune aging can occur via T cell redistribution in the absence of cellular aging. If the latter is true, future studies are needed to determine the causal direction between cellular aging and T cell differentiation in the context of immune aging.

Our data show that SPs had consistently older immune aging markers compared to NSPs and HIV-negative controls. It is worth noting that although the largest differences were seen between SP and HIV-negative control groups, our models generally detected no differences between the SP and UP groups. Similarly, although our models were not designed to detect differences between cART-controlled NSPs and HIV-negative controls, our analyses strongly

implied no differences between these two groups. These results suggest that cART is not only effective at preventing AIDS but is also effective at preventing HIV-induced immune aging. Conversely, these data also suggest that although SPs may benefit from slower HIV disease progression, these individuals who are not treated with cART experience HIV-induced immune aging to a degree comparable with their peers living with uncontrolled disease progression. We hypothesize that SPs mitigate HIV disease progression at the expense of their immune capacity, perhaps with a sustained and comparatively high-level immune response that, over time, appears to translate into shorter PBMC subset TL and an expanded CD8 T_{EM} as seen in the SP participants in this study.

An exception to this pattern was observed with CD4:CD8 T cell ratio, where SPs had a higher ratio than UPs and NSPs, but a lower ratio than HIV-negative controls. This could in theory reflect an intrinsic protection against the HIV-mediated CD4 T cell attrition among SPs that is mitigated but not completely prevented by cART among NSPs. Alternatively, differences in CD4:CD8 T cell ratio could be driven by differences in CD8 T cell expansion between HIV groups. The latter is implicated by the strong association between SP status and CD8 T cell differentiation. However, our own data argue against the latter proposition, as no difference was seen in CD8 T cell differentiation between SP and UP groups, yet SPs had significantly higher CD4:CD8 T cell ratio than UPs. These results imply that HIV-mediated CD8 differentiation and PBMC TL shortening is likely governed by a distinct mechanism than HIV-induced CD4 attrition. SPs appear to be protected from CD4 T cell depletion but undergo greater CD8 T cell differentiation than their cART-treated peers. Hence, these data strongly support the benefits of cART treatment in SPs. More research is needed, including data on absolute CD4 and CD8 T

cell counts per volume of blood, to further explain the differences in CD4:CD8 T cell ratio in these HIV groups.

The immune markers that appeared most strongly modulated by HIV status were also those that showed the strongest association with chronological age. Specifically, SPs had shorter TL in all PBMC subsets, a reduced CD8 T_N population, and an expanded CD8 T_{EM} population, after adjusting for relevant confounders. The skewing of CD8 T cells away from the less differentiated naïve phenotype and towards the most differentiated memory phenotype is seen with older age in healthy individuals [18,105], as is shorter TL in PBMCs [342]. The effect of age on CD8 T_N and T_{EM} compartment sizes was reproduced in our models, and the effect of HIV group was greater than that of a decade of aging. However, no association was detected between older age and shorter CD8 T cell or B cell TL, suggesting that the effect of age on CD8 T cell differentiation is greater than its effect on CD8 T cell TL, or that the variability of CD8 T cell TL is influenced by a confounder that is unaccounted for in our analysis. Likewise, contrary to the literature, we found no association between WB mtDNA content nor LTL with age, although a non-significant trend was observed between shorter LTL and older age. We were likely limited by sample size here (N=102), as it was not an objective of our study to reproduce known effects of age-related WB biomarkers.

Although it was not our goal to characterize the role of sex in immune aging, sex was included as an explanatory variable in our models to adjust for its known effect on immune aging. It is well accepted that females have longer LTL than males [26,27]. A more detailed analysis within cell subsets has also shown that in adults, females have longer TL in lymphocytes, naïve T cells, and

B cells, but not granulocytes and memory T cells [343]. However, this is apparently contradicted by a meta-analysis suggesting that females may have shorter telomeres in the bulk PBMC population [26], which comprises mostly lymphocytes. The source of this discrepancy remains unclear, though the authors noted that effect sizes were somewhat modulated by measurement methods [26]. Our data are consistent with the meta-analysis, showing in a single sample of adult individuals that women had higher LTL, yet shorter TL in the CD4 and proliferative CD8 T cell compartments. We also observed non-significantly shorter ($P<0.09$) TL in the remaining PBMC subsets among women. Our multivariable modelling offered a potential explanation to this apparent contradiction. Although women had somewhat shorter TL in specific PBMC subsets, women also had much larger populations of cell types with relatively little replication history and inherently longer TL, with the net effect being longer LTL. Our data showed that being female was independently associated with having T cell distributions with larger naïve and smaller differentiated populations. This included larger CD4 and CD8 T_N compartments, smaller CD4 T_{EM} populations, and a larger proliferative:senescent CD8 T cell ratio. Further research is necessary to clarify the differences in immune aging between males and females, including studies on differences in lymphocyte:neutrophil ratio, which could greatly influence LTL measurements as well.

It is known that the presence of chronic/latent coinfections has an impact on HIV disease progression and immune aging. We considered past or present infection with HCV or CMV as explanatory variables to further understand the differences we detected between HIV groups. The effect of CMV on immune aging is well known and is described in chapter 1. In line with previous evidence, we observed consistent associations between CMV infection and shorter TL

in T cell subsets. Furthermore, we found CMV to be concomitantly associated with larger T_{EM} populations in both CD4 and CD8 T cell compartments, and with a smaller T_N population only among CD8 T cells. Our data also showed associations between HCV and a reduced CD4:CD8 T cell ratio as well as an expanded CD4 T_{reg} population. These associations were independent of HIV, suggesting that an accumulation of viral coinfections in PLWH is accompanied by a corresponding decline in immune aging markers. Furthermore, the inclusion of CMV and HCV infection history into our models allowed us to interpret the effect of HIV status as independent of those coinfections. However, our data did not allow us to account for active vs. cleared HCV, nor for active vs. latent CMV infection, so the extent to which the effects seen in our data were driven by active infections remains unknown. Nevertheless, these data highlight the importance of considering coinfections such as HCV and CMV in studies characterizing the immune consequences of HIV.

A secondary objective of this study was to establish a holistic profile of accelerated immune aging among people living with HIV using the numerous markers studied here. First, multivariable linear regressions were used to determine which markers were adversely affected by HIV-mediated immune aging. Then, dimensionality reduction visualization using PCA and t-sne provided a more integrated understanding of how these markers were related to one another and visualized the extent to which participants from different HIV groups were different from one another compared to the intrinsic variability of participants within groups. In agreement with the other linear regressions conducted in this study, the PCAs demonstrated collinearity between TL of different PBMC subsets as well as an inverse association between CD8 T_N and T_{EM} population sizes. CD4:CD8 and proliferative:senescent CD8 T cell ratios were also more

related to measures of cell subset compartment size rather than subset TL. While shorter PBMC TL and more differentiated CD8 T cell populations are both markers of older age, our PCAs showed relatively little relationship between them, suggesting that cellular aging within subsets may be a distinct process from immune aging in the form of cell subset redistribution.

Although the multivariable linear regressions demonstrated robust differences between HIV groups, the most obvious interpretation of the plots generated by the dimensionality reduction visualization techniques was that the variation between individuals within groups remains much greater than the variation between groups. In the PCA models, a recurring pattern was observed where the SP and HIV-negative control groups were the most dissimilar. In addition, the UPs were on average more similar to SPs while the NSPs were more similar to the HIV-negative controls. The t-sne plots showed a similar trend, with the exception of the UP group, which appeared to exhibit greater variability due to reduced sample size. Overall, the HIV group confidence intervals greatly overlapped on the PCA plots, and distinct clusters did not form in the t-sne plots. Nevertheless, these models helped visualize the holistic effect of HIV-mediated accelerated immune aging, and together with the multivariable models, highlight specific immune markers that are most affected by HIV.

The primary strength of our study was a well-powered age- and sex-matched design that compared an extensive panel of immune aging markers between four HIV groups. One of these matched groups consisted of SPs, a rare population that is comparatively under-studied, allowing us the unique and novel opportunity to broadly characterize immune aging in this group compared to other more common HIV groups, as well as HIV-negative controls. This study also

benefited from statistical methodology that captures the effect of numerous immune aging markers and their potential confounders. The methodology relied on a systematic approach used to refine and develop models in a way that minimized potential human bias. Aside from age and sex, our analyses adjusted for numerous sociodemographic and clinical confounders known to influence immune aging, such as ethnicity, BMI, tobacco smoking, and chronic/latent viral coinfections. However, we did not have information on current CMV or HCV replication, hence could not tease out the potential effect of active infections with these two viruses. Furthermore, we lacked data on other forms of environmental stresses such as psychosocial stresses that may also play a role in immune aging. This should be explored in future studies.

Another limitation of our study was a potential cohort effect. While SP and UP groups were recruited from two pan-Canadian cohorts, NSPs and HIV-negative controls were recruited from only one of them. Therefore, it is possible that differences between those two groups and others were driven by a cohort effect rather than the effect of HIV. However, we have applied stringent QC throughout all aspects of our data collection to ensure only high-quality data were included in the analyses. Additionally, we have done sensitivity analyses to ensure that dead cells and missing data did not introduce bias. These measures mitigated the potential of a cohort effect driving our results. Lastly, the effectiveness of our dimensionality reduction strategies to capture differences between HIV groups was reduced by the inherent dimensionality of our dataset. Although the many immune aging markers included in these models were helpful in showing the trend between groups, even participants within groups likely differed along many other dimensions that were not captured in our models.

In summary, this study fulfilled its primary objective and demonstrated that SPs experience exacerbated immune aging compared to cART-controlled NSP and HIV-negative control groups. We robustly showed that SP control of HIV replication is associated with the cost of accelerated immune aging, and strongly suggest that SPs, even elite controllers, would benefit from cART. Furthermore, these results provide insight on the immune aging consequences of HIV and other chronic viruses such as CMV. By doing so, this study not only furthers the understanding of the specific effects of HIV, but also helps us understand the role of chronic viral infections in aging in general.

Chapter 5: Conclusion

5.1 Summary of findings and translational significance

The overarching goal of my PhD research was to investigate HIV infection as a human model of aging using well-established markers of immune aging in a well-controlled cohort of PLWH and HIV-negative controls across Canada.

TL and mtDNA content are two markers of cellular aging that are widely used in clinical research and feature prominently in the data presented here. My first objective was to adapt an MMqPCR technique previously designed to measure TL for use in measuring mtDNA content. The updated technique shows a two-fold improvement in time and cost-effectiveness over conventional monoplex qPCR and mitigates the variability introduced by human pipetting error. Furthermore, the MMqPCR mtDNA content assay is highly reproducible as established by multiple operators, is highly concordant with monoplex qPCR as measured using biospecimens from various tissues, and has a low limit of detection. The latter benefits my own research specifically because measuring mtDNA in relatively small cell subsets, such as senescent CD8 T cells, can be challenging without an assay that maintains high accuracy and precision despite low quantity of input material. This updated technique is ideal for high-throughput applications and can benefit a wide range of research applications. As more data are collected across a variety of research fields, the predictive properties of mtDNA content in blood continue to be better defined. Once these properties are sufficiently characterized, it is possible that WB mtDNA content may be incorporated as part of composite assessments, such as the Framingham risk

score for heart disease, or as part of routine clinical tests. Iterative improvements on the methodology, such as the one described here, are a crucial part of this process.

My next objective was to characterize the effects of HIV and HIV-related clinical parameters on TL and mtDNA content in WB. Because LTL and WB mtDNA content are relatively easy to measure, I was able to conduct this study using 312 WLWH and 300 HIV-negative controls, including 296 participants with longitudinal biospecimens. In well-controlled analyses adjusting for age, ethnicity, and substance use, I found that uncontrolled HIV viremia exacerbated the attrition rate of both markers. For example, LTL loss occurs at a rate of approximately 30 bp/year in the general population, whereas uncontrolled HIV viremia is associated with LTL loss of greater than 100 bp/year. This finding reinforces the importance of cART and explicitly demonstrates the immune consequences of losing HIV control. I also found an inverse yin and yang relationship between the rates of LTL loss and WB mtDNA content loss, whereby faster LTL attrition was associated with slower WB mtDNA content loss. This phenomenon is consistent with the mitochondrial protective function of telomerase, which localizes to mitochondria and protects them from damage while neglecting telomere maintenance during circumstances of oxidative stress. This mechanism suggests that the immediate protection of mitochondria from oxidative damage is favoured over the long-term benefits of telomere maintenance. The data presented here may be the *in vivo* consequence of this mechanism, in which the accumulation of oxidative challenges to the mitochondria over many years results in slower mtDNA content loss at the cost of faster TL attrition. Although this association is robust, it needs to be confirmed in an independent cohort. If the relationship proves to be reproducible in independent studies, it will be essential in future aging studies to incorporate both markers.

For example, when studying a disease known to affect LTL, analyses would benefit from considering the influence of WB mtDNA content in the sample. Furthermore, as mentioned above, both LTL and WB mtDNA content may be incorporated in routine standard of care testing in the future. A better understanding of the relationship between the two could greatly increase their predictive value.

Finally, my last objective was to further explore HIV as a human model of immune aging by studying SPs, a rare population of PLWH who have the natural ability to impede disease progression in the absence of treatment. A group of 57 SPs were sex- and age-matched with cART-controlled NSPs, UPs who were not on cART, as well as HIV-negative controls. The scarcity of the SP population limited the power relative to the previous study. To compensate, I measured a wider range of immune markers, including TL and mtDNA within relevant immune cellular subsets, as well as T cell differentiation. These markers have previously been established to decline with age, and most of them are also considered to be markers of HIV-mediated accelerated immune aging. I hypothesized that the SPs' ability to naturally control HIV would translate into protection against HIV-mediated accelerated immune aging. In contrast, my data definitively show that SPs have immune aging markers related to older age compared to HIV-negative controls and even cART-controlled PLWH. SPs have shorter immune subset-specific TL and more differentiated CD8 T cell populations. This is also visualized holistically using dimensionality reduction techniques that illustrate the dissimilarity between SPs and NSPs while taking into account the many relevant markers of immune aging simultaneously. This is the first study showing the immune consequences of naturally controlling HIV compared to a matched group of PLWH on cART with undetectable viremia.

These data highlight the importance of never compromising cART control of HIV, even in SPs. Furthermore, in the context of HIV as a human model of aging, these analyses among SPs raise the possibility that accelerated immune aging in HIV may be more related to the immune response to HIV rather than immune compromise from HIV disease progression. This is supported by the evidence showing that HIV-mediated accelerated immune aging is considerably alleviated by cART. However, successful cART does not completely eliminate the immune response to HIV, as seen by low levels of inflammation and immune activation that have been documented in people living with cART-controlled HIV. If treatment exists whereby the immune response to HIV is completely abolished, perhaps HIV-mediated accelerated immune aging would be eradicated as well.

Overall, in the pursuit of characterizing HIV as a human model of aging, my research supports a paradigm in which immune aging is in part driven by the accumulation of immune challenges that deplete the finite capacity of the immune system. In a chronic disease such as HIV infection, this effect is exacerbated, resulting in an apparent accelerated aging phenotype in PLWH. In HIV specifically, my research highlights the consequences of uncontrolled viremia and reinforces the benefits of cART.

5.2 Future directions

5.2.1 Confirming relevance in other populations in independent cohorts

When observational studies reveal novel findings, the first priority is always to confirm the findings in an independent cohort in order to address the potential biases inherent to

observational studies. Here, the analyses characterizing the immune consequences of HIV benefit from using well-controlled groups representing a relatively narrow slice of the global population. A future study should determine whether these findings hold true in other populations that would ideally represent genetic, environmental, societal, and/or cultural factors dissimilar to the sample used here. For example, ethnicity, income, diet, physical activity, access to healthcare, personality, as well as psychosocial stresses such as childhood trauma have all been linked to differences in TL. These potential confounders may also have unpredictable interactions that may exaggerate or hide the effect of HIV on immune aging. Future studies should aim to capture such factors and thereby strengthen the robustness of the findings presented in the current study.

One specific population that should receive particular focus is children who are affected by HIV, who intrinsically have differences in immunity compared to adults, such as much higher normal ranges of WBC and CD4 counts. A subset of these children acquired HIV perinatally and has therefore lived with HIV during infancy, a time of underdeveloped immunity. Another subset is individuals who are exposed to HIV *in utero* but are not infected. These HEU individuals are exposed to *in utero* maternal cART and potentially pro-inflammatory HIV milieu. Because of the relative recency of HIV and cART, these populations are only now beginning to reach early middle age. What were previously pediatric studies on these populations are beginning to evolve into aging studies in adults. It is unknown how differently these growing populations will experience the accelerated immune aging seen in elderly PLWH today.

A future study should also aim to investigate parameters of HIV immune response and integrate them into the panel of immune markers investigated in the current study. For example, the size of the HIV-specific CD8 T cell population, HLA typing, and markers of immune activation could be incorporated into the current analysis of immune aging. Metrics of immune aging themselves could also be expanded to include, for example, DNA methylation markers associated with older age and accumulation of mtDNA mutations. Increasing the dimensions by which HIV immune consequences are characterized may help pinpoint the mechanisms behind, and potentially identify predictors of, resistance against HIV-mediated immune aging.

Addressing the connection between immune aging markers and age-related comorbidities can perhaps be considered the final domain of HIV and aging research. This would ideally be addressed with a prospective cohort of PLWH in which comorbidities such as HIV-associated neurocognitive disorders, retinopathy, low bone mineral density, and frailty can be recorded. Such a study would include follow-up visits for longitudinal analyses over a long enough period of time to capture the incidence of these age-related comorbidities. These data would allow researchers to identify which immune aging markers have the greatest capacity to predict comorbidities, and potentially identify mechanisms behind the increased incidence of some of these comorbidities in HIV. It could also identify factors modifiable through prevention or treatment to attenuate immune aging and promote healthy aging.

5.2.2 Exploring other chronic/latent viral infections as human models of aging

The impact of HIV on accelerated immune aging is relatively well-characterized. However, there is also evidence of similar effects in other chronic/latent viral infections, especially CMV.

The immune consequences associated with CMV, as well as with HIV-CMV coinfection, are briefly outlined in chapter 1. The effect of CMV on CD8 T cell differentiation is comparable to, if not greater than, the effect of HIV. However, it is more difficult to study the effect of CMV because of its asymptomatic nature in the general population of healthy adults and because of the unpredictability of its periodic reactivations. It is possible that any effects of CMV on accelerated immune aging are related to these transient episodes of viral replication. A future study to address the impact of CMV would have to be carefully designed with frequent visits in order to capture the frequency and severity of reactivations. By doing so, it may be possible to identify a unique population of individuals who are more naturally resistant to CMV reactivations. This population would be analogous to the SP population in HIV and may shed light on the mechanisms by which CMV induces accelerated immune aging. An argument was made at the outset of chapter 1 regarding the societal cost of HIV-mediated immune aging. With more data, it is possible that a stronger argument can be made for that of CMV.

To further broaden the concept of chronic/latent viral infections as human models of aging, it is reasonable that the accumulation of multiple infections would have proportionately, or perhaps even disproportionately, larger effects on immune aging. Some of the more common viruses like HCV, EBV, HSV-1 and -2, and VZV have been associated with shorter TL as well as higher prevalence of age-related comorbidities. Future studies that characterize lifetime cumulative viral burden in the general population may find it to be a major driver of biological aging. It is conceivable that better prevention and control of a wide array of chronic/latent viral infections using tools such as vaccines and antiviral treatments would extend lifespan and lead to healthier aging. If so, this would represent an evolution in the paradigm of aging research.

References

1. United Nations. Department of Economic and Social Affairs. World population ageing, 1950-2050. *Choice Rev Online*. 2002;40(03):40-1307-40-1307. doi:10.5860/CHOICE.40-1307
2. Kline KA, Bowdish DME. Infection in an aging population. *Curr Opin Microbiol*. 2016;29:63-67. doi:10.1016/j.mib.2015.11.003
3. Stowe RP, Kozlova E V, Yetman DL, Walling DM, Goodwin JS, Glaser R. Chronic herpesvirus reactivation occurs in aging. *Exp Gerontol*. 2007;42(6):563-570. doi:10.1016/j.exger.2007.01.005
4. Thomasini RL, Pereira DS, Pereira FSM, Mateo EC, Mota TN, Guimarães GG, Pereira LSM, Lima CX, Teixeira MM, Teixeira ALJ. Aged-associated cytomegalovirus and Epstein-Barr virus reactivation and cytomegalovirus relationship with the frailty syndrome in older women. *PLoS One*. 2017;12(7):e0180841. doi:10.1371/journal.pone.0180841
5. D'Alessio DJ, Cox Jr. PM, Dick EC. Failure of Inactivated Influenza Vaccine to Protect an Aged Population. *JAMA*. 1969;210(3):485-489. doi:10.1001/jama.1969.03160290037007
6. Bernstein E, Kaye D, Abrutyn E, Gross P, Dorfman M, Murasko DM. Immune response to influenza vaccination in a large healthy elderly population. *Vaccine*. 1999;17(1):82-94. doi:10.1016/s0264-410x(98)00117-0
7. Franceschi C, Garagnani P, Parini P, Giuliani C, Santoro A. Inflammaging: a new immune–metabolic viewpoint for age-related diseases. *Nat Rev Endocrinol*. 2018;14(10):576-590. doi:10.1038/s41574-018-0059-4

8. Mozaffarian D, Benjamin EJ, Go AS, Arnett DK, Blaha MJ, Cushman M, de Ferranti S, Després J-P, Fullerton HJ, Howard VJ, Huffman MD, Judd SE, Kissela BM, Lackland DT, Lichtman JH, Lisabeth LD, Liu S, Mackey RH, Matchar DB, McGuire DK, Mohler ER 3rd, Moy CS, Muntner P, Mussolino ME, Nasir K, Neumar RW, Nichol G, Palaniappan L, Pandey DK, Reeves MJ, Rodriguez CJ, Sorlie PD, Stein J, Towfighi A, Turan TN, Virani SS, Willey JZ, Woo D, Yeh RW, Turner MB. Heart Disease and Stroke Statistics—2015 Update. *Circulation*. 2015;131(4):e29-e322. doi:10.1161/CIR.0000000000000152

9. Dhingra R, Vasan RS. Age as a cardiovascular risk factor. *Med Clin North Am*. 2012;96(1):87-91. doi:10.1016/j.mcna.2011.11.003

10. Kim IH, Kisseleva T, Brenner DA. Aging and liver disease. *Curr Opin Gastroenterol*. 2015;31(3):184-191. doi:10.1097/MOG.0000000000000176

11. Stevens LA, Viswanathan G, Weiner DE. Chronic kidney disease and end-stage renal disease in the elderly population: current prevalence, future projections, and clinical significance. *Adv Chronic Kidney Dis*. 2010;17(4):293-301. doi:10.1053/j.ackd.2010.03.010

12. Coresh J, Astor BC, Greene T, Eknoyan G, Levey AS. Prevalence of chronic kidney disease and decreased kidney function in the adult US population: Third national health and nutrition examination survey. *Am J Kidney Dis*. 2003;41(1):1-12. doi:https://doi.org/10.1053/ajkd.2003.50007

13. Reginster J-Y, Burlet N. Osteoporosis: A still increasing prevalence. *Bone*. 2006;38(2, Supplement 1):4-9. doi:https://doi.org/10.1016/j.bone.2005.11.024

14. Dix D. The Role of Aging in Cancer Incidence: An Epidemiological Study. *J Gerontol*.

1989;44(6):10-18. doi:10.1093/geronj/44.6.10

15. Pawelec G. Age and immunity: What is “immunosenescence”? *Exp Gerontol*. 2018;105:4-9. doi:10.1016/j.exger.2017.10.024

16. Müezzinler A, Zaineddin AK, Brenner H. A systematic review of leukocyte telomere length and age in adults. *Ageing Res Rev*. 2013;12(2):509-519. doi:10.1016/j.arr.2013.01.003

17. Wikby A, Ferguson F, Forsey R, Thompson J, Strindhall J, Löfgren S, Nilsson B-O, Ernerudh J, Pawelec G, Johansson B. An immune risk phenotype, cognitive impairment, and survival in very late life: impact of allostatic load in Swedish octogenarian and nonagenarian humans. *J Gerontol A Biol Sci Med Sci*. 2005;60(5):556-565. doi:10.1093/gerona/60.5.556

18. Fagnoni FF, Vescovini R, Passeri G, Bologna G, Pedrazzoni M, Lavagetto G, Casti A, Franceschi C, Passeri M, Sansoni P. Shortage of circulating naive CD8+ T cells provides new insights on immunodeficiency in aging. *Blood*. 2000;95(9):2860-2868. doi:10.1182/blood.v95.9.2860.009k35_2860_2868

19. Frenck RW, Blackburn EH, Shannon KM. The rate of telomere sequence loss in human leukocytes varies with age. *Proc Natl Acad Sci*. 2002;95(10):5607-5610. doi:10.1073/pnas.95.10.5607

20. Zeichner SL, Palumbo P, Feng Y, Xiao X, Gee D, Sleasman J, Goodenow M, Biggar R, Dimitrov D. Rapid telomere shortening in children. *Blood*. 1999;93(9):2824-2830.

21. Daniali L, Benetos A, Susser E, Kark JD, Labat C, Kimura M, Desai K, Granick M, Aviv A. Telomeres shorten at equivalent rates in somatic tissues of adults. *Nat Commun*. 2013;4:1-7. doi:10.1038/ncomms2602

22. Kuznetsova T, Codd V, Brouilette S, Thijs L, González A, Jin Y, Richart T, Van Der Harst P, Díez J, Staessen JA, Samani NJ. Association between left ventricular mass and telomere length in a population study. *Am J Epidemiol*. 2010;172(4):440-450. doi:10.1093/aje/kwq142

23. Chen W, Kimura M, Kim S, Cao X, Srinivasan SR, Berenson GS, Kark JD, Aviv A. Longitudinal versus cross-sectional evaluations of leukocyte telomere length dynamics: Age-dependent telomere shortening is the rule. *Journals Gerontol - Ser A Biol Sci Med Sci*. 2011;66 A(3):312-319. doi:10.1093/gerona/glq223

24. Hjelmborg JB, Dalgård C, Möller S, Steenstrup T, Kimura M, Christensen K, Kyvik KO, Aviv A. The heritability of leucocyte telomere length dynamics. *J Med Genet*. 2015;52(5):297-302. doi:10.1136/jmedgenet-2014-102736

25. Slagboom P, Droog S, Boomsma D. Genetic determination of telomere size in humans: a twin study of three age groups. *Am J Hum Genet*. 1994;55(5):876-882.

26. Gardner M, Bann D, Wiley L, Cooper R, Hardy R, Nitsch D, Martin-Ruiz C, Shiels P, Sayer AA, Barbieri M, Bekaert S, Bischoff C, Brooks-Wilson A, Chen W, Cooper C, Christensen K, De Meyer T, Deary I, Der G, Roux AD, Fitzpatrick A, Hajat A, Halaschek-Wiener J, Harris S, Hunt SC, Jagger C, Jeon HS, Kaplan R, Kimura M, Lansdorp P, Li C, Maeda T, Mangino M, Nawrot TS, Nilsson P, Nordfjall K, Paolisso G, Ren F, Riabowol K, Robertson T, Roos G, Staessen J a., Spector T, Tang N, Unryn B, van der Harst P, Woo J, Xing C, Yadegarfar ME, Park JY, Young N, Kuh D, von Zglinicki T, Ben-Shlomo Y. Gender and telomere length: Systematic review and meta-analysis. *Exp Gerontol*. 2014;51:15-27. doi:10.1016/j.exger.2013.12.004

27. Benetos A, Okuda K, Lajemi M, Kimura M, Thomas F, Skurnick J, Labat C, Bean K,

Aviv A. Telomere Length as an Indicator of Biological Aging. *Hypertension*. 2001;37(2):381-385. doi:10.1161/01.hyp.37.2.381

28. Aviv A, Srinivasan SR, Eckfeldt JH, Chen W, Hunt SC, Kimura M, Berenson GS, Gardner JP. Leukocyte telomeres are longer in AfricanAmericans than in whites: the National Heart, Lung, and Blood Institute Family Heart Study and the Bogalusa Heart Study. *Aging Cell*. 2008;7(4):451-458. doi:10.1111/j.1474-9726.2008.00397.x

29. Diez Roux A V., Ranjit N, Jenny NS, Shea S, Cushman M, Fitzpatrick A, Seeman T. Race/ethnicity and telomere length in the Multi-Ethnic Study of Atherosclerosis. *Aging Cell*. 2009;8(3):251-257. doi:10.1111/j.1474-9726.2009.00470.x

30. Cassidy A, De Vivo I, Liu Y, Han J, Prescott J, Hunter DJ, Rimm EB. Associations between diet, lifestyle factors, and telomere length in women. *Am J Clin Nutr*. 2010;91(5):1273-1280. doi:10.3945/ajcn.2009.28947

31. Nettleton JA, Diez-Roux A, Jenny NS, Fitzpatrick AL, Jacobs DRJ. Dietary patterns, food groups, and telomere length in the Multi-Ethnic Study of Atherosclerosis (MESA). *Am J Clin Nutr*. 2011;143(5):1405-1412. doi:10.3945/ajcn.2008.26429

32. Paul L. Diet, nutrition and telomere length. *J Nutr Biochem*. 2011;22(10):895-901. doi:10.1016/j.jnutbio.2010.12.001

33. Ludlow AT, Zimmerman JB, Witkowski S, Hearn JW, Hatfield BD, Roth SM. Relationship between physical activity level, telomere length, and telomerase activity. *Med Sci Sports Exerc*. 2008;40(10):1764-1771. doi:10.1249/MSS.0b013e31817c92aa

34. LaRocca TJ, Seals DR, Pierce GL. Leukocyte telomere length is preserved with aging in endurance exercise-trained adults and related to maximal aerobic capacity. *Mech Ageing Dev*. 2010;131(2):165-167. doi:10.1016/j.mad.2009.12.009

35. Astuti Y, Wardhana A, Watkins J, Wulaningsih W. Cigarette smoking and telomere length: A systematic review of 84 studies and meta-analysis. *Environ Res*. 2017;158:480-489. doi:10.1016/j.envres.2017.06.038

36. Müezzinler A, Mons U, Dieffenbach AK, Butterbach K, Saum KU, Schick M, Stammer H, Boukamp P, Holleczek B, Stegmaier C, Brenner H. Smoking habits and leukocyte telomere length dynamics among older adults: Results from the ESTHER cohort. *Exp Gerontol*. 2015;70:18-25. doi:10.1016/j.exger.2015.07.002

37. Valdes AM, Andrew T, Gardner JP, Kimura M, Oelsner E, Cherkas LF, Aviv A, Spector TD. Obesity, cigarette smoking, and telomere length in women. *Lancet*. 2005;366(9486):662-664. doi:10.1016/S0140-6736(05)66630-5

38. Song Z, Figura G Von, Liu Y, Kraus JM, Torrice C, Dillon P, Rudolph-watabe M, Ju Z, Kestler HA, Sanoff H, Rudolph KL. Lifestyle impacts on the aging-associated expression of biomarkers of DNA damage and telomere dysfunction in human blood. *Aging Cell*. 2010;9(4):607-615. doi:10.1111/j.1474-9726.2010.00583.x

39. McGrath M, Wong JYY, Michaud D, Hunter DJ, De Vivo I. Telomere Length, Cigarette Smoking, and Bladder Cancer Risk in Men and Women. *Cancer Epidemiol Biomarkers Prev*. 2007;16(4):815-819. doi:10.1158/1055-9965.EPI-06-0961

40. Huzen J, Wong LSM, van Veldhuisen DJ, Samani NJ, Zwinderman AH, Codd V, Cawthon RM, Benus GFJD, van der Horst ICC, Navis G, Bakker SJL, Gansevoort RT, de Jong PE, Hillege HL, van Gilst WH, de Boer RA, Van der Harst P. Telomere length loss due to smoking and metabolic traits. *J Intern Med*. 2014;275(2):155-163. doi:10.1111/joim.12149

41. Zhou D, Shen Q, Cui D, He S, Wang T, Qi G, Yang Z, Ye J, Li C, Liu Y, Cao L, Wu J,

He L. Drug addiction is associated with leukocyte telomere length. *Sci Rep*. 2013;3(1):1-6. doi:10.1038/srep01542

42. Zanet DAL, Thorne A, Singer J, Maan EJ, Sattha B, Le Campion A, Soudeyns H, Pick N, Murray M, Money DM, Côté HCF. Association between short leukocyte telomere length and HIV infection in a cohort study: No evidence of a relationship with antiretroviral therapy. *Clin Infect Dis*. 2014;58(9):1322-1332. doi:10.1093/cid/ciu051

43. Gonzalez-Serna A, Ajaykumar A, Gadawski I, Muñoz-Fernández MA, Hayashi K, Harrigan PR, Côté HCF. Rapid Decrease in Peripheral Blood Mononucleated Cell Telomere Length After HIV Seroconversion, but Not HCV Seroconversion. *J Acquir Immune Defic Syndr*. 2017;76(1):e29-e32. doi:10.1097/QAI.0000000000001446

44. Bestilny LJ, Gill MJ, Mody CH, Riabowol KT. Accelerated replicative senescence of the peripheral immune system induced by HIV infection. *Aids*. 2000;14(7):771-780. doi:10.1097/00002030-200005050-00002

45. Lawn SD, Weiss HA, Christ T, McGlynn L, Port J, Barclay K, Wood R, Shiels PG, Pathai S, Bekker L-G, Gilbert CE, McGuinness D. Accelerated biological ageing in HIV-infected individuals in South Africa. *Aids*. 2013;27(15):2375-2384. doi:10.1097/qad.0b013e328363bf7f

46. Liu JCY, Leung JM, Ngan DA, Nashta NF, Guillemi S, Harris M, Lima VD, Um SJ, Li Y, Tam S, Shaipanich T, Raju R, Hague C, Leipsic JA, Bourbeau J, Tan WC, Harrigan PR, Sin DD, Montaner J, Man SFP. Absolute leukocyte telomere length in HIV-infected and uninfected individuals: Evidence of accelerated cell senescence in HIV-associated chronic obstructive pulmonary disease. *PLoS One*. 2015;10(4):1-13. doi:10.1371/journal.pone.0124426

47. Gianesin K, Noguera-Julian A, Zanchetta M, Del Bianco P, Petrara MR, Freguja R, Rampon O, Fortuny C, Camós M, Mozzo E, Giaquinto C, De Rossi A. Premature aging and immune senescence in HIV-infected children. *Aids*. 2016;30(9):1363-1373. doi:10.1097/QAD.0000000000001093

48. Talmud PJ, Maubaret CG, Abelak K, Humphries SE, Stephens JW, Salpea KD, Cooper JA. Association of telomere length with type 2 diabetes, oxidative stress and UCP2 gene variation. *Atherosclerosis*. 2009;209(1):42-50. doi:10.1016/j.atherosclerosis.2009.09.070

49. Zee RYL, Castonguay AJ, Barton NS, Germer S, Martin M. Mean leukocyte telomere length shortening and type 2 diabetes mellitus: a case-control study. *Transl Res*. 2010;155(4):166-169. doi:10.1016/j.trsl.2009.09.012

50. Sampson MJ, Winterbone MS, Hughes JC, Dozio N, Hughes DA. Monocyte telomere shortening and oxidative DNA damage in type 2 diabetes. *Diabetes Care*. 2006;29(2):283-289. doi:10.2337/diacare.29.02.06.dc05-1715

51. Forero DA, González-Giraldo Y, López-Quintero C, Castro-Vega LJ, Barreto GE, Perry G. Meta-analysis of Telomere Length in Alzheimer's Disease. *Journals Gerontol - Ser A Biol Sci Med Sci*. 2016;71(8):1069-1073. doi:10.1093/gerona/glw053

52. Panossian LA, Porter VR, Valenzuela HF, Zhu X, Reback E, Masterman D, Cummings JL, Effros RB. Telomere shortening in T cells correlates with Alzheimer's disease status. *Neurobiol Aging*. 2003;24(1):77-84. doi:10.1016/s0197-4580(02)00043-x

53. Thomas P, O' Callaghan NJ, Fenech M. Telomere length in white blood cells, buccal cells and brain tissue and its variation with ageing and Alzheimer's disease. *Mech Ageing Dev*. 2008;129(4):183-190. doi:10.1016/j.mad.2007.12.004

54. Ma H, Zhou Z, Wei S, Liu Z, Pooley KA, Dunning AM, Svenson U, Roos G, Hosgood

3rd HD, Shen M, Wei Q. Shortened telomere length is associated with increased risk of cancer: a meta-analysis. *PLoS One*. 2011;6(6):e20466-e20466. doi:10.1371/journal.pone.0020466

55. Willeit P, Willeit J, Mayr A, Weger S, Oberhollenzer F, Brandstätter A, Kronenberg F, Kiechl S. Telomere Length and Risk of Incident Cancer and Cancer Mortality. *JAMA*. 2010;304(1):69-75. doi:10.1001/jama.2010.897

56. Fitzpatrick AL, Kronmal RA, Gardner JP, Psaty BM, Jenny NS, Tracy RP, Walston J, Kimura M, Aviv A. Leukocyte telomere length and cardiovascular disease in the cardiovascular health study. *Am J Epidemiol*. 2007;165(1):14-21. doi:10.1093/aje/kwj346

57. Bekaert S, De Meyer T, Rietzschel ER, De Buyzere ML, De Bacquer D, Langlois M, Segers P, Cooman L, Van Damme P, Cassiman P, Van Criekinge W, Verdonck P, De Backer GG, Gillebert TC, Van Oostveldt P. Telomere length and cardiovascular risk factors in a middle-aged population free of overt cardiovascular disease. *Aging Cell*. 2007;6(5):639-647. doi:10.1111/j.1474-9726.2007.00321.x

58. Brouilette S, Singh RK, Thompson JR, Goodall AH, Samani NJ. White cell telomere length and risk of premature myocardial infarction. *Arterioscler Thromb Vasc Biol*. 2003;23(5):842-846. doi:10.1161/01.ATV.0000067426.96344.32

59. Cawthon RM, Smith KR, O'Brien E, Sivatchenko A, Kerber RA. Association between telomere length in blood and mortality in people aged 60 years or older. *Lancet*. 2003;361(9355):393-395. doi:10.1016/S0140-6736(03)12384-7

60. Fitzpatrick AL, Kronmal RA, Kimura M, Gardner JP, Psaty BM, Jenny NS, Tracy RP, Hardikar S, Aviv A. Leukocyte telomere length and mortality in the cardiovascular health study. *Journals Gerontol - Ser A Biol Sci Med Sci*. 2011;66(4):421-429.

doi:10.1093/gerona/glq224

61. Epel ES, Merkin SS, Cawthon R, Blackburn EH, Adler NE, Pletcher MJ, Seeman TE. The rate of leukocyte telomere shortening predicts mortality from cardiovascular disease in elderly men. *Aging (Albany NY)*. 2008;1(1):81-88. doi:10.18632/aging.100007

62. Mengel-From J, Thinggaard M, Dalgård C, Kyvik KO, Christensen K, Christiansen L. Mitochondrial DNA copy number in peripheral blood cells declines with age and is associated with general health among elderly. *Hum Genet*. 2014;133(9):1149-1159. doi:10.1007/s00439-014-1458-9

63. Tritschler H, Andreetta F, Moraes C, Bonilla E, Arnaudo E, Danon M, Glass S, Zelaya B, Vamos E, Telerman-Toppet N, Shanske S, Kadenbach B, DiMauro S, Schon E. Mitochondrial myopathy of childhood associated with depletion of mitochondrial DNA. *Neurology*. 1992;42(1):209-217. doi:10.1212/wnl.42.1.209

64. Pisano A, Cerbelli B, Perli E, Pelullo M, Bargelli V, Preziuso C, Mancini M, He L, Bates MG, Lucena JR, Della Monica PL, Familiari G, Petrozza V, Nediani C, Taylor RW, D'Amati G, Giordano C. Impaired mitochondrial biogenesis is a common feature to myocardial hypertrophy and end-stage ischemic heart failure. *Cardiovasc Pathol*. 2016;25(2):103-112. doi:10.1016/j.carpath.2015.09.009

65. Yen M-Y, Chen C-S, Wang A, Wei Y-H. Increase of mitochondrial DNA in blood cells of patients with Leber's hereditary optic neuropathy with 11778 mutation. *Br J Ophthalmol*. 2002;86(9):1027-1030. doi:10.1136/bjo.86.9.1027

66. Spinazzola A, Zeviani M. Disorders of nuclear-mitochondrial intergenomic communication. *Biosci Rep*. 2007;27(1-3):39-51. doi:10.1007/s10540-007-9036-1

67. Dimmock D, Tang LY, Schmitt ES, Wong LJC. Quantitative evaluation of the

mitochondrial DNA depletion syndrome. *Clin Chem*. 2010;56(7):1119-1127. doi:10.1373/clinchem.2009.141549

68. Miura T, Goto M, Hosoya N, Odawara T, Kitamura Y, Nakamura T, Iwamoto A. Depletion of mitochondrial DNA in HIV-1-infected patients and its amelioration by antiretroviral therapy. *J Med Virol*. 2003;70(4):497-505. doi:10.1002/jmv.10423

69. Chiappini F, Teicher E, Saffroy R, Pham P, Falissard B, Barrier A, Chevalier S, Debuire B, Vittecoq D, Lemoine A. Prospective evaluation of blood concentration of mitochondrial DNA as a marker of toxicity in 157 consecutively recruited untreated or HAART-treated HIV-positive patients. *Lab Invest*. 2004;84(7):908-914. doi:10.1038/labinvest.3700113

70. Miró O, López S, Martínez E, Pedrol E, Milinkovic A, Deig E, Garrabou G, Casademont J, Gatell JM, Cardellach F. Mitochondrial effects of HIV infection on the peripheral blood mononuclear cells of HIV-infected patients who were never treated with antiretrovirals. *Clin Infect Dis*. 2004;39:710-716. doi:10.1086/423176

71. Casula M, Bosboom-Dobbelaer I, Smolders K, Otto S, Bakker M, de Baar MP, Reiss P, de Ronde A. Infection with HIV-1 induces a decrease in mtDNA. *J Infect Dis*. 2005;191(9):1468-1471. doi:10.1086/429412

72. Maagaard A, Holberg-Petersen M, Kvittingen E a., Sandvik L, Bruun JN. Depletion of mitochondrial DNA copies/cell in peripheral blood mononuclear cells in HIV-1-infected treatment-naïve patients. *HIV Med*. 2006;7(1):53-58. doi:10.1111/j.1468-1293.2005.00336.x

73. Côté HCF, Brumme ZL, Craib KJP, Alexander CS, Wynhoven B, Ting L, Wong H, Harris M, Harrigan PR, O'Shaughnessy M V., Montaner JSG. Changes in mitochondrial DNA as

a marker of nucleoside toxicity in HIV-infected patients. *N Engl J Med*. 2002;346(11):811-820. doi:10.1056/NEJMoa012035

74. Sun J, Longchamps RJ, Piggott DA, Castellani CA, Sumpter JA, Brown TT, Mehta SH, Arking DE, Kirk GD. Association between HIV infection and mitochondrial DNA copy number in peripheral blood: A population-based, prospective cohort study. *J Infect Dis*. 2019;219(8):1285-1293. doi:10.1093/infdis/jiy658

75. Lee HK, Song JH, Shin CS, Park DJ, Park KS, Lee KU, Koh CS. Decreased mitochondrial DNA content in peripheral blood precedes the development of non-insulin-dependent diabetes mellitus. *Diabetes Res Clin Pract*. 1998;42(3):161-167. doi:10.1016/S0168-8227(98)00110-7

76. Delbarba A, Abate G, Prandelli C, Marziano M, Buizza L, Arce Varas N, Novelli A, Cuetos F, Martinez C, Lanni C, Memo M, Uberti D. Mitochondrial Alterations in Peripheral Mononuclear Blood Cells from Alzheimer's Disease and Mild Cognitive Impairment Patients. *Oxid Med Cell Longev*. 2016;2016. doi:10.1155/2016/5923938

77. Wang Z, Liu VWS, Xue WC, Cheung ANY, Ngan HYS. Association of decreased mitochondrial DNA content with ovarian cancer progression. *Br J Cancer*. 2006;95(8):1087-1091. doi:10.1038/sj.bjc.6603377

78. Meierhofer D. Decrease of mitochondrial DNA content and energy metabolism in renal cell carcinoma. *Carcinogenesis*. 2004;25(6):1005-1010. doi:10.1093/carcin/bgh104

79. Chen S, Xie X, Wang Y, Gao Y, Xie X, Yang J, Ye J. Association between leukocyte mitochondrial DNA content and risk of coronary heart disease: A case-control study. *Atherosclerosis*. 2014;237(1):220-226. doi:10.1016/j.atherosclerosis.2014.08.051

80. Lee HC, Lu CY, Fahn HJ, Wei YH. Aging- and smoking-associated alteration in the

relative content of mitochondrial DNA in human lung. *FEBS Lett*. 1998;441(2):292-296. doi:10.1016/S0014-5793(98)01564-6

81. Masayesva BG, Mambo E, Taylor RJ, Goloubeva OG, Zhou S, Cohen Y, Minhas K, Koch W, Sciubba J, Alberg AJ, Sidransky D, Califano J. Mitochondrial DNA content increase in response to cigarette smoking. *Cancer Epidemiol Biomarkers Prev*. 2006;15(1):19-24. doi:10.1158/1055-9965.EPI-05-0210

82. Hosgood HD, Liu CS, Rothman N, Weinstein SJ, Bonner MR, Shen M, Lim U, Virtamo J, Cheng W ling, Albanes D, Lan Q. Mitochondrial DNA copy number and lung cancer risk in a prospective cohort study. *Carcinogenesis*. 2010;31(5):847-849. doi:10.1093/carcin/bgq045

83. Knez J, Winckelmans E, Plusquin M, Thijs L, Cauwenberghs N, Gu Y, Staessen JA, Nawrot TS, Kuznetsova T. Correlates of Peripheral Blood Mitochondrial DNA Content in a General Population. *Am J Epidemiol*. 2016;183(2):138-146. doi:10.1093/aje/kwv175

84. Liu C-S, Tsai C-S, Kuo C-L, Chen H-W, Lii C-K, Ma Y-S, Wei Y-H. Oxidative Stress-related Alteration of the Copy Number of Mitochondrial DNA in Human Leukocytes. *Free Radic Res*. 2003;37(12):1307-1317. doi:10.1080/10715760310001621342

85. Xing J, Chen M, Wood CG, Lin J, Spitz MR, Ma J, Amos CI, Shields PG, Benowitz NL, Gu J, De Andrade M, Swan GE, Wu X. Mitochondrial DNA content: Its genetic heritability and association with renal cell carcinoma. *J Natl Cancer Inst*. 2008;100(15):1104-1112. doi:10.1093/jnci/djn213

86. Vaziri H, Benchimol S. From telomere loss to p53 induction and activation of a DNA-damage pathway at senescence: the telomere loss/DNA damage model of cell aging. *Exp Gerontol*. 1996;31(1-2):295-301. doi:10.1016/0531-5565(95)02025-x

87. Artandi SE, Attardi LD. Pathways connecting telomeres and p53 in senescence, apoptosis, and cancer. *Biochem Biophys Res Commun*. 2005;331(3):881-890. doi:https://doi.org/10.1016/j.bbrc.2005.03.211

88. Sahin E, Colla S, Liesa M, Moslehi J, Müller FL, Guo M, Cooper M, Kotton D, Fabian AJ, Walkey C, Maser RS, Tonon G, Foerster F, Xiong R, Wang YA, Shukla SA, Jaskelioff M, Martin ES, Heffernan TP, Protopopov A, Ivanova E, Mahoney JE, Kost-Alimova M, Perry SR, Bronson R, Liao R, Mulligan R, Shirihai OS, Chin L, DePinho RA. Telomere dysfunction induces metabolic and mitochondrial compromise. *Nature*. 2011;470(7334):359-365. doi:10.1038/nature09787.Telomere

89. Ahmed S, Passos JF, Birket MJ, Beckmann T, Brings S, Peters H, Birch-Machin M a, von Zglinicki T, Saretzki G. Telomerase does not counteract telomere shortening but protects mitochondrial function under oxidative stress. *J Cell Sci*. 2008;121:1046-1053. doi:10.1242/jcs.019372

90. Haendeler J, Dröse S, Büchner N, Jakob S, Altschmied J, Goy C, Spyridopoulos I, Zeiher AM, Brandt U, Dimmeler S, Judith H, Stefan D, Nicole B, Sascha J, Joachim A, Christine G, Ioakim S, M. ZA, Ulrich B, Stefanie D. Mitochondrial telomerase reverse transcriptase binds to and protects mitochondrial DNA and function from damage. *Arterioscler Thromb Vasc Biol*. 2009;29(6):929-935. doi:10.1161/ATVBAHA.109.185546

91. Tyrka AR, Carpenter LL, Kao H-T, Porton B, Philip NS, Ridout SJ, Ridout KK, Price LH. Association of telomere length and mitochondrial DNA copy number in a community sample of healthy adults. *Exp Gerontol*. 2015;66:17-20. doi:10.1016/j.exger.2015.04.002

92. Zole E, Ranka R. Mitochondrial DNA copy number and telomere length in peripheral blood mononuclear cells in comparison with whole blood in three different age groups.

Arch Gerontol Geriatr. 2019;83:131-137. doi:10.1016/j.archger.2019.04.007

93. Kim JH, Kim HK, Ko JH, Bang H, Lee DC. The Relationship between Leukocyte Mitochondrial DNA Copy Number and Telomere Length in Community-Dwelling Elderly Women. *PLoS One*. 2013;8(6):1-8. doi:10.1371/journal.pone.0067227

94. Alegria-Torres JA, Velazquez-Villafana M, Lopez-Gutierrez JM, Chagoyan-Martinez MM, Rocha-Amador DO, Costilla-Salazar R, Garcia-Torres L. Association of Leukocyte Telomere Length and Mitochondrial DNA Copy Number in Children from Salamanca, Mexico. *Genet Test Mol Biomarkers*. 2016;20(11):654-659. doi:10.1089/gtmb.2016.0176

95. Campa D, Barrdahl M, Santoro A, Severi G, Baglietto L, Omichessan H, Tumino R, Bueno-de-Mesquita HB, Peeters PH, Weiderpass E, Chirlaque MD, Rodríguez-Barranco M, Agudo A, Gunter M, Dossus L, Krogh V, Matullo G, Trichopoulou A, Travis RC, Canzian F, Kaaks R. Mitochondrial DNA copy number variation, leukocyte telomere length, and breast cancer risk in the European Prospective Investigation into Cancer and Nutrition (EPIC) study. *Breast Cancer Res*. 2018;20(1):1-10. doi:10.1186/s13058-018-0955-5

96. Aubert G, Hills M, Lansdorp PM. Telomere length measurement-Caveats and a critical assessment of the available technologies and tools. *Mutat Res - Fundam Mol Mech Mutagen*. 2012;730(1-2):59-67. doi:10.1016/j.mrfmmm.2011.04.003

97. Kimura M, Stone RC, Hunt SC, Skurnick J, Lu X, Cao X, Harley CB, Aviv A. Measurement of telomere length by the Southern blot analysis of terminal restriction fragment lengths. *Nat Protoc*. 2010;5(9):1596-1607. doi:10.1038/nprot.2010.124

98. Baerlocher GM, Vulto I, de Jong G, Lansdorp PM. Flow cytometry and FISH to measure the average length of telomeres (flow FISH). *Nat Protoc*. 2006;1(5):2365-2376.

doi:10.1038/nprot.2006.263

99. Cawthon RM. Telomere measurement by quantitative PCR. *Nucleic Acids Res*. 2002;30(10):e47. doi:10.1093/nar/30.10.e47

100. Cawthon RM. Telomere length measurement by a novel monochrome multiplex quantitative PCR method. *Nucleic Acids Res*. 2009;37(3):1-7. doi:10.1093/nar/gkn1027

101. Hsieh AYY, Saberi S, Ajaykumar A, Hukezalie K, Gadawski I, Sattha B, Côté HCF. Optimization of a Relative Telomere Length Assay by Monochromatic Multiplex Real-Time Quantitative PCR on the LightCycler 480: Sources of Variability and Quality Control Considerations. *J Mol Diagnostics*. 2016;18(3):425-437. doi:10.1016/j.jmoldx.2016.01.004

102. Hsieh AYY, Budd M, Deng D, Gadawska I, Côté HCF. A Monochrome Multiplex Real-Time Quantitative PCR Assay for the Measurement of Mitochondrial DNA Content. *J Mol Diagnostics*. 2018;20(5):612-620. doi:10.1016/j.jmoldx.2018.05.001

103. Olsson J, Wikby A, Johansson B, Löfgren S, Nilsson BO, Ferguson FG. Age-related change in peripheral blood T-lymphocyte subpopulations and cytomegalovirus infection in the very old: The Swedish longitudinal OCTO immune study. *Mech Ageing Dev*. 2001;121(1-3):187-201. doi:10.1016/S0047-6374(00)00210-4

104. Wikby A, Månsson IA, Johansson B, Strindhall J, Nilsson SE. The immune risk profile is associated with age and gender: Findings from three Swedish population studies of individuals 20-100 years of age. *Biogerontology*. 2008;9(5):299-308. doi:10.1007/s10522-008-9138-6

105. Di Benedetto S, Derhovanessian E, Steinhagen-Thiessen E, Goldeck D, Müller L, Pawelec G. Impact of age, sex and CMV-infection on peripheral T cell phenotypes: results from

the Berlin BASE-II Study. *Biogerontology*. 2015;16(5):631-643. doi:10.1007/s10522-015-9563-2

106. Czesnikiewicz-Guzik M, Lee W-W, Cui D, Hiruma Y, Lamar DL, Yang Z-Z, Ouslander JG, Weyand CM, Goronzy JJ. T cell subset-specific susceptibility to aging. *Clin Immunol*. 2008;127(1):107-118. doi:10.1016/j.clim.2007.12.002

107. Hakim FT, Memon SA, Cepeda R, Jones EC, Chow CK, Kasten-Sportes C, Odom J, Vance BA, Christensen BL, Mackall CL, Gress RE. Age-dependent incidence, time course, and consequences of thymic renewal in adults. *J Clin Invest*. 2005;115(4):930-939. doi:10.1172/jci22492

108. den Braber I, Mugwagwa T, Vrisekoop N, Westera L, Mögling R, Bregje de Boer A, Willems N, Schrijver EHR, Spierenburg G, Gaiser K, Mul E, Otto SA, Ruiter AFC, Ackermans MT, Miedema F, Borghans JAM, de Boer RJ, Tesselaar K. Maintenance of Peripheral Naive T Cells Is Sustained by Thymus Output in Mice but Not Humans. *Immunity*. 2012;36(2):288-297. doi:10.1016/j.immuni.2012.02.006

109. Effros RB. Replicative senescence in the immune system: impact of the Hayflick limit on T-cell function in the elderly. *Am J Hum Genet*. 1998;62(5):1003-1007. doi:10.1086/301845

110. Valenzuela HF, Effros RB. Divergent Telomerase and CD28 Expression Patterns in Human CD4 and CD8 T Cells Following Repeated Encounters with the Same Antigenic Stimulus. *Clin Immunol*. 2002;105(2):117-125. doi:https://doi.org/10.1006/clim.2002.5271

111. Campisi J, Kim SH, Lim CS, Rubio M. Cellular senescence, cancer and aging: the telomere connection. *Exp Gerontol*. 2001;36(10):1619-1637. doi:10.1016/s0531-

5565(01)00160-7

112. Campisi J. Cellular senescence and apoptosis: how cellular responses might influence aging phenotypes. *Exp Gerontol*. 2003;38(1):5-11. doi:https://doi.org/10.1016/S0531-5565(02)00152-3

113. Childs BG, Baker DJ, Kirkland JL, Campisi J, van Deursen JM. Senescence and apoptosis: dueling or complementary cell fates? *EMBO Rep*. 2014;15(11):1139-1153. doi:10.15252/embr.201439245

114. Effros RB, Boucher N, Porter V, Zhu X, Spaulding C, Walford RL, Kronenberg M, Cohen D, Schachter F. Decline in CD28+ T cells in centenarians and in long-term T cell cultures: a possible cause for both in vivo and in vitro immunosenescence. *Exp Gerontol*. 1994;29(6):601-609. doi:10.1016/0531-5565(94)90073-6

115. Tchkonia T, Zhu Y, van Deursen J, Campisi J, Kirkland JL. Cellular senescence and the senescent secretory phenotype: therapeutic opportunities. *J Clin Invest*. 2013;123(3):966-972. doi:10.1172/JCI64098

116. Spaulding C, Guo W, Effros RB. Resistance to apoptosis in human CD8+ T cells that reach replicative senescence after multiple rounds of antigen-specific proliferation. *Exp Gerontol*. 1999;34(5):633-644. doi:10.1016/S0531-5565(99)00033-9

117. Azuma M, Phillips JH, Lanier LL. CD28- T lymphocytes. Antigenic and functional properties. *J Immunol*. 1993;150(4):1147-1159.

118. Saurwein-Teissl M, Lung TL, Marx F, Gschösser C, Asch E, Blasko I, Parson W, Böck G, Schönitzer D, Trannoy E, Grubeck-Loebenstein B. Lack of Antibody Production Following Immunization in Old Age: Association with CD8+CD28− T Cell Clonal Expansions and an Imbalance in the Production of Th1 and Th2 Cytokines. *J Immunol*.

2002;168(11):5893-5899. doi:10.4049/jimmunol.168.11.5893

119. Jin HT, Anderson AC, Tan WG, West EE, Ha SJ, Araki K, Freeman GJ, Kuchroo VK, Ahmed R. Cooperation of Tim-3 and PD-1 in CD8 T-cell exhaustion during chronic viral infection. *Proc Natl Acad Sci U S A*. 2010;107(33):14733-14738. doi:10.1073/pnas.1009731107

120. Sakaguchi S, Sakaguchi N, Asano M, Itoh M, Toda M. Immunologic self-tolerance maintained by activated T cells expressing IL-2 receptor alpha-chains (CD25). Breakdown of a single mechanism of self-tolerance causes various autoimmune diseases. *J Immunol*. 1995;155(3):1151-1164. doi:10.4049/jimmunol.167.1.98

121. Dieckmann D, Plottner H, Berchtold S, Berger T, Schuler G. Ex vivo isolation and characterization of CD4+CD25+ T cells with regulatory properties from human blood. *J Exp Med*. 2001;193(11):1303-1310. doi:10.1084/jem.193.11.1303

122. Lages CS, Suffia I, Velilla PA, Huang B, Warshaw G, Hildeman DA, Belkaid Y, Chougnet C. Functional regulatory T cells accumulate in aged hosts and promote chronic infectious disease reactivation. *J Immunol*. 2008;181(3):1835-1848. doi:10.4049/jimmunol.181.3.1835

123. Kawashiri S-Y, Kawakami A, Okada A, Koga T, Tamai M, Yamasaki S, Nakamura H, Origuchi T, Ida H, Eguchi K. CD4+CD25highCD127low/- Treg Cell Frequency from Peripheral Blood Correlates with Disease Activity in Patients with Rheumatoid Arthritis. *J Rheumatol*. 2011;38(12):2517-2521. doi:10.3899/jrheum.110283

124. Bennett CL, Christie J, Ramsdell F, Brunkow ME, Ferguson PJ, Whitesell L, Kelly TE, Saulsbury FT, Chance PF, Ochs HD. The immune dysregulation, polyendocrinopathy, enteropathy, X-linked syndrome (IPEX) is caused by mutations of FOXP3. *Nat Genet*.

2001;27(1):20-21. doi:10.1038/83713

125. McClymont SA, Putnam AL, Lee MR, Esensten JH, Liu W, Hulme MA, Hoffmüller U, Baron U, Olek S, Bluestone JA, Brusko TM. Plasticity of Human Regulatory T Cells in Healthy Subjects and Patients with Type 1 Diabetes. *J Immunol*. 2011;186(7):3918-3926. doi:10.4049/jimmunol.1003099

126. Kitz A, de Marcken M, Gautron A-S, Mitrovic M, Hafler DA, Dominguez-Villar M. AKT isoforms modulate Th1-like Treg generation and function in human autoimmune disease. *EMBO Rep*. 2016;17(8):1169-1183. doi:10.15252/embr.201541905

127. Boettler T, Spangenberg HC, Neumann-haefelin C, Panther E, Urbani S, Ferrari C, Blum HE, von Weizsäcker F, Thimme R. T cells with a CD4+CD25+ regulatory phenotype suppress in vitro proliferation of virus-specific CD8+ T cells during chronic hepatitis C virus infection. *J Virol*. 2005;79(12):7860-7867. doi:10.1128/JVI.79.12.7860-7867.2005

128. Gregg R, Smith CM, Clark FJ, Dunnion D, Khan N, Chakraverty R, Nayak L, Moss PA. The number of human peripheral blood CD4+ CD25high regulatory T cells increases with age. *Clin Exp Immunol*. 2005;140(3):540-546. doi:10.1111/j.1365-2249.2005.02798.x

129. Rosenkranz D, Weyer S, Tolosa E, Gaenslen A, Berg D, Leyhe T, Gasser T, Stoltze L. Higher frequency of regulatory T cells in the elderly and increased suppressive activity in neurodegeneration. *J Neuroimmunol*. 2007;188(1-2):117-127. doi:10.1016/j.jneuroim.2007.05.011

130. Santner-Nanan B, Seddiki N, Zhu E, Quent V, Kelleher A, De St Groth BF, Nanan R. Accelerated age-dependent transition of human regulatory T cells to effector memory phenotype. *Int Immunol*. 2008;20(3):375-383. doi:10.1093/intimm/dxm151

131. Hwang K-AA, Kim H-RR, Kang I. Aging and human CD4(+) regulatory T cells. *Mech*

Ageing Dev. 2009;130(8):509-517. doi:10.1016/j.mad.2009.06.003

132. Frasca D, Diaz A, Romero M, Landin AM, Phillips M, Lechner SC, Ryan JG, Blomberg BB. Intrinsic defects in B cell response to seasonal influenza vaccination in elderly humans. *Vaccine*. 2010;28(51):8077-8084. doi:10.1016/j.vaccine.2010.10.023

133. Frasca D, Diaz A, Romero M, Blomberg BB. The generation of memory B cells is maintained, but the antibody response is not, in the elderly after repeated influenza immunizations. *Vaccine*. 2016;34(25):2834-2840. doi:10.1016/j.vaccine.2016.04.023

134. Chong Y, Ikematsu H, Yamaji K, Nishimura M, Nabeshima S, Kashiwagi S, Hayashi J. CD27+ (memory) B cell decrease and apoptosis-resistant CD27− (naive) B cell increase in aged humans: implications for age-related peripheral B cell developmental disturbances. *Int Immunol*. 2005;17(4):383-390. doi:10.1093/intimm/dxh218

135. Colonna-Romano G, Bulati M, Aquino A, Scialabba G, Candore G, Lio D, Motta M, Malaguarnera M, Caruso C. B cells in the aged: CD27, CD5, and CD40 expression. *Mech Ageing Dev*. 2003;124(4):389-393. doi:https://doi.org/10.1016/S0047-6374(03)00013-7

136. Colonna-Romano G, Bulati M, Aquino A, Pellicano M, Vitello S, Lio D, Candore G, Caruso C, Pellicanò M, Vitello S, Lio D, Candore G, Caruso C. A double-negative (IgD−CD27−) B cell population is increased in the peripheral blood of elderly people. *Mech Ageing Dev*. 2009;130(10):681-690. doi:https://doi.org/10.1016/j.mad.2009.08.003

137. Listì F, Candore G, Modica MA, Russo M, Lorenzo GDI, Esposito-Pellitteri M, Colonna-Romano G, Aquino A, Bulati M, Lio D, Franceschi C, Caruso C. A Study of Serum Immunoglobulin Levels in Elderly Persons That Provides New Insights into B Cell Immunosenescence. *Ann N Y Acad Sci*. 2006;1089(1):487-495. doi:10.1196/annals.1386.013

138. Davydov AN, Obraztsova AS, Lebedin MY, Turchaninova MA, Staroverov DB, Merzlyak EM, Sharonov G V, Kladova O, Shugay M, Britanova O V, Chudakov DM. Comparative Analysis of B-Cell Receptor Repertoires Induced by Live Yellow Fever Vaccine in Young and Middle-Age Donors. *Front Immunol*. 2018;9:2309. doi:10.3389/fimmu.2018.02309

139. Gibson KL, Wu Y, Barnett Y, Duggan O, Vaughan R, Kondeatis E, Nilsson B-O, Wikby A, Kipling D, Dunn-walters DK. B-cell diversity decreases in old age and is correlated with poor health status. *Aging Cell*. 2009;8(1):18-25. doi:10.1111/j.1474-9726.2008.00443.x

140. Tabibian-keissar H, Hazanov L, Schiby G, Rosenthal N, Rakovsky A, Michaeli M, Shahaf GL, Pickman Y, Rosenblatt K, Melamed D, Dunn-Walters D, Mehr R, Barshack I. Aging affects B-cell antigen receptor repertoire diversity in primary and secondary lymphoid tissues. *Eur J Immunol*. 2016;46(2):480-492. doi:10.1002/eji.201545586

141. Frasca D, Landin AM, Lechner SC, Ryan JG, Schwartz R, Riley RL, Blomberg BB. Aging Down-Regulates the Transcription Factor E2A, Activation-Induced Cytidine Deaminase, and Ig Class Switch in Human B Cells. *J Immunol*. 2008;180(8):5283-5290. doi:10.4049/jimmunol.180.8.5283

142. Frasca D, Diaz A, Romero M, Blomberg BB. Human peripheral late / exhausted memory B cells express a senescent-associated secretory phenotype and preferentially utilize metabolic signaling pathways. *EXG*. 2017;87:113-120. doi:10.1016/j.exger.2016.12.001

143. UNAIDS. Global HIV and AIDS statistics 2019 Fact sheet. *Glob HIV AIDs ststistics, World AIDS day 2019 Fact Sheet*. 2019;1(June):1-6.

144. Kahn JO, Walker BD. Acute Human Immunodeficiency Virus Type 1 Infection. *N Engl J*

Med. 1998;339(1):33-39. doi:10.1056/NEJM199807023390107

145. Weiss RA. How does HIV cause AIDS? *Science*. 1993;260(5112):1273-1279. doi:10.1126/science.8493571

146. World Health Organization. Guideline on When To Start Antiretroviral Therapy and on Pre-Exposure Prophylaxis for HIV. 2015;(September):1-76.

147. World Health Organization. The use of anti retro-viral drugs for treatment and prevention of HIV infection. 2013;(June):176-180.

148. Clotet B, Feinberg J, van Lunzen J, Khuong-Josses M-A, Antinori A, Dumitru I, Pokrovskiy V, Fehr J, Ortiz R, Saag M, Harris J, Brennan C, Fujiwara T, Min S. Once-daily dolutegravir versus darunavir plus ritonavir in antiretroviral-naive adults with HIV-1 infection (FLAMINGO): 48 week results from the randomised open-label phase 3b study. *Lancet*. 2014;383(9936):2222-2231. doi:https://doi.org/10.1016/S0140-6736(14)60084-2

149. Rockstroh JK, Dejesus E, Lennox JL, Yazdanpanah Y, Saag MS, Wan H, Rodgers AJ, Walker ML, Miller M, Dinubile MJ, Nguyen BY, Teppler H, Leavitt R, Sklar P. Durable efficacy and safety of raltegravir versus efavirenz when combined with tenofovir/emtricitabine in treatment-naive HIV-1-infected patients: Final 5-year results from STARTMRK. *J Acquir Immune Defic Syndr*. 2013;63(1):77-85. doi:10.1097/QAI.0b013e31828ace69

150. Hukezalie KR, Thumati NR, Côté HCF, Wong JMY. In Vitro and Ex Vivo Inhibition of Human Telomerase by Anti-HIV Nucleoside Reverse Transcriptase Inhibitors (NRTIs) but Not by Non-NRTIs. *PLoS One*. 2012;7(11). doi:10.171/journal.pone.0047505

151. Leeansyah E, Cameron PU, Solomon A, Tennakoon S, Velayudham P, Gouillou M, Spelman T, Hearps A, Fairley C, Smit DV, Pierce AB, Armishaw J, Crowe SM, Cooper

DA, Koelsch KK, Liu JP, Chuah J, Lewin SR. Inhibition of telomerase activity by human immunodeficiency virus (HIV) nucleos(t)ide reverse transcriptase inhibitors: A potential factor contributing to HIV-associated accelerated aging. *J Infect Dis*. 2013;207(7):1157-1165. doi:10.1093/infdis/jit006

152. Chen CH, Vazquez-Padua M, Cheng YC. Effect of anti-human immunodeficiency virus nucleoside analogs on mitochondrial DNA and its implication for delayed toxicity. *Mol Pharmacol*. 1991;39(5):625-628.

153. Lewis W, Day BJ, Copeland WC. Mitochondrial toxicity of NRTI antiviral drugs: An integrated cellular perspective. *Nat Rev Drug Discov*. 2003;2(10):812-822. doi:10.1038/nrd1201

154. Autenrieth CS, Beck EJ, Stelzle D, Mallouris C, Mahy M, Ghys P. Global and regional trends of people living with HIV aged 50 and over: Estimates and projections for 2000–2020. *PLoS One*. 2018;13(11):1-11. doi:10.1371/journal.pone.0207005

155. Palella Jr. FJ, Baker RK, Moorman AC, Chmiel JS, Wood KC, Brooks JT, Holmberg SD, Investigators HIVOS. Mortality in the highly active antiretroviral therapy era: changing causes of death and disease in the HIV outpatient study. *J Acquir Immune Defic Syndr*. 2006;43(1):27-34. doi:10.1097/01.qai.0000233310.90484.16

156. Bhaskaran K, Hamouda O, Sannes M, Boufassa F, Johnson AM, Lambert PC, Porter K, CASCADE Collaboration for the. Changes in the Risk of Death After HIV Seroconversion Compared With Mortality in the General Population. *JAMA*. 2008;300(1):51-59. doi:10.1001/jama.300.1.51

157. Triant VA, Lee H, Hadigan C, Grinspoon SK. Increased acute myocardial infarction rates and cardiovascular risk factors among patients with human immunodeficiency virus

disease. *J Clin Endocrinol Metab*. 2007;92(7):2506-2512. doi:10.1210/jc.2006-2190

158. Obel N, Thomsen HF, Kronborg G, Larsen CS, Hildebrandt PR, Sørensen HT, Gerstoft J. Ischemic Heart Disease in HIV-Infected and HIV-Uninfected Individuals: A Population-Based Cohort Study. *Clin Infect Dis*. 2007;44(12):1625-1631. doi:10.1086/518285

159. Freiberg MS, Chang C-CH, Kuller LH, Skanderson M, Lowy E, Kraemer KL, Butt AA, Bidwell Goetz M, Leaf D, Oursler KA, Rimland D, Rodriguez Barradas M, Brown S, Gibert C, McGinnis K, Crothers K, Sico J, Crane H, Warner A, Gottlieb S, Gottdiener J, Tracy RP, Budoff M, Watson C, Armah KA, Doebler D, Bryant K, Justice AC. HIV Infection and the Risk of Acute Myocardial Infarction. *JAMA Intern Med*. 2013;173(8):614-622. doi:10.1001/jamainternmed.2013.3728

160. Hooshyar D, Hanson DL, Wolfe M, Selik RM, Buskin SE, McNaghten AD. Trends in perimortal conditions and mortality rates among HIV-infected patients. *AIDS*. 2007;21(15):2093-2100. doi:10.1097/QAD.0b013e3282e9a664

161. Neuhaus J, Jacobs Jr DR, Baker J V, Calmy A, Duprez D, La Rosa A, Kuller LH, Pett SL, Ristola M, Ross MJ, Shlipak MG, Tracy R, Neaton JD. Markers of inflammation, coagulation, and renal function are elevated in adults with HIV infection. *J Infect Dis*. 2010;201(12):1788-1795. doi:10.1086/652749

162. Thomas J, Doherty SM. HIV Infection—A Risk Factor for Osteoporosis. *JAIDS J Acquir Immune Defic Syndr*. 2003;33(3). doi:10.1097/00126334-200307010-00001

163. Kooij KW, Wit FW, Bisschop PH, Schouten J, Stolte IG, Prins M, van der Valk M, Prins JM, van Eck-Smit BL, Lips P, Reiss P. Low Bone Mineral Density in Patients With Well-Suppressed HIV Infection: Association With Body Weight, Smoking, and Prior Advanced HIV Disease. 2015;211(4):539-548. doi:10.1093/infdis/jiu499

164. Cooley TP. Non-AIDS-defining cancer in HIV-infected people. *Hematol Oncol Clin North Am*. 2003;17(3):889-899. doi:10.1016/s0889-8588(03)00038-8

165. Lange CG, Lederman MM, Medvik K, Asaad R, Wild M, Kalayjian R, Valdez H. Nadir CD4+ T-cell count and numbers of CD28+ CD4+ T-cells predict functional responses to immunizations in chronic HIV-1 infection. *AIDS*. 2003;17(14):2015-2023. doi:10.1097/00002030-200309260-00002

166. Moir S, Malaspina A, Ogwaro KM, Donoghue ET, Hallahan CW, Ehler LA, Hwu P, Baseler M, Orenstein JM, Liu S, Adelsberger J, Chun TW, Mican JAM, Fauci AS. HIV-1 induces phenotypic and functional perturbations of B cells in chronically infected individuals. *Proc Natl Acad Sci U S A*. 2001;98(18):10362-10367. doi:10.1073/pnas.181347898

167. De Milito A, Nilsson A, Titanji K, Thorstensson R, Reizenstein E, Narita M, Grutzmeier S, Sönnerborg A, Chiodi F. Mechanisms of hypergammaglobulinemia and impaired antigen-specific humoral immunity in HIV-1 infection. *Blood*. 2004;103(6):2180-2186. doi:10.1182/blood-2003-07-2375

168. Yen Y-F, Chuang P-H, Jen I-A, Chen M, Lan Y-C, Liu Y-L, Lee Y, Chen Y-H, Chen Y-MA. Incidence of autoimmune diseases in a nationwide HIV/AIDS patient cohort in Taiwan, 2000-2012. *Ann Rheum Dis*. 2017;76(4):661-665. doi:10.1136/annrheumdis-2016-209815

169. Lebrun D, Hentzien M, Cuzin L, Rey D, Joly V, Cotte L, Allavena C, Dellamonica P, Servettaz A, Bani-Sadr F. Epidemiology of autoimmune and inflammatory diseases in a French nationwide HIV cohort. *AIDS*. 2017;31(15):2159-2166. doi:10.1097/QAD.0000000000001603

170. Birx D, Redfield R, Tencer K, Fowler A, Burke D, Tosato G. Induction of interleukin-6 during human immunodeficiency virus infection. *Blood*. 1990;76(11):2303-2310. doi:10.1182/blood.V76.11.2303.2303

171. Lafeuillade A, Poizot-Martin I, Quilichini R, Gastaut JA, Kaplanski S, Farnarier C, Mege JL, Bongrand P. Increased interleukin-6 production is associated with disease progression in HIV infection. *AIDS*. 1991;5(9):1139-1140. doi:10.1097/00002030-199109000-00014

172. Deeks SG. HIV Infection, Inflammation, and Aging. *Annu Rev Med*. 2011;62:141-155. doi:10.1146/annurev-med-042909-093756

173. Desai S, Landay A. Early immune senescence in HIV disease. *Curr HIV/AIDS Rep*. 2010;7(1):4-10. doi:10.1007/s11904-009-0038-4

174. Zapata HJ, Shaw AC. Aging of the human innate immune system in HIV infection. *Curr Opin Immunol*. 2014;29(1):127-136. doi:10.1016/j.coi.2014.06.007

175. Pathai S, Bajillan H, Landay AL, High KP. Is HIV a model of accelerated or accentuated aging? *Journals Gerontol - Ser A Biol Sci Med Sci*. 2014;69(7):833-842. doi:10.1093/gerona/glt168

176. Wolthers KC, Bea G, Wisman A, Otto SA, de Roda Husman AM, Schaft N, de Wolf F, Goudsmit J, Coutinho RA, van der Zee AG, Meyaard L, Miedema F. T cell telomere length in HIV-1 infection: no evidence for increased CD4+ T cell turnover. *Science*. 1996;274(5292):1543-1547. doi:10.1126/science.274.5292.1543

177. Palmer LD, Weng NP, Levine BL, June CH, Lane HC, Hodes RJ. Telomere length, telomerase activity, and replicative potential in HIV infection: Analysis of CD4+ and CD8+ T cells from HIV-discordant monozygotic twins. *J Exp Med*. 1997;185(7):1381-1386. doi:10.1084/jem.185.7.1381

178. Effros RB, Allsopp R, Chiu CP, Hausner M a, Hirji K, Wang L, Harley CB, Villeponteau B, West MD, Giorgi J V. Shortened telomeres in the expanded CD28-CD8+ cell subset in HIV disease implicate replicative senescence in HIV pathogenesis. *AIDS*. 1996;10(8):F17-F22. doi:10.1097/00002030-199607000-00001

179. Rickabaugh TM, Kilpatrick RD, Hultin LE, Hultin PM, Hausner MA, Sugar CA, Althoff KN, Margolick JB, Rinaldo CR, Detels R, Phair J, Effros RB, Jamieson BD. The dual impact of HIV-1 infection and aging on naïve CD4 + T-cells: Additive and distinct patterns of impairment. *PLoS One*. 2011;6(1). doi:10.1371/journal.pone.0016459

180. Buggert M, Frederiksen J, Noyan K, Svärd J, Barqasho B, Sönnerborg A, Lund O, Nowak P, Karlsson AC. Multiparametric Bioinformatics Distinguish the CD4/CD8 Ratio as a Suitable Laboratory Predictor of Combined T Cell Pathogenesis in HIV Infection. *J Immunol*. 2014;192(5):2099-2108. doi:10.4049/jimmunol.1302596

181. Serrano-Villar S, Pérez-Elías MJ, Dronda F, Casado JL, Moreno A, Royuela A, Pérez-Molina JA, Sainz T, Navas E, Hermida JM, Quereda C, Moreno S. Increased risk of serious non-AIDS-related events in HIV-infected subjects on antiretroviral therapy associated with a low CD4/CD8 ratio. *PLoS One*. 2014;9(1). doi:10.1371/journal.pone.0085798

182. Mussini C, Lorenzini P, Cozzi-Lepri A, Lapadula G, Marchetti G, Nicastri E, Cingolani A, Lichtner M, Antinori A, Gori A, d'Arminio Monforte A. CD4/CD8 ratio normalisation and non-AIDS-related events in individuals with HIV who achieve viral load suppression with antiretroviral therapy: An observational cohort study. *Lancet HIV*. 2015;2(3):e98-e106. doi:10.1016/S2352-3018(15)00006-5

183. Dion M-L, Poulin J-F, Bordi R, Sylvestre M, Corsini R, Kettaf N, Dalloul A, Boulassel

M-R, Debré P, Routy J-P, Grossman Z, Sékaly R-P, Cheynier R. HIV Infection Rapidly Induces and Maintains a Substantial Suppression of Thymocyte Proliferation. *Immunity*. 2004;21(6):757-768. doi:10.1016/j.immuni.2004.10.013

184. Wang L, Robb CW, Cloyd MW. HIV induces homing of resting T lymphocytes to lymph nodes. *Virology*. 1997;228(2):141-152. doi:10.1006/viro.1996.8397

185. Douek DC. Disrupting T-cell Homeostasis: how HIV-1 Infection Causes Disease. *Aids Rev*. 2003;(5):172-177.

186. Finkel TH, Tudor-Williams G, Banda NK, Cotton MF, Curiel T, Monks C, Baba TW, Ruprecht RM, Kupfer A. Apoptosis occurs predominantly in bystander cells and not in productively infected cells of HIV- and SIV-infected lymph nodes. *Nat Med*. 1995;1(2):129-134. doi:10.1038/nm0295-129

187. Doitsh G, Galloway NLK, Geng X, Yang Z, Monroe KM, Zepeda O, Hunt PW, Hatano H, Sowinski S, Muñoz-Arias I, Greene WC. Cell death by pyroptosis drives CD4 T-cell depletion in HIV-1 infection. *Nature*. 2013;505(7484):509-514. doi:10.1038/nature12940

188. Moore RD, Keruly JC. CD4+ Cell Count 6 Years after Commencement of Highly Active Antiretroviral Therapy in Persons with Sustained Virologic Suppression. *Clin Infect Dis*. 2007;44(3):441-446. doi:10.1086/510746

189. Mutoh Y, Nishijima T, Inaba Y, Tanaka N, Kikuchi Y, Gatanaga H, Oka S. Incomplete Recovery of CD4 Cell Count, CD4 Percentage, and CD4/CD8 Ratio in Patients With Human Immunodeficiency Virus Infection and Suppressed Viremia During Long-term Antiretroviral Therapy. *Clin Infect Dis*. 2018;67(6):927-933. doi:10.1093/cid/ciy176

190. Hazenberg MD, Otto SA, Van Benthem BHB, Roos MTL, Coutinho RA, Lange JMA, Hamann D, Prins M, Miedema F. Persistent immune activation in HIV-1 infection is

associated with progression to AIDS. *Aids*. 2003;17(13):1881-1888. doi:10.1097/00002030-200309050-00006

191. Trickey A, May MT, Schommers P, Tate J, Ingle SM, Guest JL, Gill MJ, Zangerle R, Saag M, Reiss P, Monforte ADA, Johnson M, Lima VD, Sterling TR, Cavassini M, Wittkop L, Costagliola D, Sterne JAC. CD4:CD8 Ratio and CD8 Count as prognostic markers for mortality in human immunodeficiency virus-infected patients on antiretroviral therapy: The antiretroviral therapy cohort collaboration (ART-CC). *Clin Infect Dis*. 2017;65(6):959-966. doi:10.1093/cid/cix466

192. Borrow P, Lewicki H, Hahn BH, Shaw GM, Oldstone MB. Virus-specific CD8+ cytotoxic T-lymphocyte activity associated with control of viremia in primary human immunodeficiency virus type 1 infection. *J Virol*. 1994;68(9):6103-6110. doi:10.1128/jvi.68.9.6103-6110.1994

193. Wilson JDK, Ogg GS, Allen RL, Davis C, Shaunak S, Downie J, Dyer W, Workman C, Sullivan JS, McMichael AJ, Rowland-Jones SL. Direct visualization of HIV-1-specific cytotoxic T lymphocytes during primary infection. *Aids*. 2000;14(3):225-233. doi:10.1097/00002030-200002180-00003

194. Emu B, Moretto WJ, Hoh R, Krone M, Martin JN, Nixon DF, Deeks SG, McCune JM. Composition and function of T cell subpopulations are slow to change despite effective antiretroviral treatment of HIV disease. *PLoS One*. 2014;9(1). doi:10.1371/journal.pone.0085613

195. Rönsholt FF, Ullum H, Katzenstein TL, Gerstoft J, Ostrowski SR. T-cell subset distribution in HIV-1-infected patients after 12 years of treatment-induced viremic suppression. *J Acquir Immune Defic Syndr*. 2012;61(3):270-278.

doi:10.1097/QAI.0b013e31825e7ac1

196. Cao W, Mehraj V, Trottier B, Baril J-G, Leblanc R, Lebouche B, Cox J, Tremblay C, Lu W, Singer J, Li T, Routy J-P, Group MPHIVIS, Vézina S, Charest L, Milne M, Huchet E, Lavoie S, Friedman J, Duchastel M, Villielm F, Côté P, Potter M, Lessard B, Charron MA, Dufresne S, Turgeon ME, Rouleau D, Labrecque L, Fortin C, de Pokomandy A, Hal-Gagné V, Munoz M, Deligne B, Martel-Laferrière V, Gilmore N, Fletcher M, Szabo J. Early Initiation Rather Than Prolonged Duration of Antiretroviral Therapy in HIV Infection Contributes to the Normalization of CD8 T-Cell Counts. *Clin Infect Dis*. 2016;62(2):250-257. doi:10.1093/cid/civ809

197. Helleberg M, Kronborg G, Ullum H, Ryder LP, Obel N, Gerstoft J. Course and clinical significance of CD8+ T-cell counts in a large cohort of HIV-infected individuals. *J Infect Dis*. 2015;211(11):1726-1734. doi:10.1093/infdis/jiu669

198. Roederer M, Dubs JG, Anderson MT, Raju PA, Herzenberg LA, Herzenberg LA. CD8 naive T cell counts decrease progressively in HIV-infected adults. *J Clin Invest*. 1995;95(5):2061-2066. doi:10.1172/JCI117892

199. Vrisekoop N, van Gent R, de Boer AB, Otto SA, Borleffs JCC, Steingrover R, Prins JM, Kuijpers TW, Wolfs TFW, Geelen SPM, Vulto I, Lansdorp P, Tesselaar K, Borghans JAM, Miedema F. Restoration of the CD4 T Cell Compartment after Long-Term Highly Active Antiretroviral Therapy without Phenotypical Signs of Accelerated Immunological Aging. *J Immunol*. 2008;181(2):1573-1581. doi:10.4049/jimmunol.181.2.1573

200. Papagno L, Spina CA, Marchant A, Salio M, Rufer N, Little S, Dong T, Chesney G, Waters A, Easterbrook P, Dunbar PR, Shepherd D, Cerundolo V, Emery V, Griffiths P, Conlon C, McMichael AJ, Richman DD, Rowland-Jones SL, Appay V. Immune

activation and CD8+ T-cell differentiation towards senescence in HIV-1 infection. *PLoS Biol*. 2004;2(2). doi:10.1371/journal.pbio.0020020

201. Borthwick NJ, Bofill M, Gombert WM, Akbar AN, Medina E, Sagawa K, Lipman MC, Johnson MA, Janossy G. Lymphocyte activation in HIV-1 infection. II. Functional defects of CD28− T cells. *AIDS*. 1994;8(4):431-442. doi:10.1097/00002030-199404000-00004

202. Kalayjian RC, Landay A, Pollard RB, Taub DD, Gross BH, Francis IR, Sevin A, Pu M, Spritzler J, Chernoff M, Namkung A, Fox L, Martinez A, Waterman K, Fiscus SA, Sha B, Johnson D, Slater S, Rousseau F, Lederman MM. Age-Related Immune Dysfunction in Health and in Human Immunodeficiency Virus (HIV) Disease: Association of Age and HIV Infection with Naive CD8 + Cell Depletion, Reduced Expression of CD28 on CD8 + Cells, and Reduced Thymic Volumes. *J Infect Dis*. 2003;187(12):1924-1933. doi:10.1086/375372

203. Jimenez VC, Wit FWNM, Joerink M, Maurer I, Harskamp AM, Schouten J, Prins M, Van Leeuwen EMM, Booiman T, Deeks SG, Reiss P, Kootstra NA. T-Cell Activation Independently Associates with Immune Senescence in HIV-Infected Recipients of Long-term Antiretroviral Treatment. *J Infect Dis*. 2016;214(2):216-225. doi:10.1093/infdis/jiw146

204. Day CL, Kaufmann DE, Kiepiela P, Brown JA, Moodley ES, Reddy S, Mackey EW, Miller JD, Leslie AJ, DePierres C, Mncube Z, Duraiswamy J, Zhu B, Eichbaum Q, Altfeld M, Wherry EJ, Coovadia HM, Goulder PJR, Klenerman P, Ahmed R, Freeman GJ, Walker BD. PD-1 expression on HIV-specific T cells is associated with T-cell exhaustion and disease progression. *Nature*. 2006;443(7109):350-354. doi:10.1038/nature05115

205. Trautmann L, Janbazian L, Chomont N, Said EA, Gimmig S, Bessette B, Boulassel M-R,

Delwart E, Sepulveda H, Balderas RS, Routy J-P, Haddad EK, Sekaly R-P. Upregulation of PD-1 expression on HIV-specific CD8+ T cells leads to reversible immune dysfunction. *Nat Med*. 2006;12(10):1198-1202. doi:10.1542/peds.2007-0846PPPP

206. Jones RB, Ndhlovu LC, Barbour JD, Sheth PM, Jha AR, Long BR, Wong JC, Satkunarajah M, Schweneker M, Chapman JM, Gyenes G, Vali B, Hyrcza MD, Yue FY, Kovacs C, Sassi A, Loutfy M, Halpenny R, Persad D, Spotts G, Hecht FM, Chun TW, McCune JM, Kaul R, Rini JM, Nixon DF, Ostrowski MA. Tim-3 expression defines a novel population of dysfunctional T cells with highly elevated frequencies in progressive HIV-1 infection. *J Exp Med*. 2008;205(12):2763-2779. doi:10.1084/jem.20081398

207. Tavenier J, Langkilde A, Haupt TH, Henriksen JH, Jensen FK, Petersen J, Andersen O. Immunosenescence of the CD8+ T cell compartment is associated with HIV-infection, but only weakly reflects age-related processes of adipose tissue, metabolism, and muscle in antiretroviral therapy-treated HIV-infected patients and controls. *BMC Immunol*. 2015;16(1):1-14. doi:10.1186/s12865-015-0136-6

208. Jensen SS, Fomsgaard A, Larsen TK, Tingstedt JL, Gerstoft J, Kronborg G, Pedersen C, Karlsson I. Initiation of antiretroviral therapy (ART) at different stages of HIV-1 disease is not associated with the proportion of exhausted CD8+ T Cells. *PLoS One*. 2015;10(10):1-14. doi:10.1371/journal.pone.0139573

209. Epple HJ, Loddenkemper C, Kunkel D, Tröger H, Maul J, Moos V, Berg E, Ullrich R, Schulzke JD, Stein H, Duchmann R, Zeitz M, Schneider T. Mucosal but not peripheral FOXP3+ regulatory T cells are highly increased in untreated HIV infection and normalize after suppressive HAART. *Blood*. 2006;108(9):3072-3078. doi:10.1182/blood-2006-04-016923

210. Mozos A, Garrido M, Carreras J, Plana M, Diaz A, Alos L, Campo E, Garcia F, Martinez A. Redistribution of FOXP3-positive regulatory T cells from lymphoid tissues to peripheral blood in HIV-infected patients. *J Acquir Immune Defic Syndr*. 2007;46(5):529-537. doi:10.1097/QAI.0b013e31815b69ae

211. Tsunemi S, Iwasaki T, Imado T, Higasa S, Kakishita E, Shirasaka T, Sano H. Relationship of CD4+CD25+ regulatory T cells to immune status in HIV-infected patients. *Aids*. 2005;19(9):879-886. doi:10.1097/01.aids.0000171401.23243.56

212. Montes M, Lewis DE, Sanchez C, Lopez de Castilla D, Graviss EA, Seas C, Gotuzzo E, White ACJ. Foxp3+ regulatory T cells in antiretroviral-naive HIV patients. *AIDS*. 2006;20(12):52-58. doi:10.1093/tropej/44.1.52

213. Lim A, Tan D, Price P, Kamarulzaman A, Tan H-YY, James I, French MA. Proportions of circulating T cells with a regulatory cell phenotype increase with HIV-associated immune activation and remain high on antiretroviral therapy. *AIDS*. 2007;21(12):1525-1534. doi:10.1097/QAD.0b013e32825eab8b

214. Bi X, Suzuki Y, Gatanaga H, Oka S. High frequency and proliferation of CD4+FOXP3+ Treg in HIV-1-infected patients with low CD4 counts. *Eur J Immunol*. 2009;39(1):301-309. doi:10.1002/eji.200838667

215. Schulze zur Wiesch J, Thomssen A, Hartjen P, Toth I, Lehmann C, Meyer-Olson D, Colberg K, Frerk S, Babikir D, Schmiedel S, Degen O, Mauss S, Rockstroh J, Staszewski S, Khaykin P, Strasak A, Lohse AW, Fatkenheuer G, Hauber J, van Lunzen J. Comprehensive Analysis of Frequency and Phenotype of T Regulatory Cells in HIV Infection: CD39 Expression of FoxP3+ T Regulatory Cells Correlates with Progressive Disease. *J Virol*. 2011;85(3):1287-1297. doi:10.1128/jvi.01758-10

216. Oswald-Richter K, Grill SM, Shariat N, Leelawong M, Sundrud MS, Haas DW, Unutmaz D. HIV infection of naturally occurring and genetically reprogrammed human regulatory T-cells. *PLoS Biol*. 2004;2(7):955-966. doi:10.1371/journal.pbio.0020198

217. Apoil PA, Puissant B, Roubinet F, Abbal M, Massip P, Blancher A. FOXP3 mRNA levels are decreased in peripheral blood CD4+ lymphocytes from HIV-positive patients. *J Acquir Immune Defic Syndr*. 2005;39(4):381-385. doi:10.1097/01.qai.0000169662.30783.2d

218. Eggena MP, Barugahare B, Jones N, Okello M, Mutalya S, Kityo C, Mugyenyi P, Cao H. Depletion of Regulatory T Cells in HIV Infection Is Associated with Immune Activation. *J Immunol*. 2005;174(7):4407-4414. doi:10.4049/jimmunol.174.7.4407

219. Baker CAR, Clark R, Ventura F, Jones NG, Guzman D, Bangsberg DR, Cao H. Peripheral CD4 loss of regulatory T cells is associated with persistent viraemia in chronic HIV infection. *Clin Exp Immunol*. 2007;147(3):533-539. doi:10.1111/j.1365-2249.2006.03319.x

220. Prendergast A, Prado JG, Kang YH, Chen F, Riddell LA, Luzzi G, Goulder P, Klenerman P. HIV-1 infection is characterized by profound depletion of CD161+ Th17 cells and gradual decline in regulatory T cells. *AIDS*. 2010;24(4):491-502. doi:10.1097/QAD.0b013e3283344895

221. Montes M, Sanchez C, Lewis DE, Graviss EA, Seas C, Gotuzzo E, White AC. Normalization of FoxP3+ regulatory T cells in response to effective antiretroviral therapy. *J Infect Dis*. 2011;203(4):496-499. doi:10.1093/infdis/jiq073

222. Andersson J, Boasso A, Nilsson J, Zhang R, Shire NJ, Lindback S, Shearer GM, Chougnet CA. Cutting Edge: The Prevalence of Regulatory T Cells in Lymphoid Tissue Is Correlated with Viral Load in HIV-Infected Patients. *J Immunol*. 2005;174(6):3143-3147.

doi:10.4049/jimmunol.174.6.3143

223. Nilsson J, Boasso A, Velilla PA, Zhang R, Vaccari M, Franchini G, Shearer GM, Andersson J, Chougnet C. HIV-1-driven regulatory T-cell accumulation in lymphoid tissues is associated with disease progression in HIV/AIDS. *Blood*. 2006;108(12):3808-3817. doi:10.1182/blood-2006-05-021576

224. Pion M, Jaramillo-Ruiz D, Martínez A, Muñoz-Fernández MA, Correa-Rocha R. HIV infection of human regulatory T cells downregulates Foxp3 expression by increasing DNMT3b levels and DNA methylation in the FOXP3 gene. *AIDS*. 2013;27(13):2019-2029. doi:10.1097/QAD.0b013e32836253fd

225. Méndez-Lagares G, Jaramillo-Ruiz D, Pion M, Leal M, Muñoz-Fernández MA, Pacheco YM, Correa-Rocha R. HIV infection deregulates the balance between regulatory T cells and IL-2-producing CD4 T cells by decreasing the expression of the IL-2 receptor in Treg. *J Acquir Immune Defic Syndr*. 2014;65(3):278-282. doi:10.1097/QAI.0000000000000092

226. De Milito A, Mörch C, Sönnerborg A, Chiodi F. Loss of memory (CD27) B lymphocytes in HIV-1 infection. *AIDS*. 2001;15(8):957-964. doi:10.1097/00002030-200105250-00003

227. Moir S, Ho J, Malaspina A, Wang W, DiPoto AC, Shea MAO, Roby G, Kottilil S, Arthos J, Proschan MA, Chun T, Fauci AS. Evidence for HIV-associated B cell exhaustion in a dysfunctional memory B cell compartment in HIV-infected viremic individuals. *J Exp Med*. 2008;205(8):1797-1805. doi:10.1084/jem.20072683

228. Lane HC, Masur H, Edgar LC, Whalen G, Rook AH, Fauci AS. Abnormalities of B-Cell Activation and Immunoregulation in Patients with the Acquired Immunodeficiency Syndrome. *N Engl J Med*. 1983;309(8):453-458. doi:10.1056/NEJM198308253090803

229. Janoff EN, Douglas JM, Gabriel M, Blaser MJ, Davidson AJ, Cohn DL, Judson FN.

Class-Specific Antibody Response to Pneumococcal Capsular Polysaccharides in Men Infected with Human Immunodeficiency Virus Type 1. *J Infect Dis*. 1988;158(5):983-990. doi:10.1093/infdis/158.5.983

230. Cagigi A, Pensieroso S, Ruffin N, Sammicheli S, Thorstensson R, Pan-hammarström Q, Hejdeman B, Nilsson A, Chiodi F. Relation of activation-induced deaminase (AID) expression with antibody response to A (H1N1) pdm09 vaccination in HIV-1 infected patients. *Vaccine*. 2013;31(18):2231-2237. doi:10.1016/j.vaccine.2013.03.002

231. Moir S, Malaspina A, Ho J, Wang W, Dipoto AC, O'Shea MA, Roby G, Mican JM, Kottilil S, Chun T-W, Proschan MA, Fauci AS. Normalization of B Cell Counts and Subpopulations after Antiretroviral Therapy in Chronic HIV Disease. *J Infect Dis*. 2008;197(4):572-579. doi:10.1086/526789

232. Amu S, Lavy-Shahaf G, Cagigi A, Hejdeman B, Nozza S, Lopalco L, Mehr R, Chiodi F. Frequency and phenotype of B cell subpopulations in young and aged HIV-1 infected patients receiving ART. *Retrovirology*. 2014;11(1):76. doi:10.1186/s12977-014-0076-x

233. Rinaldi S, Pallikkuth S, George VK, de Armas LR, Pahwa R, Sanchez CM, Pallin MF, Pan L, Cotugno N, Dickinson G, Rodriguez A, Fischl M, Alcaide M, Gonzalez L, Palma P, Pahwa S. Paradoxical aging in HIV: immune senescence of B Cells is most prominent in young age. *Aging (Albany NY)*. 2017;9(4):1307-1325. doi:10.18632/aging.101229

234. Hart M, Steel A, Clark SA, Moyle G, Nelson M, Henderson DC, Wilson R, Gotch F, Gazzard B, Kelleher P. Loss of Discrete Memory B Cell Subsets Is Associated with Impaired Immunization Responses in HIV-1 Infection and May Be a Risk Factor for Invasive Pneumococcal Disease. *J Immunol*. 2007;178(12):8212 LP - 8220. doi:10.4049/jimmunol.178.12.8212

235. Lin J, Epel E, Cheon J, Kroenke C, Sinclair E, Bigos M, Wolkowitz O, Mellon S, Blackburn E. Analyses and comparisons of telomerase activity and telomere length in human T and B cells: Insights for epidemiology of telomere maintenance. *J Immunol Methods*. 2010;352(1-2):71-80. doi:10.1016/j.jim.2009.09.012

236. Monteiro J, Batliwalla F, Ostrer H, Gregersen PK. Shortened telomeres in clonally expanded CD28-CD8+ T cells imply a replicative history that is distinct from their CD28+CD8+ counterparts. *J Immunol*. 1996;156(10):3587-3590.

237. Robertson JD, Gale RE, Wynn RF, Dougal M, Linch DC, Testa NG, Chopra R. Dynamics of telomere shortening in neutrophils and T lymphocytes during ageing and the relationship to skewed X chromosome inactivation patterns. *Br J Haematol*. 2000;109(2):272-279. doi:10.1046/j.1365-2141.2000.01970.x

238. Côté HCF, Hsieh AYY. Leukocyte Telomere Length in HIV Infection: A Marker of Persistent Immune Aging or Transient Immune Reconstitution? *J Infect Dis*. 2018;218(10):1521-1522. doi:10.1093/infdis/jiy365

239. Doisne J-M, Urrutia A, Lacabaratz-Porret C, Goujard C, Meyer L, Chaix M-L, Sinet M, Venet A. CD8+ T Cells Specific for EBV, Cytomegalovirus, and Influenza Virus Are Activated during Primary HIV Infection. *J Immunol*. 2004;173(4):2410 LP - 2418. doi:10.4049/jimmunol.173.4.2410

240. Appay V, Dunbar PR, Callan M, Klenerman P, Gillespie GMA, Papagno L, Ogg GS, King A, Lechner F, Spina CA, Little S, Havlir D V., Richman DD, Gruener N, Pape G, Waters A, Easterbrook P, Salio M, Cerundolo V, McMichael AJ, Rowland-Jones SL. Memory CD8+ T cells vary in differentiation phenotype in different persistent virus infections. *Nat Med*. 2002;8(4):379-385. doi:10.1038/nm0402-379

241. Zuhair M, Smit GSA, Wallis G, Jabbar F, Smith C, Devleesschauwer B, Griffiths P. Estimation of the worldwide seroprevalence of cytomegalovirus: A systematic review and meta-analysis. *Rev Med Virol*. 2019;29(3):1-6. doi:10.1002/rmv.2034

242. Lang DJ, Kovacs AA, Zaia JA, Doelkin G, Niland JC, Aledort L, Azen SP, Fletcher MA, Gauderman J, Gjerset GJ. Seroepidemiologic studies of cytomegalovirus and Epstein-Barr virus infections in relation to human immunodeficiency virus type 1 infection in selected recipient populations. Transfusion Safety Study Group. *J Acquir Immune Defic Syndr*. 1989;2(6):540-549.

243. Robain M, Carré N, Dussaix E, Salmon-Ceron D, Meyer L. Incidence and sexual risk factors of cytomegalovirus seroconversion in HIV-infected subjects. The SEROCO Study Group. *Sex Transm Dis*. 1998;25(9):476-480. doi:10.1097/00007435-199810000-00006

244. Turner JE, Campbell JP, Edwards KM, Howarth LJ, Pawelec G, Aldred S, Moss P, Drayson MT, Burns VE, Bosch JA. Rudimentary signs of immunosenescence in Cytomegalovirus-seropositive healthy young adults. *Age (Omaha)*. 2014;36(1):287-297. doi:10.1007/s11357-013-9557-4

245. Schmaltz HN, Fried LP, Xue Q-L, Walston J, Leng SX, Semba RD. Chronic Cytomegalovirus Infection and Inflammation Are Associated with Prevalent Frailty in Community-Dwelling Older Women. *J Am Geriatr Soc*. 2005;53(5):747-754. doi:10.1111/j.1532-5415.2005.53250.x

246. Roberts ET, Haan MN, Dowd JB, Aiello AE. Cytomegalovirus antibody levels, inflammation, and mortality among elderly Latinos over 9 years of follow-up. *Am J Epidemiol*. 2010;172(4):363-371. doi:10.1093/aje/kwq177

247. Simanek AM, Dowd JB, Pawelec G, Melzer D, Dutta A, Aiello AE. Seropositivity to

cytomegalovirus, inflammation, all-cause and cardiovascular disease-related mortality in the United States. *PLoS One*. 2011;6(2):e16103-e16103. doi:10.1371/journal.pone.0016103

248. Casazza JP, Betts MR, Picker LJ, Koup RA. Decay kinetics of human immunodeficiency virus-specific CD8+ T cells in peripheral blood after initiation of highly active antiretroviral therapy. *J Virol*. 2001;75(14):6508-6516. doi:10.1128/JVI.75.14.6508-6516.2001

249. Kalams SA, Goulder PJ, Shea AK, Jones NG, Trocha AK, Ogg GS, Walker BD. Levels of human immunodeficiency virus type 1-specific cytotoxic T-lymphocyte effector and memory responses decline after suppression of viremia with highly active antiretroviral therapy. *J Virol*. 1999;73(8):6721-6728.

250. Karrer U, Sierro S, Wagner M, Oxenius A, Hengel H, Koszinowski UH, Phillips RE, Klenerman P. Memory Inflation: Continuous Accumulation of Antiviral CD8 + T Cells Over Time. *J Immunol*. 2003;170(4):2022-2029. doi:10.4049/jimmunol.170.4.2022

251. Hadrup SR, Strindhall J, Køllgaard T, Seremet T, Johansson B, Pawelec G, thor Straten P, Wikby A. Longitudinal Studies of Clonally Expanded CD8 T Cells Reveal a Repertoire Shrinkage Predicting Mortality and an Increased Number of Dysfunctional Cytomegalovirus-Specific T Cells in the Very Elderly. *J Immunol*. 2006;176(4):2645-2653. doi:10.4049/jimmunol.176.4.2645

252. Champagne P, Ogg GS, King AS, Knabenhans C, Ellefsen K, Nobile M, Appay V, Rizzardi GP, Fleury S, Lipp M, Förster R, Rowland-Jones S, Sékaly RP, McMichael AJ, Pantaleo G. Skewed maturation of memory HIV-specific CD8 T lymphocytes. *Nature*. 2001;410(6824):106-111. doi:10.1038/35065118

253. Lee SA, Sinclair E, Hatano H, Hsue PY, Epling L, Hecht FM, Bangsberg DR, Martin JN, McCune JM, Deeks SG, Hunt PW. Impact of HIV on CD8+ T cell CD57 expression is distinct from that of CMV and aging. *PLoS One*. 2014;9(2):1-10. doi:10.1371/journal.pone.0089444

254. Heath JJ, Fudge NJ, Gallant ME, Grant MD. Proximity of cytomegalovirus-specific CD8+ T cells to replicative senescence in human immunodeficiency virus-infected individuals. *Front Immunol*. 2018;9:201. doi:10.3389/fimmu.2018.00201

255. van de Berg PJEJ, Griffiths SJ, Yong S-L, Macaulay R, Bemelman FJ, Jackson S, Henson SM, ten Berge IJM, Akbar AN, van Lier RAW. Cytomegalovirus Infection Reduces Telomere Length of the Circulating T Cell Pool. *J Immunol*. 2010;184(7):3417-3423. doi:10.4049/jimmunol.0903442

256. Aiello AE, Jayabalasingham B, Simanek AM, Diez-Roux A, Feinstein L, Meier HCS, Needham BL, Dowd JB. The impact of pathogen burden on leukocyte telomere length in the Multi-Ethnic Study of Atherosclerosis. *Epidemiol Infect*. 2017;145(14):3076-3084. doi:10.1017/S0950268817001881

257. Dowd JB, Bosch JA, Steptoe A, Blackburn EH, Lin J, Rees-Clayton E, Aiello AE. Cytomegalovirus is associated with reduced telomerase activity in the Whitehall II cohort. *Exp Gerontol*. 2013;48(4):385-390. doi:10.1016/j.exger.2013.01.016

258. Freeman ML, Mudd JC, Shive CL, Younes SA, Panigrahi S, Sieg SF, Lee SA, Hunt PW, Calabrese LH, Gianella S, Rodriguez B, Lederman MM. CD8 T-cell expansion and inflammation linked to CMV coinfection in ART-treated HIV infection. *Clin Infect Dis*. 2016;62(3):392-396. doi:10.1093/cid/civ840

259. Barrett L, Stapleton SN, Fudge NJ, Grant MD. Immune resilience in HIV-infected

individuals seronegative for cytomegalovirus. *Aids*. 2014;28(14):2045-2049. doi:10.1097/QAD.0000000000000405

260. Naeger DM, Martin JN, Sinclair E, Hunt PW, Bangsberg DR, Hecht F, Hsue P, McCune JM, Deeks SG. Cytomegalovirus-specific T cells persist at very high levels during long-term antiretroviral treatment of HIV disease. *PLoS One*. 2010;5(1):e8886-e8886. doi:10.1371/journal.pone.0008886

261. Hunt PW, Martin JN, Sinclair E, Epling L, Teague J, Jacobson MA, Tracy RP, Corey L, Deeks SG. Valganciclovir reduces T cell activation in HIV-infected individuals with incomplete CD41 T cell recovery on antiretroviral therapy. *J Infect Dis*. 2011;203(10):1474-1483. doi:10.1093/infdis/jir060

262. Lichtner M, Cicconi P, Vita S, Cozzi-Lepri A, Galli M, Lo Caputo S, Saracino A, De Luca A, Moioli M, Maggiolo F, Marchetti G, Vullo V, Monforte ADA. Cytomegalovirus coinfection is associated with an increased risk of severe non-AIDS-defining events in a large cohort of HIV-infected patients. *J Infect Dis*. 2015;211(2):178-186. doi:10.1093/infdis/jiu417

263. Aramă V, Mihăilescu R, Rădulescu M, Aramă SŞ, Streinu-Cercel A, Youle M, group C-HS, Bartholomeusz A, Locarnini S. Clinical relevance of the plasma load of cytomegalovirus in patients infected with HIV—A survival analysis. *J Med Virol*. 2014;86(11):1821-1827. doi:10.1002/jmv.24027

264. Parrinello CM, Sinclair E, Landay AL, Lurain N, Sharrett AR, Gange SJ, Xue X, Hunt PW, Deeks SG, Hodis HN, Kaplan RC. Cytomegalovirus immunoglobulin G antibody is associated with subclinical carotid artery disease among HIV-infected women. *J Infect Dis*. 2012;205(12):1788-1796. doi:10.1093/infdis/jis276

265. Strathdee SA, Veugelers PJ, Page-Shafer KA, McNulty A, Moss AR, Schechter MT, van Griensven GJ, Coutinho RA. Lack of consistency between five definitions of nonprogression in cohorts of HIV-infected seroconverters. *AIDS*. 1996;10(9):959-965. doi:10.1097/00002030-199610090-00005

266. Salhi Y, Costagliola D. Long-term nonprogression in HIV infection. Clinical Epidemiology Group from the Centre d'Information et de Soins de l'Immunodéficience Humaine. *J Acquir Immune Defic Syndr*. 1997;16(5):409-411. doi:10.1097/00042560-199712150-00018

267. Petrucci A, Dorrucci M, Alliegro MB, Pezzotti P, Rezza G, Sinicco A, Lazzarin A, Angarano G. How many HIV-infected individuals may be defined as long-term nonprogressors? A report from the Italian Seroconversion Study. Italian Seroconversion Study Group (ISS). *J Acquir immune Defic Syndr Hum retrovirology*. 1997;14(3):243-248. doi:10.1097/00042560-199703010-00008

268. Sheppard HW, Lang W, Ascher MS, Vittinghoff E, Winkelstein W. The characterization of non-progressors: long-term HIV-1 infection with stable CD4+ T-cell levels. *AIDS*. 1993;7(9):1159-1166.

269. Buchbinder SP, Katz MH, Hessol NA, O'Malley PM, Holmberg SD. Long-term HIV-1 infection without immunologic progression. *AIDS*. 1994;8(8):1123-1128. doi:10.1097/00002030-199408000-00014

270. Grabar S, Selinger-Leneman H, Abgrall S, Pialoux G, Weiss L, Costagliola D. Prevalence and comparative characteristics of long-term nonprogressors and HIV controller patients in the French Hospital Database on HIV. *Aids*. 2009;23(9):1163-1169. doi:10.1097/QAD.0b013e32832b44c8

271. Sajadi MM, Constantine NT, Mann DL, Charurat M, Dadzan E, Kadlecik P, Redfield RR. Epidemiologic characteristics and natural history of HIV-1 natural viral suppressors. *J Acquir Immune Defic Syndr*. 2009;50(4):403-408. doi:10.1097/QAI.0b013e3181945f1e

272. Okulicz JF, Marconi VC, Landrum ML, Wegner S, Weintrob A, Ganesan A, Hale B, Crum-Cianflone N, Delmar J, Barthel V, Quinnan G, Agan BK, Dolan MJ. Clinical Outcomes of Elite Controllers, Viremic Controllers, and Long-Term Nonprogressors in the US Department of Defense HIV Natural History Study. *J Infect Dis*. 2009;200(11):1714-1723. doi:10.1086/646609

273. Madec Y, Boufassa F, Avettand-Fenoel V, Hendou S, Melard A, Boucherit S, Surzyn J, Meyer L, Rouzioux C. Early control of HIV-1 infection in long-term nonprogressors followed since diagnosis in the ANRS SEROCO/HEMOCO cohort. *J Acquir Immune Defic Syndr*. 2009;50(1):19-26. doi:10.1097/QAI.0b013e31818ce709

274. Lambotte O, Boufassa F, Madec Y, Nguyen A, Goujard C, Meyer L, Rouzioux C, Venet A, Delfraissy J-F. HIV Controllers: A Homogeneous Group of HIV-1—Infected Patients with Spontaneous Control of Viral Replication. *Clin Infect Dis*. 2005;41(7):1053-1056. doi:10.1086/433188

275. Pereyra F, Palmer S, Miura T, Block BL, Wiegand A, Rothchild AC, Baker B, Rosenberg R, Cutrell E, Seaman MS, Coffin JM, Walker BD. Persistent low-level viremia in HIV-1 elite controllers and relationship to immunologic parameters. *J Infect Dis*. 2009;200(6):984-990. doi:10.1086/605446

276. Hatano H, Delwart EL, Norris PJ, Lee T-H, Dunn-Williams J, Hunt PW, Hoh R, Stramer SL, Linnen JM, McCune JM, Martin JN, Busch MP, Deeks SG. Evidence for Persistent Low-Level Viremia in Individuals Who Control Human Immunodeficiency Virus in the

Absence of Antiretroviral Therapy. *J Virol*. 2009;83(1):329-335. doi:10.1128/jvi.01763-08

277. Pereyra F, Addo MM, Kaufmann DE, Liu Y, Miura T, Rathod A, Baker B, Trocha A, Rosenberg R, Mackey E, Ueda P, Lu Z, Cohen D, Wrin T, Petropoulos CJ, Rosenberg ES, Walker BD. Genetic and Immunologic Heterogeneity among Persons Who Control HIV Infection in the Absence of Therapy. *J Infect Dis*. 2008;197(4):563-571. doi:10.1086/526786

278. Benkirane M, Jin DY, Chun RF, Koup RA, Jeang KT. Mechanism of transdominant inhibition of CCR5-mediated HIV-1 infection by ccr5Δ32. *J Biol Chem*. 1997;272(49):30603-30606. doi:10.1074/jbc.272.49.30603

279. Samson M, Libert F, Doranz BJ, Rucker J, Liesnard C, Farber C-M, Saragosti S, Lapouméroulie C, Cognaux J, Forceille C, Muyldermans G, Verhofstede C, Burtonboy G, Georges M, Imai T, Rana S, Yi Y, Smyth RJ, Collman RG, Doms RW, Vassart G, Parmentier M. Resistance to HIV-1 infection in Caucasian individuals bearing mutant alleles of the CCR-5 chemokine receptor gene. *Nature*. 1996;382(6593):722-725. doi:10.1038/382722a0

280. Liu R, Paxton WA, Choe S, Ceradini D, Martin SR, Horuk R, MacDonald ME, Stuhlmann H, Koup RA, Landau NR. Homozygous Defect in HIV-1 Coreceptor Accounts for Resistance of Some Multiply-Exposed Individuals to HIV-1 Infection. *Cell*. 1996;86(3):367-377. doi:10.1016/S0092-8674(00)80110-5

281. Dean M, Carrington M, Winkler C, Huttley GA, Smith MW, Allikmets R, Goedert JJ, Buchbinder SP, Vittinghoff E, Gomperts E, Donfield S, Vlahov D, Kaslow R, Saah A, Rinaldo C, Detels R, O'Brien SJ. Genetic restriction of HIV-1 infection and progression to

AIDS by a deletion allele of the CKR5 structural gene. Hemophilia Growth and Development Study, Multicenter AIDS Cohort Study, Multicenter Hemophilia Cohort Study, San Francisco City Cohort, ALIVE . *Science*. 1996;273(5283):1856-1862. doi:10.1126/science.273.5283.1856

282. Rappaport J, Cho Y-Y, Hendel H, Schwartz EJ, Schachter F, Zagury J-F. 32 bp CCR-5 gene deletion and resistance to fast progression in HIV-1 infected heterozygotes. *Lancet*. 1997;349(9056):922-923. doi:10.1016/S0140-6736(05)62697-9

283. Zimmerman PA, Buckler-White A, Alkhatib G, Spalding T, Kubofcik J, Combadiere C, Weissman D, Cohen O, Rubbert A, Lam G, Vaccarezza M, Kennedy PE, Kumaraswami V, Giorgi J V, Detels R, Hunter J, Chopek M, Berger EA, Fauci AS, Nutman TB, Murphy PM. Inherited Resistance to HIV-1 Conferred by an Inactivating Mutation in CC Chemokine Receptor 5: Studies in Populations with Contrasting Clinical Phenotypes, Defined Racial Background, and Quantified Risk. *Mol Med*. 1997;3(1):23-36. doi:10.1007/BF03401665

284. Alvarez V, López-Larrea C, Coto E. Mutational analysis of the CCR5 and CXCR4 genes (HIV-1 co-receptors) in resistance to HIV-1 infection and AIDS development among intravenous drug users. *Hum Genet*. 1998;102(4):483-486. doi:10.1007/s004390050726

285. Kaslow RA, Carrington M, Apple R, Park L, Muñoz A, Saah AJ, Goedert JJ, Winkler C, O'Brien SJ, Rinaldo C, Detels R, Blattner W, Phair J, Erlich H, Mann DL. Influence of combinations of human major histocompatibility complex genes on the course of HIV–1 infection. *Nat Med*. 1996;2(4):405-411. doi:10.1038/nm0496-405

286. Migueles SA, Sabbaghian MS, Shupert WL, Bettinotti MP, Marincola FM, Martino L, Hallahan CW, Selig SM, Schwartz D, Sullivan J, Connors M. HLA B*5701 is highly

associated with restriction of virus replication in a subgroup of HIV-infected long term nonprogressors. *Proc Natl Acad Sci*. 2000;97(6):2709 LP - 2714. doi:10.1073/pnas.050567397

287. Horton H, Frank I, Baydo R, Jalbert E, Penn J, Wilson S, McNevin JP, McSweyn MD, Lee D, Huang Y, De Rosa SC, McElrath MJ. Preservation of T Cell Proliferation Restricted by Protective HLA Alleles Is Critical for Immune Control of HIV-1 Infection. *J Immunol*. 2006;177(10):7406-7415. doi:10.4049/jimmunol.177.10.7406

288. Elahi S, Dinges WL, Lejarcegui N, Laing KJ, Collier AC, Koelle DM, McElrath MJ, Horton H. Protective HIV-specific CD8+ T cells evade Treg cell suppression. *Nat Med*. 2011;17(8):989-995. doi:10.1038/nm.2422

289. Pereyra F, Jia X, McLaren PJ, Telenti A, de Bakker PIW, Walker BD, Ripke S, Brumme CJ, Pulit SL, Carrington M, Kadie CM, Carlson JM, Heckerman D, Graham RR, Plenge RM, Deeks SG, Gianniny L, Crawford G, Sullivan J, Gonzalez E, Davies L, Camargo A, Moore JM, Beattie N, Gupta S, Crenshaw A, Burtt NP, Guiducci C, Gupta N, Gao X, Qi Y, Yuki Y, Piechocka-Trocha A, Cutrell E, Rosenberg R, Moss KL, Lemay P, O'Leary J, Schaefer T, Verma P, Toth I, Block B, Baker B, Rothchild A, Lian J, Proudfoot J, Alvino DML, Vine S, Addo MM, Allen TM, Altfeld M, Henn MR, Le Gall S, Streeck H, Haas DW, Kuritzkes DR, Robbins GK, Shafer RW, Gulick RM, Shikuma CM, Haubrich R, Riddler S, Sax PE, Daar ES, Ribaudo HJ, Agan B, Agarwal S, Ahern RL, Allen BL, Altidor S, Altschuler EL, Ambardar S, Anastos K, Anderson B, Anderson V, Andrady U, Antoniskis D, Bangsberg D, Barbaro D, Barrie W, Bartczak J, Barton S, Basden P, Basgoz N, Bazner S, Bellos NC, Benson AM, Berger J, Bernard NF, Bernard AM, Birch C, Bodner SJ, Bolan RK, Boudreaux ET, Bradley M, Braun JF, Brndjar JE, Brown

SJSTSJ, Brown K, Zhao M. The major genetic determinants of HIV-1 control affect HLA class I peptide presentation. *Science*. 2010;330(6010):1551-1557. doi:10.1126/science.1195271

290. Deacon NJ, Tsykin A, Solomon A, Smith K, Ludford-Menting M, Hooker DJ, McPhee DA, Greenway AL, Ellett A, Chatfield C, Lawson VA, Crowe S, Maerz A, Sonza S, Learmont J, Sullivan JS, Cunningham A, Dwyer D, Dowton D, Mills J. Genomic Structure of an Attenuated Quasi Species of HIV-1 from a Blood Transfusion Donor and Recipients. *Science*. 1995;270(5238):988-991. doi:10.1126/science.270.5238.988

291. Kirchhoff F, Greenough TC, Brettler DB, Sullivan JL, Desrosiers RC. Absence of Intact nef Sequences in a Long-Term Survivor with Nonprogressive HIV-1 Infection. *N Engl J Med*. 1995;332(4):228-232. doi:10.1056/NEJM199501263320405

292. Navis M, Schellens I, van Baarle D, Borghans J, van Swieten P, Miedema F, Kootstra N, Schuitemaker H. Viral Replication Capacity as a Correlate of HLA B57/B5801-Associated Nonprogressive HIV-1 Infection. *J Immunol*. 2007;179(5):3133-3143. doi:10.4049/jimmunol.179.5.3133

293. Quiñones-Mateu ME, Ball SC, Marozsan AJ, Torre VS, Albright JL, Vanham G, van Der Groen G, Colebunders RL, Arts EJ. A dual infection/competition assay shows a correlation between ex vivo human immunodeficiency virus type 1 fitness and disease progression. *J Virol*. 2000;74(19):9222-9233. doi:10.1128/jvi.74.19.9222-9233.2000

294. Blaak H, Brouwer M, Ran LJ, de Wolf F, Schuitemaker H. In Vitro Replication Kinetics of Human Immunodeficiency Virus Type 1 (HIV-1) Variants in Relation to Virus Load in Long-Term Survivors of HIV-1 Infection. *J Infect Dis*. 1998;177(3):600-610. doi:10.1086/514219

295. Blankson JN, Bailey JR, Thayil S, Yang H-C, Lassen K, Lai J, Gandhi SK, Siliciano JD, Williams TM, Siliciano RF. Isolation and Characterization of Replication-Competent Human Immunodeficiency Virus Type 1 from a Subset of Elite Suppressors. *J Virol*. 2007;81(5):2508-2518. doi:10.1128/jvi.02165-06

296. Crowell TA, Gebo KA, Blankson JN, Korthuis PT, Yehia BR, Rutstein RM, Moore RD, Sharp V, Nijhawan AE, Mathews WC, Hanau LH, Corales RB, Beil R, Somboonwit C, Edelstein H, Allen SL, Berry SA. Hospitalization rates and reasons among HIV elite controllers and persons with medically controlled HIV infection. *J Infect Dis*. 2015;211(11):1692-1702. doi:10.1093/infdis/jiu809

297. Richardson MW, Sverstiuk A, Hendel H, Cheung TW, Zagury JF, Rappaport J. Analysis of telomere length and thymic output in fast and slow/non- progressors with HIV infection. *Biomed Pharmacother*. 2000;54(1):21-31. doi:10.1016/S0753-3322(00)88637-0

298. Gaardbo JC, Hartling HJ, Ronit A, Thorsteinsson K, Madsen HO, Springborg K, Gjerdrum LMR, Birch C, Laye M, Ullum H, Andersen ÅB, Nielsen SD. Different Immunological Phenotypes Associated with Preserved CD4+ T Cell Counts in HIV-Infected Controllers and Viremic Long Term Non-Progressors. *PLoS One*. 2013;8(5):1-10. doi:10.1371/journal.pone.0063744

299. Lichterfeld M, Mou D, Cung TDH, Williams KL, Waring MT, Huang J, Pereyra F, Trocha A, Freeman GJ, Rosenberg ES, Walker BD, Yu XG. Telomerase activity of HIV-1 specific CD8+ T cells: Constitutive up-regulation in controllers and selective increase by blockade of PD ligand 1 in progressors. *Blood*. 2008;112:3679-3687. doi:10.1182/blood-2008-01-135442

300. Cao W, Jamieson BD, Hultin LE, Hultin PM, Effros RB, Detels R. Premature aging of T

cells is associated with faster HIV-1 disease progression. *J Acquir Immune Defic Syndr*. 2009;50(2):137-147. doi:10.1097/QAI.0b013e3181926c28

301. Hunt PW, Brenchley J, Sinclair E, McCune JM, Roland M, Page-Shafer K, Hsue P, Emu B, Krone M, Lampiris H, Douek D, Martin JN, Deeks SG. Relationship between T cell activation and CD4+ T cell count in HIV-seropositive individuals with undetectable plasma HIV RNA levels in the absence of therapy. *J Infect Dis*. 2008;197(1):126-133. doi:10.1086/524143

302. Williams GC. Pleiotropy, Natural Selection, and the Evolution of Senescence. *Evolution (N Y)*. 1957;11(4):398-411. doi:10.2307/2406060

303. Anderson S, Bankier AT, Barrell BG, de Bruijn MH, Coulson AR, Drouin J, Eperon IC, Nierlich DP, Roe BA, Sanger F, Schreier PH, Smith AJ, Staden R, Young IG. Sequence and organization of the human mitochondrial genome. *Nature*. 1981;290(5806):457-465. doi:10.1038/290457a0

304. Fukuhara H. Relative Proportions of Mitochondrial and Nuclear DNA in Yeast under Various Conditions of Growth. *Eur J Biochem*. 1969;11(1):135-139. doi:10.1111/j.1432-1033.1969.tb00750.x

305. Moraes CT, Kenyon L, Hao H. Mechanisms of human mitochondrial DNA maintenance: the determining role of primary sequence and length over function. *Mol Biol Cell*. 1999;10(10):3345-3356. doi:10.1091/mbc.10.10.3345

306. Fisher RP, Clayton DA. A transcription factor required for promoter recognition by human mitochondrial RNA polymerase. Accurate initiation at the heavy- and light-strand promoters dissected and reconstituted in vitro. *J Biol Chem*. 1985;260(20):11330-11338.

307. Virbasius J V, Scarpulla RC. Activation of the human mitochondrial transcription factor A

gene by nuclear respiratory factors: a potential regulatory link between nuclear and mitochondrial gene expression in organelle biogenesis. *Proc Natl Acad Sci U S A*. 1994;91(4):1309-1313. doi:10.1073/pnas.91.4.1309

308. Lee H-C, Wei Y-H. Mitochondrial biogenesis and mitochondrial DNA maintenance of mammalian cells under oxidative stress. *Int J Biochem Cell Biol*. 2005;37(4):822-834. doi:10.1016/j.biocel.2004.09.010

309. Barrientos A, Casademont J, Cardellach F, Estivill X, Urbano-Marquez A, Nunes V. Reduced steady-state levels of mitochondrial RNA and increased mitochondrial DNA amount in human brain with aging. *Mol Brain Res*. 1997;52(2):284-289. doi:10.1016/S0169-328X(97)00278-7

310. Lee HC, Yin PH, Lu CY, Chi CW, Wei YH. Increase of mitochondria and mitochondrial DNA in response to oxidative stress in human cells. *Biochem J*. 2000;348 Pt 2(Pt 2):425-432. doi:10.1042/bj3480425

311. He X, Qu F, Zhou F, Zhou X, Chen Y, Guo X. High leukocyte mtDNA content contributes to poor prognosis through ROS-mediated immunosuppression in hepatocellular carcinoma patients. *Oncotarget*. 2014;7(16). doi:10.18632/oncotarget.8071

312. Song J, Oh JY, Sung YA, Pak YK, Park KS, Lee HK. Peripheral blood mitochondrial DNA content is related to insulin sensitivity in offspring of type 2 diabetic patients. *Diabetes Care*. 2001;24(5):865-869. doi:10.2337/diacare.24.5.865

313. Malik AN, Parsade CK, Ajaz S, Crosby-Nwaobi R, Gnudi L, Czajka A, Sivaprasad S. Altered circulating mitochondrial DNA and increased inflammation in patients with diabetic retinopathy. *Diabetes Res Clin Pract*. 2015;110(3):257-265. doi:10.1016/j.diabres.2015.10.006

314. Cote HC, Day AG, Heyland DK. Longitudinal increases in mitochondrial DNA levels in blood cells are associated with survival in critically ill patients. *Crit Care*. 2007;11(4):R88. doi:10.1186/cc6096

315. Miro O, Lopez S, Martinez E, Rodriguez-Santiago B, Blanco JL, Milinkovic A, Miro JM, Nunes V, Casademont J, Gatell JM, Cardellach F. Reversible mitochondrial respiratory chain impairment during symptomatic hyperlactatemia associated with antiretroviral therapy. *AIDS Res Hum Retroviruses*. 2003;19(11):1027-1032. doi:10.1089/088922203322588387

316. Arnaudo E, Shanske S, DiMauro S, Schon EA, Moraes CT, Schon EA, Dalakas M. Depletion of muscle mitochondrial DNA in AIDS patients with zidovudine-induced myopathy. *Lancet*. 1991;337(8740):508-510. doi:10.1016/0140-6736(91)91294-5

317. Dalakas MC, Semino-Mora C, Leon-Monzon M. Mitochondrial alterations with mitochondrial DNA depletion in the nerves of AIDS patients with peripheral neuropathy induced by 2’3’-dideoxycytidine (ddC). *Lab Invest*. 2001;81(11):1537-1544. doi:10.1038/labinvest.3780367

318. Shikuma CM, Hu N, Milne C, Yost F, Waslien C, Shimizu S, Shiramizu B. Mitochondrial DNA decrease in subcutaneous adipose tissue of HIV-infected individuals with peripheral lipoatrophy. *Aids*. 2001;15(14):1801-1809. doi:10.1097/00002030-200109280-00009

319. Yu M. Generation, function and diagnostic value of mitochondrial DNA copy number alterations in human cancers. *Life Sci*. 2011;89(3-4):65-71. doi:10.1016/j.lfs.2011.05.010

320. Wen SL, Zhang F, Feng S. Decreased copy number of mitochondrial DNA: A potential diagnostic criterion for gastric cancer. *Oncol Lett*. 2013;6(4):1098-1102. doi:10.3892/ol.2013.1492

321. Fernandes J, Michel V, Camorlinga-Ponce M, Gomez A, Maldonado C, De Reuse H, Torres J, Touati E. Circulating mitochondrial DNA level, a noninvasive biomarker for the early detection of gastric cancer. *Cancer Epidemiol Biomarkers Prev*. 2014;23(11):2430-2438. doi:10.1158/1055-9965.EPI-14-0471

322. Côté H, Brumme Z, Chan J, Guillemi S, Montaner J, Harrigan P. HIV therapy, hepatitis C virus infection, antibiotics and obesity, a mitochondria killer mix? *Aids*. 2006;20(9):1343-1345. doi:10.1097/01.aids.0000232250.89404.00

323. Stringer HAJ, Sohi GK, Maguire JA, Côté HCF. Decreased skeletal muscle mitochondrial DNA in patients with statin-induced myopathy. *J Neurol Sci*. 2013;325(1-2):142-147. doi:10.1016/j.jns.2012.12.023

324. Schick BA, Laaksonen R, Frohlich JJ, Päivä H, Lehtimäki T, Humphries KH, Côté HCF. Decreased Skeletal Muscle Mitochondrial DNA in Patients Treated with High-Dose Simvastatin. *Clin Pharmacol Ther*. 2007;81(5):650-653. doi:10.1038/sj.clpt.6100124

325. Zanet DL, Saberi S, Oliveira L, Sattha B, Gadawski I, Côté HCF. Blood and Dried Blood Spot Telomere Length Measurement by qPCR: Assay Considerations. *PLoS One*. 2013;8(2). doi:10.1371/journal.pone.0057787

326. Kogelnik A. MITOMAP: a human mitochondrial genome database. *Nucleic Acids Res*. 1996;24(1):177-179. doi:10.1093/nar/24.1.177

327. Ruijter JM, Ramakers C, Hoogaars WMH, Karlen Y, Bakker O, van den Hoff MJB, Moorman AFM. Amplification efficiency: linking baseline and bias in the analysis of quantitative PCR data. *Nucleic Acids Res*. 2009;37(6):e45-e45. doi:10.1093/nar/gkp045

328. Lin LI-K. A Concordance Correlation Coefficient to Evaluate Reproducibility. *Biometrics*. 1989;45(1):255-268. doi:10.1017/CBO9781107415324.004

329. Morton NE. Parameters of the human genome. *Proc Natl Acad Sci U S A*. 1991;88(17):7474-7476. doi:10.1073/pnas.88.17.7474

330. Serth J, Kuczyk MA, Paeslack U, Lichtinghagen R, Jonas U. Quantitation of DNA extracted after micropreparation of cells from frozen and formalin-fixed tissue sections. *Am J Pathol*. 2000;156(4):1189-1196. doi:10.1016/S0002-9440(10)64989-9

331. Ghatak S, Muthukumaran RB, Nachimuthu SK. A simple method of genomic DNA extraction from human samples for PCR-RFLP analysis. *J Biomol Tech*. 2013;24(4):224-231. doi:10.7171/jbt.13-2404-001

332. Memon AA, Zöller B, Hedelius A, Wang X, Stenman E, Sundquist J, Sundquist K. Quantification of mitochondrial DNA copy number in suspected cancer patients by a well optimized ddPCR method. *Biomol Detect Quantif*. 2017;13:32-39. doi:10.1016/j.bdq.2017.08.001

333. Kim MY, Lee JW, Kang HC, Kim E, Lee DC. Leukocyte mitochondrial DNA (mtDNA) content is associated with depression in old women. *Arch Gerontol Geriatr*. 2011;53(2):2009-2012. doi:10.1016/j.archger.2010.11.019

334. Cui H, Huang P, Wang Z, Zhang Y, Zhang Z, Xu W, Wang X, Han Y, Guo X. Association of decreased mitochondrial DNA content with the progression of colorectal cancer. *BMC Cancer*. 2013;13(1):110. doi:10.1186/1471-2407-13-110

335. Urata M, Koga-Wada Y, Kayamori Y, Kang D. Platelet contamination causes large variation as well as overestimation of mitochondrial DNA content of peripheral blood mononuclear cells. *Ann Clin Biochem*. 2008;45(Pt 5):513-514. doi:10.1258/acb.2008.008008

336. Hurtado-Roca Y, Ledesma M, Gonzalez-Lazaro M, Moreno-Loshuertos R, Fernandez-

Silva P, Enriquez JA, Laclaustra M. Adjusting MtDNA Quantification in Whole Blood for Peripheral Blood Platelet and Leukocyte Counts. *PLoS One*. 2016;11(10):e0163770. doi:10.1371/journal.pone.0163770

337. Budd MA, Calli K, Samson L, Bowes J, Hsieh AYY, Forbes JC, Bitnun A, Singer J, Kakkar F, Alimenti A, Maan EJ, Suzanne Lewis ME, Gentile C, Côté HCF, Brophy JC. Blood mitochondrial DNA content in HIV-exposed uninfected children with autism spectrum disorder. *Viruses*. 2018;10(2). doi:10.3390/v10020077

338. Morin A, Liu JC, Xu S, Jones M, Fishbane N, Kobor M, Sin DD, Horvath S, Harrigan PR, Man SFP, Montaner J, Hayashi K, Leung JM, Milloy M-J, MacIsaac J. Longitudinal study of surrogate aging measures during human immunodeficiency virus seroconversion. *Aging (Albany NY)*. 2017;9(3):687-705. doi:10.18632/aging.101184

339. Pavanello S, Hoxha M, Dioni L, Bertazzi PA, Snenghi R, Nalesso A, Ferrara SD, Montisci M, Baccarelli A. Shortened telomeres in individuals with abuse in alcohol consumption. *Int J Cancer*. 2011;129(4):983-992. doi:10.1002/ijc.25999

340. Heckbert SR, Mukamal KJ, Dixit S, Lin J, Vittinghoff E, Roberts JD, Marcus GM, Whooley MA, Leung C, Fitzpatrick AL. Alcohol consumption and leukocyte telomere length. *Sci Rep*. 2019;9(1):1-10. doi:10.1038/s41598-019-38904-0

341. El-Far M, Kouassi P, Sylla M, Zhang Y, Fouda A, Fabre T, Goulet JP, Van Grevenynghe J, Lee T, Singer J, Harris M, Baril JG, Trottier B, Ancuta P, Routy JP, Bernard N, Tremblay CL. Proinflammatory isoforms of IL-32 as novel and robust biomarkers for control failure in HIV-infected slow progressors. *Sci Rep*. 2016;6(November 2015):1-18. doi:10.1038/srep22902

342. Lin Y, Damjanovic A, Metter EJ, Nguyen H, Truong T, Najarro K, Morris C, Longo DL,

Zhan M, Ferrucci L, Hodes RJ, Weng N. Age-associated telomere attrition of lymphocytes in vivo is co-ordinated with changes in telomerase activity, composition of lymphocyte subsets and health conditions. *Clin Sci (Lond)*. 2015;128(6):367-377. doi:10.1042/CS20140481

343. Aubert G, Baerlocher GM, Vulto I, Poon SS, Lansdorp PM. Collapse of telomere homeostasis in hematopoietic cells caused by heterozygous mutations in telomerase genes. *PLoS Genet*. 2012;8(5):e1002696. doi:10.1371/journal.pgen.1002696